LEABHARLANN CHOLÁISTE NA TRÍONÓIDE, BAILE ÁTHA CLIATH | TRINITY COLLEGE LIBRARY DUBLIN
Ollscoil Átha Cliath | The University of Dublin

Terms and Conditions of Use of Digitised Theses from Trinity College Library Dublin

Copyright statement

All material supplied by Trinity College Library is protected by copyright (under the Copyright and Related Rights Act, 2000 as amended) and other relevant Intellectual Property Rights. By accessing and using a Digitised Thesis from Trinity College Library you acknowledge that all Intellectual Property Rights in any Works supplied are the sole and exclusive property of the copyright and/or other IPR holder. Specific copyright holders may not be explicitly identified. Use of materials from other sources within a thesis should not be construed as a claim over them.

A non-exclusive, non-transferable licence is hereby granted to those using or reproducing, in whole or in part, the material for valid purposes, providing the copyright owners are acknowledged using the normal conventions. Where specific permission to use material is required, this is identified and such permission must be sought from the copyright holder or agency cited.

Liability statement

By using a Digitised Thesis, I accept that Trinity College Dublin bears no legal responsibility for the accuracy, legality or comprehensiveness of materials contained within the thesis, and that Trinity College Dublin accepts no liability for indirect, consequential, or incidental, damages or losses arising from use of the thesis for whatever reason. Information located in a thesis may be subject to specific use constraints, details of which may not be explicitly described. It is the responsibility of potential and actual users to be aware of such constraints and to abide by them. By making use of material from a digitised thesis, you accept these copyright and disclaimer provisions. Where it is brought to the attention of Trinity College Library that there may be a breach of copyright or other restraint, it is the policy to withdraw or take down access to a thesis while the issue is being resolved.

Access Agreement

By using a Digitised Thesis from Trinity College Library you are bound by the following Terms & Conditions. Please read them carefully.

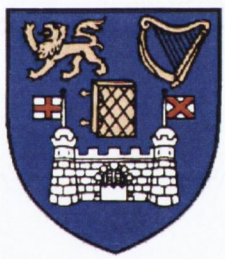
I have read and I understand the following statement: All material supplied via a Digitised Thesis from Trinity College Library is protected by copyright and other intellectual property rights, and duplication or sale of all or part of any of a thesis is not permitted, except that material may be duplicated by you for your research use or for educational purposes in electronic or print form providing the copyright owners are acknowledged using the normal conventions. You must obtain permission for any other use. Electronic or print copies may not be offered, whether for sale or otherwise to anyone. This copy has been supplied on the understanding that it is copyright material and that no quotation from the thesis may be published without proper acknowledgement.

β-Adrenoceptor-mediated Regulation of Matrix Metalloproteinase-9 in Fibroblasts

A thesis submitted to the

University of Dublin,

Trinity College



In fulfilment of the requirement

for the degree of

Doctor of Philosophy

By

Anne Rietz

Dipl.-Biochem. (M.Sc.)

2011

TRINITY COLLEGE
27 JUL 2011
LIBRARY DUBLIN
THESIS
9260

Declaration

I declare that, expect where otherwise acknowledged this thesis is entirely my own work and that it has not been submitted previously for a Higher Degree at this or any other university.

I agree that the Library may lend or copy this thesis on request.



Anne Rietz

Summary Methods and Results

Adrenoceptor signalling in fibroblasts: Intracellular cAMP levels were measured by a direct cAMP enzyme immunoassay. Isoprenaline (ISO, 1 μM) increased intracellular cAMP concentration by 1.3 and 4.8 fold, $P<0.05$, after 10 min in the NIH3T3 fibroblasts and human cardiac ventricular fibroblasts (HCVF) respectively. These effects were abolished by pre-treatment with propranolol (PROP, 10 μM; $P<0.05$). Nuclear translocation of phospho-CREB was increased by isoprenaline (0.1 μM) and phenylephrine (10 μM) increased in NIH3T3 fibroblasts ($P<0.05$). Western blot analysis indicated that isoprenaline (1 μM) and phenylephrine (10 μM) caused a biphasic increase in p38 MAPK and a sustained increase in ERK1/2 MAPK activation over a 30 min period in NIH3T3 fibroblasts. However, in HCVF cells, isoprenaline (1 μM) decreased ERK1/2 MAPK phosphorylation by 70% after 30 min, an effect abolished by propranolol (10 μM; ISO vs. ISO/PROP: 0.30±0.06 vs.1.05±0.10 AU; $P<0.05$). In NIH3T3 fibroblasts, isoprenaline and phenylephrine did not alter NFκB promoter activation at any concentration or time point studied. Isoprenaline (1 μM) decreased NFκB p65 (Ser^{536}) phosphorylation over a 30 min period, while IκBα expression was unaltered in NIH3T3 fibroblasts. In HCVF cells, isoprenaline did not modify NFκB phosphorylation or IκBα expression. Phenylephrine (10 μM) did not affect either NFκB phosphorylation or IκBα expression in NIH3T3 and HCVF cells, while TNFα increased both NFκB phosphorylation and IκBα degradation in NIH3T3 and HCVF cells ($P<0.05$). MMP-9 activity was not affected by either isoprenaline (0.1, 1 μM) or phenylephrine (10, 50 μM) in NIH3T3 cells as measured by gelatin-zymography. MMP-9 promoter activity was measured in NIH3T3 cells transiently transfected with a luciferase promoter construct corresponding to -1285 bp to +20 bp of the MMP-9 promoter. Isoprenaline (0.1, 1 μM) and phenylephrine (10, 50 μM) did not alter promoter activity at any time or concentration studies. Furthermore, in NIH3T3 and HCVF cells they did not

alter MMP-9 mRNA expression as measured by real-time PCR. However, TNFα increased MMP-9 activity, MMP-9 transcription, and MMP-9 mRNA expression ($P<0.05$).

Phosphoprotein phosphatase inhibition and β-adrenoceptor stimulation: Okadaic acid inhibited PP2A activity in NIH3T3 cells by 70% compared to control ($P<0.05$). Furthermore, it did not cell viability at any concentration studied (OA 100 nM vs. control: 88.13±2.50 vs. 100±3.69%) as measured by a MTT-assay. Okadaic acid increased MMP-9 activity in a dose-dependent manner in NIH3T3 fibroblasts (40 nM OA vs. control: 137.9±3.39 vs. 100±6.54%; $P<0.05$) and hepatic stellate cells (LX-2; 40 nM: OA vs. control: 2.83±0.40 vs. 1.0±0.16 AU; $P<0.05$). Okadaic acid (40 nM) also increased MMP-9 mRNA expression in HCVF cells by 2 fold (OA vs. control: 3.4±0.56 vs. 1±0.0 5 AU; $P<0.05$). In NIH3T3 fibroblasts SB202190 (5 μM), a p38 MAPK inhibitor prevented okadaic acid (40 nM) induced MMP-9 expression (OA vs. OA/SB 202190: 43.31±6.51 vs. 14.77±3.68%; $P<0.05$), while a MEK1/2 inhibitor (U0126, 5 μM) had no effect (OA vs. OA/U0126: 35.80±6.34 vs. 36.45±8.50%). Okadaic acid (40 nM) did not alter p38 MAPK and ERK1/2 MAPK activation over a 7.5 min period. However, it decreased phospho-ERK1/2 MAPK by 70% in HCVF cells after 30 min ($P<0.05$). Surprisingly, isoprenaline (1 μM) abolished okadaic induced MMP-activity and expression in NIH3T3 fibroblasts ($P<0.05$), and MMP-9 mRNA expression in HCVF cells ($P<0.05$). Knockdown of β-arrestin 2 by transient transfection with siRNA specific for murine β-arrestin 2 abolished the inhibitory effects of isoprenaline on okadaic acid induced MMP-9 activity, while okadaic acid induced MMP-9 activity was unaffected ($P<0.05$). Isoprenaline mediated activation of p38 MAPK and ERK1/2 MAPK was unaltered by okadaic acid. Although isoprenaline transiently induced PP2A activity over a 30 min period ($P<0.05$), it did not alter okadaic acid mediated PP2A inhibition after 24 hrs (OA vs. OA/ISO: 26.8±3.36 vs. 20.3±0.20%). Transient transfection of NIH3T3 cells with MMP-9 promoter constructs

containing targeted mutation of the AP-1 and NFκB consensus motifs revealed that okadaic acid requires the distal (-533 bp) and the proximal (-79 bp) AP-1 binding sites, but not the NFκB (-600 bp) binding site for induction of MMP-9 promoter activity. Isoprenaline and okadaic acid did not alter NFκB promoter activity in NIH3T3 fibroblasts. Pre-treatment with a NFκB inhibitor (1 μM) did not alter okadaic acid induced MMP-9 expression in NIH3T3 fibroblasts. However, when the NFκB binding site of the MMP-9 promoter was mutated ($P<0.05$) isoprenaline did not prevent okadaic acid induced MMP-9 promoter activity.

Effects of adrenoceptor blockade on TNFα modulated MMP-9 and TIMP-1: Recombinant murine TNFα (100 ng/ml) increased MMP-9 activity (TNFα vs. control: 100.0±3.97 vs. 21.1±2.97%; $P<0.05$), MMP-9 expression (TNFα vs. control: 32.69±1.92 vs. 8.00±1.01 ng/ml; $P<0.05$) and MMP-9 promoter activity after 24 hrs in NIH3T3 fibroblasts. Prazosin (PRAZ; 10 μM), and carvedilol (CARV; 10 μM) inhibited TNFα induced MMP-9 activity, expression and promoter activity (TNFα/PRAZ vs. TNFα/DMSO: 23.90±0.82 vs. 33.95±2.23 ng/ml; $P<0.05$). However, propranolol (PROP; 10 μM), ICI 118,551 (ICI; 10 μM), atenolol (ATENO; 10 μM), or DMSO (0.4% v/v) did not alter TNFα induced MMP-9 (TNFα/ICI vs. TNFα: 31.42±2.48 vs. 28.18±3.55 ng/ml). Using 5'-end deletion mutants of the MMP-9 promoter (-1285/+20), it was established that the cis-acting elements upstream of -571 bp are required for TNFα activation of MMP-9. TNFα increased NFκB promoter activity by 30 fold. Interestingly, this was attenuated by pre-treatment with prazosin (10 μM), carvedilol (10 μM), propranolol (10 μM), and ICI 118,551 (10 μM) in NIH3T3 fibroblasts (TNFα/PROP vs. TNFα: 17.01±2.74 vs. 29.39±3.93; $P<0.05$). Transient transfection of NIH3T3 cells with mutated MMP-9 promoter constructs revealed that TNFα requires the distal AP-1 (-533 bp) and the NFκB (-600 bp) binding sites, for induction of MMP-9 promoter activity. Prazosin did not prevent

TNFα induced MMP-9 promoter activity when the proximal AP-1 (-79) binding site was mutated (TNFα/PRAZ vs. TNFα/DMSO: 2.02±0.20 vs. 2.08±0.20).

TNFα increased TIMP-1 expression by ~10 ng/ml in conditioned medium of NIH3T3 cells (TNFα vs. control: 9.64±1.17 vs. 0.0±1.08 ng/ml; $P<0.05$). Carvedilol and ICI 118,551 reduced basal TIMP-1 expression compared to control by 5 ng/ml and 4 ng/ml, respectively ($P<0.05$). Pre-treatment with carvedilol and ICI 118,551 prevented TNFα induced TIMP-1 expression ($P<0.05$), while prazosin, propranolol and atenolol had no effect. Surprisingly, TNFα decreased TIMP-$1_{(-1718/+988)}$-luc and TIMP-$1_{(-738/+96)}$-luc promoter activity by 50%. Carvedilol reduced basal TIMP-$1_{(-1718/+988)}$-luc promoter activity by 50% ($P<0.05$), but did not alter basal TIMP-$1_{(-738/+96)}$-luc promoter activity. Prazosin, propranolol, ICI 118,551, and atenolol did not alter TIMP-1 promoter activity.

Contents

Page

Declaration

Summary Methods and Results

Acknowledgments I

Publications and Presentations II

Abbreviations III

List of Figures VI

List of Tables X

Chapter 1. Introduction

1.1 G-protein coupled receptors 1

1.1.1 History and structure of G-protein coupled receptors (GPCR) 1

1.1.1.1 G-proteins 2

1.1.1.2 Standard model of GPCR signalling 4

1.2 Adrenoceptors 7

1.2.1 Classification of adrenoceptors 7

1.2.2 Structure of adrenoceptors 9

1.2.3 Adrenoceptor mediated signalling 10

1.2.3.1 α_1-Adrenoceptor signalling – Role in smooth muscle contraction 10

1.2.3.2 α_2-Adrenoceptor signalling 11

1.2.3.3 β-Adrenoceptor signalling 12

1.2.4 Arrestins and adrenoceptor signalling 15

1.2.5 Physiological role of adrenoceptors 18

1.2.6 Adrenoceptors in disease 20

1.2.7 β-Adrenoceptor antagonists 21

1.3 Fibroblasts 23

1.3.1 Fibroblasts and tissue remodelling 23

1.3.2 Collagens 25

1.4 Regulation of the extracellular matrix 28

1.4.1 The physiological function of the extracellular matrix....28
1.4.2 Classification of matrix metalloproteinases (MMPs)....28
1.4.3 Structure of MMPs....32
1.4.4 Regulation of MMP activity....35
1.4.4.1 Transcriptional regulation....36
1.4.4.1.1 The MMP-9 promoter....37
1.4.4.2 Post-transcriptional regulation of MMPs....39
1.4.4.3 Regulation of MMP activity....41
1.4.5 MMPs in health and disease....42
1.5 Adrenoceptors and MMPs....45
1.6 Protein phosphatases and adrenoceptor regulation....46
1.7 Overview of the Pharmacological reagents used as part of this thesis....50
1.8 Aims....52

Chapter 2. Materials

2.1 Materials....55
2.2 Consumables....56
2.3 Enzymes....57
2.4 Prokaryotic cells....57
2.5 Eukaryotic cells....58
2.6 Antibodies....59
2.7 DNA and RNA....60
2.7.1 Oligonucleotides....60
2.7.1.1 PCR primers....60
2.7.1.2 Real-time RT-PCR primers....61
2.7.1.3 siRNA....61
2.7.2 Vectors and eukaryotic expression vectors....62
2.8 Equipment....63

Chapter 3. Characterisation of adrenoceptor signalling in human and murine fibroblasts: Implications for MMP-9 Regulation

3.1 Introduction....67
3.2 Methods....70
3.2.1 Generation of the MM-9 promoter constructs....70
3.2.2 Cell culture....74

3.2.3 Preparation of pharmacological reagents 74
3.2.4 Measurement of cAMP levels 75
3.2.5 Assessment of cell viability (MTT-assay) 75
3.2.6 Gelatin-zymography 76
3.2.7 Real-time RT-PCR 77
3.2.7.1 RNA isolation and RT-PCR 77
3.2.7.2 Real-time RT-PCR 78
3.2.8 Transient transfection and Dual-Luciferase reporter assay 80
3.2.9 CREB activation assay using High-content analysis (HCA) 81
3.2.10 Western blot analysis 81
3.2.11 Validation of the cloning and Real-time RT-PCR methodology 83
3.2.11.1 Validation of the MMP-9 promoter constructs 83
3.2.11.2 Validation of mRNA quality and Real-time RT-PCR cycling efficiency 89
3.2.12 Data and statistical analysis 92
3.3 Results 93
3.3.1 Effect of adrenoceptor stimulation on cell viability 93
3.3.2 Effect of β-adrenoceptor stimulation on intracellular cAMP levels in fibroblasts 93
3.3.3 Effect of adrenoceptor stimulation on phospho-CREB translocation 94
3.3.4 Effect of adrenoceptor stimulation on ERK1/2 and p38 MAPK phosphorylation 94
3.3.5 Effect of adrenoceptor stimulation on NFκB promoter activity 95
3.3.6 Regulation of NFκB and IκBα signal transduction 96
3.3.7 Effect of adrenoceptor stimulation on MMP-9 activity 96
3.3.8 Effect of adrenoceptor stimulation on MMP-9 promoter activity and mRNA expression 97
3.4 Discussion 110

Chapter 4. Okadaic acid Induces MMP-9 Expression in Fibroblast: Crosstalk between Protein Phosphatase Inhibition and β-Adrenoceptor Signalling

4.1 Introduction 117
4.2 Methods 119
4.2.1 Cell culture 119
4.2.2 Determination of MMP-9 expression and activity 119

4.2.3 Cell viability (MTT-assay) 120
4.2.4 Quantitative Real-time RT-PCR 120
4.2.5 Knockdown of β-arrestin 2 by siRNA 121
4.2.6 Determination of protein concentration (Bradford-assay) 121
4.2.7 PP2A activity assay 122
4.2.8 Mutation of the NFκB and AP-1 binding sites in the MMP-9 promoter construct 123
4.2.9 Western blot analysis 127
4.2.10 Data and statistical analysis 127
4.3 Results 129
4.3.1 Effects of okadaic acid on cell viability and MMP-9 activity 129
4.3.2 Effect of isoprenaline on okadaic acid induced MMP-9 abundance 129
4.3.3 The effect of β-arrestin 2 knockdown in NIH3T3 cells 130
4.3.4 Effect of okadaic acid and isoprenaline on PP2A activity 130
4.3.5 Effects of okadaic acid and isoprenaline on p38 and ERK1/2 MAPK signalling pathways 131
4.3.6 Assessment of the role of AP-1 and NFκB transcription factor binding sites on MMP-9 promoter activity 132
4.3.7 Effects of okadaic acid and isoprenaline on NFκB and IκBα 133
4.4 Discussion 145

Chapter 5. Adrenoceptor antagonists differentially regulate TNFα-induced MMP-9 and TIMP-1 expression in NIH3T3 fibroblasts

5.1 Introduction 153
5.2 Methods 155
5.2.1 Cell culture 155
5.2.2 Drug treatment of NIH3T3 fibroblasts 155
5.2.3 Gelatin-zymography 155
5.2.4 Determination of MMP-9 and TIMP-1 protein expression 156
5.2.5 Transient transfection and Dual-Luciferase reporter assay 156
5.2.6 Data and statistical analysis 157
5.3 Results 158
5.3.1 The effects of TNFα and adrenoceptor antagonists on MMP-9 activity and expression 158

5.3.2 Effect of 5'-end cis elements on TNFα modulated MMP-9 promoter activity..... 159
5.3.3 Effects of TNFα and adrenoceptor antagonists on NFκB promoter activity.. 160
5.3.4 Effects of TNFα and adrenoceptor antagonism on MMP-9 promoter activity..... 161
5.3.5 Effects of TNFα and adrenoceptor antagonists on TIMP-1 expression 162
5.3.6 Effects of TNFα and adrenoceptor antagonists on TIMP-1 promoter activity..... 163
5.4 Discussion 174

Chapter 6. Conclusions

6.1 Conclusions 183

Chapter 7. Appendix

7.1 MMP-9 promoter insert sequences aligned to NCBI Accession NT_011362.10. 189
7.2 Predicted transcription factor binding site of the MMP-9 promoter mutants 193
7.3 MMP-9 promoter mutant sequences aligned to wild type MMP-9 promoter construct 197

Chapter 8. Reference list

Acknowledgments

I am deeply appreciative of my supervisor Dr. Paul Spiers for the opportunity to undertake this work. I am very thankful for his great support, his good humour, the stimulating discussions, the encouragement, the trust, and the patience with me throughout this study. I further thank him for being very understanding and helpful throughout my difficulties with my father's illness.

I am also especially grateful to Dr. Pierce Kavanagh and Mr. Ken Scott for their very kind patience help, support, good humour and open ears throughout my time in the Department of Pharmacology & Therapeutics. Likewise, I am very thankfully to Dr. Steffi Gieseler and Jenny Svärd, for their patience and encouraging discussions. I am very delighted to have the opportunity to become friends with these people, who also helped me through a very difficult time in my life. Furthermore, I wish to thank Omar AlSharef, Alan Kennedy, and Mrs. Una Doyle for the encouraging time in the Department, and all the other staff of the Department of Pharmacology & Therapeutics.

I am grateful for the inspiring discussions with Dr. Martina Hennessy, Dr. Anthony Davies, and Prof. Yuri Volkov. Furthermore, I am obliged to Dr. Steven Smith, Dr. Anthony Davies, and Dr. Aiden Corvin for access to specialised equipment.

I am very thankful to Mandy Riedel and Maika Holzapfel who supported and encouraged me all the time.

Finally, my deepest gratitude goes to my lovely parents, who gave me the freedom, the possibility, and the support in anything, and who further listened to me so patiently, whether they understood or not. I deeply appreciate the encouragement of my parents that I shall persist, although I could not be there to help them through my father illness (amyotrophic lateral sclerosis). I therefore would like to dedicate this thesis to my parents.

The Health Research Board (project grant (RP/2006/51) for funding this PhD studentship.

Publications and Presentations

Full papers

Rietz A, Volkov Y, Hennessy M, Davies A & Spiers JP. Characterisation of β-adrenoceptor signalling in human and murine fibroblasts: Implications for MMP-9 Regulation. *In preparation*

Rietz A, Volkov Y, Hennessy M, Davies A, & Spiers JP. Okadaic acid Induces MMP-9 Expression in Fibroblast: Linking Protein Phosphatase Inhibition and β-Adrenergic Signalling. *submitted*

Rietz A, Volkov Y, Hennessy M, Davies A, & Spiers JP. Adrenoceptor antagonists differentially regulate TNFα-induced MMP-9 and TIMP-1 expression in NIH3T3 fibroblasts. *submitted*

Abstracts:

Oral:

Rietz A, Davies A, Hennessy M, Volkov Y, & Spiers JP. Adrenoceptor modulation of matrix metalloproteinase-9 (MMP-9) activity and promoter activity in murine fibroblasts (NIH3T3): Not all that it seems! *British Pharmacological Society*, BPS Winter Meeting, Brighton, December 2008

Poster presentations:
Rietz A, Davies A, Hennessy M, Volkov Y, & Spiers JP. Adrenoceptor modulation of matrix metalloproteinase-9 (MMP-9) activity and promoter activity in murine fibroblasts (NIH3T3): Not all that it seems! 2nd School of Medicine Postgraduate Research Day; Trinity College Dublin, 2008

Rietz A, Hennessy M, Davies A, Volkov Y, & Spiers JP. Adrenoceptor agonists do not alter matrix metalloproteinase-9 (MMP-9) activity and promoter activity in murine fibroblasts (NIH3T3): Lack of involvement of NFκB. *European Journal of Heart Failure Supplements*. 2009; **8**:A1270, Heart failure Congress. Nice, France, 2009

Rietz A, Hennessy M, Davies A, Volkov Y, & Spiers JP. Combined blockade of α1 and β-adrenoceptors is essential for inhibition of TNFα-induced MMP-9 expression and activity in NIH3T3 fibroblasts. 11th Annual Meeting of the Institute of Molecular Medicine, Trinity College Dublin, 2009

Rietz A, Hennessy M, Davies A, Volkov Y, & Spiers JP. Combined blockade of α_1 and β-adrenoceptors is essential for inhibition of TNFα-induced MMP-9 expression and activity in NIH3T3 fibroblasts. *Proceedings of the British Pharmacological Society,* BPS Winter Meeting, London, December 2009

Rietz A, Hennessy M, Davies A, Volkov Y, & Spiers JP. β-adrenergic stimulation inhibits okadaic acid-induced MMP-9 response in fibroblasts: A novel regulatory mechanism. XX World Congress of the International Society for Heart Research. Kyoto, Japan, 2010

Prizes/Awards:
International Society for Heart Research Travel Award (European Section); Heart failure Congress. Nice, France, 2009
International Society for Heart Research Travel Award (ISHR International); XX World Congress of the International Society for Heart Research. Kyoto, Japan, 2010

Abbreviations

AU	Arbitrary Unit
ATENO	Atenolol
bp	base pair(s)
BHI	Brain heart infusion
BSA	Bovine serum albumin
cAMP	Cyclic adenosine monophosphate
CARV	Carvedilol
cDNA	Copy deoxyribonucleic acid
C_{final}	final concentration
cfu	colony forming units
CIP	Calf Intestinal Alkaline Phosphatase
CREB	cAMP response element binding protein
DAG	Diacylglycerol
dH_2O	Distilled water
DMSO	Dimethylsulphoxide
DNA	Deoxyribonucleic acid
DNase	Deoxyribonuclease
dNTP	Deoxynucleotide triphosphate
E.coli	*Escherichia coli*
EDTA	Ethylene diamine tetraacetic acid
ELISA	Enzyme-linked immuno-sorbant assay
ERK 1/2	Extracellular signal-regulated kinase 1/2
FBS	Foetal bovine serum
GAPDH	Glyceraldehyde-3-phosphate dehydrogenase
HCVF	Human cardiac ventricular fibroblasts

HRP	Horseradish peroxidase
ICI	ICI 118,551
IgG	Immunoglobulin G
IκBα	Nuclear factor kappa-light-chain-enhancer of activated B cells inhibitor, alpha
IL	Interleukin
IP_3	Inositol-1,4,5,-triphosphate
IPTG	Isopropyl β-D-1-thiogalactopyranoside
ISO	Isoprenaline
kb	Kilo base pairs
kDa	Kilodaton
LB	Luria Broth
LPS	Lipopolysaccharide
M	mol/l
MAPK	mitogen-activated protein kinase
MMP-2	Matrix metalloproteinase-2
MMP-9	Matrix metalloproteinase-9
mRNA	Messenger Ribonucleic Acid
NCS	Newborn calf serum
NFκB	Nuclear factor kappa-light-chain-enhancer of activated B cells
OA	Okadaic acid
PAGE	Polyacrylamide gel electrophoresis
PBS	Phosphate-buffered saline
PCR	Polymerase chain reaction
PE	Phenylephrine

PKA	Protein kinase A
PKC	Protein kinase C
PLC	Phospholipase C
PMA	Phorbol-12-myristate-13-acetate
PRAZ	Prazosin
PROP	Propranolol
RNA	Ribonucleic acid
RT-PCR	Reverse transcription-polymerase chain reaction
SDS	Sodium dodecyl sulphate
SEM	Standard error of the mean
siRNA	Small interfering RNA
TAE	Tris-acetate-EDTA buffer
Taq-Polymerase	*Thermus aquaticus* DNA polymerase
TE	Tris-EDTA buffer
TNFα	Tumour necrosis factor α
Tris	Tris(hydroxymethyl)aminomethane
U	Unit
UV	Ultraviolet
v/v	volume/volume
w/v	weight/volume
X-Gal	5-Bromo-4-chloro-3-indolyl-β-D-galactopyranoside

List of Figures

Figure 1.1 The G-protein coupled receptor. 3

Figure 1.2 Schematic representation of G-protein mediated receptor signalling. 6

Figure 1.3 Classification of adrenoceptors. 9

Figure 1.4 A schematic representation of possible signal transduction pathways linking α_1-adrenoceptors to myocyte contraction. 11

Figure 1.5 A simplified model depicting β_1- and β_2-adrenoceptor signalling pathways in the human myocardium 14

Figure 1.6 Schematic model of β_2-adrenoceptor signalling and the role of arrestin 17

Figure 1.7 Role of α-adrenoceptors in the murine cardiovascular system 19

Figure 1.8 A schematic representation of "The vicious cycle in heart failure." 21

Figure 1.9 Origin of myofibroblasts. 25

Figure 1.10 Domain structure of the major MMP classes. 30

Figure 1.11 A ribbon model depicting the structure of the human proMMP-9. 34

Figure 1.12 Regulation of MMPs. 35

Figure 1.13 Schematic representation of transcription factor binding sites in the human MMP-9 promoter. 39

Figure 1.14 Activation of proMMPs. 40

Figure 1.15 A schematic representation of the temporal expression pattern for MMPs and TIMP in the liver following a chronic toxic insult 45

Figure 1.16 Regulation of the β-adrenoceptor signalling pathway by protein phosphatases. 49

Figure 1.17 Overview of the physiological actions of drugs targeting adrenoceptors. 51

Figure 3.1 A representative agarose gel (1% w/v) of the MMP-9 promoter inserts generated by PCR. 85

Figure 3.2 A representative mini gel (1% w/v agarose) showing the banding pattern of the MMP-9 pGEM®-T Easy vectors following digestion with *Hind*III/*Xho*I..... 85

Figure 3.3 Analysis of insertion and orientation of MMP-9 inserts in the pGL-3 Basic plasmids. 88

Figure 3.4 Assessment of the integrity of the RNA samples isolated using TRI reagent. .. 90

Figure 3.5 PCR amplification efficiency for mouse MMP-9 and β-actin primers using mouse control cDNA. 90

Figure 3.6 A representative melting curve analysis for mouse β-actin. 91

Figure 3.7 Effect of adrenoceptor stimulation on the cell viability in NIH3T3 fibroblasts. 99

Figure 3.8 Effect of β-adrenoceptor stimulation on cAMP production in (A) mouse (NIH3T3) and (B) human ventricular cardiac fibroblasts (HCVF). 100

Figure 3.9 Effect of adrenoceptor stimulation on phospho-CREB translocation in NIH3T3 cells. 101

Figure 3.10 Temporal effects of adrenoceptor stimulation on phosphorylation of ERK1/2 and p38 MAPK in NIH3T3. 102

Figure 3.11 Effect of adrenoceptor stimulation and blockade on phospho-ERK1/2 MAPK in HCVF cells. 103

Figure 3.12 Effect of adrenoceptor stimulation on NFκB promoter activity in NIH3T3 cells. 104

Figure 3.13 Temporal effects of isoprenaline and phenylephrine on NFκB phosphorylation and IκBα expression in NIH3T3 cells. 105

Figure 3.14 Temporal effects of isoprenaline and phenylephrine on NFκB phosphorylation and IκBα expression in HCVF cells. 106

Figure 3.15 Effect of adrenoceptor stimulation on MMP-9 activity in NIH3T3 fibroblasts. 107

Figure 3.16 Effect of adrenoceptor stimulation on MMP-9 promoter activity in NIH3T3 fibroblasts. 108

Figure 3.17 Effect of adrenoceptor stimulation on MMP-9 mRNA expression in (A) NIH3T3 and (B) HCVF fibroblasts. 109

Figure 4.1 Schematic representation illustrating known transcription factor binding sites, and the location of the mutated AP-1 and NFκB binding sites on the p1285-luc MMP-9 promoter. 124

Figure 4.2 Characterisation of the pGL-3 Basic plasmids containing the mutated MMP-9 inserts by restriction enzyme digestion. 125

Figure 4.3 Effects of okadaic acid on cell viability and MMP-9 gelatinase activity in NIH3T3 fibroblasts and LX-2 cells. 135

Figure 4.4 Effect of okadaic acid (OA; 40 nM) and isoprenaline (ISO; 1.0 μM), alone and in combination, on MMP-9 abundance in conditioned medium from NIH3T3 fibroblasts. 136

Figure 4.5 Effect of okadaic acid (OA; 40 nM) and isoprenaline (ISO; 1.0 μM), alone or in combination, on mRNA expression in HVCFs. 137

Figure 4.6 The effect of β-arrestin 2 knockdown on MMP-9 activity in NIH3T3 cells. ... 138

Figure 4.7 Effect of okadaic acid and isoprenaline on PP2A activity in NIH3T3 fibroblasts. 139

Figure 4.8 Effect of SB202190 and U0126 on okadaic acid induced MMP-9 expression. 140

Figure 4.9 Effects of okadaic acid, isoprenaline alone and in combination on phospho-p38 and phospho-ERK1/2 levels in NIH3T3 and HCVF cells. 141

Figure 4.10 Effect of mutation of the AP-1 and NFκB transcription factor binding sites on MMP-9 promoter activity following exposure to okadaic acid and isoprenaline. 142

Figure 4.11 Early effects of okadaic acid and isoprenaline on NFκB and IκBα signalling. 143

Figure 4.12 Late effects of okadaic acid and isoprenaline on NFκB and IκBα signalling. 144

Figure 4.13 Schematic diagram presenting the key findings in NIH3T3 fibroblasts. 150

Figure 5.1 Effect of α_1- and β-adrenoceptor antagonists on basal or TNFα stimulated gelatinase activity in conditioned medium from NIH3T3 cells. 164

Figure 5.2 Effect of α_1- and β-adrenoceptor antagonists on basal or TNFα stimulated MMP-9 protein expression in conditioned medium from NIH3T3 cells..... 165

Figure 5.3 Schematic representation illustrating the position of the cis acting elements in the 5'-end deletion mutants of the MMP-9 promoter..... 166

Figure 5.4 Effect of TNFα on promoter activity of the 5'-end deletion mutants of the MMP-9 promoter. 167

Figure 5.5 Effect of adrenoceptor antagonism on TNFα-induced NFκB promoter activity. 168

Figure 5.6 Effect of adrenoceptor antagonists on TNFα-mediated MMP-9 promoter activity in NIH3T3 cells transfected with p1285-luc..... 169

Figure 5.7 Effect of mutation of the AP-1 and NFκB transcription factor binding sites on TNFα-mediated MMP-9 promoter activity in NIH3T3 fibroblasts. 170

Figure 5.8 Effect of TNFα and adrenoceptor antagonists on TIMP-1 expression in NIH3T3 fibroblasts..... 171

Figure 5.9 Schematic representation detailing the major transcription factors binding sites present in the TIMP-1 luciferase promoter constructs..... 172

Figure 5.10 Effect of TNFα and adrenoceptor antagonism on TIMP-1 promoter activity. 173

List of Tables

Table 1.1 Classification and substrate specificity of the major MMPs. 31

Table 2.1 Pharmacological reagents, recombinant proteins, and materials. 55

Table 2.2 Consumables. 56

Table 2.3 A list of enzymes and their suppliers used. 57

Table 2.4 A list of antibodies, their source, conjugation, dilution and suppliers. 59

Table 2.5 Primers for MMP-9 promoter constructs. 60

Table 2.6 QuantiTec Primers for real-time RT-PCR. 61

Table 2.7 A list of vectors, their properties, and suppliers used. 62

Table 2.8 A list of equipment and supplier. 63

Table 3.1 Primers for MMP-9 promoter constructs. 71

Table 3.2 PCR-program for the desired MMP-9 promoter constructs. 71

Table 3.3 Composition of the resolving and stacking gels used for gelatin-zymography. ..77

Table 3.4 Real-time theromcycler conditions 80

Table 3.5 Composition of the resolving and stacking gels used in western blot analysis. ..83

Table 3.6 Alignment of the MMP-9 promoter sequence from the p1285-pGEM®-T Easy plasmid to that of NCBI Accession NT_011362.10. 86

Table 4.1 A summary table showing sequence around the NFκB and AP-1 binding sites of the wild type and mutated MMP-9 promoters. 126

Table 7.1 Alignment of the MMP-9 promoter sequence from the p657-pGEM®-T Easy plasmid to that of NCBI Accession NT_011362.10. 189

Table 7.2 Alignment of the MMP-9 promoter sequence from the p571-pGEM®-T Easy plasmid to that of NCBI Accession NT_011362.10. 190

Table 7.3 Alignment of the MMP-9 promoter sequence from the p540-pGEM®-T Easy plasmid to that of NCBI Accession NT_011362.10. 191

Table 7.4 Alignment of the MMP-9 promoter sequence inserted into a p523-pGEM®-T Easy plasmid to that of NCBI Accession NT_011362.10. 192

Table 7.5 Predicted transcription factor binding sites of a p1285-luc sequence part (50 bp) containing the NFκB-binding site. 193

Table 7.6 Predicted transcription factor binding sites of a p1285-luc sequence part (50 bp) containing the mutated NFκB-binding site. 193

Table 7.7 Predicted transcription factor binding sites of a p1285-luc sequence part (50 bp) containing the AP-$1_{(-533)}$ binding site. 194

Table 7.8 Predicted transcription factor binding sites of a p1285-luc sequence part (50 bp) containing mutated AP-$1_{(-533)}$ binding site. 194

Table 7.9 Predicted transcription factor binding sites of a p1285-luc sequence part (50 bp) containing the AP-$1_{(-79)}$ binding site. 195

Table 7.10 Predicted transcription factor binding sites of a p1285-luc sequence part (50 bp) containing the mutated AP-$1_{(-79)}$ binding site. 196

Table 7.11 Alignment of obtained sequence for p1285-luc NFκ$B_{(-600)}$ against p1285-luc using BLAST. 197

Table 7.12 Alignment of obtained sequence for p1285-luc AP-$1_{(-533)}$ against p1285-luc using BLAST. 199

Table 7.13 Alignment of obtained sequence for p1285-luc AP-$1_{(-79)}$ against p1285-luc using BLAST. 201

Anyone who has never made a mistake has never tried anything new.

Albert Einstein

For my parents

Curiosity is the key to problem solving.

Galileo Galilei

Chapter 1.

Introduction

1.1 G-protein coupled receptors

1.1.1 History and structure of G-protein coupled receptors (GPCR)

G-protein coupled receptors (GPCRs) are one of the largest (approx. 800) and most diverse protein groups encoded by the genome[1]. Based upon evolutionary similarity the human GPCRs are classified into five main groups: rhodopsin, secretin, glutamate, adhesion and frizzled receptor groups[2]. Within this grouping, the rhodopsin family is the largest with 672 family members[1]. Historically, Ehrlich first described the binding of biological active molecules to specific sites in cells[3]. However, Langley and Dale used classical physiological and pharmacological experiments to investigate the responses of mammalian extracts, and put forward the idea of a "receptive substance"[3]. This developed into the classical receptor theory of dose-response data, kinetics, affinity, and efficacy in drug actions[3]. Our understanding of receptor function was extended by the discovery of key signal-transduction molecules such as, cAMP, adenylyl cyclase, protein kinase A (PKA) and G-proteins[3-5]. These facilitate amplification of the ligand-receptor interaction and provide mechanisms for controlling signal transduction.

GPCRs are integral membrane proteins, which are predicted to consist of seven transmembrane-spanning α-helices, and are also known as 7-TM receptors. The N-Terminus (NH_2-) is positioned extracellularly (extracellular domain), the predicted seven α-helices pass through the membrane with varying polypeptide loops (transmembrane domain), and the C-Terminus (COOH-) is located intracellularly. Furthermore, they are predicted to contain three interhelical loops on both sides of the membrane. Besides posttranscriptional modification, most GPCRs are posttranslationally modified through phosphorylation, glycosylation, or palmitoylation. Phosphorylation of GPCR by G-protein coupled receptor kinases (GRK) results in receptor desensitisation, while phosphorylation

by PKA modifies their coupling specificity[6]. Glycosylation of the receptor determines its localisation and modifies function in a receptor subtype specific manner. Likewise, palmitoylation of highly conserved cysteine residues of the C-terminal cytoplasmatic tail is also thought to modulate GPCR function[6]. It is also well documented that acetylation, ubiquitinylation, and myristoylation also modify GPCR function[1].

From a structural perspective GPCR function can be modulated through homo- or hetero-oligomerisation[1]. For example, some GPCRs are unable to bind a ligand or initiate signal transduction as monomers, but become active on forming oligomers (homomeric/heteromeric receptors)[1]. Other GPCRs are biological active as monomers and show new activities on oligomerisation (receptor homomers/heteromers). For example, co-expression of a binding-defective mutant and a signal-defective mutant of the luteinizing hormone receptor rescues receptor functionality in vitro and in vivo[7, 8].

1.1.1.1 G-proteins

The function of a receptor is to transmit an extracellular stimulus across the cell membrane through physical interaction, and elicit an amplified intracellular chemical signal. This is achieved via interaction of the intracellular domain of the receptor with a heterotrimeric G-protein. This in turn activates a variety of effector systems including adenylyl cyclase, and phospholipase Cβ (Figure 1.1). G-proteins belong to the super family of GTPases, which are hydrolase enzymes, owing to their ability to bind and hydrolyze GTP. They may be classified as either monomeric or heterotrimeric. Ras and Rho are monomeric G proteins and are often referred to as small GTPases. The heterotrimeric class of G-proteins consists of three different polypeptide subunits: Gα, Gβ, and Gγ. In man there are 21 Gα subunits encoded by 16 genes, 6 Gβ subunits encoded by 5 genes, and 12 Gγ subunits[9]. Heterotrimeric G-proteins are typically subdivided into four main classes: $G\alpha_s$, $G\alpha_i$, $G\alpha_q$,

and $G\alpha_{12}$ by virtue of their primary sequence similarity to $G\alpha$[10]. The conserved GTPase domain of the $G\alpha$ subunit provides the binding surfaces for the $G\beta\gamma$ dimer, GPCR and the effector proteins[10]. The composition of the heterotrimeric G-protein determines signal transduction with regard to specificity and efficiency of the receptor, and effector interaction. Compared to the size and diversity of the GPCR superfamily, they interact with a relatively small group of G-proteins.

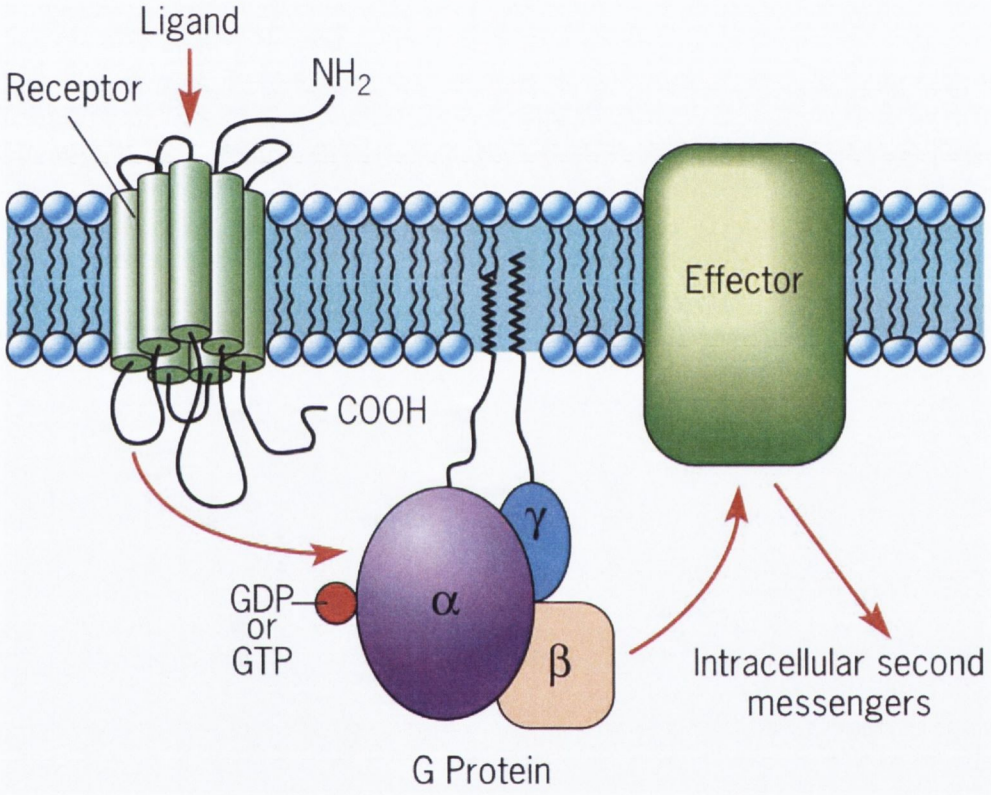


Figure 1.1 The G-protein coupled receptor.

A diagrammatic representation showing the relationship between a G-Protein-coupled receptor (left), the heterotrimeric G-protein with its subunits (middle), and the effector protein (right). Taken from Karp *et al.*, 2005[11].

1.1.1.2 Standard model of GPCR signalling

In the resting state, the Gα-unit forms a stable complex with GDP and Gβγ (Figure 1.2). It is unclear whether this stable complex is associated with the GPCR prior to agonist stimulation (precoupled model), or whether it resides in close proximity to the receptor and undergoes lateral diffusion within the plasma membrane upon receptor activation (collision model)[10]. The former model is supported by the coupling specificity of some G proteins to receptors and the fast intracellular response, however it does not adequately account for the observed signal amplification[10]. Irrespective of the model, ligand binding induces a conformational change in the receptor resulting in binding of the GDP-bound heterotrimeric G-protein to the receptor. This interaction initiates exchange of GDP for GTP on the Gα subunit (Step 1). This in turn causes a conformational change in the Gαβγ complex leading to its release from the GPCR as well as the dissociation of the Gβγ subunit from Gα subunit (Step 2). At this stage, both subunits are able to interact with effector molecules, and initiate a multitude of signal transduction cascades (e.g. cAMP and Ca^{2+} signalling pathways). Intrinsic GTPase activity associated with the Gα subunit hydrolyses GTP to GDP. GTPase-accelerating proteins known as regulators of G-protein signalling (RGS; Step 3) augment GTP hydrolysis. Hydrolysis typically occurs within a few seconds after the Gα complex is bound to the effector. The Gα and Gβγ subunit then reform the stabilised complex and return the system to its initial state (Step 4). The cycle can continue, as the now inactive Gα subunit is able to bind to the ligand-bound GPCR again. However, at this point G-protein receptor kinases (GRKs) can prevent re-activation of the GPCR through phosphorylation of its cytosolic domain. The phosphorylated receptor can bind arrestin preventing re-association of the G-protein and hence receptor desensitisation (Step 5). Binding of arrestin to receptor also initiates recruitment of endocytic machinery, leading to receptor internalisation. Once internalised the ligand dissociates from the ligand-receptor complex and the receptor may be recycled back to the

plasma membrane or targeted for degradation (Step 6)[12]. This process is highly regulated and prevents over-activation of GPCR signalling, which is associated with a number of pathological and disease states ranging from cancer to neurodegenerative disorders. It is also of note that GPCR signalling can also be modulated independently of G-proteins[13].

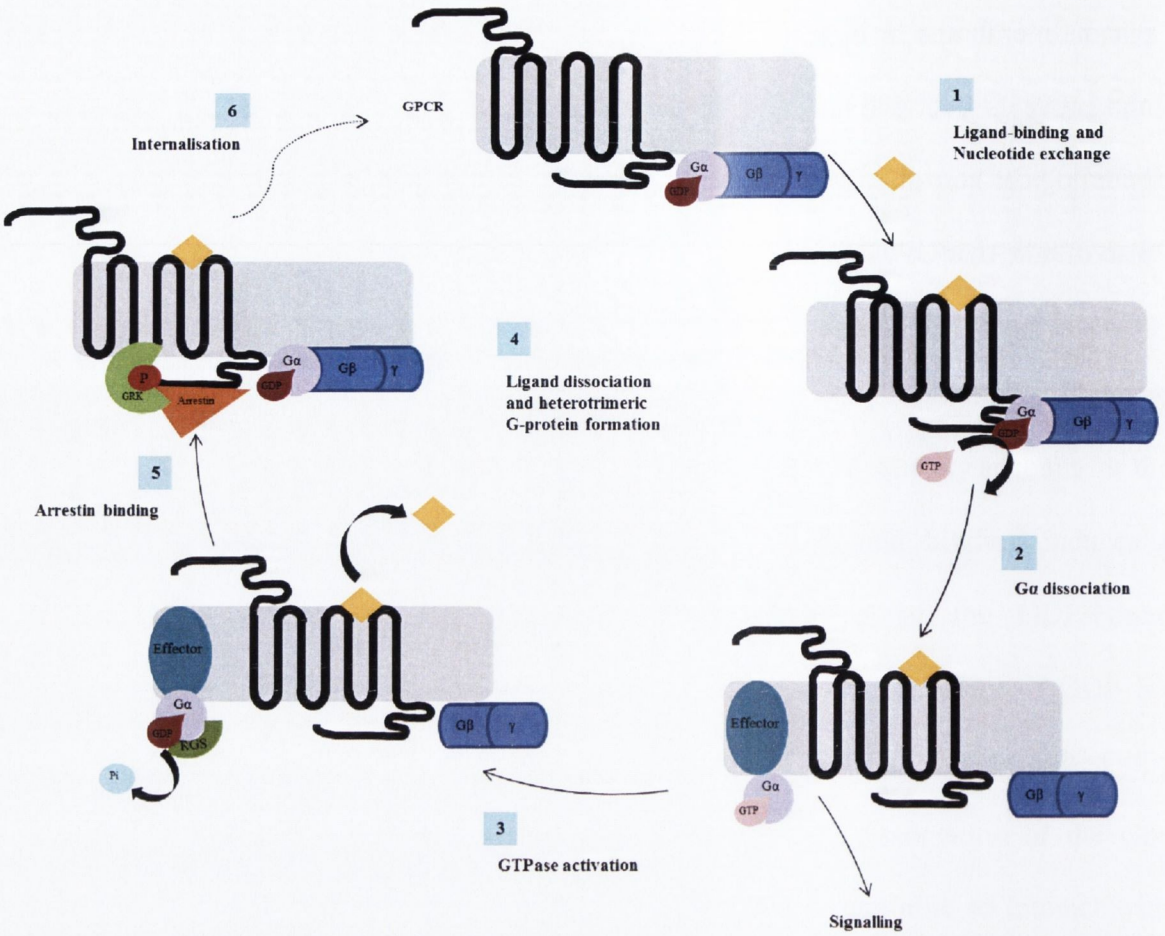


Figure 1.2 Schematic representation of G-protein mediated receptor signalling.

Binding of a ligand (yellow diamond) to a GPCR induces a conformational change in the receptor resulting in binding of a heterotrimeric G-protein and exchange of GDP for GTP (Step 1). Nucleotide exchange induces dissociation of the Gα subunit from the Gβγ subunit and allowing both complexes to interact with effector molecules and initiate signal transduction (Step 2). Intrinsic GTPase activity associated with the Gα subunit hydrolyses GTP to GDP. Hydrolysis is enhanced by RGS (regulator of G-protein signalling; Step 3). Generation of the GDP-bound Gα subunit permits the system to return to its initial state (Step 4). In order to prevent overstimulation of the GPCR, G-protein coupled kinases (GRK) phosphorylate the cytosolic domain of the GPCR leading to binding of arrestin and uncoupling of the heterotrimeric G-protein from the GPCR (Step 5). Binding of arrestin also initiates receptor internalisation. Once internalised the receptor can be either degraded or recycled back to the plasma membrane (Step 6).

1.2 Adrenoceptors

1.2.1 Classification of adrenoceptors

Adrenoceptors belong to the rhodopsin family of GPCRs and are cell surface glycoproteins. They were first classified as α and β-adrenoceptors by Ahlquist in 1948[14], and shown to mediate the effects of sympathetic nerve stimulation. Adrenoceptors are now subdivided into three main groups of α_1, α_2, and β-adrenoceptors based on their pharmacological profile, physiological responses, and tissue location (Figure 1.3). These groupings have been further subdivided (Figure 1.3).

α-Adrenoceptors are subdivided into α_1 and α_2 based upon their anatomical localisation; α_1-adrenoceptors are found post-synaptically, while α_2-adrenoceptors usually occur pre-synaptically. As such, α_1-adrenoceptors modulate effector tissues while α_2-adrenoceptors regulate neurotransmitter release from sympathetic nerve endings. However, α_2-adrenoceptors are also found both pre- and post-junctionally, with pre-junctional receptors being auto-inhibitory. Both α-adrenoceptors subtypes regulate the vascular tone. However, both α_1 and α_2 do not form a homogeneous group. In the past century, several researchers have suggested, based on observed discrepancies in pharmacological and functional pattern that there must be more than one subtype of α_1-adrenoceptor[11, 15, 16]. This was confirmed following cloning of the genes for three distinct α_1-adrenoceptor subtypes (α_{1A}, α_{1B}, α_{1D})[17]. A clear sub-classification based upon tissue distribution/localisation, or functional aspects is difficult. Although, α_{1A}-adrenoceptors are expressed in the human heart and liver, while α_{1B}-adrenoceptors have been found in the rat heart and liver[17]. The α_{1D}-adrenoceptor is clearly expressed in the rat and human aorta. There may be an additional subtype of α_1-adrenoceptor, which has a low affinity binding profile for prazosin. This subtype if often

referred to as an atypical or α_{1L}-adrenoceptor[17]. However, a gene for this receptor subtype remains to be identified and cloned.

α_2-Adrenoceptors receptors are also subdivided into three main groups: $\alpha_{2A/D}$, α_{2B}, and α_{2C}. The α_{2D}-subtype is a rodent specific homolog of the mammalian α_{2A}-adrenoceptor. They have been subdivided based on functional and radio-ligand binding assays. Existence of the individual receptor subtypes has been confirmed through cloning and expression[18].

The β-adrenoceptors are subdivided into three main subclasses: β_1-, β_2-, and β_3-adrenoceptors. Adrenaline and noradrenaline are equipotent at the β_1-Adrenoceptors. Although they are predominantly expressed in the heart they are also found in the kidney and adipocytes[19]. They are generally located in and around the synaptic cleft[20]. The β_2-adrenoceptors are mainly expressed in the smooth muscle (vascular, bronchial, gastrointestinal, and genitor-urinary) and skeletal muscle cells. They are often located remotely from the adrenergic nerve terminals and tend to be activated via circulating adrenaline. This may explain why they have a higher affinity for adrenaline than for noradrenaline[20]. β_2-adrenoceptors are also expressed in the heart, but to a lesser extent than β_1-adrenoceptors; the β_1:β_2-adrenoceptor ratio in the human heart is around 70:30%[21].

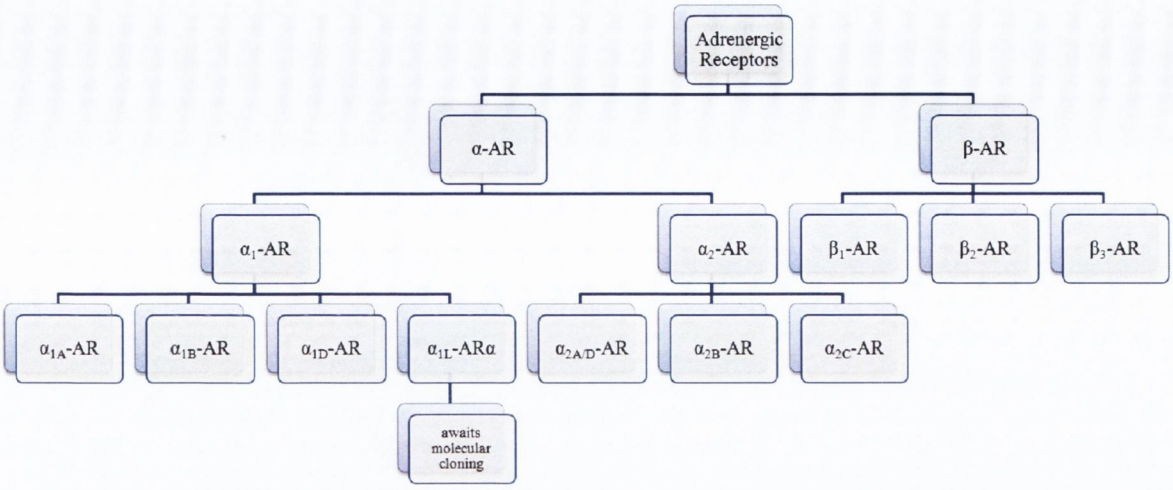


Figure 1.3 Classification of adrenoceptors.

This schema shows the different subtypes of adrenoceptors (AR), identified by pharmacological and molecular cloning approaches.

1.2.2 Structure of adrenoceptors

Adrenoceptors recognize and selectively bind the catecholamines, noradrenaline, and adrenaline. Catecholamines bind to the ligand-binding pocket which resides in the hydrophobic trans-membrane domain of the receptors[22]. Protein sequencing indicates that α- and β-adrenoceptors share approximately 30-40% amino acid homology. Within the α_1- and α_2-adrenoceptor subtypes, there is approximately 75% identity with regard to their amino acid sequences in the transmembrane domain. β-Adrenoceptors share approximately 60% amino acid sequence identity within their transmembrane domain. Interestingly, β_1- and β_2-adrenoceptors are more similar to each other than to β_3-adrenoceptor. Indeed, the human β_1-and β_2-adrenoceptors are 67% identical in their transmembrane domains, and the residues surrounding the ligand-binding pocket appear to be identical. However, two residues close to the ligand-binding pocket, which are different in human β_1-and β_2-adrenoceptor, appear to be responsible for ligand selectivity[23-25]. Data from the crystal

structures reveal that GPCRs have an open ligand-binding pocket[23-25]. Furthermore, the β_1-adrenoceptor has a unique helix within the cytoplasmatic loop 2 of the transmembrane domain that is essential for receptor activation[23, 25].

1.2.3 Adrenoceptor mediated signalling

1.2.3.1 α_1-Adrenoceptor signalling – Role in smooth muscle contraction

Upon α_1-adrenoceptor stimulation, members of the $G\alpha_{q/11}$-family of G-proteins are released from their heterotrimeric complex and activate the β isoform of phospholipase C (PLCβ). Activated PLCβ then hydrolyses membrane-bound polyphosphoinositides, resulting in the generation of two second messengers, diacylglycerol (DAG) and inositol-1,4,5-triphosphate (IP_3). IP_3 binds to IP_3 receptors on intracellular organelles such as the sarcoplasmic reticulum (SR) which release stored Ca^{2+} (Figure 1.4)[26]. DAG interacts and enhances the affinity of protein kinase C (PKC) for Ca^{2+}, and initiates its translocation to the plasma membrane. PKC is only activated in the presence of Ca^{2+}, DAG and phosphatidylserine[27]. Once activated PKC phosphorylates numerous substrates including membrane proteins such as ion channels, pumps and ion-exchange proteins, many of which are associated with regulation of intracellular Ca^{2+} concentrations and facilitate entry of extracellular Ca^{2+}[17]. Ultimately, the increase in cytosolic Ca^{2+} leads to a contraction of most smooth muscle cells through stimulation of myosin light chain kinase (MLCK) and inhibition of myosin light chain phosphatase (MLCP, Figure 1.4). α_1-Adrenoceptor activation can also activate phospholipase A2, leading to release of arachidonic acid and cAMP production[28]. In the rat heart, the positive inotropic effects of α_1-adrenoceptor stimulation are coupled to $G\alpha_s$ and results in cAMP production and inhibition of the K^+-efflux[29].

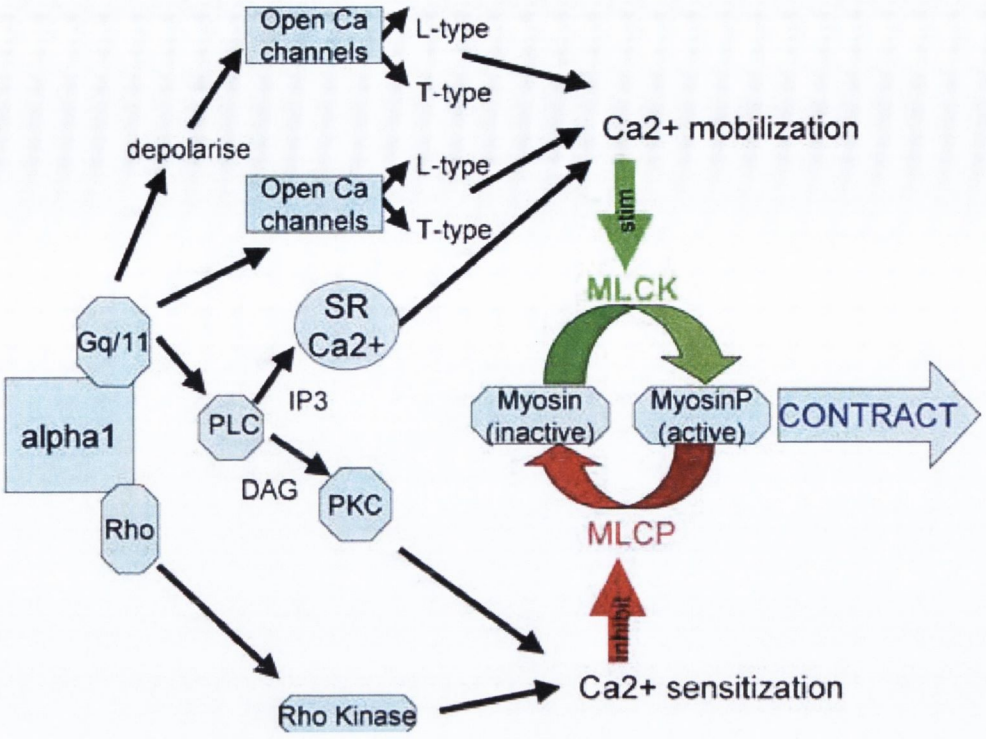


Figure 1.4 A schematic representation of possible signal transduction pathways linking α_1-adrenoceptors to myocyte contraction.

alpha1 α_1-adrenoceptor; DAG diacylglycerol; Gq/11 $G\alpha_{q/11}$- protein family; IP3 inositol-1,4,5,-triphosphate, MLCK myosin light chain kinase; MLCP myosin light chain phosphatase; PKC protein kinase C; PLC phospholipase C; Rho Rho GTPase; SR sarcoplasmic reticulum. Diagram taken from Docherty J.R. , 2010[30].

1.2.3.2 α_2-Adrenoceptor signalling

α_2-Adrenoceptors mediate their effects through the $G\alpha_i$ family of G-proteins. When coupled to the $G\alpha_o$, α_2-adrenoceptor stimulation can inhibit voltage-gated Ca^{2+} channels, while coupling to $G\alpha_{i\ 1,\ 2,\ 3}$ is associated with inhibition of adenylyl cyclase[31, 32]. Furthermore, when released, the $\beta\gamma$ subunit of $G\alpha_i$ can activate K^+-channels resulting in membrane hyperpolarization[31-33]. Other second messenger systems linked the α_2-adrenoceptors include phospholipase D activation, arachidonic acid mobilisation, and increased intracellular Ca^{2+} availability[34,35]. α_2-Adrenoceptors are also coupled to the mitogen-activated protein kinase (MAPK) cascade. It is unclear how this occurs, but it may

be mediated through βγ subunits in a pertussis toxin-sensitive G protein dependent manner[36]. However, the process may be more complex as α_2-adrenoceptors also activate MAPK via a pathway involving arachidonic acid, matrix metalloproteinases, and epidermal growth factor receptor transactivation[37, 38].

1.2.3.3 β-Adrenoceptor signalling

β-Adrenoceptors are the prototypical GPCR for studying cell signalling. In the classical signalling cascade, β-adrenoceptors activate adenylyl cyclase (AC) by coupling to a $G\alpha_s$-protein. The resulting increase in cAMP results in activation of cyclic AMP-dependent protein kinase A (PKA; Figure 1.5). PKA phosphorylates numerous cellular proteins involved in metabolism, growth, muscle contraction and cell survival or death[39]. It can also translocate to the nucleus where it phosphorylates the cAMP response element-binding protein (CREB). Once activated, CREB binds to CRE-specific DNA sequence which regulate gene expression.

With regard to cell contraction, PKA phosphorylates and activates sarcolemmal L-type Ca^{2+}-channels. This is mediated through an A kinase anchoring protein (AKAP79) leading to the influx of extracellular Ca^{2+} and cell contraction[40]. In addition, PKA can increase cardiac contractility through phosphorylation of sarcoplasmic ryanodine receptors (RyR2) and phospholamban (PLB)[41]. As PLB inhibits sarcoplasmic reticulum (SR) Ca^{2+} ATPase (SERCA2a) activity, β-adrenoceptor-PKA-mediated phosphorylation of PLBs removes it inhibition of SERCA2a. This leads to increased uptake of Ca^{2+} from the cytoplasm into the SR through SERCA2a and aids relaxation[41]. As a consequence of the increase in Ca^{2+} loading of the SR, more Ca^{2+} is available for release during the next cardiac contraction, which will be enhanced[41].

β_2-Adrenoceptors have a unique ability to couple not only to $G\alpha_s$-protein but also to $G\alpha_i$-protein in the human myocardium (Figure 1.5)[42, 43]. A switch from $G\alpha_s$-protein to $G\alpha_i$-protein coupling seems to occur during persistent agonist stimulation[39]. It leads to activation of phosphoinositide 3-kinase (PI3K), which inhibits $G\alpha_s$/cAMP/PKA induced phosphorylation events and therefore the associated positive inotropic effects[39]. There are indications that PKA phosphorylates the β_2-adrenoceptor itself, which induces the switch in coupling from $G\alpha_s$- to $G\alpha_i$-protein[44].

cAMP/PKA mediated signalling is counterbalanced by cAMP phosphodiesterases (PDE) and protein phosphatases (PP)[41]. PDE degrade cAMP and therefore inhibit the actions of PKA. In addition to PKA as the main effector of cAMP-directed signalling, a new class of proteins is emerging as regulators in PKA-independent cAMP signalling. These are referred to as exchange proteins directly activated by cAMP (EPAC). Their primary function is to activate GTPases by promoting the exchange of GDP for GTP on the Ras family of small GTPases, Rap1 and Rap2.

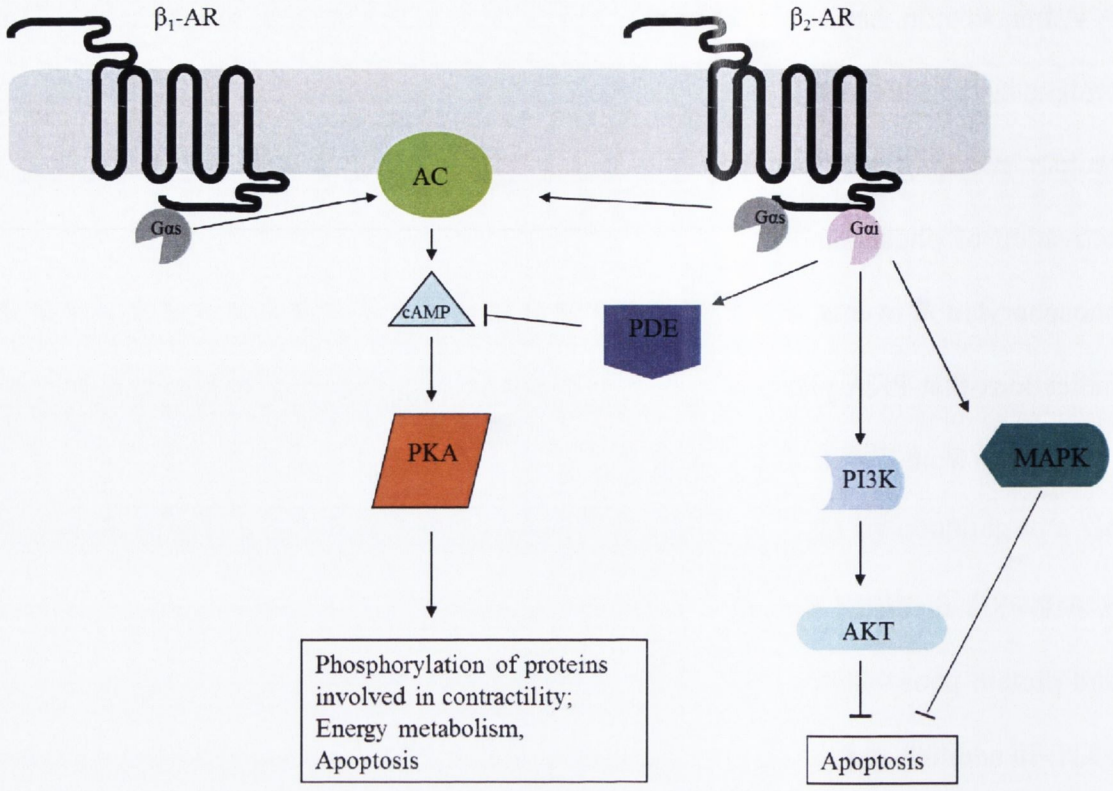


Figure 1.5 A simplified model depicting β_1- and β_2-adrenoceptor signalling pathways in the human myocardium.

AC adenylyl cyclase; AKT protein kinase B; AR adrenoceptor; cAMP cyclic AMP; Gαs $G\alpha_s$ protein family; Gαi $G\alpha_i$ protein family; MAPK mitogen-activated protein kinase; PDE cAMP phosphodiesterases; PI3K phosphoinositide 3-kinase; PKA protein kinase A. This figure is based upon Xiao *et al.*, 2006[39].

1.2.4 Arrestins and adrenoceptor signalling

The arrestin family consists of four members, two are found in the retina (visual arrestins; arrestin-1 and arrestin-4), whereas the other two are distributed throughout the body (non-visual arrestins; β-arrestin-1 and β-arrestin-2). The arrestins are responsible for desensitisation and internalisation of GPCR (Figure 1.6). As stated earlier (section 1.1.1.2), GRK phosphorylates the cytosolic tail of a GPCR inducing a conformational change in the receptor which allows arrestin to bind. Binding of arrestin prevents the G-proteins from re-associating with the receptor (Figure 1.6). This is referred to as receptor uncoupling or desensitisation. Furthermore, arrestins play an active role in receptor internalisation, as they direct activated receptors to clathrin-coated pits[45]. This step is critical for receptor recycling and degradation. The latter is responsible for receptor down regulation following chronic exposure to an agonist.

Over the past ten years, the role of arrestins has been revised and it is now apparent that they play a major role as scaffolding proteins[46]. Within this context, their major functions are: (i) GPCR internalisation, (ii) recruitment of enzymes responsible for second messenger degradation (PDE4D, diacylglycerol kinase (DGK))[47, 48], and (iii) activation of non-classical signalling cascades (MAPK family, Figure 1.6)[46]. β-arrestins are also involved in terminating signal transduction. This is exemplified by the work of Baillie *et al.,* which shows that by recruiting PDE4D, β-arrestins mediate the switch from uncoupling of the β_2-adrenoceptor from $G\alpha_s$-protein after PKA phosphorylation to re-coupling to $G\alpha_i$-protein[47].

As a scaffolding protein, β-arrestins have an important role in several non-classical signalling pathways: (i) following ubiquitinylation they stabilize the receptor/β-arrestin/ERK complex leading to receptor sequestration, (ii) they mediate delayed

phosphorylation of ERK1/2 MAPK independently of cAMP, and (iii) they facilitate nuclear translocation of activated kinases[49-52]. α_2-Adrenoceptors have a similar requirement of β-arrestins for the activation of ERK1/2[52]. As scaffolding proteins, β-arrestin can couple β_2-adrenoceptors to MAPK signalling independent of G-protein involvement[50, 53]. However, others have shown that β_2-adrenoceptor stimulation activates MAPK signalling through a G-protein and β-arrestin independent but Src-dependent mechanism[52]. Additionally, arrestins seem to participate in the regulation of some transcription factors[46].

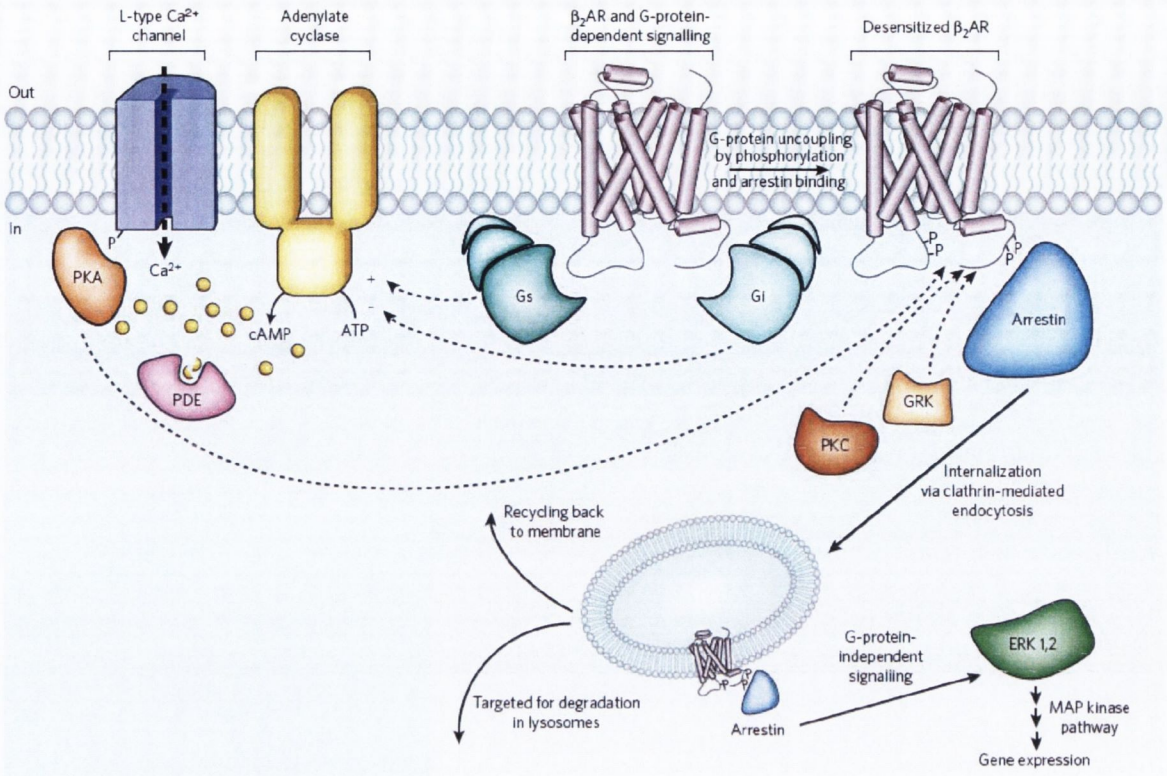


Figure 1.6 Schematic model of β_2-adrenoceptor signalling and the role of arrestin. Following ligand binding, β_2-adrenoceptors (β_2AR) can couple to $G\alpha_s$ or $G\alpha_i$ differentially regulating the cellular responses (see 1.2.2.3 for more information). Signal termination is achieved through phosphorylation of G-protein-coupled receptor kinase (GRK) and subsequent coupling to arrestin. Arrestin prevents G-protein activation and initiates receptor internalisation, and can activate extracellular signal-regulated kinases (ERK). Taken from Rosenbaum *et al.*, 2009[24].

1.2.5 Physiological role of adrenoceptors

The physiological consequences of α_1-adrenoceptor stimulation are diverse. They regulate glycogenolysis (liver) and affect temperature control of the human body[30]. In the heart, they mediate positive inotropic and chronotropic effects[30, 54]. While in the vasculature and genitourinary systems they are also coupled to smooth muscle cell contraction[32]. Transgenic mice with a deletion of the gene targeting either the α_1-adrenoceptor or a combined α_{1AB} and α_{1BD}-adrenoceptor genes are viable, fertile and appear normal[55]. However, these studies demonstrate that α_{1A}-adrenoceptors play a crucial role in maintaining basal blood pressure, whereas the α_{1B}-adrenoceptors are important for mediating responses to exogenous agonists[55]. α_{1D}-Adrenoceptors appear to be involved in both (Figure 1.7)[18, 55]. $\alpha_{2A/D}$- and α_{2B}-Adrenoceptors regulate arterial contraction, while α_{2C}-adrenoceptors mediate venous vasoconstriction[18]. Gilsbach *et al.* have shown that α_{2A}-adrenoceptors protect against cardiac hypertrophy and fibrosis in mice at baseline. However, after chronic pressure overload, receptors are desensitised and in turn may contribute to the pathological progression of this condition[56]. Interestingly, α_2-adrenoceptor agonists appear to have neuroprotective properties in experimental models of cerebral ischemia[57]. However, the underlying mechanisms are not fully understood.

β-Adrenoceptors are of great therapeutic importance as they regulate blood pressure and vascular tone. β_1-Adrenoceptors regulate cardiac function, while β_2-adrenoceptors cause relaxation of smooth muscle cells in the vasculature, bronchus and uterus. β-Adrenoceptors also modulate energy and fat metabolism (glycogenolysis, lipolysis, and thermogenesis) in humans[19, 58]. Although, β_1-adrenoceptors are predominant over β_2-adrenoceptors in the human myocardium, the functional responses of β_1- compared to β_2-adrenoceptors are similar. This may be explained by a more effective coupling of β_2-adrenoceptors to adenylyl cyclase than β_1-adrenoceptors[21]. Within the heart, β_1-adrenoceptor activation

leads to an increase in force and rate of contraction. While in the kidney they control renin release and therefore have indirect effects on arterial blood pressure[21]. Nevertheless, β_2-adrenoceptor (terbutaline) activation is also associated with positive inotropic and chronotropic effects in the healthy human heart[59], but to a less extent than β_1-adrenoceptors in the isolated rat heart[60].

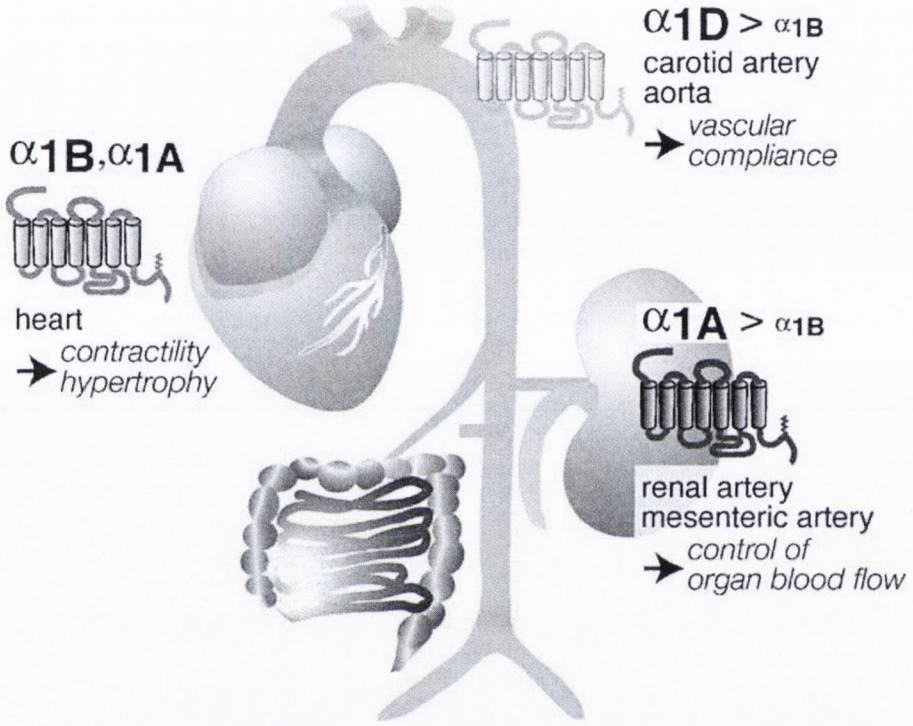


Figure 1.7 Role of α-adrenoceptors in the murine cardiovascular system.

α_{1A}- and α_{1B}-Adrenoceptors are abundantly expressed in the heart, where they mediate cardiac growth and contractility. α_{1D}-Adrenoceptors are predominantly expressed in large blood vessels (e.g. aorta), and mediate vasoconstriction. However, α_{1A}-adrenoceptors are also expressed in arteries and increase blood pressure through effects on vascular tone. This illustration was taken from Philipp *et al.*, 2004[61].

1.2.6 Adrenoceptors in disease

Chronic α_1-adrenoceptor stimulation induces hypertrophy and cell growth[17], which appears to involve the PKC family. In particular, PKCα has emerged as the main PKC isoform associated with regulation of hypertrophy in murine cardiac myocytes[62]. The main G-protein coupling α_1-adrenoceptors to cardiac hypertrophy is the α-subunit of $G\alpha_q$-protein[63, 64]. In heart failure, β-adrenoceptors are desensitised and down-regulated[65, 66], whereas α_1-adrenenoceptor density is unaffected. Therefore, their relative density with respect to the total adrenoceptor population is upregulated[20], and they have been postulated to take on a more important role in maintaining cardiac function in heart failure[32]. Indeed, in a mouse model of heart failure, this appears to be restricted to the right ventricle[67].

β-Adrenoceptor signalling is a crucial compensatory mechanism for maintenance of cardiac function in heart failure. El-Armouche *et al.* defined heart failure as "a clinical syndrome that represents the common final pathway of a variety of diseases characterised by compromised contractile function of the heart"[41]. As the heart fails, sympathetic drive to the heart is increased in an attempt to maintain cardiac output. This is achieved by increasing heart rate and force of contraction. However, this puts further demand on the heart over time leading to other compensatory mechanisms and loss of response to the chronic increase in sympathetic drive. In particular, chronic stimulation of β-adrenoceptors increases energy consumption, induces cardiac myocyte apoptosis, hypertrophy, and is arrhythmogenic and fibrogenic (Figure 1.8)[41]. The loss of functional response to chronic stimulation is frequently attributed to their desensitisation and down-regulation. As a result of this, the ratio of β_1- to β_2-adrenoceptors is shifted towards the β_2-adrenoceptor in ventricle[68]. Together, these mechanisms would appear to be part of a mechanism to limit the detrimental effects of chronic adrenoceptor stimulation.

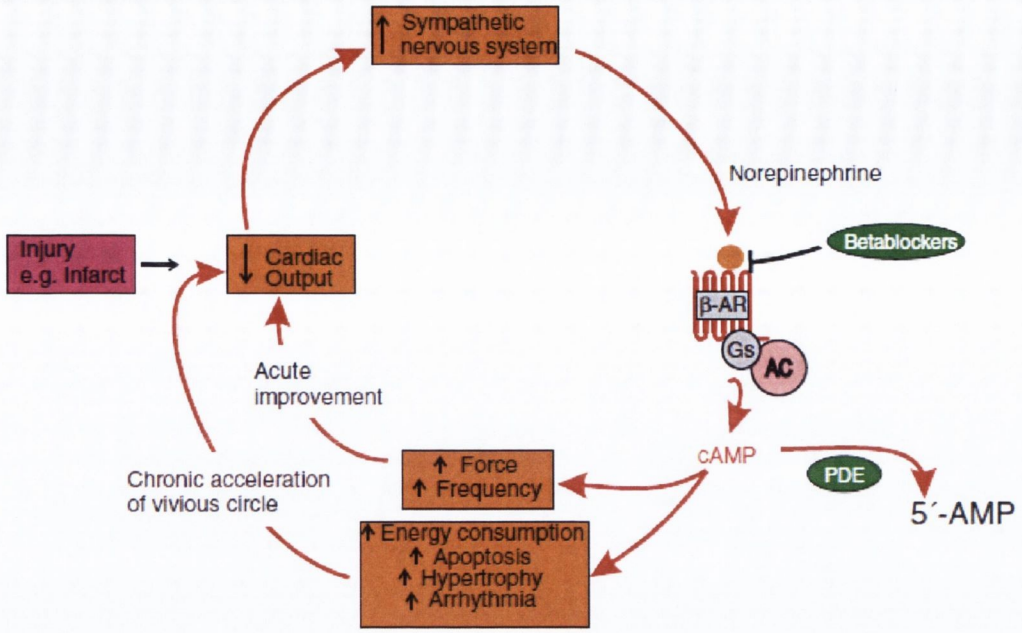


Figure 1.8 A schematic representation of "The vicious cycle in heart failure." See text for full description. Modified from El-Armouche *et al.*, 2009[41].

1.2.7 β-Adrenoceptor antagonists

Propranolol was the first β-adrenoceptor antagonist to be synthesised and is a non-selective agent with similar activity for β_1- and β_2-adrenoceptors[20]. It was originally licensed for the treatment of angina pectoris, but its use has extended to the treatment of hypertension, cardiac arrhythmias, and myocardial infarction. More recently, it has been used in the treatment of post-traumatic stress disorder and migraine. Propranolol is a competitive β-adrenoceptor antagonists and decreases chronotropic, inotropic, and vasodilator responses. Propranolol also shows some inverse agonist characteristics as it can simultaneously signal through $G\alpha_s$-coupled and G-protein independent mechanisms[69]. Furthermore, its anti-hypertrophic properties were independent of its β-adrenoceptor properties in a rat model of heart failure[70].

Second generation β-blockers such as metoprolol were developed to be more cardioselective, in that they are more selective towards β_1-adrenoceptors. As treatment of hypertension evolved, further research led to the development of the third generation β-blockers, which possess vasodilating properties[20]. Labetolol and carvedilol are noted members of the third generation of β-blockers. Their role moved from the treatment of hypertension towards treatment of heart failure. They are a non-selective β-adrenoceptor antagonist with α-adrenoceptor blocking properties[20, 71].

Carvedilol is the most commonly prescribed drug for the management of congestive heart failure[20]. Clinical trial data indicate that it increases the survival rate compared to metoprolol in mild to severe heart failure patients[72, 73]. So what is so special about carvedilol? Apart from being a nonselective β-blocker, it has antioxidant, anti-inflammatory, anti-proliferative, and anti-arrhythmic properties and is an α_1-adrenoceptor antagonist. In addition, it has recently been shown to activate β-arrestin signalling independently from G-protein signalling[74]. Therefore, it does not only display antagonistic action, it further expands its actions by acting as a biased ligand[74]. It is therefore difficult to attribute its beneficial action to one particular mechanism, which in effect may be a culmination of its pleiotrophic nature. Nonetheless, α_1-adrenoceptor antagonists and antioxidants per se do not appear to be beneficial in the treatment of heart failure[75]. Furthermore, metoprolol (β_1-adrenoceptor antagonists) can reverse β_1-adrenoceptor downregulation in heart failure[76, 77], or may even re-couple β_2-adrenoceptors to their signal transduction pathway[78]. However, these effects are not observed with carvedilol[79]. Despite this, the consensus is that β-adrenoceptor antagonists reduce mortality and morbidity in heart failure through improvements in ventricular structure and function, heart rate reduction, blood pressure reduction, and inhibition of the renin-angiotensin system[80].

1.3 Fibroblasts

1.3.1 Fibroblasts and tissue remodelling

Fibroblasts are the most prominent cell type in connective tissue and responsible for maintaining, altering, and repairing connective tissue. They have key roles in wound healing, inflammation, and aging[81]. An understanding of their biological role is difficult to determine as they form a heterogeneous group of cells (Figure 1.9)[81]. Indeed, fibroblasts not only show a phenotypic and functional heterogeneity among organs, but also within the same organ system (e.g. myofibroblast, tumour stromal fibroblast).

Fibroblast are described morphologically as elongated, spindle-shaped cells, but may also be present with different characteristics as they have numerous subpopulations[81]. From a functional perspective they are involved in: (i) the synthesis and secretion of structural (e.g., collagens) and non-structural (e.g., growth factors) extracellular matrix proteins, (ii) organisation and remodelling of the extracellular matrix (ECM) through proteinase secretion, and (iii) cell-cell communication[81].

In the myocardium, cardiac fibroblasts (CF) make up to 60-70% of cells and together with cardiomyocytes account for approximately 90% of the cell population[82]. CFs are activated by numerous environmental stimuli including, mechanical stretch, electrical stimuli, and oxygen levels, and are associated with wound healing and repair. Cardiac fibroblasts are the main regulators of ECM proteins and thereby maintain the structure of the myocardium following injury[83]. This is accomplished through increased production of growth factors, and proinflammatory cytokines (TNFα, IL-1, IL-6, and TGFβ), matrix protein synthesis and degradation, proliferation, and migration. CF migration towards the site of injury is regulated by cytokines and is under tight control of MMP expression and activity[82-84]. The

latter facilitates migration and proliferation at the site of the injury through degradation of fibrillar collagen in the surrounding tissue[82, 85-87]. This mechanism is protective in the short-term (wound healing). In addition, at the site of injury, CFs change their phenotype to that of a myofibroblast[88, 89]. This is a generalised response to injury applicable across different organs. In this situation, myofibroblasts actively regulate the remodelling process by increasing MMP secretion and collagen turnover. Myofibroblasts express contractile proteins and facilitate migration, proliferation, and secretion[82]. Myofibroblasts are derived from endogenous fibroblast or fibroblast-like cells, epithelial-mesenchymal transition and bone marrow derived cells (Figure 1.9)[90]. Interestingly, in most tissues, myofibroblasts undergo apoptosis in order to stop the tissue repair response. However, in the heart, myofibroblasts can persist for months following injury, which may contribute to pathological remodelling[82, 91]. CFs play a central role in tissue remodelling associated with hypertension, myocardial infarction, and heart failure. Furthermore, increased sympathetic drive as part of the compensatory mechanism in response to diminishing cardiac function may increase fibrosis through β_2-adrenoceptor stimulation as noradrenaline increases CF proliferation[84, 92]. Indeed, adult cardiac fibroblasts predominantly express β_2-adrenoceptors[84].

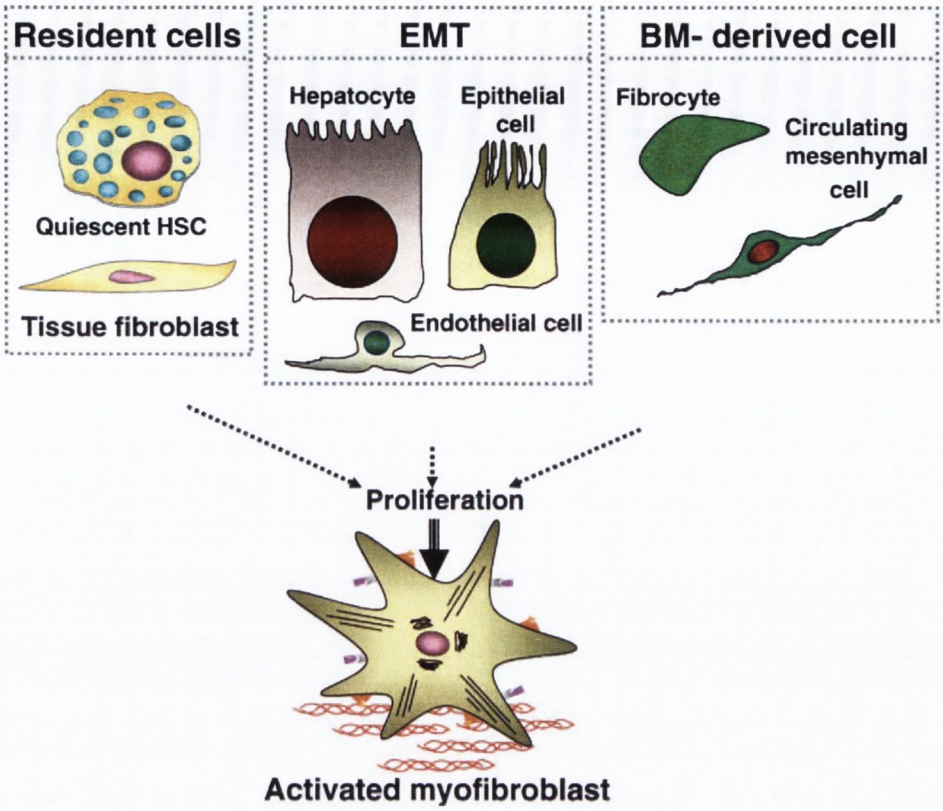


Figure 1.9 Origin of myofibroblasts.

Myofibroblasts originate from endogenous fibroblast or fibroblast-like cells, epithelial-mesenchymal transition (EMT) and bone marrow (BM)-derived cells. Figure adapted from Kisseleva *et al.*, 2008[90].

1.3.2 Collagens

Collagens are an important part of the extracellular matrix (ECM), as they play a leading role in maintaining the integrity of various tissues. To date 28 different collagen types have been identified in vertebrates[93] and they account for 25% of whole body protein content in mammals. All collagens contain at least one triple helical domain which is formed by three polypeptide chains (α chains), which are wound around each other into a triple helix. Every third amino acid in the α chain is a glycine, giving a repetitive sequence of $(Gly\text{-}X\text{-}Y)_n$. Positions X and Y are frequently occupied by proline and 4-hydroxyproline, which adds stability to the triple helix. Hydrogen bonds also help to stabilise the triple helix. The

majority of the collagens are homodimers, but they can also exist as heterotrimeric complexes. Structurally, they all contain non-triple helical domain at their N- and C-termini.

Collagens are classified on the basis of function and domain homology[93]. The major classes are fibril-forming collagens, fibril-associated collagens with interrupted triple helices (FACITs), network-forming collagens and transmembrane collagens. The fibril-forming collagens are the most abundant and widespread family member, making up about 90% of total collagen. Fibril-forming collagens include collagen types I, II, III, V, XI, XXIV, and XXVII[93-95]. Characteristically, they assemble into highly orientated supramolecular aggregates containing a typical quarter-staggered fibril-array as a suprastructure[96, 97]. They exist as homotrimers (type II and III), heterotrimers (type XI), or as a combination of both (type I and V). Within this group, Type I collagen is the most abundant collagen in man. The triple helix of collagen type I is usually formed as a heterodimer, consisting of two identical α1(I)-chains and one α2(I)-chain. The triple helical fibres are integrated in a network with type III collagen or type V collagen *in vivo*[97-99]. Fibril-forming collagens and their associated collagens are the main products synthesised by fibroblasts, osteoblasts, and chrondocytes. Types V and XI collagens are heterotrimers composed of three different α-chains. Type V collagen supports the organic bone matrix, corneal stroma, and the interstitial matrix of muscles, liver, lungs and placenta by the formation of heterofibrils with types I and III collagens[97]. Furthermore, type XI is mainly found in articular cartilage together with type II collagen. In some tissues, types V and XI exist as a hybrid of type V/XI molecules[100].

The FACIT collagens consist of collagen types IX, XII, XIV, XVI, XIX, XX, XXI and XXII[93]. Structurally they contain "collagenous domains" which are interrupted by short-

non helical domains which associate with various fibrils[97]. Collagen IX, co-distributes with collagen II primarily in the cartilage and vitreous humour. Collagen type IV, VIII and X belong to the group of network-forming collagens. Collagen type IV is the most important structural component of basement membranes, integrating laminins, nidogens, and other components to form a two-dimensional stable supramolecular aggregate[97]. It is structurally characterised by a "7S domain", which is made of four collagen IV interacting through their N-termini, forming an important interaction node[101]. Collagen IV has a C-terminal globular domain (NC1), which forms a network by head-to-head interaction between two NC1 domains. Its triple helix is flexible, as the central part consists of short interruptions of Gly-X-Y repeats. Collagen VIII is a major component of descemet's membrane and vascular subendothelial matrices, whereas collagen type X is mainly found in the hypertrophic cartilage.

Transmembrane collagens are characterised by a short cytosolic N-terminal domain and long interrupted triple helical extracellular domains. This class of collagens includes type XIII, XVII, XXIII, XXV, ectodysplasin A, and gliomedin[93]. Type VI collagen tetramers aggregate into filaments forming an independent microfibrillar network in nearly all connective tissue except bone[102, 103]. Furthermore, type VI collagen is required for the maintenance of the integrity of muscle fibers[104].

1.4 Regulation of the extracellular matrix

1.4.1 The physiological function of the extracellular matrix

Communication between cells is mediated through cell-cell and cell-matrix interactions. These interactions regulate morphological changes, differentiation, apoptosis, tissue repair, and cell migration. Proteolysis of the extracellular matrix (ECM) and cell-surface proteins can alter cell responses through local changes in the microenvironment[105]. The ECM is a gel-like matrix consisting of the interstitial matrix and the basement membrane. It is composed of two main components, glycosaminoglycans (GAGs) and fibrous proteins. GAGs like chrondroitin sulphate, heparin and keratin sulphate are found covalently bound to core proteins (e.g. perlecan, agrin, aggrecan and decorin). These secreted proteoglycans are involved in cell adhesion and binding of latent growth factors. The fibrous proteins have structural (e.g. collagen, elastin) and adhesive (e.g. fibronectin, laminin) functions. Furthermore, the ECM can function as a "store room" for various growth factors, proteinases and cytokines[106]. The ECM is in a dynamic state as it undergoes constant remodelling in response to its local environment. Remodelling is delicate balance between synthesis and degradation. The ECM is degraded by matrix metalloproteinase and several serine, aspartate, and cysteine proteases (e.g. plasmin, cathepsin D, cathepsin G).

1.4.2 Classification of matrix metalloproteinases (MMPs)

Matrix metalloproteinases (MMPs) are a family of zinc-containing endopeptidases, which belong to a larger family called the metzincin-superfamily[107]. To date, 28 MMPs have been identified[108]. They were initially classified on the basis of a combination of their substrate specificity and cellular localisation as collagenases, gelatinases, stromelysins, and the membrane-type MMPs (MT-MMPs; table 1.1). However, many of the family members

have multiple and often overlapping substrates. As the MMP genes became better characterised, classification moved towards a new classification system based on domain structure arose (Figure 1.10)[109]. Under this system, the MMPS are assigned to one of five major groups: the matrilysins, collagenases/stromelysins, gelatinases, transmembrane MT-MMPs and glycosyl-phosphatidyl inositol (GPI)-linked MT-MMPs (Figure 1.11)[108-111]. The Matrilysins include MMP-7 (matrilysin) and MMP-26 (endometase), while the collagenase/stromelysins are the largest group and include MMP-1, 3, 8, 10, 11, 12, 14, 18, and some others. MMP-2 (gelatinase A) and MMP-9 (gelatinase B) belong to the gelatinase subgroup while MMP-14, 15, 16, and 24 are examples of MT-MMPs. Members of the GPI-linked MT-MMP subgroup are MMP-17 and MMP-25[108]. However, as more MMPs have been discovered, shortcomings of this system have become evident[108-111]. Ra *et al.* expanded this classification to include subdivisions based on their "secretion" or anchoring ability, and their furin-recognition motif[112]. The most widely used classification is the original classification that is based upon the domain structure and will be used throughout this thesis.

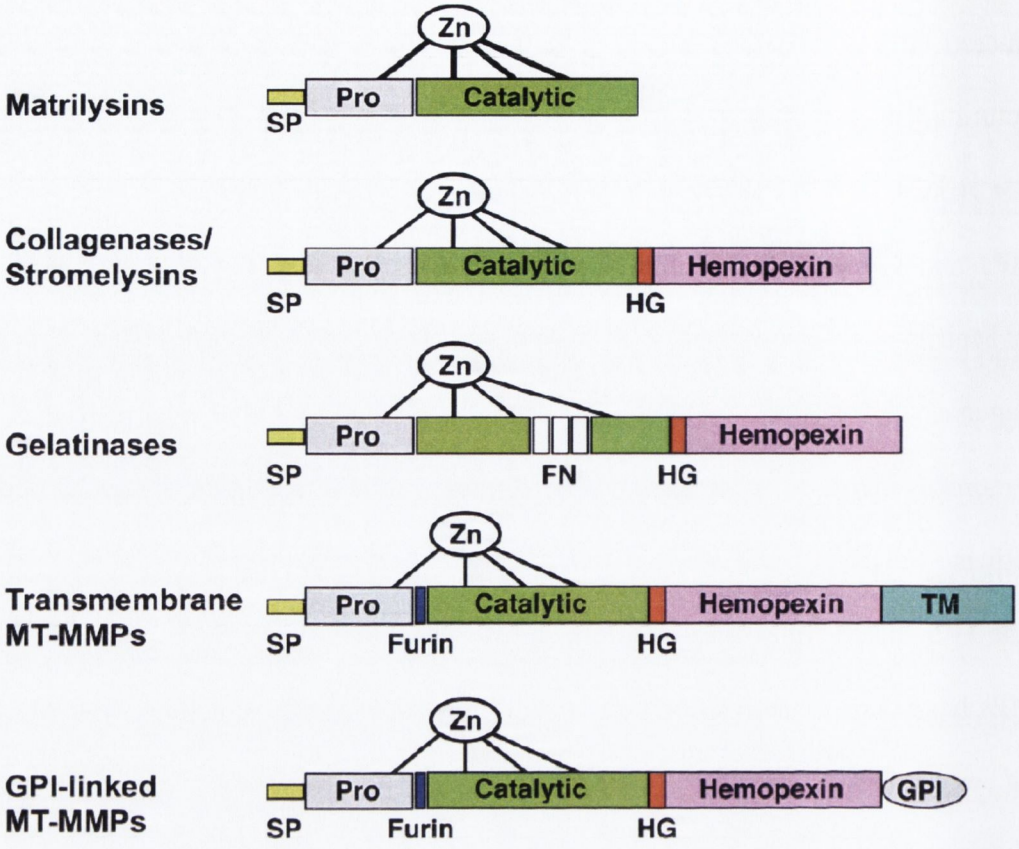


Figure 1.10 Domain structure of the major MMP classes.

The major domains consist of the signal peptide (SP; predomain), propeptide domain (Pro), catalytic domain with a zinc (Zn) binding motif and a "cysteine switch –residue" in the propeptide domain, the hinge region (HG), the hemopexin domain, and in some cases either a transmembrane domain (TM) or GPI-anchor domain (GPI). In certain MMPs, a furin cleavage site resides between the propeptide domain and catalytic domain. In the catalytic domain of the gelatinases, there is a triple repeat of a type II fibronectin domain (FN). Taken from Brauer P.R., 2006[109].

Table 1.1 Classification and substrate specificity of the major MMPs.

This table is adapted from the work of Brauer P.R., 2006[109], and Sternlicht *et al.*, 2001[108].

Enzyme	MMP class	Collagen substrate	Other ECM substrates
Matrilysin			
Matrilysin	MMP-7	I, III, IV, IX, X, XI	Aggrecan, decorin, elastin, entactin, fibronectin, gelatines, laminin, osteonectin, tenascin, vitronectin, proMMP-2, -7,
Collagenases/ Stromelysins			
Collagenase-1	MMP-1	I, II, III, VII, VIII, X, XI	Aggrecan, entactin, fibronectin, gelatines, laminin, tenascin, vitronectin, proMMP-1, -2
Collagenase-2	MMP-8	I, II, III	Aggrecan
Collagenase-3	MMP-13	I, II, III, VI, IX, X	Aggrecan, fibronectin, gelatines, laminin, osteonectin, tenascin, proMMP-9, -13
Stromelysin-1	MMP-3	III, IV, V, IX, X, XI	Aggrecan, decorin, elastin, entactin, fibronectin, gelatines, laminin, osteonectin, tenascin, vitronectin, proMMP-1, -3, -7, -9, -13,
Stromelysin-2	MMP-10	III, IV, and V	Aggrecan, elastin, fibronectin, gelatines, laminin, proMMP-1, -7, -8, -9
Stromelysin-3	MMP-11	IV	Aggrecan, laminin, fibronectin,
Gelatinases			
Gelatinase A	MMP-2	I, IV, V, VI, VII, X, and XI	Aggrecan, elastin, entactin, fibronectin, gelatines, laminin, vitronectin, proMMP-1, -9, -13
Gelatinase B	MMP-9	IV, V, VI, XI, and XIV	Aggrecan, decorin, elastin, entactin, fibronectin, gelatines, laminin, osteonectin, vitronectin
Membrane-type MMPs			
MT1-MMP	MMP-14	I, II, and III	Aggrecan, entactin, fibronectin, gelatines, laminin, vitronectin, proMMP-2, -13
MT2-MMP	MMP-15	-	Aggrecan, entactin, fibronectin, laminin, tenascin, proMMP-2
MT3-MMP	MMP-16	III	Aggrecan, Fibronectin, laminin, vitronectin, proMMP-2,
MT5-MMP	MMP-24		Fibronectin, proMMP-2

1.4.3 Structure of MMPs

Structurally many MMPs share the common domain structure of a predomain, propeptide, catalytic domain, proline-rich linker, and a C-terminal hemopexin binding domain[110, 111]. The first domain is a hydrophobic signal sequence (predomain) that is located at the N-terminal site of the propeptide domain. The predomain directs their synthesis to the endoplasmic reticulum and is removed afterwards[108]. They are then released as inactive proenzymes, and are activated through proteolytic cleavage. The latency is mediated by the propeptide domain (prodomain; ~80 amino acids), which has an auto-inhibitory effect on the full-length enzyme. This is achieved through a cysteine residue, which acts as the fourth zinc-binding ligand to keep the enzyme inactive ("cysteine switch-residue").

The catalytic domain (~180 amino acids) is highly conserved across all MMPs, and consists of a five-stranded β-sheet, three α-helices, two zinc ions, and one to three calcium ions. The catalytic activity is dependent on the binding of a zinc ion to a conserved HEXXHXXGXXH motif. Within this region, the three histidine (His) residues chelate the zinc ion at the active site forming a zinc-binding motif[113]. In the active enzyme, a water molecule makes up the fourth position. The conserved glutamate residue is involved in fixation of the zinc-bound water molecule, and acts first as a catalytic base, and then as an acid during the hydrolysis of a peptide bond of the target substrate. In addition, MMPs contain a second zinc, which contributes to structural integrity.

The catalytic domain contains a second conserved structure. This consists of a structurally super-imposable methionine, which is positioned eight residues on the C-terminal side of the histidine residues (zinc-binding motif) and forms a methionine-turn in the active site-helix ("Met-turn"). The reason for its strict conservation is not clear. It has been suggested to be essential for the structural integrity of the active site through stabilisation of the zinc

binding[113], while some mutational studies supported this, others do not[114, 115]. The main determinant of substrate specificity is the hydrophobic S_1 pocket in the active site. This S_1 pocket is not uniform in size or shape across MMPs. For example, the S_1-pocket for MMP-9 (gelatinase B) and MMP-2 (gelatinase A) is described as a "tunnel leading toward solvent", whereas the S_1-pocket for stromelysin is described as a "tunnel leading out to solvent"[116].

Another characteristic common across MMPs is the ability to cleave peptide bonds in front of a hydrophobic residue (Leu, Ile, Met, Phe or Tyr), which fits into the S_1-pocket. MMPs seldom cleave peptide bonds where a charged residue is in this position, although, MMP-12 is an exception to this rule, as it cleaves X-Lys[117]. In addition to interactions at the active site, some substrates also interact with non-catalytic domains of the MMPs. This is particularly true for large macromolecules of the ECM. For instance, within the catalytic domain of MMP-9 and MMP-2 there are three repeats of a type II fibronectin binding domain to which collagens, gelatin, and laminin bind[118, 119]. With the exception of matrilysin, the catalytic domain of other MMPs is connected to a C-terminal hemopexin-like domain (~210 residues) through a flexible hinge or linker region (variable and proline rich). Near the end of the hinge region, there is a unique type V-collagen-like insert in MMP-9, whose function is not yet clear. Indeed, a MMP-9 mutant missing this region had similar enzyme activity and substrate specificity against gelatin and type V collagen as wild type MMP-9[120]. The C-terminal hemopexin-like domain has a four-bladed propeller structure, which mediates protein-protein interactions. The "propeller" is closed by cysteine-residues at the beginning and end of this domain. The loss of this domain affects collagenolytic activity, but not the collagen-binding specificity of the enzyme. Therefore, this domain contributes to substrate recognition as well as enzyme activation, protease localisation, internalisation and degradation[121].

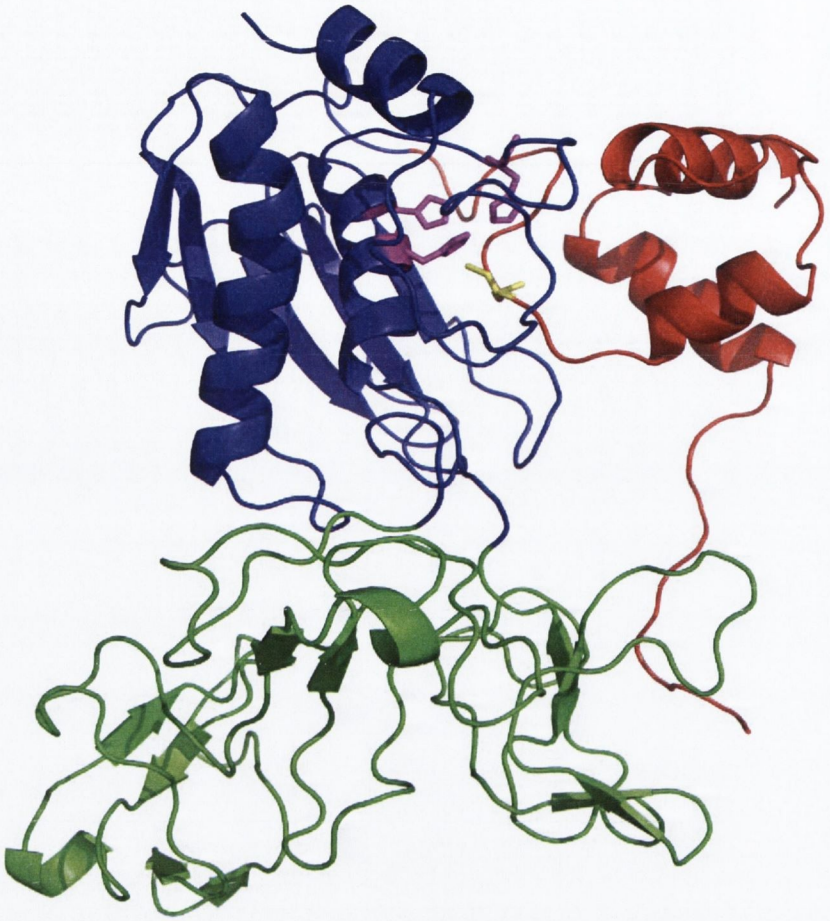


Figure 1.11 A ribbon model depicting the structure of the human proMMP-9.

The propeptide domain (red) is inserted in the active cleft of the catalytic domain (blue) and therefore blocks substrate access to the catalytic zinc. The three catalytic histidine residues (His401, His405 and His411) are marked in magenta, and the critical cysteine-residue (Cys99), also called cysteine-switch, is marked in yellow. The three fibronectin domains are shown in green. The image does not show the full proMMP-9 structure, as the C-terminal end is truncated. This model was prepared from the Brookhaven Protein Data Bank entry (1L6J), deposited by Elkins et al.[122], using PyMOL[123].

1.4.4 Regulation of MMP activity

The activity of MMPs is tightly regulated at many levels including: (i) transcriptional, (ii) activation of the proenzyme, and (iii) inhibition by endogenous inhibitors (Figure 1.12)[117].

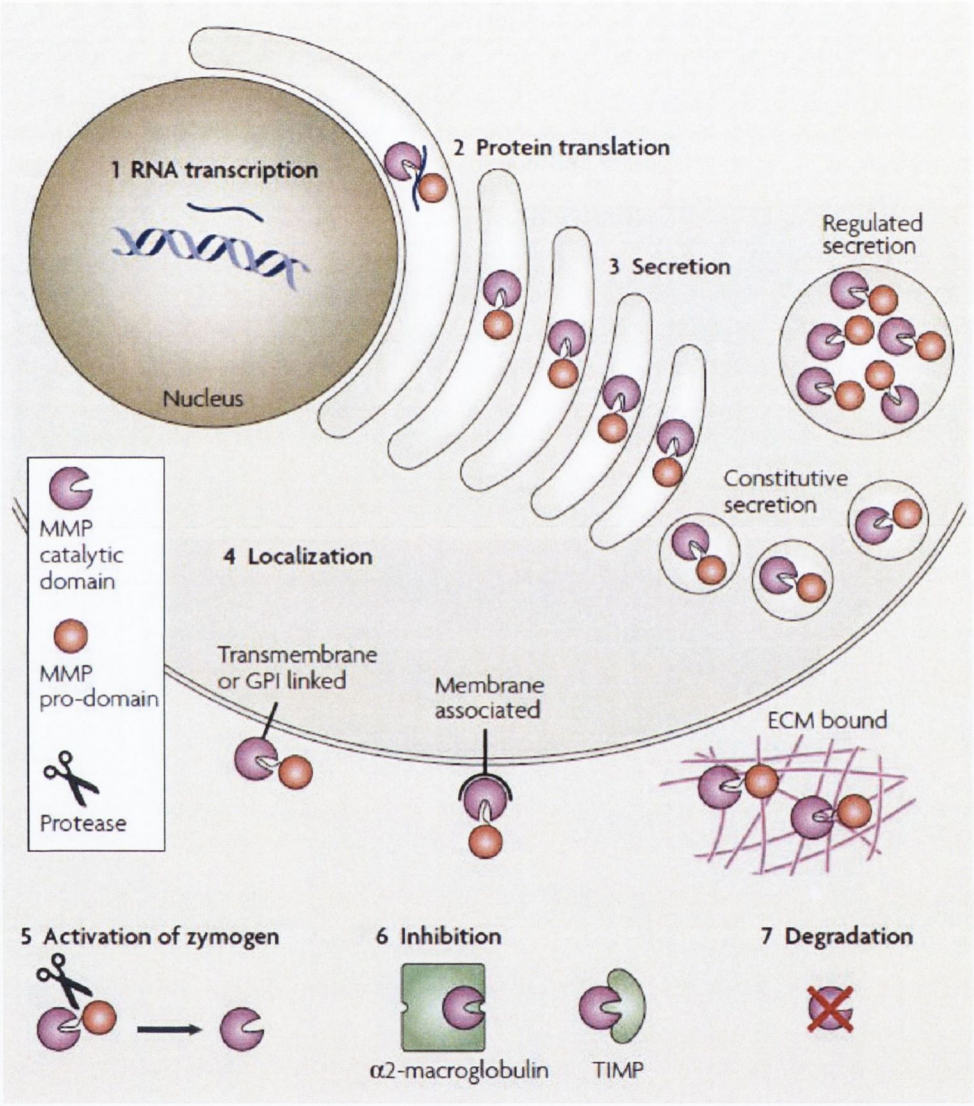


Figure 1.12 Regulation of MMPs.

MMP expression and activity are tightly controlled at the level of: (1) transcriptional control, (2) protein synthesis, (3) secretion and intracellular trafficking, (4) localisation, (5) proenzyme activation, (6) endogenous protein inhibitors and (7) degradation. Indirect regulation is mediated by the access and the availability of substrates. This figure has been taken from Page-McCaw *et al.*, 2007[121].

1.4.4.1 Transcriptional regulation

At the transcriptional level, MMP expression is regulated through gene specific promoter sequences. However, across the different MMP classes there are some common cis-acting elements which fall into three main groups[124]. Group 1 is characterised by a TATA box and an activator protein-1 (AP-1) binding site in the proximal region of the promoter (~70 bp), this element allows regulation through transcription factors belonging to fos and jun families[124]. Although phorbol esters (tumour promoters) can induce MMP expression through this AP-1 site, it appears to cell type specific[108, 125]. Furthermore, the majority of group 1 MMPs also have a PEA3 binding site. Examples of MMPs within group 1 are MMP-1, -3, -7, -9, -10, -12, -13, -19, and -26[126]. The second group includes MMP-8, MMP-11, and MMP-21; this group contains only the TATA box and not the proximal AP-1 binding site. Their regulation is described as being relatively simple and different from the first group. The third and last group of MMP promoters lacks both the TATA box and AP-1 binding site. The expression of MMP-2, -14, -28 fall into this group and are mainly expressed constitutively.

The AP-1 binding site, with or without the PEA3 binding site, is responsible for the expression of MMPs in response to growth hormones and cytokines (e.g. interferons, interleukins, TNFα, TGF-β)[83, 126, 127]. These growth hormones and cytokines activate a MAPK-signalling cascade resulting in trans-activation of the MMP promoter. In particular, p38-MAPK can increase c-jun and c-fos expression resulting in transcriptional activation of genes containing AP-1 transcription factor binding sites in their promoter region. These elements also represent a convergence point for MMP induction by ECM proteins, as the integrin family of cell surface receptors activates focal adhesion kinase, which mediates transcriptional activation of AP-1 and/or PEA3 by MAPK signalling pathways[126, 128]. Although not discussed here, MMP expression is also modulated by polymorphisms, DNA

methylation and through alterations in chromatin structure[126, 129]. Of recent interest is the post-transcriptional regulation of MMP gene expression, via regulation of mRNA stability[126].

1.4.4.1.1 The MMP-9 promoter

MMP-9 which is also known as gelatinase B, 92kDa gelatinase, and 92kDa Type IV collagenase was first identified by Sopata *et al.* in human polymorphonuclear leukocytes in 1974[130]. MMP-9 is primarily released in an inducible manner in response to a variety of stimuli including tumour promoters, cytokines, growth factors, hormones, and through cell-cell interactions[131]. However, it is basally expressed in keratinocytes, monocytes, tissue macrophages, cardiac fibroblasts, and polymorphonuclear leukocytes[83, 131]. As indicated above (section 1.4.4.1), MMPs can be classified into one of three groups based upon the presence of conserved motifs within their promoter sequence. MMP-9 belongs to group 1 as it has both a TATA box and activator protein-1 (AP-1) transcription factor-binding site. As with other MMPs, transcriptional regulation of MMP-9 is tightly controlled. The three major MAPK signalling cascades that transmit extracellular stimuli to MMP-9 gene transcription are (i) Ras/Raf/ERK1/2, (ii) JNK/SAPK, and p38 MAPK pathway[131].

The full-length human MMP-9 promoter sequence is 2.2 kb long and contains several consensus sequences for NFκB, AP-1, TIE, Sp1/GC and PEA3 (Figure 1.13)[131-133]. Within the MMP-9 promoter sequence there are at least five potential AP-1 binding sites[131], the last (-927 bp) of which overlaps a possible Stat3 binding site[134]. Members of the c-fos and c-jun family of transcription factors are potential binding partners at these elements. Furthermore, MMP-9 contains a highly conserved NFκB subtype p65 binding site (-600 bp)[135]and a binding site for NFκB subtype p50 at position -328 bp. This is interesting as

many inflammatory cytokines (e.g. IL1α, TNFα) regulate gene transcription through the NFκB signalling pathway. However, the NFκB binding motif at position -328 bp does not mediate TNFα or TGF-β responses of the MMP-9 promoter in dermal fibroblasts[135]. While the promoter region also contain a TGF-β inhibitory element (TIE)[136], it has been demonstrated that TGF-β mediated inhibition of MMP-9 is regulated through the NFκB binding site (-600 bp), and does not involve the TIE motif in RAW264.7 cells[137]. The MMP-9 promoter also contains a $(CA)_n$ repeat (-131 bp) which is a microsatellite polymorphism ranging from 13 to 27 repeats. Although longer repeats have been associated with increased promoter activity[126], Demacq *et al.* did not find a correlation between this polymorphism and plasma MMP-9 levels in healthy volunteers[138]. Nevertheless, some genetic studies have reported an association between the CA polymorphism and susceptibility to atherosclerosis and multiple sclerosis[139, 140]. Interestingly, shortening of the microsatellite sequence inhibits MMP-9 gene expression[141].

The majority of the cis-regulating elements appear to regulate the MMP-9 promoter in a synergistic manner. For example, the proximal AP-1 binding site cooperates with the NFκB (-600 bp) and Sp1 binding sites to mediate cytokine and phorbol ester induced MMP-9 promoter activity[133]. In addition, phorbol esters initiate formation of a ternary co-activator complex involving the CREB-binding protein/p300, co-activator associated arginine methyltransferase 1, and the p160 steroid receptor co-activator (SRC) family member GRIP1, which synergistically activates MMP-9 promoter activity[142]. Although NFκB is necessary for the synergistic up-regulation of MMP-9 by cytokines and growth factors, the proximal AP-1 binding site also has a contributory role[127].

In mice, it appears that upstream from the MMP-9 promoter there are elements that regulate cell type specific expression of MMP-9[143]. Although not discussed, several

epigenetic mechanisms including methylation[144] and chromatin remodelling[145] are also involved in transcriptional regulation of MMP-9.

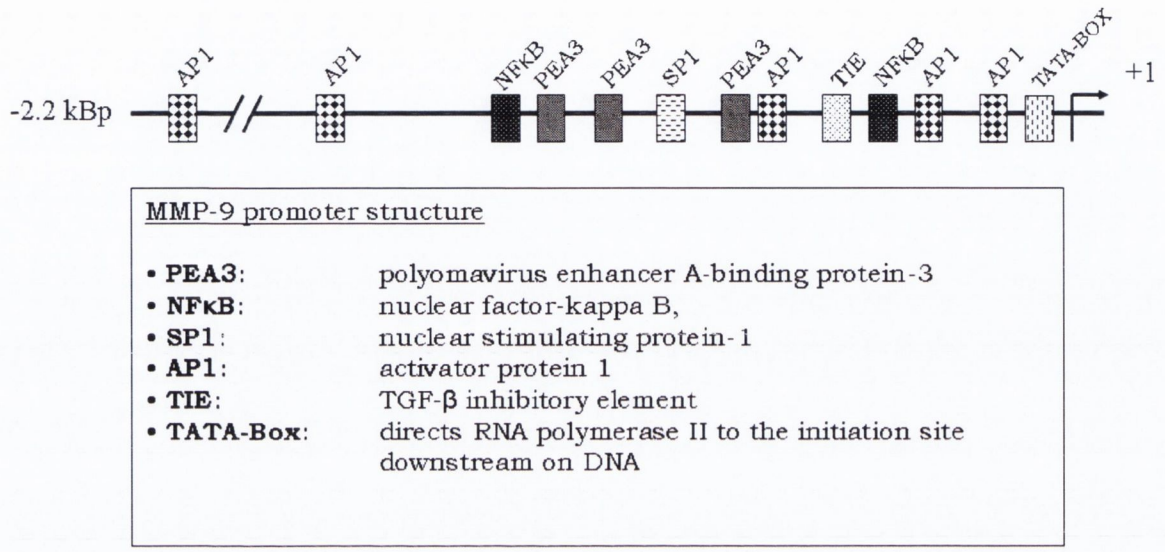


Figure 1.13 Schematic representation of transcription factor binding sites in the human MMP-9 promoter.

Modified from Van den Steen *et al.*, 2002[131].

1.4.4.2 Post-transcriptional regulation of MMPs

Once synthesised, MMPs are stored in granules and either constitutively released or secreted in response to a variety of signals[108]. They are normally released in a latent or proMMP form, which is activated through proteolytic or oxidative cleavage of a conserved cysteine switch in the propeptide domain (Figure 1.14). Proteolytic activation predominantly takes place in the extracellular space and has mainly been studied *in vitro*[112]. However, some proMMPs (e.g. MMP-14, MMP-15, MMP-16) that contain a furin-like enzyme recognition site between the propeptide domain and catalytic domain are activated intracellularly by furin, which is a serine protease[108, 146]. However, the best documented

non-furin mechanism of activation *in vitro* is the activation of proMMP-2 by active MT1-MMP (MMP-14) at the cell surface[112]. ProMMP-2 activation requires the cooperative action of MMP-14 and TIMP-2 in a 1:1:1 stoichiometry *in vitro*, with the amount of TIMP-2 regulating the activation process. The role of TIMP-2 in regulating proMMP-2 activation is supported by *in vivo* data showing that TIMP-2 KO mice only express proMMP-2[147]. However, it appears that MMP-14 is not involved in this process *in vivo* (for review see[112]). Although serine proteases (e.g. plasmin) can also active proMMPs *in vitro*[112], it is unclear if they do so *in vivo* (for review see[112]). With regard to proMMP-9 activation, MMP-3 has been shown to activate it, which in turn is activated by plasmin *in vitro*[148, 149], while elastase, trypsin, MMP-2, MMP-3 activate it *in vitro* (Table 1.1)[131]. Mast cell chymases have also been shown to activate proMMP-2 and-9 *in vitro* and *in vivo*[150, 151]. MMPs can also be activated non-enzymatically by reactive oxygen species (ROS) through oxidation of prodomain thiol groups which promotes autolytic cleavage *in vitro*[112]and *in vivo*[152].

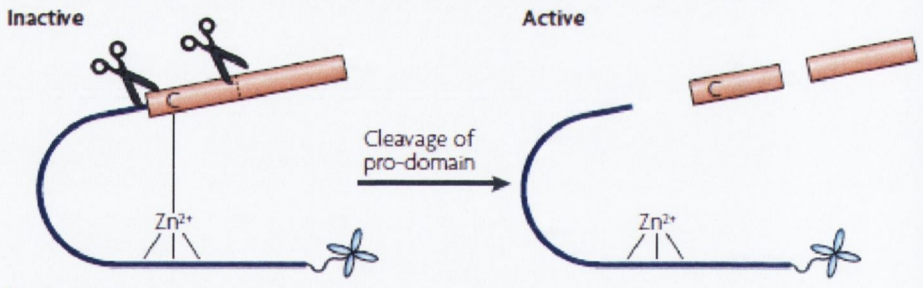


Figure 1.14 Activation of proMMPs.

Matrix metalloproteinases (MMPs) are expressed as proenzymes. A conserved cysteine residue acts as the fourth zinc-binding partner preventing from being catalytic active. The proteolytic removal of the pre- and prodomain results in activation of MMPs. Figure from Page-McCaw *et al.*[121].

1.4.4.3 Regulation of MMP activity

Several endogenous inhibitors regulate MMP activity. The principal inhibitor is α_2-macroglobulin, an endopeptidase inhibitor. α_2-Macroglobulin contains a bait region which is cleaved by proteases (e.g. serine-, cysteine-and metalloproteases), resulting in a conformational change in the structure of α_2-macroglobulin which traps the protease[153]. The trapped enzyme remains active and is restricted from interaction with large protein substrates[153]. Tissue factor pathway inhibitor-2, β-amyloid precursor protein, reversion-inducing-cysteine-rich protein with Kazal motifs (RECK), and chlorotoxin are reported to inhibit MMP activity[117]. With regard to MMP-9, its hemopexin domain and O-glycosylated domain (hinge region) are important in modulating extracellular release through interaction with cargo receptors[154]. It has also been suggested that MMP-9 activity is retained at the cell membrane by interaction with CD44 (a membrane anchor)[155, 156]. However, the most studied group, and probably the group with the greatest influence on MMP activity are the tissue inhibitors of metalloproteinases (TIMPs).

In vertebrates there are four members in this protease inhibitor family: TIMP-1, TIMP-2, TIMP-3 and TIMP-4[117]. TIMPs have a molecular mass between 21-29 kDa and their N-terminal domain is responsible for binding to MMPs in a 1:1 stoichiometry[117]. TIMPs are broad-spectrum inhibitors of MMPs, and their affinity and specificity varies across the different MMPs[157]. For example, TIMP-1 has relatively low affinity for MMP-14, MMP-16, MMP-19, and MMP-24, whereas it binds to MMP-3, MMP-7, and MMP-9 with a higher affinity than TIMP-2[158-162]. In contrast, TIMP-2 has higher affinity for MMP-2[161]. TIMP-3, which is tightly bound to the ECM, has the broadest inhibitory spectrum as it also inhibits members of the disintegrin and metalloproteinases (ADAMs) and ADAMs with thrombospondin motifs (ADAMTS) families[157]. With regard to the MMP-2 and MMP-9 (gelatinases), TIMPs show a unique ability to bind reversibly to the latent isoforms. For

example, TIMP-2, TIMP-3, and TIMP-4 bind to proMMP-2, whereas TIMP-1 and TIMP-3 bind proMMP-9[147, 157]. Interestingly, formation of a TIMP-2/proMMP-2 complex has been identified as a part of the activation complex of proMMP-2[147]. The biological function of the other MMP/TIMP complexes remains to be established. As a result of their ability to inhibit MMP activity, they have important roles in modulating proliferation, migration, invasion and apoptosis of cells. Evidence from studies utilising MMP inhibitors would indicate that some of these effects are likely to be independent of MMP inhibition (for review see[157]). The data regarding degradation MMPs are sparse and unclear. For instance, MMP-9 is degraded in the proteasome but not in the lysosomes of U937 cells[163], while proteasome inhibition decreases MMP-9 abundance in epithelial cells[164]. Furthermore, MMP-1 degradation is associated with the proteasomal path in dermal fibroblasts[165], while MMP-2 abundance is decreased by proteasome inhibition in mice[166].

1.4.5 MMPs in health and disease

Elevated MMP levels and a MMP/TIMP imbalance are indicative of ECM remodelling and are associated with ageing and diseases such as heart failure, liver fibrosis, atherosclerosis, and cancer. Aging is associated with remodelling of the vasculature, which is manifest as increased vascular stiffening. Several studies have shown that age-related changes in the vasculature are associated with increased MMP-2 expression in the aorta or aged rats[167], non-human primates[168] and man[169]. This is reflected in increased plasma levels of MMP-2 and MMP-7, TIMP-1, TIMP-2 and TIMP-4, but decreased MMP-9 plasma levels[170]. The latter is an interesting finding as aging is a major risk factor of cardiovascular disease, hence there is on-going discussion as to whether increased MMP-9 levels is a possible marker/risk factor for cardiovascular disease[171]. Despite this, numerous reports have shown MMP levels are increased in patients and animal models of atherosclerosis, heart failure and myocardial infarction[168, 172-180].

MMPs appear to influence atherosclerotic plaque formation in different ways. In fact, MMP activity may contribute to pathogenesis of atherosclerosis as they degrade ECM components enabling vascular smooth muscle cells to migrate through the elastica interna into the intima of the vessel wall, where they proliferate. This contributes to atherosclerotic plaque growth, which is initiated by structural changes that lead to the accumulation of cells, ECM and lipids in the intimal layer of the diseased artery[181, 182]. Geometrical vascular remodelling can be expansive (outward or positive remodelling) or constrictive (inward or negative remodelling). In outward remodelling, the lumen is preserved and MMP-9 and MMP-2 are associated with destabilisation of the arterial wall. Indeed, rupture of a atherosclerotic plaque appears to occur in arteries that undergo outward remodelling[182]. It is suspected that locally overexpressed MMPs overcome endogenous TIMP inhibition triggering plaque rupture, this initiates thrombus formation and acute vascular events. These events lead to reduced blood flow or vessel occlusion, and subsequent tissue death. In particular, Brown *et al.* found that active MMP-9 is expressed in the lesions of patients with unstable angina, but not in those with stable angina[183], implying a deleterious role of active MMP-9 in this process. In inward or constrictive remodelling, the diameter of the vessel lumen is reduced through hyperplasia of the intima. Although this is considered to be structurally stable, the vessel tends to become stenotic resulting in reduced blood flow.

The maintenance of an appropriate MMP/TIMP balance is required to prevent a shift from a physiological to pathological state. Within the myocardium, the ECM is required for proper alignment of the myocytes and myofibrils, which facilitates optimal myocardial contraction and relaxation within a collagen network. During cardiac remodelling, the collagen network is preferentially degraded by MMP-1. While overexpression of human

MMP-1 in a transgenic mouse model leads to myocardial hypertrophy, it also increased collagen type III deposition, whereas prolonged expression showed a loss of interstitial collagen along with decreased contractile function[184]. This study eloquently demonstrates that disruption of the ECM leads to the initial compensatory mechanisms (myocardial hypertrophy and collagen deposition) and is followed by progressive loss of contractile function as seen in heart failure. The ECM breakdown may result in myocyte hypertrophy due to increased haemodynamic stress, or/and because of interrupted signalling between myocytes. In patients with end stage heart failure MMP-2, -8, -9 and -19 expression, and TIMP (1, 2, 3, 4) expression and collagen type I and III deposition is increased[179] while MMP-1 expression appears to be unchanged[180]. The role of MMP-9 in myocardial infarction is strengthened by data from a knock-out study, which showed that MMP-9 knock-out protected the heart against LV enlargement and collagen accumulation following a myocardial infarction[185]. Nonetheless, the MMP and TIMP profile depends on the underlying etiology (ischemic, dilated, or inflammatory cardiomyopathy)[179] and disease stage[173, 174].

Temporal changes in MMP and TIMP expression patterns in liver disease are eloquently summarised in a review by Hemmann *et al.* 2007[186]. In this review, the authors show that MMP-13 and MMP-3 are transiently increased in the early stages of the disease, while MMP-9, MMP-2 and MMP-14 are increased later. These changes are associated with degradation of the normal liver matrix and accumulation of fibrotic scar tissue, respectively (Figure 1.15). MMP-13 is re-expressed during the recovery phase and is associated with degradation of the fibrotic live matrix. Similar temporal expression patterns are also noted for TIMP-1.

MMP-9 is also an important mediator in inflammation and is highly expressed in lymphocytes, macrophages, neutrophils, and easinophils[131]. Although MMP-9 expression is induced by various cytokines including TNFα, it is also capable of activating TNFα and IL-1β[187, 188]. Data from *in vivo* studies indicate that increased MMP-9 levels are deleterious as MMP-9 knockout protects against traumatic brain injury, allergic airway inflammation, and suppresses cell invasion and metastasis[131].

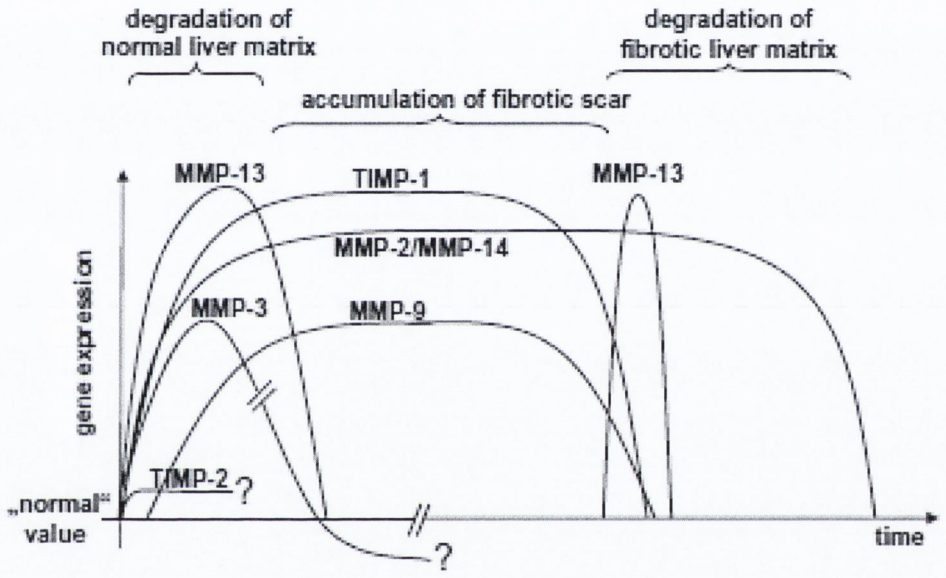


Figure 1.15 A schematic representation of the temporal expression pattern for MMPs and TIMP in the liver following a chronic toxic insult.

Taken from Hemmann *et al.*, 2007[186].

1.5 Adrenoceptors and MMPs

The interaction between adrenergic and matrix metalloproteinase systems is best illustrated with regard to the cardiovascular system. In rat model of heart failure induced by chronic infusion of noradrenaline (NA) MMP-2 activity is increased. This increase is attributed to direct stimulation of cardiac adrenoceptors, since MMP-2 expression is prevented by α-

and β-adrenoceptor blockade with carvedilol, but not when afterload is normalised using nisoldipine[189]. Furthermore, increased MMP-2 abundance following experimental MI is attenuated by metoprolol[190, 191]. Similarly, increased MMP-9 activity and abundance is abolished by atenolol in an angiotensin-II-combined tachycardia pacing induced model of heart failure in pigs[192]. This would indicate the possibility of a novel mechanism by which β-blockade may limit ventricular remodelling and diastolic dysfunction[192]. Further evidence supporting a role of adrenoceptors in modulating MMP abundance include: (i) increased MMP-2 and MT1-MMP in myocytes and conditioned media of myocytes incubated with isoprenaline[193], (ii) a positive correlation between circulating MMP-2 and NA levels in patients with congestive heart failure[194], (iii) MMP inhibition abolishes β-adrenoceptor-stimulated apoptosis[195] and myocyte hypertrophy[175], and (iv) NA up-regulates LPS-induced MMP-9 expression in human monocytes, an effect that is abolished by β_1- but not β_2- or α-blockers[196]. In addition, our group has shown that isoprenaline and phenylephrine differentially induce MMP-9 promoter activity in ECV304 cells[197]. Although, ECV304 cells were originally designated as a human endothelial cell line they are now considered as human bladder cancer epithelial cell. Finally, dibutryl-cAMP and/or forskolin, which activate protein kinase A increase MMP-9 expression in macrophages[198] and trophoblasts[199].

1.6 Protein phosphatases and adrenoceptor regulation

Reversible protein phosphorylation is a major event in the regulation of cell function. The phosphorylation state of a protein is regulated by protein kinases and protein phosphatases. Serine/threonine protein phosphatases (PP) are a major group of protein phosphatases. They are subdivided into three major groups, phosphoprotein phosphatases (PPP), metal-dependent protein phosphatases (PPMs) and aspartate-based protein phosphatases[200]. The

phosphoprotein phosphatases family comprises PP1, PP2A, PP2B (calcineurin), PP4, PP5, PP6, and PP7[200]. PP1 is endogenously regulated by inhibitor-1 (I-1), inhibitor-2 (I-2) and dopamine and cAMP regulated phosphoprotein of 32 kDa (DARPP-32)[200]. PP2A is inhibited by inhibitor 1 of PP2A (I_1^{PP2A}) and inhibitor 2 of PP2A (I_2^{PP2A})[200].

In mammals, four isoforms of the catalytic subunit of PP1 have been identified along with more than 50 regulatory subunits[201]. PP2A is a heterotrimer made of a catalytic C subunit and two regulatory (A and B). The catalytic subunit is encoded by two genes named α and β. The core enzyme is composed of a 36 kDa catalytic subunit (subunit C) and a regulatory subunit (65 kDa, subunit A), that associates with a variety of other regulatory subunits. The core complex can bind to one of several B subunits[201]. In the heart, more than 90% of total PP activity is attributed to PP1 and PP2A[41].

Several studies indicate that there appears to be an inter-relationship between phosphoprotein phosphatases and adrenoceptor signalling (Figure 1.16). In guinea pig heart, short-term β-adrenoceptor stimulation decreases PP1 activity by increasing I-1 phosphorylation[202], while PKA directly phosphorylates and activate I-1[41, 203-205]. As a result of this, PP1-mediated dephosphorylation of phospholamban B is reduced and PKA-mediated contractility is enhanced (positive feedback loop)[203-205]. In contrast, β-adrenoceptor stimulation does not alter PP2A activity in guinea pigs[202], although *in vitro* studies show it transiently increases PP2A activity in cardiomyocytes[206] and keratinocytes[207]. Furthermore, PP2A maintains I-1 phosphorylation (active) at a low level in cardiac myocytes[208].

PP1 is increased in patients with end-stage heart failure[209] suggesting that it may be implicated in disease progression or form part of a compensator process. This is supported

by a transgenic study showing that PP1 over-expressing mice, cardiac function is depressed, the heart is dilated, and the animals die prematurely[203]. Similarly, over-expression of PP2A causes cardiac hypertrophy and decreases contractile function[210], while inhibition of PP2A reduces myocardial infarct size[211]. Interestingly, chronic infusion of isoprenaline also increases PP2A-activity and decreases I-1 expression in the rat heart[212, 213]. I-1 expression is decreased in the failing human heart[214], which may be protective as knockout of I-1 protects against cardiac arrhythmias and isoprenaline-induced myocardial hypertrophy in mice[214]. Together these data indicate that it is not unreasonable to suggest that adrenoceptors may modulate tissue remodelling through effects on phosphoprotein phosphatases. However, whether this is through effects on MMPs, remains to be established.

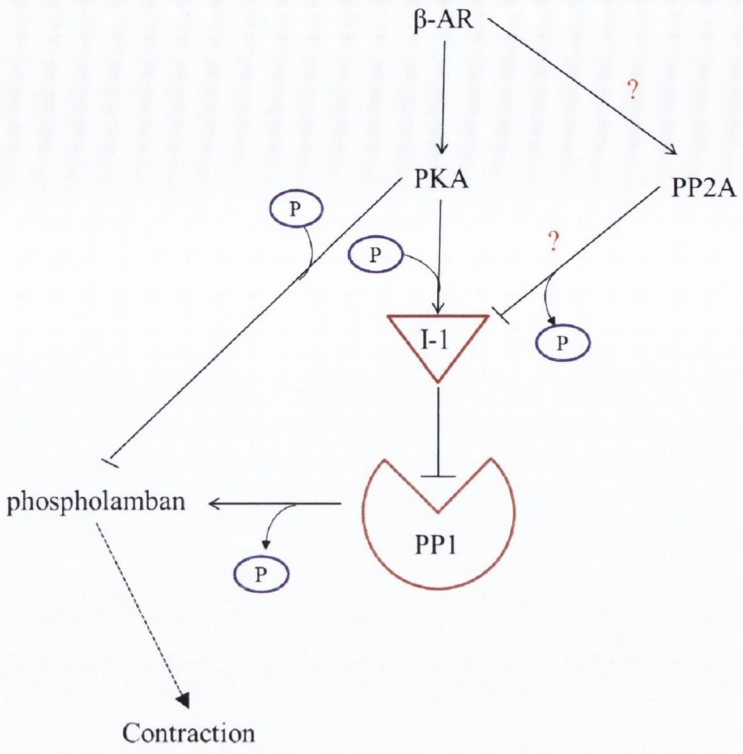
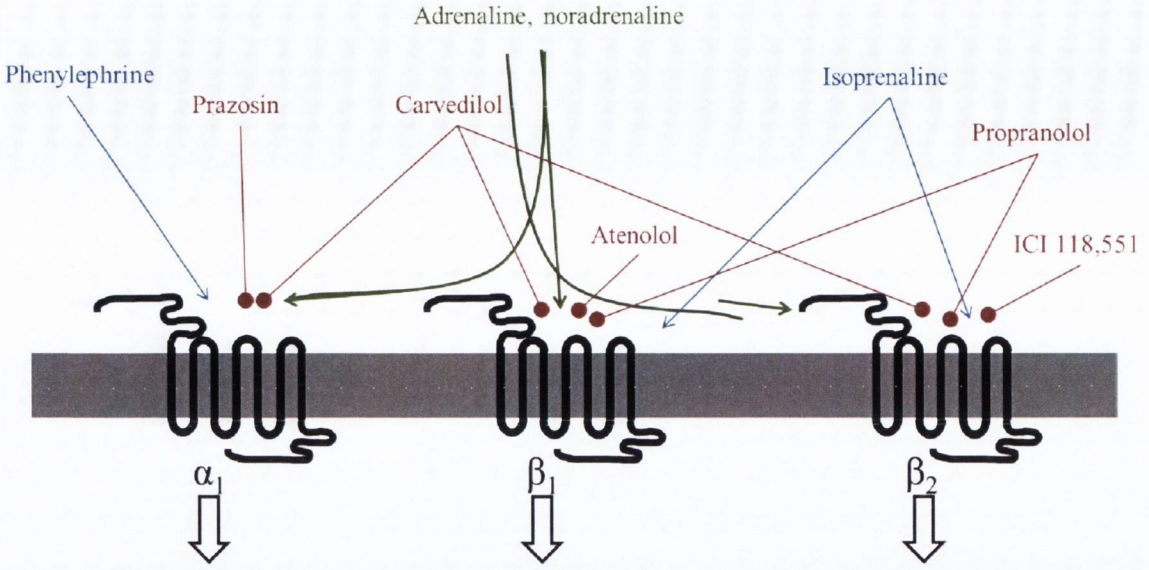


Figure 1.16 Regulation of the β-adrenoceptor signalling pathway by protein phosphatases. β-Adrenoceptor stimulation activates protein kinase A (PKA), leading to phosphorylation of the endogenous inhibitor of protein phosphatase 1 (Inhibitor-1; I-1) and inactivation of protein phosphatase 1 (PP1). As a result of this, PKA-mediated contraction is enhanced as PP1-mediated dephosphorylation of phospholamban B is reduced. This pathway may be counter regulated by β-adrenoceptor mediated activation of protein phosphatase 2A (PP2A), which has been shown to dephosphorylate and inactivate I-1.

1.7 Overview of the Pharmacological reagents used as part of this thesis

During the course of this work, a number of pharmacological reagents were employed to address the involvement of α- and β-adrenoceptors and key signalling pathways. An overview of the physiological effects of α_1-, β_1- and β_2-adrenoceptors along with their natural occurring substrates, adrenaline and noradrenaline, is presented in Figure 1.17. Two synthetic agonists, isoprenaline (4-[1-hydroxy-2-(isopropylamino)ethyl]benzene-1,2-diol), a non-selective β_1- and β_2-adrenoceptor agonist, and phenylephrine ((R)-3-[-1-hydroxy-2-(methylamino)ethyl]phenol)) an α_1-adrenoceptor agonist were also utilised. To help delineate receptor selective effects a number of adrenoceptor antagonist were used: prazosin (2-[4-(2-furoyl)piperazin-1-yl]-6,7-dimethoxyquinazolin-4-amine) an α_1-adrenoceptor antagonist, propranolol ((RS)-1-(isopropylamino)-3-(1-naphthyloxy)propan-2-ol)) a non-selective β-adrenoceptor antagonists, and atenolol ((RS)-2-{4-[2-hydroxy-3-(propan-2-ylamino)propoxy]phenyl} acetamide) and ICI 118,551 (3-(isopropylamino)-1-[(7-methyl-4-indanyl)oxy]butan-2-ol), which are β_1 and β_2-adrenoceptor antagonists, respectively. Carvedilol ((±)-[3-(9H-carbazol-4-yloxy)-2-hydroxypropyl][2-(2-methoxy phenoxy)ethyl]amine) was also employed as it is an α_1-, β_1- and β_2-adrenoceptor antagonist widely used clinically.

In addition, U0126 and SB202190, two pharmacological reagents targeting MAPK signalling pathways were employed. U0126 (1,4-diamino-2,3-dicyano-1,4-bis[2-aminophenylthio]butadiene) selectively inhibits the activation of MEK1 and MEK2 MAPK and thereby affects its downstream targets ERK1/2 MAPK[215]. SB202190 (4-(4-Fluorophenyl)-2-(4-hydroxyphenyl)-5-(4-pyridyl)-1H-imidazole) selectively inhibits p38 MAPK activity in cell based assays. Both reagents have been shown to have no or little effects on other targets related to MAPK signalling pathways[215].



Increases smooth muscle contraction in vasculature and genitourinary systems	Increases heart rate and force of contraction	Relaxation of smooth muscle cells in the vasculature, bronchus and uterus
Maintains basal blood pressure and responses to exogenous agonists	Stimulates renin secretion	Increases heart rate and force of contraction
Increases liver glycogenolysis, heart rate and force of contraction	Relaxation of coronary arteries and gastrointestinal smooth muscles	Increases liver glycogenolysis

Figure 1.17 Overview of the physiological actions of drugs targeting adrenoceptors.

1.8 Aims

The overall scope of this thesis is to investigate if adrenoceptors regulate MMP-9 abundance in murine embryonic and human cardiac ventricular fibroblasts and to delineate the underlying signalling pathways. In particular, key components of β-adrenoceptor signalling are characterised in fibroblasts. Time and concentration dependent effects of α_1- and β-adrenoceptor activation on NFκB regulation are examined, as it represents a fundamental transcriptional regulator of MMP-9 expression and is implicated in β-adrenoceptor signalling. The concentration and temporal effects of adrenoceptor stimulation on MMP-9 promoter regulation, mRNA, and enzyme activity are also studied.

Based on the emerging research linking β-adrenoceptor modulation to phosphoprotein phosphatases, the effects of phosphoprotein phosphatase inhibition on MMP-9 abundance in fibroblasts are examined. Regulatory cis-elements on the MMP-9 promoter are investigated by mutational analysis, along with the potential involvement of the p38 and ERK1/2 MAPK signalling pathways. The effect of β-adrenoceptor agonists on phosphoprotein phosphatase modulated MMP-9 abundance is considered, and their modulation by downstream targets of the β-adrenoceptor signalling is considered.

Increasing evidence indicates that β-adrenoceptors are able to modulate TNFα abundance. As TNFα is well documented to regulate MMP-9 expression, it is not unreasonable to suggest β-adrenoceptor antagonists may modulate tissue remodelling through their anti-inflammatory action. Therefore, the third study considers the effects of α_1-and β-adrenoceptor antagonists on TNFα mediated MMP-9 and TIMP-1 abundance in NIH3T3 fibroblasts. Effects on NFκB promoter activity and transcriptional regulation of MMP-9 are considered. The role of key regulatory cis-elements of the MMP-9 and TIMP-1 promoters is also investigated.

Chapter 2.

Materials

2.1 Materials

Table 2.1 compromises the main employed pharmacological reagents, recombinant proteins, and materials with their suppliers. Pharmacological reagents, chemicals, and proteins that are not mentioned were obtained from Sigma-Aldrich.

Table 2.1 Pharmacological reagents, recombinant proteins, and materials.

Compound	Supplier
(±)-Carvedilol	BIOTREND GmbH
(±)-ICI 118,551 hydrochloride	Sigma-Aldrich
(±)-Isoprenaline hydrochloride	Sigma-Aldrich
(±)-Propranolol hydrochloride	Sigma-Aldrich
(RS)-Atenolol	BIOTREND GmbH
(R)-(−)-Phenylephrine hydrochloride	Sigma-Aldrich
ChemiBlot™ Molecular Weight Markers	Millipore
DNA size standard	Finnzymes
Human liver DNA	Biochain
HyperLadder IV	Bioline
Milk powder	Marvel
NFκB-Inhibitor III	Calbiochem
Okadaic acid, ammonium salt	Calbiochem
Opti-MEM	Gibco
Prazosin hydrochloride	Sigma-Aldrich
proMMP-9 (mouse)	Anaspec
TNFα (mouse, human)	Prospec
U0126	Calbiochem

2.2 Consumables

Table 2.2 Consumables.

Product	Manufacturer
24-well plate, sterile	Sarstedt
3MM ® chromatography paper	Whatman
48-well plate, Nunclon™Δ Surface, sterile	Nunc
96-well plate, Nunclon™Δ Surface, sterile	Nunc
6-well plate, sterile	Sarstedt
Cell scraper, sterile	Sarstedt
Cryogenic vials, sterile	Corning
Hybond™-P, Hydrophobic polyvinylidene difluoride (PVDF) membrane	GE Healthcare
Filter, 0.22 μm, sterile	Millipore
Medical X-ray film	Kodak
MicroAmp® Fast Optical 96-Well Reaction Plate	Applied Biosystems
MicroAmp® Optical Adhesive Film	Applied Biosystems
Petri dish, sterile	Sarstedt
White 96-well plates	Greiner Bio-One
Serological pipettes, sterile	Corning
Syringes and needles, sterile	Becton, Dickinson and Company
T75-cell culture flask, Nunclon™Δ Surface, filter cap, sterile	Nunc

2.3 Enzymes

Table 2.3 A list of enzymes and their suppliers used.

Enzyme	Company
Deoxyribonuclease I, Amplification Grade	Invitrogen, Carlsbad, USA
HindIII Restriction Endonuclease	New England Biolabs, Ipswich, USA
M-MLV Reverse Transcriptase	Sigma-Aldrich, Saint Louis, USA
Phusion™ high-fidelity DNA Polymerase	Finnzymes, Wobrun, USA
T4 DNA Ligase	Promega, Madison, USA
Thermo-Start™ *Taq* DNA polymerase	Thermo Fisher Scientific (Abgene), Epsom, UK
XhoI Restriction Endonuclease	New England Biolabs, Ipswich, USA

2.4 Prokaryotic cells

In the experimental process of this study the bacterial strain TOP 10 *E.coli*, which was a kind gift of Dr. Deirdre Ni Eidhin, was used. The genotype of the TOP 10 *E.coli* strain is F^- *mcr*A Δ(*mrr-hsd*RMS-*mcr*BC) φ80*lacZ*ΔM15 Δ*lacX*74 *rec*A1 *ara*D139 Δ(*ara-leu*) 7697 *gal*U *gal*K *rps*L (Str^R) *end*A1 *nup*G λ-.

2.5 Eukaryotic cells

NIH3T3-cells:

NIH3T3 cells are mouse embryonic fibroblasts, which originated from a SWISS mouse embryo and spontaneously immortalized[216]. These fibroblasts grow adherent and have lost their contact inhibition. NIH3T3 fibroblasts were obtained from the European Collection of Cell Cultures.

Human cardiac fibroblasts:

The human cardiac fibroblasts are from the adult ventricle of the human heart (HCVF). These cells were a kind gift from Dr. Laragh Tormey who purchased them from TCS Cellworks, UK. HCVFs grow adherent and have a limited lifespan of 15 population doublings.

LX-2 cells:

LX-2 cells are human hepatic stellate cells, which were prepared through spontaneous immortalisation in low serum conditions and grow adherent[217]. Prof. Scott L. Friedman (Mount Sinai School of Medicine, New York) kindly donated these cells.

2.6 Antibodies

Table 2.4 A list of antibodies, their source, conjugation, dilution and suppliers.

Target	Source	Conjugate	MW (kDa)	Dilution	Supplier
β-actin	mouse	HRP	43	1:7500	Santa Cruz
β-arrestin 2 (C16D9)	rabbit	-	50	1:500	Cell Signaling Technology
IκBα (L35A5)	mouse	-	39	1:1000	Cell Signaling Technology
mouse IgG	horse	HRP		1:1000	Cell Signaling Technology
phospho-CREB	rabbit	-	43	1:500	Thermo Fisher Scientific
phospho-NFκB p65 (Ser^{536})	rabbit	-	65	1:1000	Cell Signaling Technology
phospho-p38 MAPK (Thr^{180}/Tyr^{182})	rabbit	-	43	1:1000	Cell Signaling Technology
phospho-p44/p42 MAPK (Thr^{202}/Tyr^{204})	rabbit	-	42, 44	1:1000	Cell Signaling Technology
rabbit IgG	goat	Dylight 488		1:500	Thermo Fisher Scientific
rabbit IgG	swine	HRP		1:1000	Dako

2.7 DNA and RNA

2.7.1 Oligonucleotides

2.7.1.1 PCR primers

5' -end deletions of the MMP-9 promoter were constructed using forward primers (Table 2.5), and a common reverse primer corresponding to the starting position +20 up to +1 of the MMP-9 promoter (Table 2.5).

Table 2.5 Primers for MMP-9 promoter constructs.

Starting Position	Primer Sequence
+20	5'-CCCAAGCTTTGGTGAGGGCAGAGGTGTCT-3'
-523	5'-CCGCTCGAGAAGGCTGTCAGGGAGGGAAAAAGA-3'
-540	5'-CCGCTCGAGAGAGGAAGCTGAGTCAAAGAAGGC-3'
-571	5'-CCGCTCGAGCATTCCTTCCGCCCCCAGAT-3'
-657	5'-CCGCTCGAGTACTGTCCCCTTTACTGCCCTGAA-3'
-1285	5'-CCGCTCGAGGGGAGGGAGGCTTGGCATAA-3'

2.7.1.2 Real-time RT-PCR primers

All RT-PCR primers were purchased from Qiagen as part of a predesigned QuantiTec Primer Assay. They were selected according to species and target gene of interest (Table 2.6).

Table 2.6 QuantiTec Primers for real-time RT-PCR.

Target	Species	Detected transcript	Amplicon length	Product code
MMP-9	human	NM_004994	115 bp	QT00040040
GAPDH	human	NM_002046	119 bp	QT01192646
MMP-9	mouse	NM_013599	84 bp	QT00108815
β-actin	mouse	NM_007393	77 bp	QT01136772

2.7.1.3 siRNA

The siRNAs employed in this study were purchased from Dharmacon, Thermo Fisher Scientific. ON-TARGETplus SMARTpool siRNAs are double-stranded, chemically synthesised desalted oligonucleotides. Both sense and antisense strands contain UU for a 3'-overhangs. Furthermore, these siRNAs are developed through seed-region analysis to reduce miRNA-induced off-target effects. The ON-TARGETplus SMARTpool for murine β-arrestin 2 contains a mixture of 4 siRNA targeting NM_145429. Furthermore, the negative control ON-TARGETplus Non-targeting Pool was ordered.

2.7.2 Vectors and eukaryotic expression vectors

Table 2.7 A list of vectors, their properties, and suppliers used.

Vector	Specific properties	Supplier
pGEM®-T Easy	3'-T overhang, multiple cloning site (MSC), linearised and high-copy-number vector, blue-white selection, Amp^r	Promega, Madison, USA
pGL-3 Basic	lacks eukaryotic promoter and enhancer sequences, MCS, firefly luciferase coding region (*luc*+), Amp^r	Promega, Madison, USA
pGL-3 Control	SV40 promoter and enhancer sequences, MCS, *luc*+, Amp^r	Promega, Madison, USA
pNFκB-Luc	Enhancer element sequence for NFκB binding site ((T**GGGGACTTTCC**GC)$_5$), *luc*+, Amp^r	Agilent Technologies, Santa Clara, USA
pRL-CMV	CMV immediate early enhancer/promoter region, renilla luciferase coding region (R*luc*), Amp^r	Promega, Madison, USA

2.8 Equipment

Table 2.8 A list of equipment and supplier.

Equipment	Company, Model
7900HT Fast Real-time PCR System	Applied Biosystems
Analytical balance	Mettler, AE240
Autoclave	Dixon
Automated microscopy	GE Healthcare, IN Cell Analyzer 1000 HCA
Automated pipettes	Gilson, Inc. (2 µl, 10 µl, 100 µl, 200 µl, 1000 µl, 5000 µl, Pipetman Ultra 8-channel (20–300 µl))
Centrifuge	Hettich Zentrifugen, EBA 12R/mikro 22R
Digital imaging	Fujifilm life science, LAS-4000
Inverted microscope	VWR, VistaVision™
Freezer (-80°C)	Thermofisher Scientific, Revco Value Plus
Gel documentation system	Syngene, GeneGenius
Gel electrophoreses system	Bio-Rad, Mini-Protean
Incubator (37 °C, 5% CO_2, 95 % rh)	Memmert, Inco2
Lamina flow hood	Mason Technology, BioBan 48
Luminometer	Thermofisher Scientific, Fluoroskan AscentFL
Microplate reader	BioTek, EL 808
Microplate washer	BioTek, ELx405
Micro-Volume UV-Vis Spectrophotometer	Thermofisher Scientific, Nanodrop ND 8000
Neubauer haemocytometer, improved	BRAND GMBH + CO KG, Blaubrand®
pH meter	Mettler-Toledo Inc., MP230
Thermocycler	MJ Research Inc, PTC-100

Chapter 3.

Characterisation of adrenoceptor signalling in human and murine fibroblasts: Implications for MMP-9 Regulation

3.1 Introduction

Cardiovascular remodelling is a key component to the development of hypertension and heart failure, and involves numerous cell types including fibroblasts, cardiomyocytes, smooth muscle cells, and endothelial cells. Nevertheless, fibroblasts are recognised as a pivotal cell type in this process as they are involved in the regulation and synthesis of extracellular matrix (ECM)[82, 218]. Within the heart, they respond to mechanical, chemical and electrophysiological signals[218, 219], and contribute to myocardial fibrosis[219]. The latter reflects a delicate balance between collagen synthesis and degradation, and is regulated by matrix metalloproteinases (MMPs) and tissue inhibitors of metalloproteinases (TIMPs)[177]. MMP activity is tightly controlled at the levels of transcription, activation of the precursor zymogens, through contact with components of the ECM, and by binding to their endogenous TIMPs.

Cardiovascular remodelling is characterised by fibroblast proliferation and accumulation of fibrillar collagen in response to an insult (e.g. ischemia, pressure or volume overload), resulting in adverse remodelling. This culminates in distortion of the tissue structure and increased tissue stiffness. For instance, ischemia or the loss of pump function lead to increases in the sympathetic drive in order to maintain cardiac output. This increase is also associated with cardiac myocyte hypertrophy in order to cope with the increased cardiac demand and contributes over time to cardiac stiffness. Cardiac hypertrophy is also promoted by ECM proteins and growth factors secreted by fibroblast[219]. Nonetheless, it appears that immune cells are also involved in the early stages of myocardial fibrosis as macrophages were found to accumulate and co-localise with fibroblasts in the perivascular space in a rat model of hypertension[223]. This occurred along with increased fibroblast proliferation and TGF-β1 expression. As macrophages are a major source of cytokines and growth factors, they can activate fibroblasts and vascular smooth muscle cell proliferation

along with increased MMP secretion. However, vascular endothelial cells are also secrete mitogens (e.g. endothelin-1, angiotensin II) which stimulate proliferation of neighbouring fibroblast and vascular smooth muscle cells resulting in increased collagen synthesis. These pathological characteristics are displayed in heart failure, which is a common final pathway of a multitude of disease processess[41]. The importance of the sympathetic drive in the progression of heart failure is highlighted in a β_1-and β_2-adrenoceptor knock-out mouse model[221]. These mice have a decreased cardiac hypertrophic and fibrotic phenotype after pressure overload and angiotensin II infusion than wild type mice. In agreement, chronic infusion of isoprenaline (β_1- and β_2-adrenoceptor agonist) induces myocardial fibrosis and hypertrophy in several animal models[189, 222], supporting a role of β-adrenoceptors in the development of myocardial fibrosis.

Although several species of MMP are present in the myocardium, the gelatinases, MMP-2 and MMP-9, preferentially degrade basement membrane components, which form the interface between myocytes, fibroblasts, and the extracellular matrix. Therefore, they are well positioned to modulate cardiac function and contribute to fibrotic remodelling. Indeed, MMP-2 (constitutive) and MMP-9 (inducible) abundance is increased in a number of experimental models of heart failure, as well as in the clinical condition[173, 224]. In rats, chronic infusion of noradrenaline increases MMP-2 activity through direct stimulation of cardiac adrenoceptors. This is based upon the increase being prevented by carvedilol (α- and β-adrenoceptor antagonist), but not when afterload is normalised by nisoldipine[189]. Other studies also support a role for adrenoceptors in modulating MMPs: (i) isoprenaline increases MMP-2 in myocytes and their conditioned medium[193], and (ii) in human monocytes noradrenaline up-regulation of LPS-induced MMP-9 expression is abolished by β_1- but not β_2- or α-adrenoceptor antagonists[196].

Alpha and β-adrenoceptors are members of the G-protein-coupled-receptor family, with α_1-adenoreceptors being coupled to $G\alpha_q$ and β-adrenoceptors coupled to $G\alpha_s$. While α_1-adrenoceptor stimulation activates phospholipase C and increases intracellular Ca^{2+} levels, β-adrenoceptors increase cAMP levels through activation of adenylyl cyclase. In a classical signal transduction cascade the increase in cAMP leads to the activation of protein kinase A which phosphorylates cAMP response binding element (CREB) leading to its translocation to the nucleus. However, cAMP can activate non-classical signalling pathways, including extracellular signal-regulated kinases 1/2 (ERK 1/2) and p38 MAPK pathways. Both of these pathways converge on a common downstream target mitogen- and stress-activated protein kinase (MSK1)[225, 226], which in turn can activate NFκB[227]. Furthermore, α_1- and β-adrenoceptor stimulation increases MMP-9 promoter activity through a 762-bp region of the MMP-9 promoter (from 523 to 1285 bp), which contains a NFκB transcription factor binding site, in ECV304 cells[197]. However, we do not know what upstream signalling pathway(s) couples adrenoceptors to MMP-9 expression, or if this phenomenon occurs in fibroblasts. Therefore, the aims of the first study were to: 1) characterise key aspects of β-adrenoceptor signalling in murine fibroblasts (NIH3T3) and human cardiac ventricular fibroblasts, and 2) investigate if β-adrenoceptors modulate MMP-9 expression in fibroblasts.

3.2 Methods

3.2.1 Generation of the MM-9 promoter constructs

The MMP-9 promoter and 5'-end deletion mutants were produced by polymerase chain reaction (PCR) from human liver DNA of a healthy 23-year old Caucasian male (Biochain) using sequence specific primers (Genersch *et al.*, 2000; Table 3.1)[228]. The primers contain restriction sites for *Xho*I and *Hind*III, and are analogous to the starting position +20 up to +1 bp, and -523, -540, -571, -657 and -1285 bp downstream of this. In the following procedure, the MMP-9 promoter, and its 5'-end deletion inserts are referred to as p1285, p657, p571, p540, and p523. Their predicted sizes were determined using Basic Local Alignment Search Tool (BLAST) by alignment of the primers to NCBI Accession NT_011362.10 and are 1312 bp, 683 bp, 595 bp, 566 bp, and 549 bp, respectively.

PCR-products were amplified using *Phusion*™ high-fidelity DNA polymerase. The PCR reaction mix was prepared on ice and consisted of 1X Phusion HF buffer, 200 µM dNTPs, 0.5 µM of the forward and reverse primers, 1 mM $MgCl_2$, 0.02 U/µl *Phusion*™ DNA polymerase, and 200 ng template DNA in a final volume of 50 µl. The PCR was performed on a MJ Research Inc, PTC-100 thermocyler using an optimised program each primer pair (Table 3.2). Following addition of a 6X gel loading dye (10 mM Tris HCl, pH 8.0, 1 mM EDTA, 0.25% w/v bromophenol blue, 0.25% w/v Orange G, 30% v/v glycerol) the PCR products and DNA molecular ladder (Finnzymes) were separated on a agarose gel (1% w/v agarose, 40 mM Tris acetate, pH 8.5, 1 mM EDTA, 0.1 mg/ml ethidium bromide) by electrophoresis at 80 mA. PCR-products were visualised under UV light, cut from the gel, and purified (MinElute Gel Extraction Kit; Qiagen). The concentrations of the PCR-products were determined by spectrophotometry and only products with an A_{260}/A_{280} = 1.8 to 2.0 were used.

Table 3.1 Primers for MMP-9 promoter constructs.

Starting Position	*Primer Sequence*
+20	5'-CCCAAGCTTTGGTGAGGGCAGAGGTGTCT-3'
-523	5'-CCGCTCGAGAAGGCTGTCAGGGAGGGAAAAAGA-3'
-540	5'-CCGCTCGAGAGAGGAAGCTGAGTCAAAGAAGGC-3'
-571	5'-CCGCTCGAGCATTCCTTCCGCCCCCAGAT-3'
-657	5'-CCGCTCGAGTACTGTCCCCTTTACTGCCCTGAA-3'
-1285	5'-CCGCTCGAGGGGAGGGAGGCTTGGCATAA-3'

Table 3.2 PCR-program for the desired MMP-9 promoter constructs.

Conditions	**p523**	**p540**	**p571**	**p657**	**p1285**
Initial Denaturation	1 min, 98°C	1 min, 98°C	1 min, 98°C	1 min, 98°C	1 min, 98°C
Denaturation	10 sec, 95°C	10 sec, 95°C	10 sec, 95°C	10 sec, 95°C	10 sec, 95 °C
Annealing	30 sec, 78°C	30 sec, 82°C	30 sec, 86°C	30 sec, 83°C	30 sec, 82°C
Extension	30 sec, 72°C	30 sec, 72°C	30 sec, 72°C	30 sec, 72°C	1 min, 72°C
			35 cycles		
Final Extension	10 min, 72°C	10 min, 72°C	10 min, 72°C	10 min, 72°C	10 min, 72°C

The purified PCR-products were "A-tailed" using Thermo-Start Taq DNA polymerase (0.2 U/µl) in a reaction mix consisting of the Thermo-Start PCR Buffer, 200 µM dATP, 1.5 mM $MgCl_2$ and 100 ng PCR product in a final volume of 40 µl. The DNA polymerase was activated at 95°C for 15 min and then held at 70°C for 20 min.

Following A-tailing, the PCR products were ligated into a pGEM-T Easy vector in a reaction mixture composed of the Rapid Ligation Buffer, 50 ng pGEM®-T Easy vector, 3 U/µl T4 DNA Ligase and the required amount of PCR product (16 hrs at 4°C). The amount of PCR-product used in the ligation reaction was calculated according to the following formula and a molar ratio of 3:1 insert:vector was found to be optimal[229]:

$$amount\ of\ the\ insert\ (ng) = \frac{amount\ of\ vector\ (ng) \times size\ of\ the\ insert\ (kb) \times 3}{size\ of\ the\ vector\ (kb)}$$

Chemically competent TOP10 *E.coli* (transformation efficiency of $2.5x10^8$ cfu/µg DNA) were transformed with the modified vector by heat shock (42°C for 30 seconds) and immediately placed on ice for 5 min. A negative control (empty vector) was also included. Transformed cells were then allowed to recover for 1 hr in BHI medium before being used to inoculate LB agar plates (15 g/l LB agar, 100 µg/ml ampicillin, pre-incubated with 100 µl of 100 mM IPTG and 20 µl of 50 mg/ml X-Gal for 30 min at 37°C). Plates were then incubated at 37°C overnight and several positive white colonies were lifted and grown in LB-medium (20 g/l LB medium, 100 µg/ml ampicillin) at 37°C with shaking (100 rpm, overnight).

The pGEM-T easy plasmids were isolated using a mini plasmid preparation. In brief, overnight cultures (1.5 ml) were centrifuged at 5000 rpm for 5 min and the pellets were re-

suspended in 100 µl of Mini-Buffer P1 (50 mM Tris HCl, pH 7.5, 10 mM EDTA). To this the Mini-Buffer P2 lysis buffer was added (100 µl; 1% w/v SDS, 0.2 M NaOH), the tubes gently inverted, and incubated for less than 5 min at room temperature. Proteins were precipitated by addition of Mini-Buffer P3 (100 µl; 1.32 M Sodium acetate, pH 4.8), the tubes inverted, and incubated on ice for 15 min. Samples were cleared by centrifugation (20 min at 13.000 rpm, 4°C). The supernatants were removed and the DNA precipitated by addition of isopropanol (0.7 volumes) and collected by centrifugation (20 min, 13.000 rpm, 4°C). The DNA pellets were washed with 70% (v/v) ethanol, centrifuged (10 min, 13.000 rpm, 4°C), and the ethanol was removed. DNA pellets were dissolved in TE-RNAse A buffer (10 mM Tris-HCl, pH 8.0, 1 mM EDTA, 0.1 mg/ml RNAse A) and stored at -20°C. Several plasmids were tested by restriction enzyme digestion to ensure they contained the desired MMP-9 promoter insert. Plasmid DNA (300 ng) was digested with 0.5 U/µl of *Xho*I and 0.5 U/µl *Hind*III in a NEBuffer 2 for 1hr at 37°C. Restriction digests were then separated on a 1% (w/v) agarose gel and visualised under UV light.

Positive clones were grown in LB-Amp medium at 37°C (150 rpm, overnight), and the plasmids were extracted and purified using a GenElute™ Endotoxin-Free Plasmid Midi/Maxi Kit (Sigma-Aldrich) according to the manufactures instructions. The fidelity of the MMP-9 promoter insert was verified by sequence analysis using T7 and SP6 promoter sequencing primers (DNA Sequencing Facility, University of Cambridge, UK). The pGEM®-T Easy plasmids containing the desired inserts were digested with *Xho*I and *Hind*III, separated by gel electrophoreses and purified by gel extraction. The pGL3-Basic vector was digested with *Xho*I and *Hind*III, and prevented from recombining through dephosphorylation of the 5'- phosphate groups by calf intestinal alkaline phosphatase (0.5 U per µg DNA) for 1 hr at 37°C. The linearised pGL3-vector and MMP-9 promoters were annealed and ligated at a molar ratio of 3:1. The resulting plasmid was subcloned into

TOP10 *E.coli* as described above. Insertion and orientation were verified by restriction enzyme digestion with either *Xho*I/*Hind*III (insertion) or *Kpn*I/*Hind*III (orientation). The cloned plasmids are referred to as p523-luc, p540-luc, p571-luc, p657-luc, and p1285-luc from here on.

3.2.2 Cell culture

NIH3T3 fibroblasts and human adult cardiac ventricular fibroblasts (HCVF) were cultured in Dulbecco's Modified Eagle's Medium (DMEM, 4500 mg/l glucose) supplemented with either 10% new born calf serum (NIH3T3) or 10% foetal bovine serum (HCVF) and 1 mM sodium pyruvate, 2 mM glutamine and 100 U/ml penicillin, 100 mg/ml streptomycin at 37°C, 5% CO_2. Cells were subcultured every 2-3 days using Trypsin-EDTA solution. All cell lines were regularly tested for mycoplasma contamination using MycoAlert® Mycoplasma Detection kit (Lonza). In order to determine cell number and viability, cells were stained with Trypan Blue (0.4% w/v; 1:5) for 5 min and counted (Neubauer haemocytometer). Cell number per ml of culture medium was calculated using the following equation:

$$Cells/ml = \frac{number\ of counted\ cells \times 10000 \times 6}{8\ squares \times 5}$$

3.2.3 Preparation of pharmacological reagents

All drug stocks were prepared in water, except the NFκB-Inhibitor III (C_{final}= 0.1% v/v DMSO), prazosin hydrochloride (C_{final}=0.4% v/v DMSO) and (±)-isoprenaline hydrochloride, which was dissolved in sterile millipore water containing vitamin C (antioxidant, C_{final}=100 µM). All working solutions were prepared in medium and cells exposed to the drugs for 24 hrs unless otherwise indicated.

3.2.4 Measurement of cAMP levels

NIH3T3 and HCVF fibroblasts were seeded in 6-well plates at a density of $3x10^5$ cells/well and changed to serum free DMEM 1 hr before experimentation. Cells were treated for 30 min with 3-isobutyl-1-methylxanthine (IBMX, 100 μM) ± propranolol (10 μM), or medium prior to addition of isoprenaline (1 μM), forskolin (1 μM, positive control), or medium (control) for 10 min. Cells were lysed in HCl (250 μl, 0.1 M) for 30 min and centrifuged at 600 g for 5 min. cAMP levels in the samples were measured using a cAMP Enzyme Immunoassay Kit (Sigma-Aldrich) according to the manufactures instructions. In brief, all samples were acetylated to increase sensitivity of the assay and analysed in duplicate along with the cAMP standards. The optical density was read at 405 nm with a reference wavelength of 540 nm. The cAMP concentration was calculated by subtracting the average optical density (OD) of the non-specific binding sample from each sample and standard. The cAMP standards were calculated as a percentage of the maximum binding sample. cAMP concentration of the unknowns was calculated through interpolation from the cAMP concentration response curve.

3.2.5 Assessment of cell viability (MTT-assay)

NIH3T3 fibroblasts were seeded at a density of $2x10^4$ cells/well in 48-well plates. Cells were allowed to attach for 24 hrs and the medium changed to phenol-red free DMEM containing 5% charcoal stripped foetal calf serum 18 hrs prior to the start of the experiment. Cells were treated with (±)-isoprenaline hydrochloride (ISO, 0.1 μM and 1 μM), (R)-(−)-phenylephrine hydrochloride (PE, 10 μM and 50 μM), vitamin C (VitC, 100 μM), doxorubicin hydrochloride (DOX, 1 and 5 μM) and medium for 24 hrs. Prior to the end of the incubation time thiazolyl blue tetrazolium bromide/PBS solution (5 mg/ml; 14 μl) was added to each well and incubated for one hour. Supernatants were gently removed and the

crystals dissolved in DMSO (100 µl). The absorption was measured at a wavelength of 540 nm with a reference wavelength of 650 nm using a mircoplate reader (BioTek, EL 808).

3.2.6 Gelatin-zymography

NIH3T3 fibroblasts were seeded at a density of $4x10^4$ cells/well in 24-well plates and allowed to attach for 24 hrs. Medium was changed to phenol-red free DMEM containing 5% charcoal stripped foetal calf serum 18 hrs prior to the start of the experiment. Cells were exposed to either TNFα (100 ng/ml), ISO (1 µM and 10 µM), PE (10 µM and 50 µM), VitC (100 µM), or medium alone (control). The conditioned medium was collected after 24 hrs, cleared by centrifugation (5000 g; 5 min), and mixed with a 6X non-reducing Laemmli sample buffer (0.35 mM Tris HCl, pH 6.8, 30% v/v glycerol, 10% w/v SDS, 0.06% w/v bromophenol blue). Equal volumes of the samples along with murine recombinant proMMP-9 (1 ng) were subjected to electrophoresis on an 8% SDS-polyacrylamide gel (0.75 cm thickness; 5% stacking gel; Table 3.3) co-polymerised with 0.1% (w/v) gelatin. Gels were run at 110 V for 1.5 hrs in a buffer of composition: 25 mM Tris base, 192 mM Glycine, 0.1% (w/v) SDS. Gels were then washed in Triton X-100 (2.5% v/v) for 30 min and incubated for 18 hrs at 37°C in an incubation buffer of composition 50 mM Tris HCl, pH 7.6, 10 mM $CaCl_2$, 50 M NaCl. Gels were rinsed in destain (1:3:6; glacial acetic acid: methanol: dH_2O) followed by staining (0.05% w/v coomassie brilliant blue R250 in destain solution) for 1 hr followed by destaining (5 min). Gelatinolytic activity, clear band on blue background, was quantified using a Gel documentation system. Samples were normalised to control (medium). To ensure that non-specific protease activity did not confound the results, identical gels were incubated in either incubation buffer or one supplemented with 20 mM EDTA.

Table 3.3 Composition of the resolving and stacking gels used for gelatin-zymography.

	Resolving gel (8%)	Stacking gel (5%)
dH_2O	2.6 ml	1.4 ml
Gelatin (5 mg/ml)	2 ml	-
30% (w/v) Acrylamide/Bis-acrylamide (29:1)	2.7 ml	0.33 ml
Tris HCl (1.5 M, pH 8.8)	2.5 ml	-
Tris HCl (1 M, pH 6.8)	-	0.25 ml
10% (w/v) SDS	100 µl	20 µl
10% (w/v) ammonium persulfate	100 µl	20 µl
TEMED	6 µl	2 µl

3.2.7 Real-time RT-PCR

3.2.7.1 RNA isolation and RT-PCR

NIH3T3 fibroblasts and HCVF cells were grown and treated as described previously (section 3.2.6). Total cellular RNA was extracted using TRI REAGENT™. In brief, cells were lysed in the wells by addition of TRI reagent (200 µl/well) and the content of the wells transferred to sterile eppendorf tubes. Chloroform (40 µl) was added to each sample, mixed for 15 seconds, and incubated at room temperature for 15 min. The aqueous and organic layers were separated by centrifugation (12,000 g, 15 min, 4°C) and the colourless upper aqueous phase containing the RNA was carefully transferred to a clean tube. RNA was precipitated by addition of isopropanol (100 µl) and pelleted by centrifugation (12,000 g, 10 min, 4°C). The pellet was washed with 75% (v/v) ethanol (200 µl), vortexed and pelleted by centrifugation (12,000 g, 10 min, 4°C). The resulting RNA pellet was air-dried for 5-10 min and dissolved in 0.1% (v/v) diethylpyrocarbonate (DEPC)-treated water (13

µl). Integrity of the RNA was determined by separation on a 1% (w/v) agarose gel, while concentration and possible contamination were assessed by UV spectrophotometry. Samples (1 µg) were then treated with 1 U of DNase I in 1X DNase I Reaction Buffer and incubated at room temperature (<15 min) to remove any DNA contamination. The reaction was stopped by addition of EDTA (25 mM; 1 µl) and heat inactivation at 65°C for 10 min. DNase I treated RNA was stored at -20°C until required. cDNA was synthesised (RT-PCR) by reverse transcription of 800 ng of DNase I treated RNA using M-MLV Reverse Transcriptase in a two-step reaction. RNA samples were denatured and annealed with anchored oligo$(dT)_{23}$ primers (5 µM) in a mixture containing dNTPs (1 mM) at 70°C for 10 min. The reaction was then cooled (4°C) and the remaining components added (M-MLV Reverse Transcriptase Buffer, 200 U M-MLV Reverse Transcriptase, 20 U RNase Inhibitor). This was then incubated for 10 min at room temperature, followed by 50 min at 37°C. The reaction was terminated by heat inactivation at 92°C for 10 min.

3.2.7.2 Real-time RT-PCR

Real-time RT-PCR was performed using a QuantiTect SYBR Green Assay and a QuantiTec Primer Assay (Qiagen) with primers for murine and human MMP-9 (NM_013599 and NM_004994, respectively), murine β-actin (NM_007393), or human GAPDH (NM_002046). In order to make valid comparisons between samples, amplification efficiency for each primer set was determined using a serial dilution from 40 ng of control cDNA (1, 1:3, 1:10, 1:30, 1:100). Samples were analysed in duplicate. Each assay included a no-template control and a no reverse transcriptase-control. cDNA (1.5 µl) was added to a reaction mix containing 7.5 µl of QuantiTect SYBR Green, 1.5 µl of the Primer set and 4.5 µl of RNase-free water (PCR-grade) in a fast optical 96-well plate. This was covered with an optical adhesive film, briefly shaken and analysed in a 7900HT Fast Real-time PCR System (Applied Biosystems; Table 3.4).

Correction for fluorescence fluctuations was achieved through setting ROX dye as an internal fluorescence reference. Furthermore, each real-time PCR run contained a melting point analysis ranging from 60°C to 95°C over 30 min and a continuous fluorescence measurement to identify formation of primer-dimers. Data collection and analysis was acquired using SDS software v2.2.1, in which threshold level was set to 0.4. Threshold cycle (Ct) was defined as the point where the fluorescence crosses the threshold line and was set in the exponential phase of the amplification. Amplification efficiency of the individual primer sets was obtained by plotting the mean threshold cycle (Ct) values against the logarithm of DNA mass, in order to determine slope and linearity. Relative mRNA expression was analyzed according to the following equation[230]:

$$ratio = \frac{(E_{target})^{\Delta Ct_{target}\,(control-sample)}}{(E_{ref})^{\Delta Ct_{ref}\,(control-sample)}}$$

Real-time PCR efficiency (E) was calculated using the slope of the amplification efficiency of the individual primer sets, according to $E = 10^{[-1/slope]}$. E_{target} describes real-time PCR efficiency of the target gene transcript and E_{ref} is the real-time PCR efficiency of a house-keeping gene transcript[230]. ΔCt_{target} is the difference of mean Ct value of control minus treated sample of the target gene transcript. Furthermore, the ΔCt_{ref} value describes the difference of the mean Ct value of the control minus the treated sample of the house-keeping gene transcript.

Table 3.4 Real-time theromcycler conditions

Step	Time	Temperature	Comment
Initial activation step	15 min	95°C	
Denaturation	15 sec	94°C	
Annealing	30 sec	55°C	
Extension	30 sec	72°C	Fluorescence data collection
		40 cycles	

3.2.8 Transient transfection and Dual-Luciferase reporter assay

NIH3T3 fibroblasts were seeded at a density of $2x10^4$ cells/well in 48-well plates and allowed to attach for 18 hrs. The transfection mix per well consisted of 450 ng of reporter construct, 1 ng of pRL-CMV (internal standard) and 2 µl of Polyfect in a final volume of 100 µl Opti-MEM. After complex formation (15 min) at room temperature, the mixture was added to the wells containing cells and fresh medium (200 µl/well). Cells remained in this mixture for 24 hrs before being replaced with phenol-red free DMEM containing 5% charcoal stripped foetal calf serum. Following recovery (18 hrs), cells were exposed to TNFα (100 ng/ml), ISO (0.01, 0.1, 0.5, 1, 5 µM), PE (0.2, 10, 50 µM), VitC (100 µM), NFκB-Inhibitor III (5, 10 µM), DMSO (0.1% v/v), medium alone, or in combination for the time indicated. Cells were pretreated with NFκB-Inhibitor III for 30 min prior to addition of TNFα. At the end of the experiment, cells were lysed, and the lysates were analysed for luciferase activity using a Dual-Luciferase® Reporter Assay System (Promega) according to manufacture instructions. In brief, cells were gently washed with PBS, and harvested in a passive lysis buffer through gentle rocking for 15 min. Firefly and *renilla* luciferase luminescence were acquired over a 10 second read time following sequential

addition of the luciferase assay reagent II (firefly luciferase substrate) and stop & glo reagent.

3.2.9 CREB activation assay using High-content analysis (HCA)

NIH3T3 cells were plated at a density of $1x10^4$ cells/well on 96-well plates. Prior to seeding, plates were treated with poly-L-lysine (0.1 mg/ml) for 1 hr, washed three times with PBS, and air-dried under sterile conditions. Cells were exposed to ISO (0.1 μM), PE (10), forskolin (100 μM), or medium (10% newborn calf serum complete DMEM) for 30 min. CREB activation was determined using the Cellomics® PKA and CREB Activation kit (Thermo Fisher Scientific Inc.). In brief, cells were fixed in 4% (w/v) paraformaldehyde in wash buffer, permeabilised, blocked, and incubated with the anti-phospho-CREB-primary antibody (1:500). Cells were then washed and blocked prior to addition of the secondary antibody DyLight 488 goat anti-rabbit (1:500) and the nuclear stain Hoechst 33342 (1:10000). Excess antibody and stain were removed by washing. Three individually prepared plates containing quadruplet were scanned (10 randomly selected fields per well) using automated microscopy (IN Cell Analyzer 1000 HCA platform, GE Healthcare, Buckinghamshire, England) under a 10X objective. Fluorescence was collected using excitation-emission filters at 360nm/460nm for Hoechst 33342 and 480nm/535nm for DyLight 488 goat anti-rabbit antibody. Nuclear translocation of phosphorylated CREB was measured and analyzed by IN Cell Investigator software using the nuclear trafficking analysis module (GE Healthcare).

3.2.10 Western blot analysis

Cells were seeded in 6-well plates ($3x10^5$ cells/well) and cultured in serum free DMEM for 5 hours prior to starting the experiment. Cells were preincubated with propranolol (10 μM), prazosin (10 μM), DMSO (0.4% v/v) or medium (DMEM). Cells were exposed to ISO (1

μM), PE (10 μM), UV irradiation (positive control for p38 MAPK), medium (2.5% newborn calf serum; positive control for ERK1/2), TNFα (100 ng/ml; positive control for pNFκB and IκBα) or serum free medium (control) for the times indicated. Cells were then lysed in boiling Laemmli sample buffer containing 2-β-mercaptoethanol (1% v/v), and transferred to clean tube and kept on ice. Samples were sonicated for 10 sec to shear DNA, denatured at 100°C for 5 min and centrifuged at 2000 g for 5 min at 4°C. Samples and molecular weight marker (ChemiBlot, Millipore) were subjected to 12% SDS-PAGE (5% stacking gel; Table 3.5) for 1.5 hrs at 110 V.

Polyvinylidene difluoride (PVDF) membrane was soaked in methanol (100%) for 5 min, washed three times with dH_2O and equilibrated in transfer buffer (50 mM Tris HCl, pH 8.3, 40 mM glycine, 20% v/v methanol, 0.037% w/v SDS) for 10 min. A gel sandwich consisting of three sheets of filter paper, PVDF membrane, gel and three sheets of filter paper was constructed, and placed on the transfer apparatus (Thermofisher Scientific). The proteins were semi-dry transferred at 100 mA for 1 hr. Transfer efficiency was checked by staining the membrane with 0.1% (w/v) ponceau S/5% acetic. The membrane was rinsed in TBTS buffer (10 mM Tris HCl, pH 7.4, 100 mM NaCl, 0.1% Tween 20) and blocked in 5% (w/v) low fat milk in TBST for 1 hr at room temperature. Following washing with TBST-buffer the membrane was incubated with the primary antibody in 2.5% (w/v) bovine serum albumin (BSA, Cohn Fraction V) in TBST buffer and incubation overnight at 4°C. The following primary antibodies were used: anti-phospho-ERK1/2 MAPK (Thr^{202}/Tyr^{204}, 1:1000), anti-phospho-p38 MAPK (Thr^{180}/Tyr^{182}, 1:1000), anti-phospho-NFκB p65 (Ser^{536}, 1:1000), and anti-IκBα (1:1000). On the following day, membranes were washed and incubated with either a swine anti-rabbit (1:1000) or horse anti-mouse (1:1000) horseradish peroxidase (HRP) conjugated secondary antibody. Membranes were washed in TBST and visualised by enhanced chemiluminescence[231]. In brief, membranes were exposed to a

freshly prepared chemiluminescence solution (100 mM Tris HCl, pH 8.5, 5.3 mM H_2O_2, 1.25 mM Luminol, 2.0 mM 4-iodophenylboronic acid) for 1 min, captured by digital imaging and quantified using a GeneGenius Gel documentation system. Membranes were stripped in a solution of 2.5 mM Tris-base pH 6.7, 2% (w/v) SDS, 100 mM β-mercaptoethanol for 45 min at 50°C. They were reprobed with either an alternative primary antibody or a β-actin HRP labelled antibody (1:7500) as required.

Table 3.5 Composition of the resolving and stacking gels used in western blot analysis.

	Resolving gel (12%)	**Stacking gel (5%)**
dH_2O	3.3 ml	1.4 ml
30% (w/v) Acrylamide/Bis-acrylamide (29:1)	4.0 ml	0.33 ml
Tris HCl (1.5 M, pH 8.8)	2.5 ml	-
Tris HCl (1 M, pH 6.8)	-	0.25 ml
10% (w/v) SDS	100 µl	20 µl
10% (w/v) ammonium persulfate	100 µl	20 µl
TEMED	4 µl	2 µl

3.2.11 Validation of the cloning and Real-time RT-PCR methodology

3.2.11.1 Validation of the MMP-9 promoter constructs

The purity and size of the truncated MMP-9 promoter inserts was checked by agarose gel electrophoresis. Based upon the Finnzymes DNA molecular weight ladder, the approximate sizes of the PCR-products were 550 bp, 600 bp, 650 bp, 700 bp, and 1350 bp

for the p523, p540, p571, p657, and p1285 respectively (Figure 3.1). This is in keeping with their predicted sizes of 549 bp, 566 bp, 595 bp, 683 bp, and 1312 bp, based upon sequence alignment to NT_011362.10. Following sub-cloning into a pGEM®-T Easy vector, the vectors were checked to ensure they contained the relevant insert using restriction enzyme digestion (*Xho*I/*Hind*III; Figure 3.2).

Vectors positive for an insert were sent for sequencing to ensure sequence fidelity. The plasmid insert sequences were found to have 99% homology to the NCBI Accession NT_011362.10 that encodes the sequence for the human chromosome 20, which contains the gene for MMP-9. The alignment of the p1285-insert to NCBI Accession NT_011362.10 is given in table 3.6; sequences of the other inserts are given in appendix 1. All MMP-9 promoter inserts differ from the reference sequence by an 8 bp deficit in the $(CA)_n$-microsatellite region. The sequence described in NT_011362.10 encodes a $(CA)_{23}$-repeat, whereas our 5'-end deletion mutants encode a $(CA)_{19}$-repeat. This may reflect genetic polymorphism between the template DNA used and the sequence lodged with NCBI.

Restriction digestion of the pGL3 plasmids containing the MMP-9 promoter insert with *Xho*I/*Hind*III indicate that the plasmids contain 5'-truncated inserts of the expected sizes. Furthermore, restriction digestion with *Kpn*I/*Hind*III give bands corresponding to the linearised pGL3-Basic (4.8 kb) DNA and a band corresponding to the insert size plus ~30 bp (Figure 3.3). This indicates that the MMP-9 promoter inserts are in the correct orientation within the pGL3-Basic vector. If the inserts were in the incorrect orientation, three bands corresponding to linearised pGL3-Basic DNA (4.8 kb), the insert and a band of ~30 bp would have been obtained.

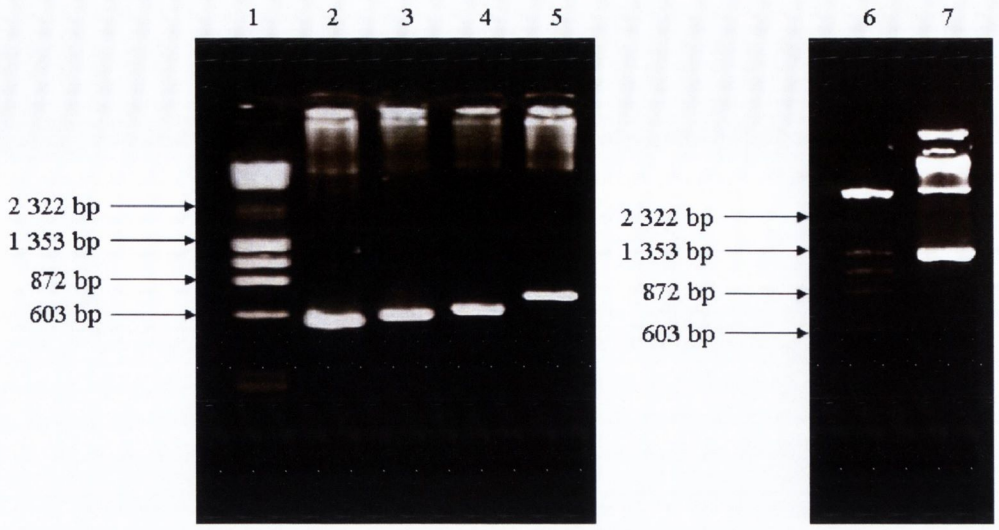


Figure 3.1 A representative agarose gel (1% w/v) of the MMP-9 promoter inserts generated by PCR.

Molecular weight marker (lane1), p523 (lane 2), p540 (lane 3), p571 (lane 4), p657 (lane 5), and p1285 (lane 7) of the human MMP-9 promoter. Lanes 1 and 6 contain the Finnzymes DNA ladder.

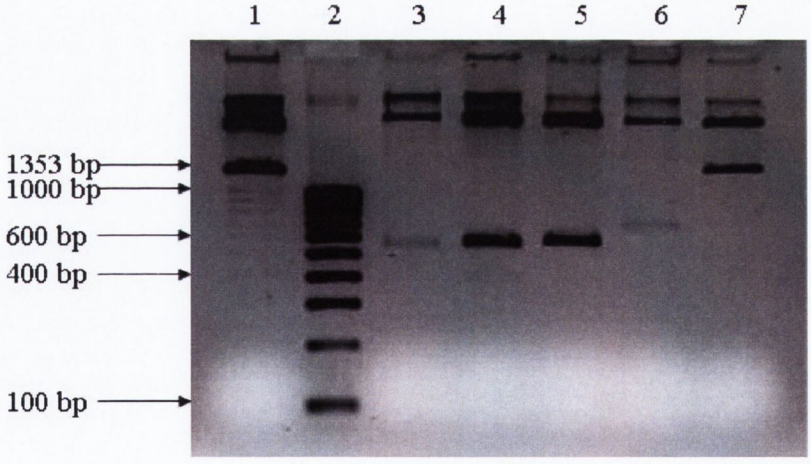


Figure 3.2 A representative mini gel (1% w/v agarose) showing the banding pattern of the MMP-9 pGEM®-T Easy vectors following digestion with *Hind*III/*Xho*I.

Finnzymes DNA marker (lane 1) and Hyperladder IV (lane 2), p523 (lanes 3 and 4), p540 (lane 5), p657 (lane 6) and p1285 (lane 7). The image is presented as a negative for clarity.

Table 3.6 Alignment of the MMP-9 promoter sequence from the p1285-pGEM®-T Easy plasmid to that of NCBI Accession NT_011362.10.

Alignment was done using Basic Local Alignment Search Tool (BLAST). Differences in the $(CA)_n$-repeats of the microsatellite region are marked in red.

```
ref|NT_011362.10| Homo sapiens chromosome 20 genomic contig

Features in this part of subject sequence:
matrix metalloproteinase 9 preproprotein preproprotein

Score = 2372 bits (1284),  Expect = 0.0
Identities = 1304/1312 (99%), Gaps = 8/1312 (0%)

Query  1         GGGAGGGAGGCTTGGCATAAGTGTGATAATTGGGGCTGGAGATTTGGCTGCATGGAGCAG  60
                 ||||||||||||||||||||||||||||||||||||||||||||||||||||||||||||
Sbjct  14832347  GGGAGGGAGGCTTGGCATAAGTGTGATAATTGGGGCTGGAGATTTGGCTGCATGGAGCAG  14832406

Query  61        GGCTGGAGAACTGAAAGGGCTCCTATAGATTATTTTCCCCCATATCCTGCCCCAATTTGC  120
                 ||||||||||||||||||||||||||||||||||||||||||||||||||||||||||||
Sbjct  14832407  GGCTGGAGAACTGAAAGGGCTCCTATAGATTATTTTCCCCCATATCCTGCCCCAATTTGC  14832466

Query  121       AGTTGAAGAATCCTAAGCTGACAAAGGGGAAGGCATTTACTCCAGGTTACACTGCAGCTT  180
                 ||||||||||||||||||||||||||||||||||||||||||||||||||||||||||||
Sbjct  14832467  AGTTGAAGAATCCTAAGCTGACAAAGGGGAAGGCATTTACTCCAGGTTACACTGCAGCTT  14832526

Query  181       AGAGCCCAATAACCTGGTTTGGTGATTCCAAGTTAGAATCATGGTCTTTTGGCAGGGTCT  240
                 ||||||||||||||||||||||||||||||||||||||||||||||||||||||||||||
Sbjct  14832527  AGAGCCCAATAACCTGGTTTGGTGATTCCAAGTTAGAATCATGGTCTTTTGGCAGGGTCT  14832586

Query  241       CGCTCTGTTGCCCAGGCTGGAGTGCAGTGACATAATCATGGCTCACTGTATCCTTGACCT  300
                 ||||||||||||||||||||||||||||||||||||||||||||||||||||||||||||
Sbjct  14832587  CGCTCTGTTGCCCAGGCTGGAGTGCAGTGACATAATCATGGCTCACTGTATCCTTGACCT  14832646

Query  301       TCTTTCTGGGCTCAAGCAATCCTCCCACCTCGGCCTCCCAAAGTGCTAAGATTACAGGAA  360
                 ||||||||||||||||||||||||||||||||||||||||||||||||||||||||||||
Sbjct  14832647  TCTTTCTGGGCTCAAGCAATCCTCCCACCTCGGCCTCCCAAAGTGCTAAGATTACAGGAA  14832706

Query  361       TGAGCCACCATACCTGGCCCTGAATCTTGGGTCTTGGCCTTAGTAATTAAAACCAATCAC  420
                 ||||||||||||||||||||||||||||||||||||||||||||||||||||||||||||
Sbjct  14832707  TGAGCCACCATACCTGGCCCTGAATCTTGGGTCTTGGCCTTAGTAATTAAAACCAATCAC  14832766

Query  421       CACCATCCGTTGCGGACTTACAACCTACAGTGTTCTAAACATTTTATATGTTTGATCTCA  480
                 ||||||||||||||||||||||||||||||||||||||||||||||||||||||||||||
Sbjct  14832767  CACCATCCGTTGCGGACTTACAACCTACAGTGTTCTAAACATTTTATATGTTTGATCTCA  14832826

Query  481       TTTAATCCTCACATCAATTTAGGGACAAAGAGCCCCCCACCCCCCGTTTTTTTTTTTACA  540
                 ||||||||||||||||||||||||||||||||||||||||||||||||||||||||||||
Sbjct  14832827  TTTAATCCTCACATCAATTTAGGGACAAAGAGCCCCCCACCCCCCGTTTTTTTTTTTACA  14832886

Query  541       GCTGAGGAAACACTTCAAAGTGGTAAGACATTTGCCCGAGGTCCTGAAGGAAGAGAGTAA  600
                 ||||||||||||||||||||||||||||||||||||||||||||||||||||||||||||
Sbjct  14832887  GCTGAGGAAACACTTCAAAGTGGTAAGACATTTGCCCGAGGTCCTGAAGGAAGAGAGTAA  14832946

Query  601       AGCCATGTCTGCTGTTTTCTAGAGGCTGCTACTGTCCCCTTTACTGCCCTGAAGATTCAG  660
                 ||||||||||||||||||||||||||||||||||||||||||||||||||||||||||||
Sbjct  14832947  AGCCATGTCTGCTGTTTTCTAGAGGCTGCTACTGTCCCCTTTACTGCCCTGAAGATTCAG  14833006

Query  661       CCTGCGGAAGACAGGGGGTTGCCCCAGTGGAATTCCCCAGCCTTGCCTAGCAGAGCCCAT  720
                 ||||||||||||||||||||||||||||||||||||||||||||||||||||||||||||
Sbjct  14833007  CCTGCGGAAGACAGGGGGTTGCCCCAGTGGAATTCCCCAGCCTTGCCTAGCAGAGCCCAT  14833066

Query  721       TCCTTCCGCCCCCAGATGAAGCAGGGAGAGGAAGCTGAGTCAAAGAAGGCTGTCAGGGAG  780
                 ||||||||||||||||||||||||||||||||||||||||||||||||||||||||||||
Sbjct  14833067  TCCTTCCGCCCCCAGATGAAGCAGGGAGAGGAAGCTGAGTCAAAGAAGGCTGTCAGGGAG  14833126

Query  781       GGAAAAAGAGGACAGAGCCTGGAGTGTGGGGAGGGGTTTGGGGAGGATATCTGACCTGGG  840
                 ||||||||||||||||||||||||||||||||||||||||||||||||||||||||||||
Sbjct  14833127  GGAAAAAGAGGACAGAGCCTGGAGTGTGGGGAGGGGTTTGGGGAGGATATCTGACCTGGG  14833186
```

```
Query  841       AGGGGGTGTTGCAAAAGGCCAAGGATGGGCCAGGGGGATCATTAGTTTCAGAAAGAAGTC  900
                  ||||||||||||||||||||||||||||||||||||||||||||||||||||||||||||
Sbjct  14833187  AGGGGGTGTTGCAAAAGGCCAAGGATGGGCCAGGGGGATCATTAGTTTCAGAAAGAAGTC  14833246

Query  901       TCAGGGAGTCTTCCATCACTTTCCCTTGGCTGACCACTGGAGGCTTTCAGACCAAGGGAT  960
                  ||||||||||||||||||||||||||||||||||||||||||||||||||||||||||||
Sbjct  14833247  TCAGGGAGTCTTCCATCACTTTCCCTTGGCTGACCACTGGAGGCTTTCAGACCAAGGGAT  14833306

Query  961       GGGGGATCCCTCCAGCTTCATCCCCCTCCCTCCCTTTCATACAGTTCCCACAAGCTCTGC  1020
                  ||||||||||||||||||||||||||||||||||||||||||||||||||||||||||||
Sbjct  14833307  GGGGGATCCCTCCAGCTTCATCCCCCTCCCTCCCTTTCATACAGTTCCCACAAGCTCTGC  14833366

Query  1021      AGTTTGCAAAACCCTACCCCTCCCCTGAGGGCCTGCGGTTTCCTGCGGGTCTGGGGTCTT  1080
                  ||||||||||||||||||||||||||||||||||||||||||||||||||||||||||||
Sbjct  14833367  AGTTTGCAAAACCCTACCCCTCCCCTGAGGGCCTGCGGTTTCCTGCGGGTCTGGGGTCTT  14833426

Query  1081      GCCTGACTTGGCAGTGGAGACTGCGGGCAGTGGAGAGAGGAGGAGGTGGTGTAAGCCCTT  1140
                  ||||||||||||||||||||||||||||||||||||||||||||||||||||||||||||
Sbjct  14833427  GCCTGACTTGGCAGTGGAGACTGCGGGCAGTGGAGAGAGGAGGAGGTGGTGTAAGCCCTT  14833486

Query  1141      TCTCATGCTGGTGCTGCCACACACACACACACACACACACACACACACACACACC-C-C  1198
                  |||||||||||||||||||||||||||||||||||||||||||||||||||||| | |
Sbjct  14833487  TCTCATGCTGGTGCTGCCACACACACACACACACACACACACACACACACACACAC  14833546

Query  1199      ------TGACCCCTGAGTCAGCACTTGCCTGTCAAGGAGGGGTGGGGTCACAGGAGCGCC  1252
                        ||||||||||||||||||||||||||||||||||||||||||||||||||||
Sbjct  14833547  ACACCCTGACCCCTGAGTCAGCACTTGCCTGTCAAGGAGGGGTGGGGTCACAGGAGCGCC  14833606

Query  1253      TCCTTAAAGCCCCCACAACAGCAGCTGCAGTCAGACACCTCTGCCCTCACCA  1304
                  ||||||||||||||||||||||||||||||||||||||||||||||||||
Sbjct  14833607  TCCTTAAAGCCCCCACAACAGCAGCTGCAGTCAGACACCTCTGCCCTCACCA  14833658
```

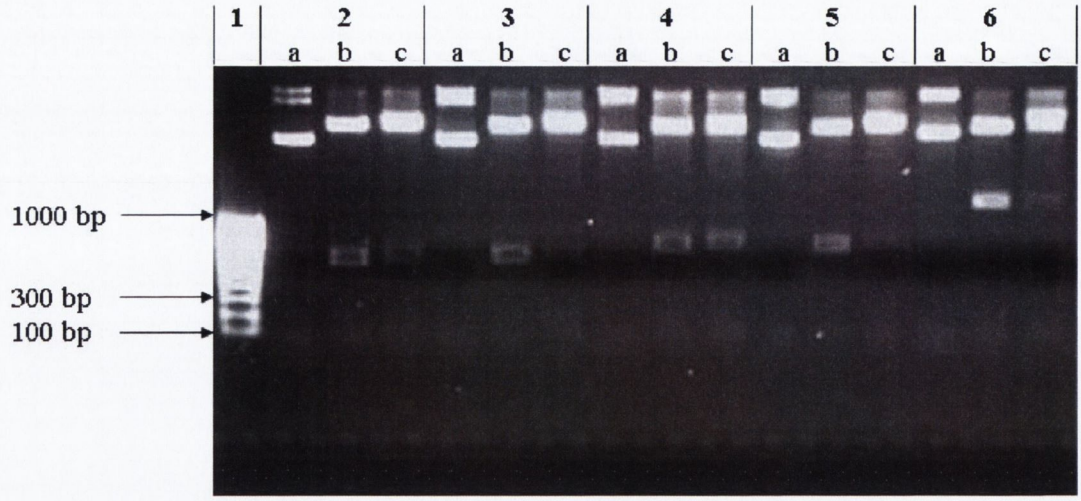


Figure 3.3 Analysis of insertion and orientation of MMP-9 inserts in the pGL-3 Basic plasmids.

A representative mini gel (1% w/v agarose) showing the banding pattern of the p523-luc (lane 2 a, b, c), p540-luc (lane 3 a, b, c), p571-luc (lane 4 a, b, c), p657-luc (lane 5 a, b, c), and p1285-luc (lane 6 a, b, c) along with Hyperladder II DNA marker (lane 1). Undigested samples are represented in the lanes labelled (a), *Hind*III/*Xho*I digested samples are represented in the lanes labelled (b), and *Hind*III/*Kpn*I digested samples are represented in the lanes labelled (c).

3.2.11.2 Validation of mRNA quality and Real-time RT-PCR cycling efficiency

The integrity of the RNA samples was investigated using agarose gel electrophoresis (Figure 3.4). As can be seen all samples showed 2 clear bands corresponding to 28S rRNA and 18S rRNA in a ratio of 2:1, respectively. There was no smearing noted between bands, which would represent RNA degradation. A third minor band corresponding to 5S rRNA was also noted.

Total RNA extracts showing the desired pattern or rRNA species were reverse transcribed and applied to real-time PCR using a QuantiTect SYBR Green PCR kit. Prior to analysis of treated samples, amplification efficiency of each used primer set was determined using a serial dilution of cDNA. Determined amplification efficiency of primer sets for human MMP-9 and GAPDH gene transcripts are 87.47% and 89.81%, respectively ($R^2 \geq 0.98$). Amplification efficiency of primer sets for murine MMP-9 and β-actin gene transcripts are 101.34% and 99.58%, respectively ($R^2 \geq 0.98$; Figure 3.5). mRNA expression was acquired using determined amplification efficiencies and the experimentally obtained Ct values according to Pfaffl[230]. Furthermore, after each real-time PCR performance a melting curve analysis was performed (Figure 3.6).

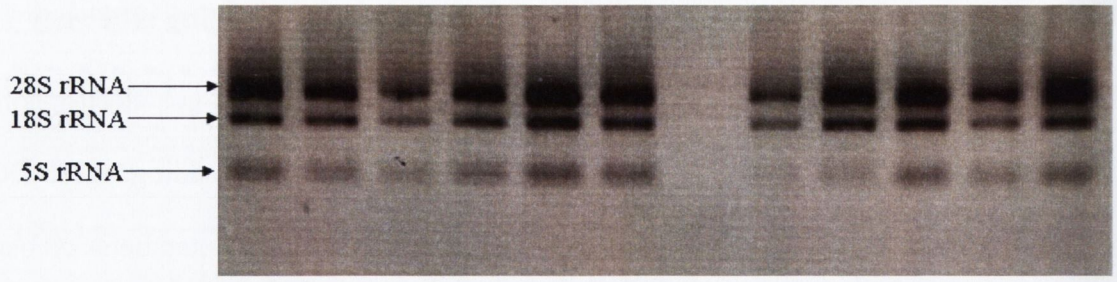


Figure 3.4 Assessment of the integrity of the RNA samples isolated using TRI reagent.

A typical midi gel (1% w/v agarose) showing 28S rRNA, 18S rRNA and 5S rRNA bands. Image is presented as a negative for clarity.

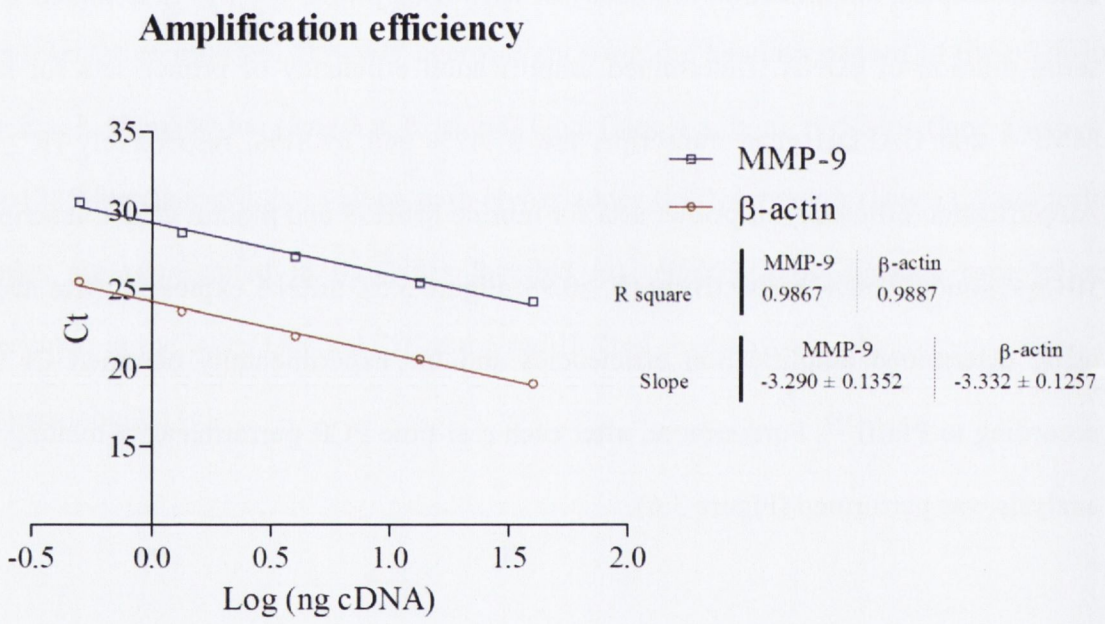


Figure 3.5 PCR amplification efficiency for mouse MMP-9 and β-actin primers using mouse control cDNA.

Amplification efficiency was determined by plotting Ct values against logarithm (Log_{10}) of DNA mass. Data are presented as Ct values vs. log DNA (mean; n=2). Comparable plots were obtained for other primer sets used in this study.

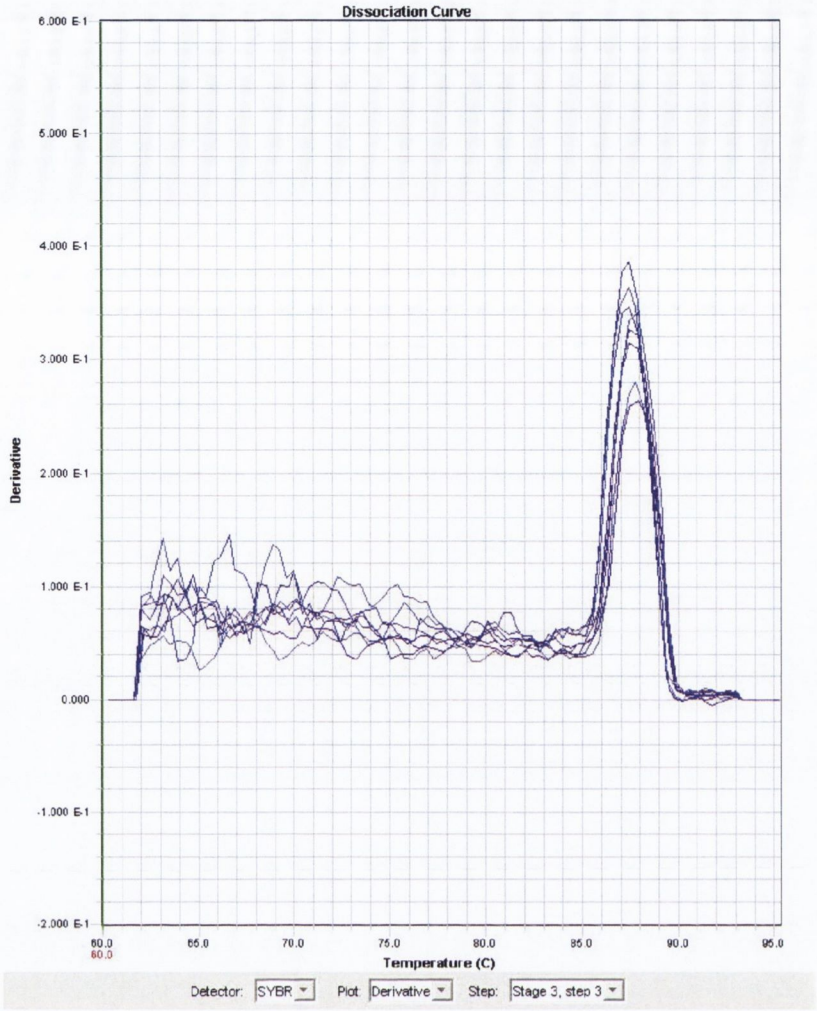


Figure 3.6 A representative melting curve analysis for mouse β-actin.

cDNA samples were amplified with using a QuantiTect primer assay targeting mouse β-actin and a QuantiTect SYBR Green Assay. Data were acquired using a 7900HT Fast Real-time PCR System (Applied Biosystems).

3.2.12 Data and statistical analysis

Cell viability, gelatin-zymography and western blot experiments were normalised to control (medium) and expressed as a percentage where indicated. Activation of CREB was quantified as a difference in cellular fluorescence intensity (DyLight 488 goat anti-rabbit antibody and Hoechst 33342) between the nucleus and cytoplasm compartments normalised to control (medium). These samples were analysed in quadruplet. Data from the luciferase reporter assays are expressed as the ratio of firefly luciferase to *renilla* luciferase normalised to control (medium) and analysed in duplicate. mRNA expression was analyzed according to Pfaffl[230], by determination of amplification efficiency for each primer set ($R^2 \geq 0.98$) and samples were analysed in duplicate. Data were analysed by one-way or two-way ANOVA with *post hoc* analysis (Bonferroni, Dunnett's) where appropriate (Graphpad Prism, version 5.02) and expressed as mean ± S.E.M. All experiments were repeated at least three independent times (n). A value of $P<0.05$ was taken to indicate statistical significance.

3.3 Results

3.3.1 Effect of adrenoceptor stimulation on cell viability

As isoprenaline and phenylephrine have been reported to have cytotoxic and apoptotic effects[232, 233], their effect on cell viability at the concentrations to be used in subsequent studies was assessed. In NIH3T3 cells isoprenaline (0.1 and 1 μM) and phenylephrine (10 and 50μM) did not alter cell viability as assessed by a MTT assay compared to untreated cells (1 μM isoprenaline vs. control: 124.3±7.34 vs. 100±5.71%; Figure 3.7). Doxorubicin (positive control) reduced metabolic activity by 40% and 80% at a concentration of 1 μM and 5 μM, respectively (Figure 3.7).

3.3.2 Effect of β-adrenoceptor stimulation on intracellular cAMP levels in fibroblasts

All cells were pretreated with IBMX to prevent phosphodiesterase-mediated breakdown of cAMP, with the exception of the untreated group. In NIH3T3 cells, IBMX (100 μM) increased the basal levels of cAMP to 14.94±2.44 pmol/ml from 4.69±0.58 pmol/ml ($P<0.05$; Figure 3.8 A), while no effect was observed in HCVF cells (Figure 3.8 B). Isoprenaline (1 μM) increased cAMP levels by 1.3 and 4.8 fold compared to IBMX treated cells in the NIH3T3 and HCVF respectively ($P<0.05$; Figure 3.8 A, B). This effect was inhibited ($P<0.05$) by propranolol (10 μM). Propranolol alone had no effect in either cell line. In NIH3T3 and HCVF cells, forskolin (1 μM, positive control) increased cAMP production by 1 and 4.2 fold compared to IBMX treated cells ($P<0.05$; Figure 3.8 A, B).

3.3.3 Effect of adrenoceptor stimulation on phospho-CREB translocation

cAMP signalling downstream of cAMP was investigated by looking at translocation of phospho-CREB to the nucleus. In untreated cells, phospho-CREB was uniformly distributed in the cytoplasm (Figure 3.9 A, C) and redistributed to the nucleus in the presence of forskolin (100 μM; 27.78±2 vs. 1.00±0.5 AU; $P<0.05$; Figure 3.9 D, F). Isoprenaline (0.1 μM) also caused phospho-CREB to redistribute from the cytoplasmic to the nuclear compartment (Figure 3.14 G, I) compared to untreated cells (3.19±0.4 vs. 1.00±0.5 AU; $P<0.05$, Figure 3.9 A, C). Interestingly, phenylephrine (10 μM) also elicited a visible translocation of phospho-CREB to the nucleus (4.65±0.4 vs. 1.00±0.5 AU; $P<0.05$; Figure 3.9 K, M) compared to untreated cells.

3.3.4 Effect of adrenoceptor stimulation on ERK1/2 and p38 MAPK phosphorylation

cAMP can also activate non-classical signalling pathways involving ERK1/2 and p38 MAPK, which are associated with activation of NFκB. Therefore, we investigated the effect of isoprenaline and phenylephrine on phosphorylation of ERK1/2 and p38 MAPK. Isoprenaline (1 μM) caused a 2.7 fold increase in the phosphorylation of ERK1/2 MAPK (7.5 min: 3.73±0.50 AU; $P<0.05$; Figure 3.10 A, B) compared to control at time 0 (1.0±0.04 AU) in NIH3T3 cells. Phenylephrine (10 μM) elicited a 2 fold increase in phosphorylation of ERK1/2 MAPK compared to the untreated control (7.5 min: 3.16±0.28 vs. 1±0.04 AU; $P<0.05$; Figure 3.10 A, B). Normal calf serum (positive control) caused a robust 3.5 fold increase in phosphorylation of ERK1/2 MAPK compared to control at 30 min (4.49±0.66 vs. 1±0.09 AU; $P<0.05$).

Isoprenaline elicited a biphasic increase in the phosphorylation of p38 MAPK, with peaks occurring at 7.5 and 30 min compared to control (30 min; 2.94±0.34 vs. 1±0.07; $P<0.05$; Figure 3.10 C, D). Phenylephrine also caused a biphasic induction of p38 MAPK phosphorylation compared to baseline values (7.5 min; 3.05±0.54 vs. 1±0.09; $P<0.05$; Figure 3.10 C, D). The magnitude of these effects are in keeping with that of the positive control (exposure to UV radiation for 15 min) which increased phospho-p38MAPK levels by 3 fold ($P<0.05$).

In HCVF cells, isoprenaline (1 μM) decreased phospho-ERK1/2 MAPK by 70% after 30 min (ISO vs. control: 0.30±0.06 vs. 1±0.03 AU; $P<0.05$), an effect blocked by the addition of propranolol (ISO vs. ISO/PROP: 0.30±0.06 vs. 1.05±0.10 AU; $P<0.05$; Figure 3.11). Although phenylephrine also decreased phospho-ERK1/2 MAPK at 30 min (phenylephrine vs. control: 0.33±0.15 vs. 1±0.03 AU; $P<0.05$ Figure 3.11), this effect was unaffected by prazosin. Neither propranolol nor prazosin altered phosphorylation of ERK1/2 MAPK.

3.3.5 Effect of adrenoceptor stimulation on NFκB promoter activity

The ERK1/2 and p38 MAPK pathways converge on a common downstream target the mitogen- and stress-activated protein kinase (MSK1)[225, 226], which in turn can activate NFκB[227]. As isoprenaline and phenylephrine can activate NFκB[234, 235] in a dose and time dependent manner we investigated the effect of adrenoceptor stimulation on NFκB promoter activity in NIH3T3 fibroblasts. Phenylephrine had no effect on NFκB promoter activity at any concentration studied (10 μM; phenylephrine vs. control: 1.72±0.25 vs. 1±0.16; Figure 3.12 A). TNFα (100 ng/ml) increased NFκB promoter activity by ~30 fold compared to control (TNFα vs. control: 31.21±5.95 vs. 1.0±0.16; $P<0.05$; Figure 3.12 A). This effect was attenuated by 85% by the $NF\kappa B_{III}$ inhibitor (10 μM; $P<0.05$; Figure 3.12 A). The $NF\kappa B_{III}$ inhibitor alone caused a small but non-significant decrease in basal NFκB

promoter activity. Furthermore, compared to matched time controls, isoprenaline (0.1 μM) did not alter NFκB promoter activity at any time point studied over 24 hrs (4hr: isoprenaline vs. control: 0.84±0.28 vs. 1±0.72; Figure 3.12 B). However, isoprenaline at the concentrations studied did not alter NFκB promoter activity after 6 hrs of treatment (5 μM vs. control: 1.40±0.14 vs. 1.0±0.20; Figure 3.12 C), while TNFα (100 ng/ml) induced NFκB promoter activity by 4 fold ($P<0.05$).

3.3.6 Regulation of NFκB and IκBα signal transduction

To complement the data from the reporter study we investigated the effects of the adrenoceptor stimulation on NFκB Ser^{536} phosphorylation and IκBα expression in NIH3T3 and HCVF fibroblasts. Isoprenaline (1 μM) decreased phosphorylation of the NFκB p65 subunit at 15 min compared to control (0.57±0.10 vs. 1±0.10; $P<0.05$; Figure 3.13) in NIH3T3 fibroblasts, but had no effect in HCVF cells (Figure 3.14). Phenylephrine did not affect levels of phospho-NFκB in NIH3T3 or HCVF cells. Neither isoprenaline nor phenylephrine altered expression of IκBα in either cell line (Figure 3.13 A and 3.14 A). TNFα increased ($P<0.05$) phosphorylation of NFκB at 15 min by 1 and 10 fold in NIH3T3 and HCVF cells compared to control (100 ng/ml; Figure 3.13 A and 3.14 A). This was accompanied by a decrease in IκBα expression by approximately 90% ($P<0.05$; Figure 3.13 A and 3.14 A) in both cell lines compared to control.

3.3.7 Effect of adrenoceptor stimulation on MMP-9 activity

Gelatinolytic activity corresponding to murine MMP-9 (95 kDa), proMMP-9 (105 kDa), proMMP-2 (72 kDa) and MMP-2 (62 kDa) activity were detected in the condition medium of NIH3T3 cells. Although active MMP-9 activity was detectable, the levels were too low for quantification. The MMP-9 gelatinolytic bands were below that of the murine

recombinant proMMP-9 internal standard (105 kDa). This likely reflects differences in post-translational modification of MMP-9. The recombinant murine proMMP-9 standard used in the present study was isolated from CHO cells and is expressed as a N-glycosylated pro-enzyme form, which migrates at 110 kDa in gelatin-zymography[236]. Furthermore, there is also data indicating that glycosylation of human MMP-9 varies depending on cell types[237, 238].

Isoprenaline and phenylephrine did not alter proMMP-9 activity in conditioned medium from NIH3T3 fibroblasts (Figure 3.15 A, C) compared to control. However, TNFα (100 ng/ml) increased proMMP-9 gelatinolytic activity by 1.6 fold compared to untreated cells (2.63±0.30 vs. 1±0.09 AU; $P<0.05$; Figure 3.15 C). Vitamin C did not alter MMP-9 activity compared to control. In HCVFs, MMP-9 activity and expression could not be quantified in conditioned medium by either enzyme-linked immunosorbent assay (Elisa) or gelatin-zymography.

3.3.8 Effect of adrenoceptor stimulation on MMP-9 promoter activity and mRNA expression

NIH3T3 fibroblasts were transfected with a full-length MMP-9 promoter construct (p1285-luc) and exposed to isoprenaline and phenylephrine for 24 hrs. At the concentrations studied, isoprenaline did not alter MMP-9 promoter activity compared control (1 μM, isoprenaline vs. control: 0.92±0.10 vs. 1.0±0.08; Figure 3.16 A). As a previous study showed that isoprenaline maximally induced MMP-9 promoter activity at 4 hrs[239], the temporal effects were also assessed. Compared to matched time controls, isoprenaline (0.1 μM) did not alter MMP-9 promoter activity at any time point studied (4hr: isoprenaline vs. control: 1.09±0.17 vs. 1±0.39; Figure 3.16 B). Phenylephrine (α_1-adrenoceptor agonist) did

not affect MMP-9 promoter activity in NIH3T3 fibroblasts at the concentrations studied compared to control (10 μM: phenylephrine vs. control: 1.31±0.32 vs. 1±0.08; Figure 3.16 A).

TNFα caused a robust induction in MMP-9 promoter activity compared to control in all experiments (TNFα vs. control: 2.56±0.33 vs. 1.0±0. 08, $P<0.05$; Figure 3.16 A). This effect was prevented by the $NF\kappa B_{III}$ inhibitor (5 μM; $P<0.05$; Figure 3.16 A). The $NF\kappa B_{III}$ inhibitor alone caused a small decrease in basal activation of the MMP-9 promoter activity, which failed to reach significance. DMSO (0.1% v/v) and vitamin C (antioxidant; 100 μM) did not affect MMP-9 promoter activity.

At the level of mRNA expression, isoprenaline (0.1, 1 μM) and phenylephrine (10, 50 μM) did not alter MMP-9 mRNA expression in NIH3T3 or HCVF cells (Figure 3.17 A, B). However, TNFα elicited a 2.4 and 180 fold increase in MMP-9 mRNA expression compared to untreated controls in NIH3T3 and HCVF cells, respectively.

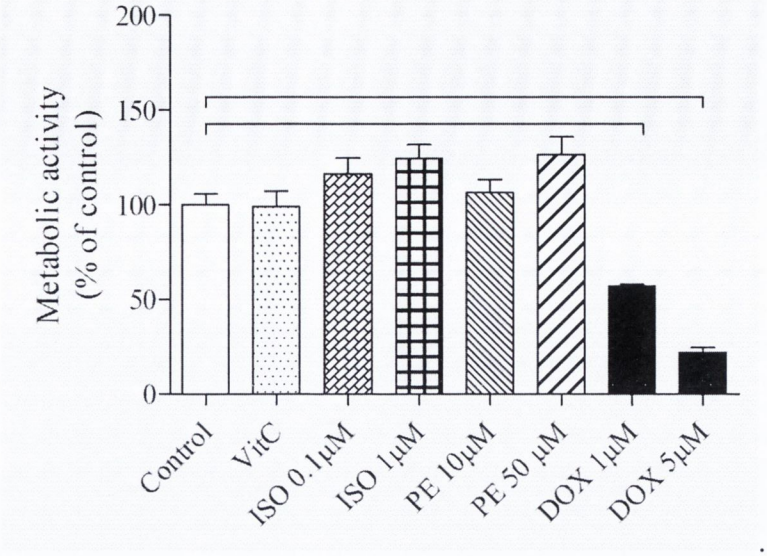


Figure 3.7 Effect of adrenoceptor stimulation on the cell viability in NIH3T3 fibroblasts. Cells were exposed to isoprenaline (ISO; 0.1 and 1 μM), phenylephrine (PE; 0.2, 10, 50 μM), vitamin C (100 μM), doxorubicin (DOX; 1 μM and 5 μM) or medium (untreated control) for 24 hrs. Data are expressed as a percentage of untreated cells (mean ± S.E.M.; n=8). Data were analysed by one-way ANOVA with *post hoc* analysis (Dunnett's). Horizontal bars indicate a statistical significance of $P<0.05$.

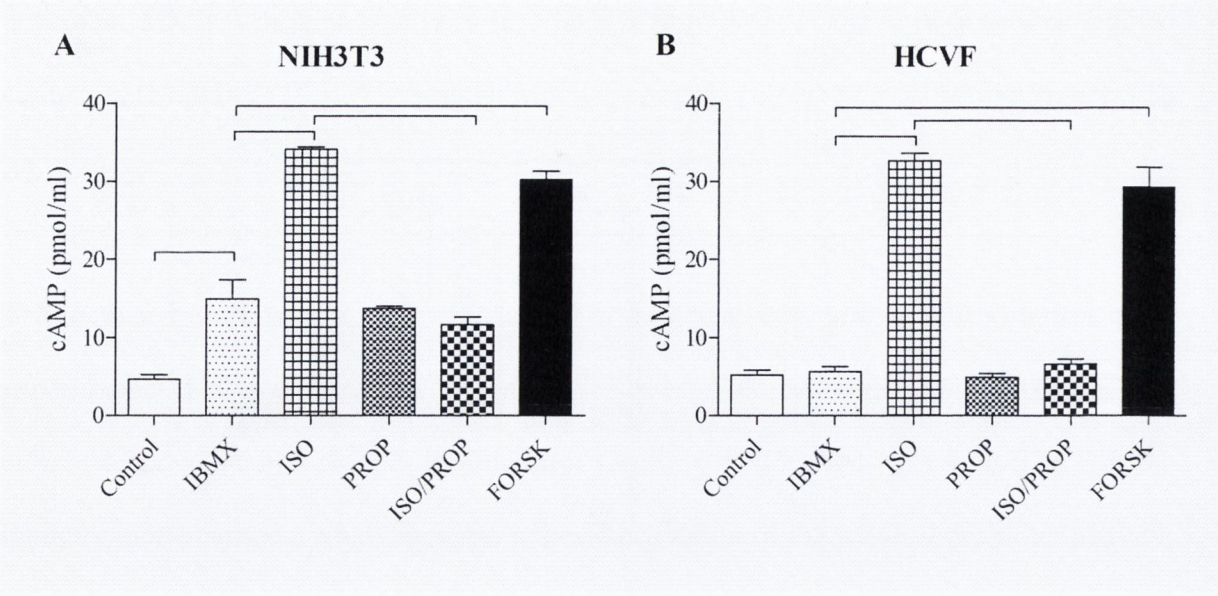


Figure 3.8 Effect of β-adrenoceptor stimulation on cAMP production in (A) mouse (NIH3T3) and (B) human ventricular cardiac fibroblasts (HCVF).

Cells were pre-incubated with IBMX (100 μM) in the absence or presence of propranolol (PROP; 10 μM) for 30 min before exposure to isoprenaline (ISO; 1 μM), forskolin (FORSK; 1 μM), or medium (control) for 10 min. cAMP levels were determined using a direct cAMP enzyme immunoassay (Sigma-Aldrich). Data are expressed as cAMP concentration (pmol/ml; mean ± S.E.M.; n=3). Data were analysed by one-way ANOVA with *post hoc* analysis (Bonferroni). Horizontal bars indicate a statistical significance of $P<0.05$.

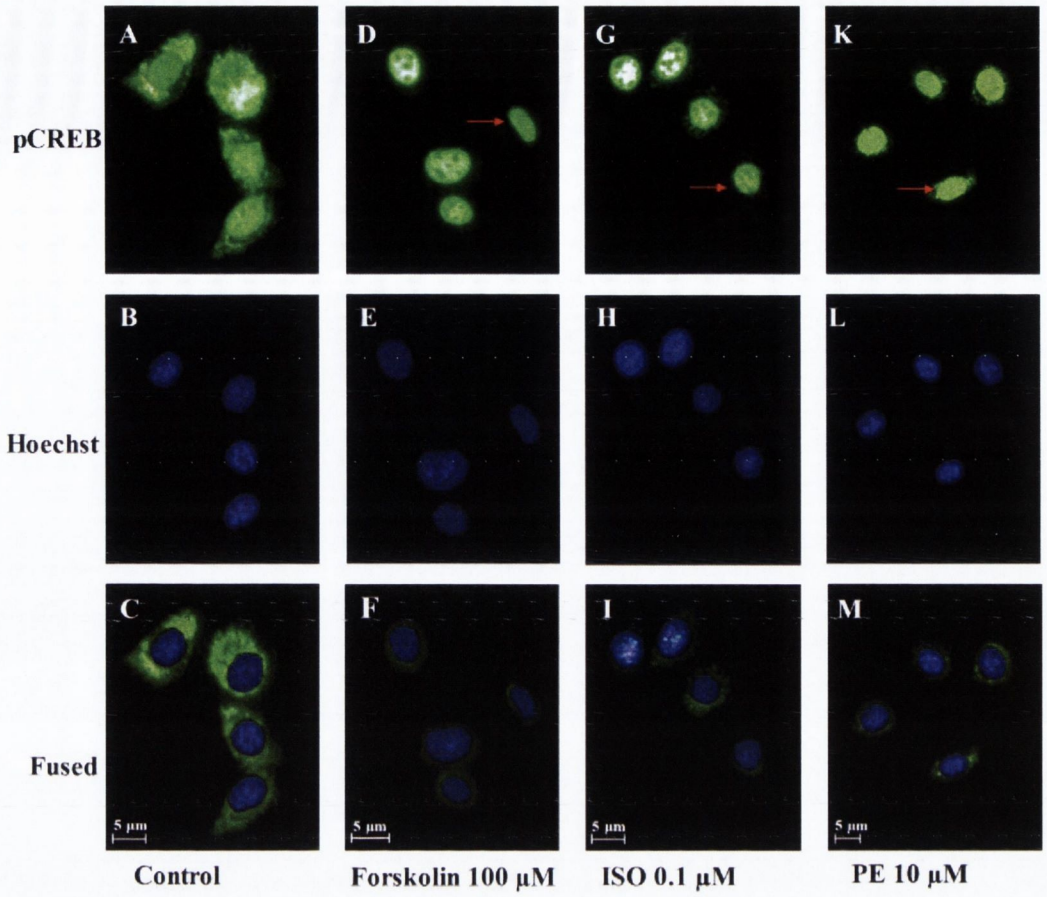


Figure 3.9 Effect of adrenoceptor stimulation on phospho-CREB translocation in NIH3T3 cells.

Nuclear translocation of phospho-CREB was determined by immunofluorescence staining (PKA and CREB Activation kit, Cellomics®) and visualised using automated microscopy (IN Cell Analyzer 1000 HCA platform, GE Healthcare). Images were analyzed by IN Cell Investigator software. Representative image fields from four independent experiments are presented for cells exposed to: medium (control; A, B, C), forskolin (100 µM; D, E, F), isoprenaline (0.1 µM; G, H, I), and phenylephrine (10 µM; K, L, M). Cellular location of phospho-CREB (pCREB) is given in row 1, while row 2 shows Hoechst staining of the nucleus and a fused image is presented in row 3. Red arrows indicate cells with nuclear translocated phospho-CREB.

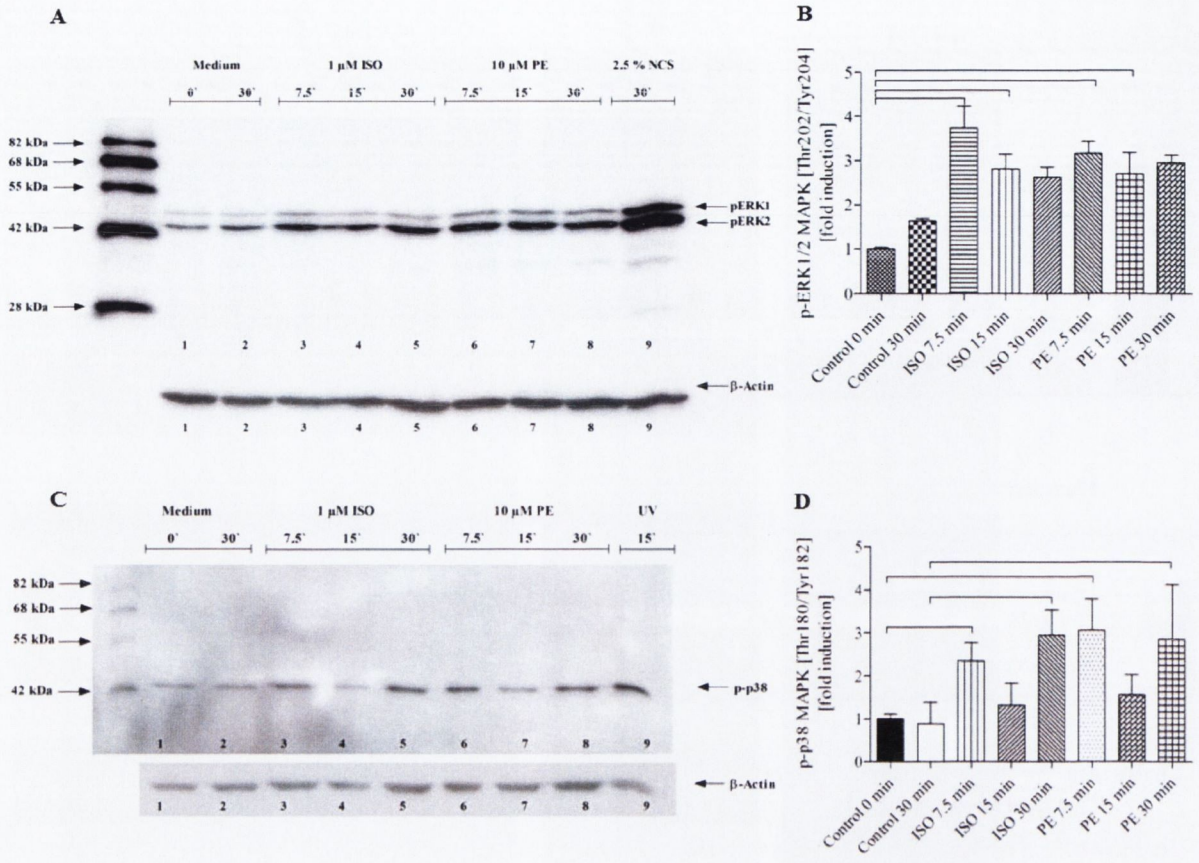


Figure 3.10 Temporal effects of adrenoceptor stimulation on phosphorylation of ERK1/2 and p38 MAPK in NIH3T3.

Western blot analysis was used to detect phosphorylation of ERK1/2 MAPK (A, B) and p38 MAPK (C, D). Cells were stimulated with isoprenaline (1 µM; lane 3-5), phenylephrine (10 µM; lane 6-8), 2.5% new born calf serum (NCS), UV radiation (positive controls; lane 9), or medium (DMEM) for the time as indicated. Expression of β-actin (internal standard) is presented in the lower blot in each image. The positions of phospho-ERK1/2 and phospho-p38 MAPK are indicated. Images are representative of four individual experiments. Data were analysed by one-way ANOVA with *post hoc* analysis (Dunnett's). Horizontal bars indicate a statistical significance of $P<0.05$.

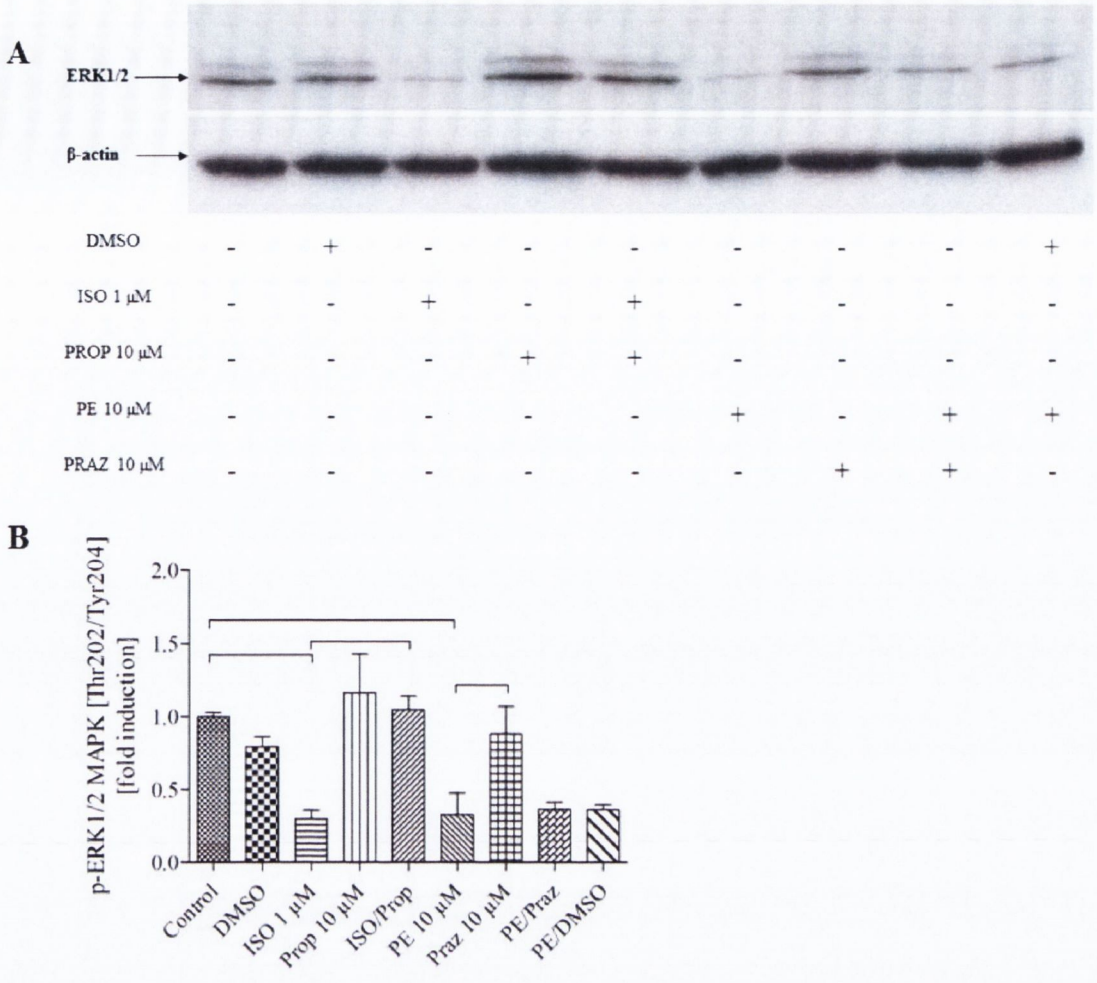


Figure 3.11 Effect of adrenoceptor stimulation and blockade on phospho-ERK1/2 MAPK in HCVF cells.

Western blot analysis was used to detect phospho-ERK1/2 MAPK (A, B). Cells were incubated with isoprenaline (1 μM), phenylephrine (10 μM), or medium (DMEM) for 30 min. Where indicated, cells were incubated with propranolol (10 μM), prazosin (10 μM), DMSO (0.4% v/v), or medium for 30 min prior to exposure to the agonists. Expression of β-actin (internal standard) is presented in the lower blot. The position of phospho-ERK1/2 is indicated. Image is representative of four individual experiments. Data were analysed by one-way ANOVA with *post hoc* analysis (Dunnett's). Horizontal bars indicate a statistical significance of $P<0.05$.

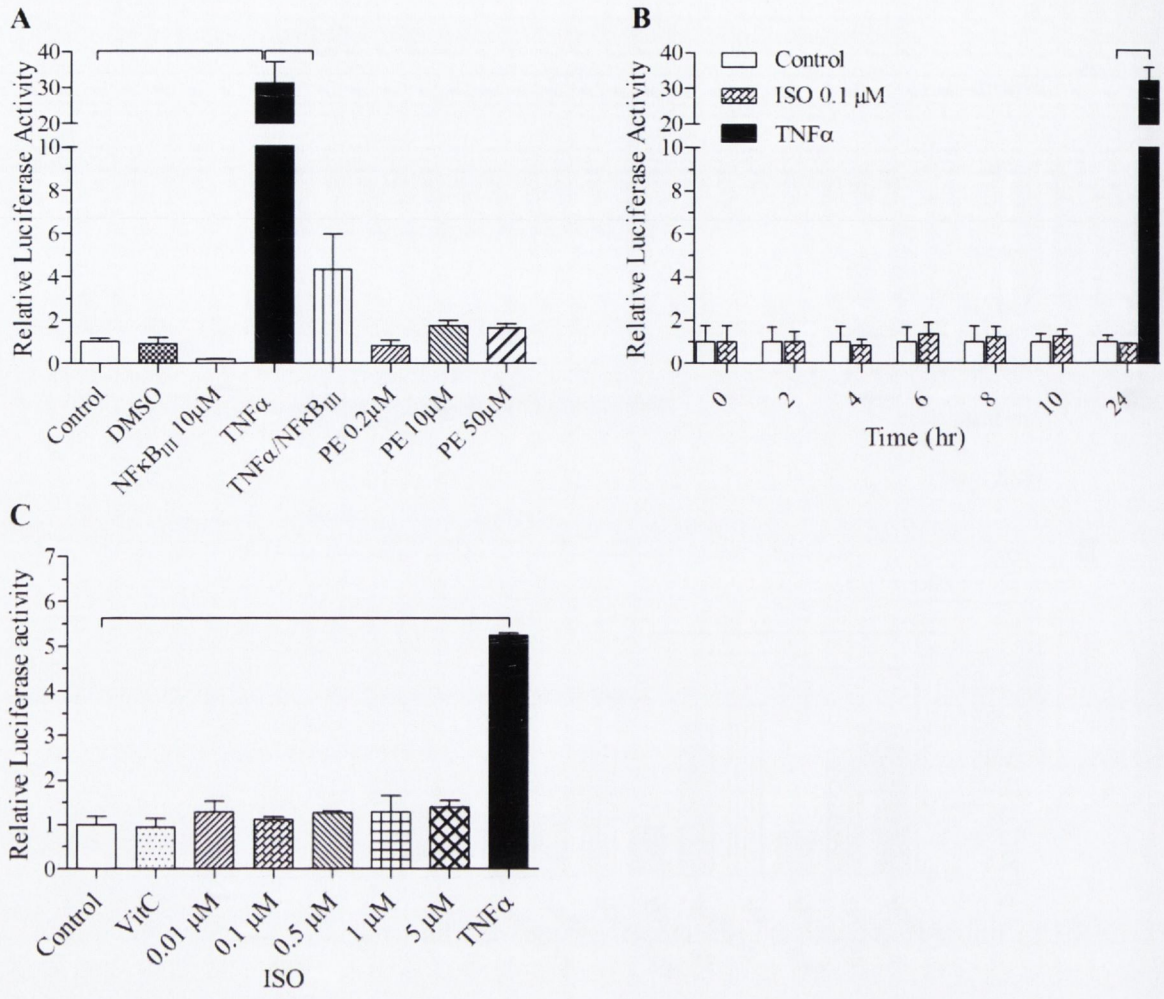


Figure 3.12 Effect of adrenoceptor stimulation on NFκB promoter activity in NIH3T3 cells.

A) NIH3T3 cells were exposed to phenylephrine (PE; 0.2, 10, 50 μM), TNFα (100 ng/ml) ± NFκB-Inhibitor III (10 μM), DMSO (solvent control) or medium (control) for 24 hrs. B) Temporal response in NFκB promoter activity following exposure to isoprenaline (0.1 μM). C) NIH3T3 cells were exposed to isoprenaline (0.01, 0.1, 0.5, 1, 5 μM), vitamin C (VitC; 100 μM), and medium (control) for 6 hrs. Luciferase activity was determined in cell lysates. Data are expressed as fold increase (mean ± S.E.M.; n=6 (A), and n=3 (B, C), respectively) relative to untreated cells transfected with NFκB-Luc. Data were analysed by one-way or two-way ANOVA as appropriate with *post hoc* analysis (Bonferroni, Dunnett's). Horizontal bars indicate a statistical significance of $P<0.05$.

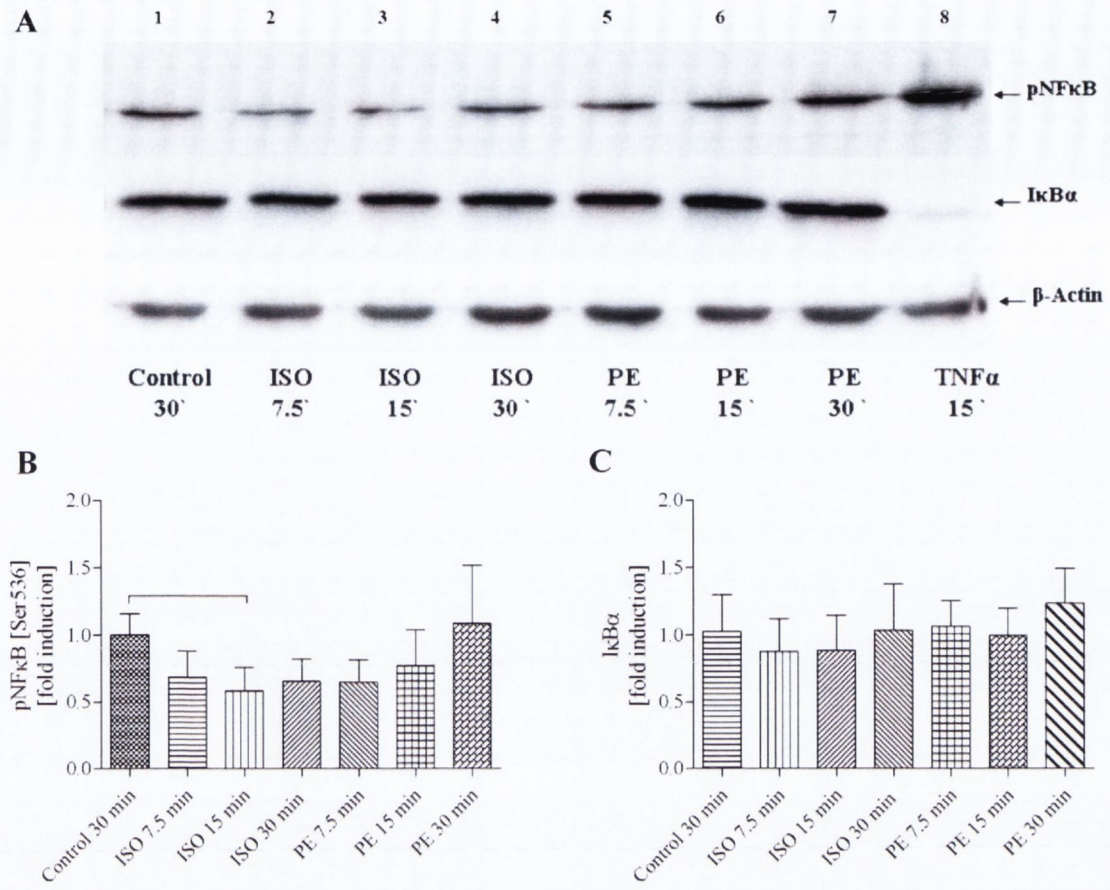


Figure 3.13 Temporal effects of isoprenaline and phenylephrine on NFκB phosphorylation and IκBα expression in NIH3T3 cells.

Cells were stimulated with isoprenaline (ISO; 1 μM; lane 2-4), phenylephrine (PE; 10 μM; lane 5-7), or TNFα (100 ng/ml). At the times indicated, cellular protein was isolated and phosphorylation of NFκB p65 (Ser^{536}) and expression of IκBα were determined by Western blot analysis. Expression of β-actin (internal standard) is presented in the lower blot of each image. The positions of phospho-NFκB (Ser^{536}) and IκBα are indicated. Images are representative of four individual experiments.

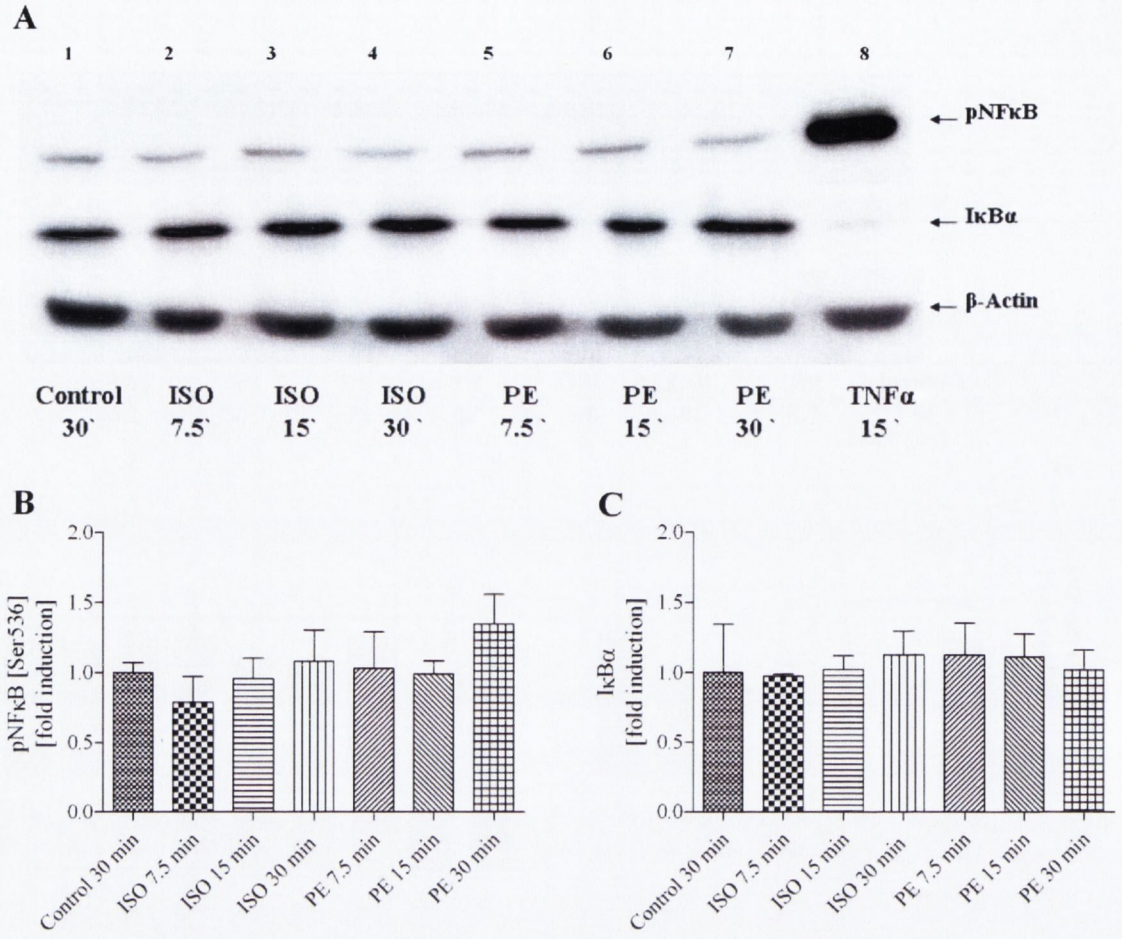


Figure 3.14 Temporal effects of isoprenaline and phenylephrine on NFκB phosphorylation and IκBα expression in HCVF cells.

Cells were stimulated with isoprenaline (ISO; 1 μM; lane 2-4), phenylephrine (PE; 10 μM; lane 5-7), or TNFα (100 ng/ml). At the times indicated, cellular protein was isolated and phosphorylation of NFκB p65 (Ser^{536}) and expression of IκBα were determined by Western blot analysis. Expression of β-actin (internal standard) is presented in the lower blot of each image. The positions of phospho-NFκB (Ser^{536}) and IκBα are indicated. Images are representative of four individual experiments.

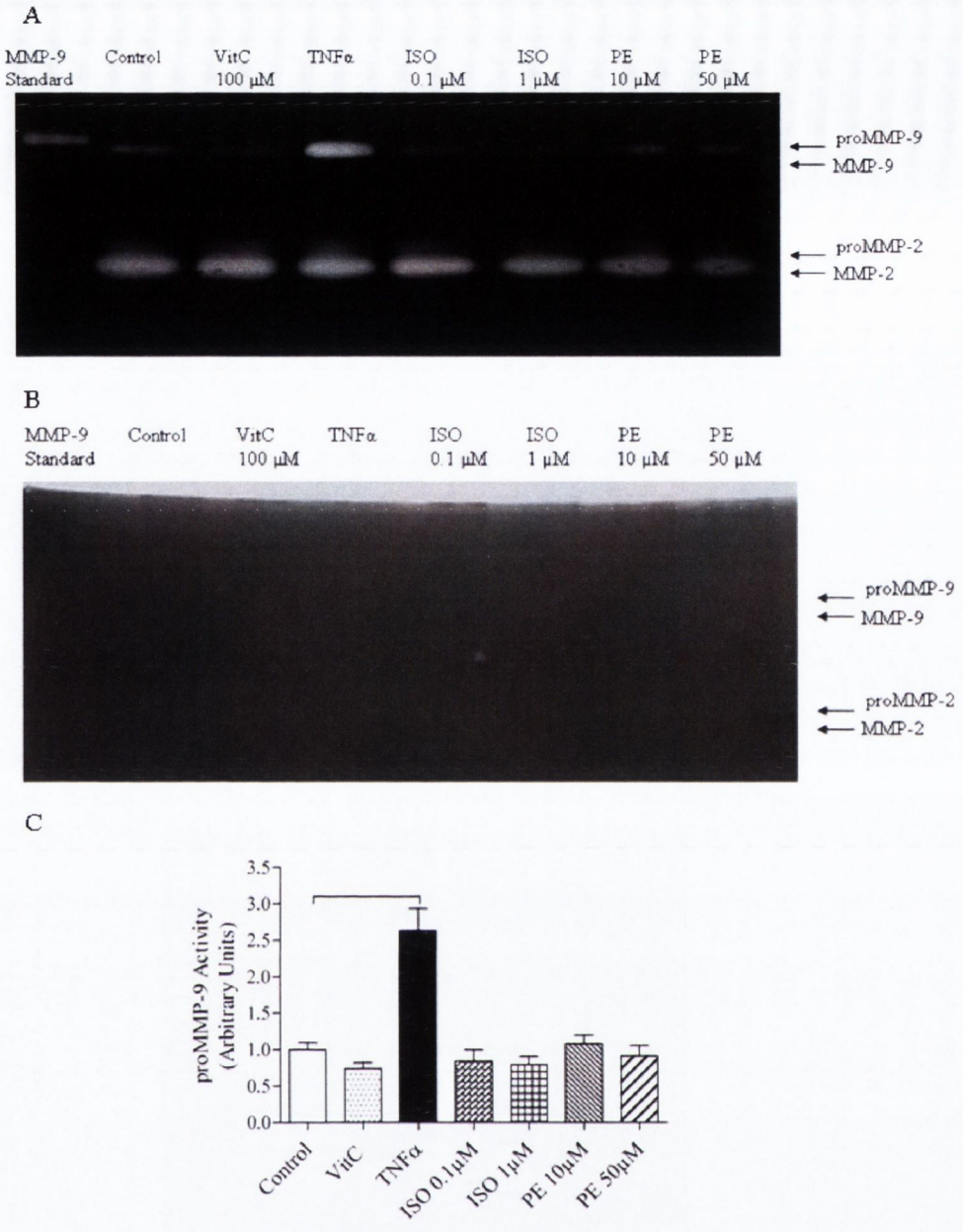


Figure 3.15 Effect of adrenoceptor stimulation on MMP-9 activity in NIH3T3 fibroblasts. Cells were exposed to isoprenaline (ISO; 0.1 and 1.0 µM), phenylephrine (PE; 10 and 50 µM), TNFα (100 ng/ml; positive control), vitamin C (100 µM) or medium (control) for 24 hrs. MMP activity in conditioned medium was assessed by gelatin-zymography. Representative zymograms showing gelatinase activity in conditioned medium from NIH3T3 cells in the absence (A) or presence of 20 mM EDTA (B) are presented. Densitometric data for proMMP-9 activity is summarised in (C). Data are normalised to untreated controls (mean ± S.E.M.; n=6). Data were analysed by one-way ANOVA with *post hoc* analysis (Dunnett's). Horizontal bars indicate a statistical significance of $P<0.05$.

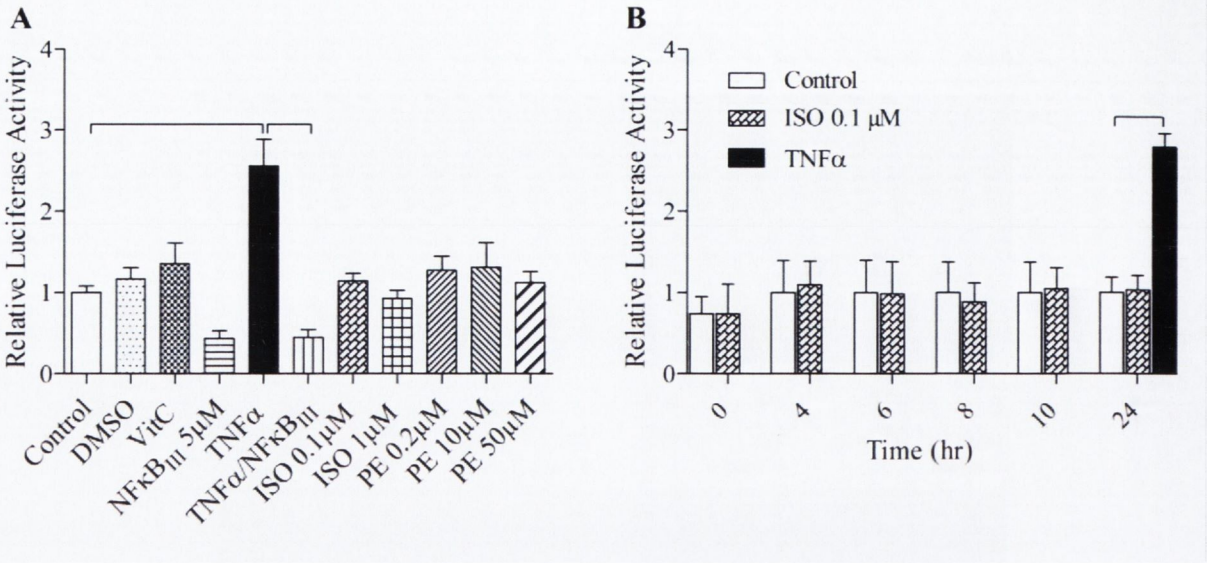


Figure 3.16 Effect of adrenoceptor stimulation on MMP-9 promoter activity in NIH3T3 fibroblasts.

A) Cells were exposed to isoprenaline (ISO; 0.1 and 1 μM), phenylephrine (PE; 0.2, 10, 50 μM), vitamin C (100 μM), TNFα (100 ng/ml) ± NFκB-Inhibitor III (5 μM), DMSO (solvent control) or medium (untreated control) for 24 hrs; B) Temporal response in MMP-9 promoter activity following exposure to isoprenaline (0.1 μM). Luciferase activity was measured in cell lysates. Data are expressed as fold increase (mean ± S.E.M.; n=3) relative to untreated cells transfected with p1285-Luc. Data were analysed by one-way or two-way ANOVA as appropriate with *post hoc* analysis (Bonferroni, Dunnett's). Horizontal bars indicate a statistical significance of $P<0.05$.

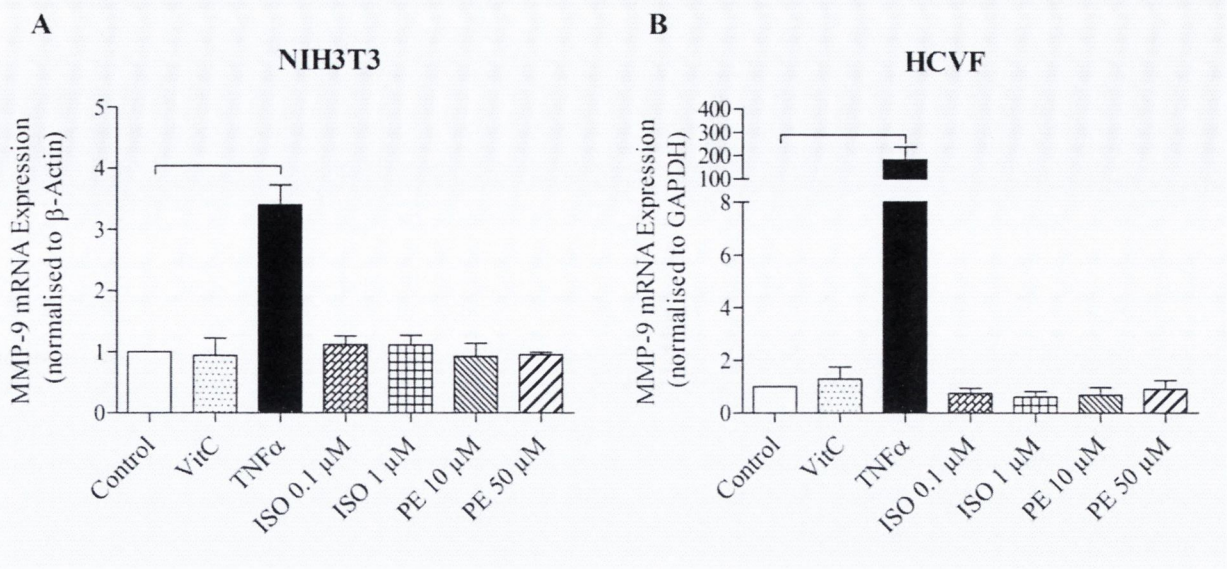


Figure 3.17 Effect of adrenoceptor stimulation on MMP-9 mRNA expression in (A) NIH3T3 and (B) HCVF fibroblasts.

Cells were exposed to isoprenaline (ISO; 0.1 and 1.0 μM), phenylephrine (PE; 10 and 50 μM, TNFα (100 ng/ml; positive control), vitamin C (100 μM) or medium (control) for 24 hrs. mRNA expressions was determined by real-time RT-PCR according to the method of Pfaffl. Data are expressed ad mean ± S.E.M. (n=4). Data were analysed by one-way ANOVA with *post hoc* analysis (Dunnett's). Horizontal bars indicate a statistical significance of $P<0.05$.

3.4 Discussion

In the present study, we show that β-adrenoceptor activation by isoprenaline increased intracellular cAMP and can be inhibited by propranolol in NIH3T3 and HCVF fibroblasts. Downstream of this, isoprenaline and forskolin (receptor independent adenylate cyclase activator) caused robust translocation of phospho-CREB from the cytoplasm to the nuclear compartment in NIH3T3 fibroblasts, as previously described in corticotrope and NIH3T3 cells[240, 241]. Interestingly, in the present study phenylephrine caused a similar effect. Markou T. *et al.* also showed that α_1-adrenoceptors can activate CREB through a MSK1 and PKA dependent signalling pathway in adult rat cardiac myocytes.[242]. Recently, Ozgen *et al.* linked this to $G\alpha_q$ mediated activation of PKC (delta isoform), which activates protein kinase D (PKD), which in turn phosphorylates CREB in cardiomyocytes[243]. However, CREB can also be phosphorylated by kinases other than PKA and PKD, such as MSK1, Ca^{2+}/calmodulin-dependent protein kinases and some MAPK-activated protein kinases[244, 245]. Indeed, we clearly demonstrate that isoprenaline and phenylephrine increase phospho-p38 MAPK and phospho-ERK1/2 MAPK in NIH3T3 fibroblasts, which is in keeping with previous reports[246, 247]. This is not a universal finding as phenylephrine can activate p38 MAPK, but inhibit ERK1/2 MAPK in RAT-1 fibroblasts[248]. Indeed, we show that phenylephrine reduces phospho-ERK1/2 MAPK levels in HCVF cells. α_1-Adrenoceptor mediated activation of ERK1/2 MAPK is dynamic in that its phosphorylation and dephosphorylation has a temporal component in cardiac myocytes[249]. In particular, ERK1/2 MAPK activation initially peaked at 5 min, which was followed by reactivation from 6 till 24 hrs. Therefore, it cannot be excluded that phenylephrine may have activated ERK1/2 in HCVF cells, as this was only studied at a single time point (30 min). In HCVFs, isoprenaline decreased phospho-ERK1/2 MAPK levels, which is in keeping with data from a study keratinocytes[207]. The temporal activation and deactivation

of ERK1/2 MAPK in response to isoprenaline may be regulated by protein phosphatases. For instance, in keratinocytes, β_2-adrenoceptor activation inactivates ERK1/2 MAPK through PP2A[207]. The fact that propranolol blocked the effects of isoprenaline on phospho-ERK1/2 MAPK expression, confirms that this effect is directly mediated by β-adrenoceptors. Interestingly, prazosin did not prevent phenylephrine decreased phospho-ERK1/2 MAPK levels. This was unexpected and is difficult to explain. However, phenylephrine may decrease phospho-ERK1/2 MAPK expression by non-specific effects independent of α_1-adrenoceptor stimulation in our cells. Alternatively, it may reflect differences in subpopulations of the α_1-adrenoceptors, as α_{1L}-adrenoceptors have a low affinity for prazosin[250, 251].

ERK 1/2 and p38 MAPK signalling pathways can converge on a common downstream target the mitogen- and stress-activated protein kinase (MSK1)[225, 226], which can activate NFκB[227]. Therefore, we investigated the effects of isoprenaline and phenylephrine on NFκB reporter activity in NIH3T3 fibroblasts. However, isoprenaline and phenylephrine did not alter NFκB promoter activity at any concentration or time point studied, despite TNFα eliciting a robust 30 fold induction in promoter activity. This was unexpected as β-adrenoceptors activate NFκB in cardiomyocytes[252, 253], cardiac–derived endothelial cells[253], rat aorta[254], and rat left ventricular myocardium[255]. Likewise, Purcell *et al.* showed that phenylephrine can alter NFκB promoter activity in rat neonatal cardiac myocytes[234]. Differences between our data and that of others may represent cell type differences, fibroblasts versus cardiomyocytes and endothelial cells.

Degradation of IκBα and site specific post-translational phosphorylation of NFκB are intrinsic events contributing to a maximal NFκB transcriptional response. In the present study, TNFα caused overt degradation of IκBα after 15 min in keeping with the

literature[256]. However, isoprenaline and phenylephrine did not alter IκBα expression in NIH3T3 and HCVF fibroblasts. Data regarding direct effects of adrenoceptor stimulation on IκBα are sparse. Although, β-agonists prevent LPS induced degradation of IκBα in THP-1 cells[257]. Interestingly, β-arrestins, which are recruited following adrenoceptor activation can directly interact with IκBα preventing its phosphorylation and degradation, and thereby inhibit NFκB activation[258, 259]. This may represent an alternative mechanism to account for the lack of effect observed in our study. In keeping with this, isoprenaline decreased phosphorylation of the p65 NFκB subunit at Ser^{536} in NIH3T3 fibroblasts. However, in HCVF cells phosphorylation was unaffected, despite TNFα causing a robust phosphorylation in NIH3T3 and HCVF fibroblasts. The observed differences in the phosphorylation of ERK1/2 and NFκB between the two fibroblast cell lines may represent cell line differences (mouse vs human) or developmental differences (embryonic vs. adult). For example, embryonic cardiac fibroblasts can promote cardiac myocyte proliferation while adult cardiac fibroblasts induce cardiac myocyte hypertrophy and have distinct gene expression profils[260].

Over recent years, evidence has emerged to indicate that adrenoceptor agonist and antagonists can modulate cardiac expression of MMP-2 *in vivo*[189] and in isolated cardiomyocyte[261]. Work by Speidl *et al.* also demonstrate that noradrenaline potentiation of LPS induced MMP-9 expression is prevented by β_1- but not β_2- or α-adrenoceptor antagonists in a leukaemic monocyte lymphoma cell line (U937)[262]. Previous work from our group expanded these findings to show that α- and β-adrenoceptors differentially regulate MMP-9 promoter activity in an epithelial bladder carcinoma cell line (ECV304). This was narrowed down to a 762bp region from -1285 to -523bp which contains transcription factor binding sites for NFκB, Sp1 and PEA3/AP-1[239]. However, in the present study isoprenaline and phenylephrine do not alter MMP-9 promoter activity,

mRNA expression or activity in NIH3T3 fibroblasts or MMP-9 mRNA expression in HCVF. This may simply represent a cell type specific finding. Alternatively, isoprenaline and phenylephrine induced activation of phospho-CREB may explain our lack of effect on NFκB and MMP-9, as CREB can reduce the ability of NFκB to interact with CREB binding protein (CBP) and thereby prevent activation[257, 263-265]. While our data reflects direct effects on the fibroblast, it may not reflect the *in vivo* situation whereby the fibroblast exists in a complex milieu of ECM and different cell types.

Nevertheless, TNFα increased MMP-9 mRNA expression in HCVF and NIH3T3 fibroblasts and MMP-9 promoter activity and enzyme activity in the latter. This would appear to be mediated through NFκB as it can be abolished by pharmacological inhibition of NFκB. This is consistent with data from several cell lines including THP-1 monocytes, ECV304 cells and fibroblasts[228, 266, 267]. This further supports our findings that adrenoceptors do not regulate MMP-9 expression in either murine fibroblasts or human ventricular fibroblasts.

In conclusion, we show that isoprenaline and phenylephrine alter p38 MAPK, ERK1/2 MAPK, and CREB signalling in fibroblasts. This occurs in a receptor dependent manner for isoprenaline as it can be blocked by propranolol, however, the phenylephrine effect is resistant to blockade by prazosin. Furthermore, isoprenaline and phenylephrine do not activate NFκB or alter MMP-9 expression in either cell line. Together these data provide evidence that although β-adrenoceptor signalling is functional in fibroblasts, they are unlikely to contribute to tissue remodelling through direct effects on MMP-9 abundance.

Chapter 4.

Okadaic acid Induces MMP-9 Expression in Fibroblast: Crosstalk between Protein Phosphatase Inhibition and β-Adrenoceptor Signalling

4.1 Introduction

In the mammalian heart more than 90% of total protein phosphatase (PP) activity is attributed to PP1 and PP2A[41]. PP1 and PP2A belong a phosphoprotein phosphatase (PPP) family that also contains PP2B (calcineurin), PP4, PP5, PP5, PP6, and PP7[200]. PP1 is regulated by endogenous inhibitor-1 (I-1), inhibitor-2 (I-2) and DARP-32[200]. Whereas, PP2A activity is inhibited by inhibitor 1 of PP2A ($I1^{PP2A}$) and inhibitor 2 of PP2A ($I2^{PP2A}$)[200]. Recent evidence indicates a close relationship between PPP regulation and adrenoceptor signalling.

There is an increasing body of evidence indicating that protein phosphatases can modulate adrenoceptor signalling and vice versa. Protein kinase A (PKA), a cAMP dependent protein kinase associated with β-adrenoceptor signalling can phosphorylate and activate I-1[41]. In doing so, it prevents dephosphorylation of phospholamban B (PLB) by PP1 and enhances PKA-mediated contractility (positive feedback loop, section 1.6, Figure 1.16)[203-205]. Furthermore, in guinea pig ventricular myocardium, β-adrenoceptor stimulation increases phosphorylation of I-1 and inhibits PP1 activity[202]. Although, PP2A activity was unaltered[202], others report that β_1-adrenoceptor stimulation increases PP2A activity in murine cardiac myocytes[206]. With respect to effects on non-classical signalling cascades, isoprenaline dephosphorylates ERK1/2 MAPK through activation of PP2A in keratinocytes[207].

Although PP1 activity is increased in patients with end-stage heart failure[209], its contribution to disease progression has not been established. Nevertheless, the hearts of mice over-expressing PP1 have clear evidence of cardiac remodelling manifest as fibrosis and ventricular dilation. Cardiac function is also compromised, and the animals have a shortened lifespan[203]. With regard to PP2A, its over-expression is associated with impaired

cardiac function, cardiac hypertrophy, decreased contractile function, and increased fibrosis in transgenic mice[210]. Intriguingly, over-expression of a catalytic inactive form of PP2A also causes dilated cardiomyopathy without altering fibrosis in transgenic mice[268].

Chronic infusion of isoprenaline increases PP1 and PP2A activity and decreases I-1 expression in the rat heart[212, 213], while inhibition of PP2A reduces myocardial infarct size[211]. There is also evidence that interleukin-18 induces PP2A activity and decreases PLB phosphorylation causing diastolic dysfunction in an animal model of asthma[269]. Interestingly, I-1 expression is decreased in the failing human heart[214], while knockout of I-1 protects against arrhythmias and isoprenaline-induced myocardial hypertrophy in mice[214]. Furthermore, okadaic acid a protein phosphatases inhibitor increases collagenase and stromelysin-1 mRNA expression in rat chondrocytes[270] and human fibrosarcoma cells[271]. Together these data support a role for PP1, PP2A and I-1 in tissue remodelling. As adrenoceptor stimulation alters protein phosphatase activity, it is possible that adrenoceptor agonists will modulate the remodelling effects of protein phosphatases. In particular, it remains to be established if phosphoprotein phosphatase inhibition affects expression of other MMPs implicated in tissue remodelling such as MMP-9, and whether this is modulated by β-adrenoceptors in fibrogenic cells. Therefore, the aims of the present study were to: 1) assess the effects of okadaic acid on MMP-9 abundance, 2) determine if isoprenaline modulates this effect, and 3) if so, investigate the underlying signalling pathway.

4.2 Methods

4.2.1 Cell culture

Mouse fibroblasts (NIH3T3) and human adult cardiac ventricular fibroblasts (HCVF) were cultured as described previously (section 3.2.2). Human hepatic stellate cells (LX-2) were cultured in DMEM (4500 mg/L glucose) supplemented with 10% foetal bovine serum, 1 mM sodium pyruvate, 2 mM glutamine, 100 U/ml penicillin, and 100 mg/ml streptomycin at 37°C, 5 % CO_2.

Cells were allowed to attach for 24 hrs, and medium was changed to phenol-red free DMEM containing 5% charcoal stripped foetal calf serum 18 hrs prior to the start of the experiment or as otherwise indicated. With the exception of SB202190 (p38 MAPK inhibitor), U0126 (MEK1/2 MAPK inhibitor), and NFκB-Inhibitor III, which were prepared in DMSO (C_{final}= ≤0.01% v/v); all other stock solutions were prepared in sterile millipore water. Isoprenaline was prepared immediate before use. All working solutions were prepared in medium. Cells were exposed to the drugs for 24 hrs, unless otherwise indicated.

4.2.2 Determination of MMP-9 expression and activity

Cells were seeded in 24-wellplates ($4x10^4$ cells/well) and exposed to either okadaic acid (1-100 nM), isoprenaline (1 μM), okadaic acid (40 nM) in combination with isoprenaline (1 μM), or medium. For the inhibitor studies, cells were pre-incubated (1 hr) with NFκB-Inhibitor III (1 μM), SB 202190 (5 μM) or U0126 (5 μM) prior to addition of okadaic acid (40 nM). Vehicle controls were DMSO and medium. Conditioned medium was collected after 24 hrs, and cell debris was removed by centrifugation (5000 g, 5 min). Samples were

diluted 1:8 in phenol-red free DMEM containing 5% charcoal stripped foetal calf serum prior to measurement of total murine MMP-9 abundance by Elisa (Total MMP-9, Quantikine ELISA Kit R&D Systems) according to manufactures protocol. The optical density was read at 450 nm with a reference wavelength of 540 nm. Samples and standards were analysed in duplicate and MMP-9 abundance determined by interpolation from the MMP-9 standard curve. MMP-9 activity was measured by gelatin-zymography as described previously (section 3.2.6).

4.2.3 Cell viability (MTT-assay)

NIH3T3 fibroblasts seeded in 48-wellplates ($2x10^4$ cells/well) were treated with okadaic acid (1-100 nM), isoprenaline (1 μM), doxorubicin hydrochloride (2.5 μM), medium or DMSO (0.2% v/v) for 24 hrs. Prior to the end of the incubation time thiazolyl blue tetrazolium bromide/PBS solution (5 mg/ml; 14 μl) was added to the wells, and incubated for one hour. The supernatants were removed and the crystals dissolved in DMSO. The absorption was measured by spectrophotometry at a wavelength of 540 nm with a reference wavelength of 650 nm (BioTek, EL 808).

4.2.4 Quantitative Real-time RT-PCR

HCVF cells were seeded at a density of $4x10^4$ cells/well in 24-well plates and allowed to attach for 24 hrs. Medium was changed to phenol-red free DMEM containing 5% charcoal stripped foetal calf serum 18 hrs prior to the start of the experiment. Cells were exposed to okadaic acid (40 nM) and isoprenaline (1 μM), alone or in combination, along with medium for 24 hrs. Quantitative real-time RT-PCR was performed as previously described (see section 3.2.7). In brief, total RNA was isolated using TRI REAGENT™, treated with DNase I and reverse transcribed using anchored oligo-dT_{23} primers and M-MLV Reverse

Transcriptase. Real-time RT-PCR was performed using a QuantiTec Primer Assay (Qiagen), with primers for human MMP-9 (NM_004994) or human GAPDH (NM_002046) and a QuantiTect SYBR Green RT-PCR Kit on a 7900HT Real-time PCR System (Applied Biosystems).

4.2.5 Knockdown of β-arrestin 2 by siRNA

NIH3T3 fibroblasts were seeded in 48-well plates ($1x10^4$ cells/well), 24 hrs before transfection. On-Target plus smart pool siRNAs targeting mouse β-arrestin 2 and On-Target plus Non-targeting pool siRNAs were reconstituted at a concentration of 20 μM in RNase-free dH_2O. Cells were transfected with 100 nM siRNAs using Dharmafect3 transfection reagent according to manufacturer's instructions. In brief, one tube containing 1.25 μl of siRNA (20 μM) and 23.75 μl serum free Opti-MEM was mixed with a second tube containing 0.5 μl Dharmafect 3 transfection reagent and 24.5 μl serum free Opti-Mem. This mixture was incubated for 20 min to allow complex formation. Following replacement of the culture medium in the plates, the transfection mix (50 μl) was added to each well. Cells were transfected for 54 hrs and then the medium was changed to phenol-red free DMEM containing 5% charcoal stripped foetal calf serum. After a further 72 hrs, cells were exposed to either okadaic acid (40 nM), isoprenaline, in combination, or medium for 24 hrs. Knockdown of β-arrestin 2 expression was confirmed in each experiment by western blot analysis using an anti-β-arrestin 2 antibody (1:500 dilution).

4.2.6 Determination of protein concentration (Bradford-assay)

The protein concentration in cell lysates was determined using Bradford reagent in accordance with the 96 well plate assay protocol supplied by the company (Sigma-Aldrich). In brief, a BSA standard curve over the concentration range 0.1-1.4 mg/ml was prepared by serial dilution. Samples, standards and blank (lysis buffer) were added to a 96-wellplate.

Bradford reagent (250 µl) was added to each well, mixed for 30 seconds and incubated for 20 min. Absorbance was measured at 650 nm. All samples were analysed in triplicate. Protein concentration of the samples was determined by interpolation of mean absorbance against protein concentration of the standards.

4.2.7 PP2A activity assay

NIH3T3 cells were grown to 60-70% confluency in T75-Flasks (Nunc). Medium was changed to phenol-red free DMEM containing 5% charcoal stripped foetal calf serum and cells were incubated for a further 18 hrs. Cells were treated with okadaic acid (40 nM), isoprenaline (1 µM), alone or in combination, along with medium (vehicle control) for the time indicated. Cells were washed twice with TBS-buffer (25 mM Tris, 150 mM NaCl, pH 7.5), and incubated on ice for 15 min in lysis buffer (50 mM HEPES, pH 7.5, 0.1 mM EDTA, 0.1 mM EGTA, 120 mM NaCl, 0.5% v/v NP-40) containing a protease inhibitor cocktail (156 µM AEBSF, 120 nM aprotinin, 6 µM bestatin 2.1 µM E-64, 3.0 µM leupeptin, 2.25 µM pepstain A). Cells were disrupted by sonicating on ice for 15 seconds. Lysates were cleared by centrifugation (5 min, 12000 g, 4°C) and protein content determined by Bradford assay. Equal amounts of protein were analysed for PP2A activity with a DuoSet IC Active PP2A Assay (R&D Systems) according to manufactures protocol. After the last incubation step, absorbance was measured within 5 min at 650 nm. All samples and standards were analysed in triplicate. PP2A activity in the samples was determined from the standard curve of absorbance versus concentration of the phosphate standards. Furthermore, each assay run contained a negative control (no lysates) as a quality control for phosphatase contamination.

4.2.8 Mutation of the NFκB and AP-1 binding sites in the MMP-9 promoter construct

The p1285-luc construct (section 3.2.1) was used as the backbone for the design of two-base pair mutations in the $NF\kappa B_{(-600)}$, $AP\text{-}1_{(-533)}$ and $AP\text{-}1_{(-79)}$ sites (Figure 4.1). All mutations were designed in accordance with transcription factor binding patterns predicted by AliBaba 2.1 (Appendix 2)[272]. The NFκB site was mutated from 5'-GGAATTCCCCA-3' to 5'-GGAACTCACCA-3' and both AP-1 sites were mutated from 5'-TGAGTCA-3' to 5'-TGAGTTG-3'. The underline indicates the mutated bases. Mutagenesis was performed by GenScript Corporation (USA). The fidelity of the pGL3-plasmids containing the mutated inserts was verified using restriction enzyme digestion (*Xho*I/*Hind*III; Figure 4.2) and sequence analysis (Table 4.1 and Appendix 3). Transient transfection was performed as previously described (see section 3.2.7). In brief, cells were transfected with 450 ng/well of the promoter constructs along with 1 ng pRL-CMV (internal standard) in Opti-Mem. After exposure to drugs, cells were harvested and lysates analysed for luciferase activity (Dual-Luciferase® Reporter Assay System, Promega).

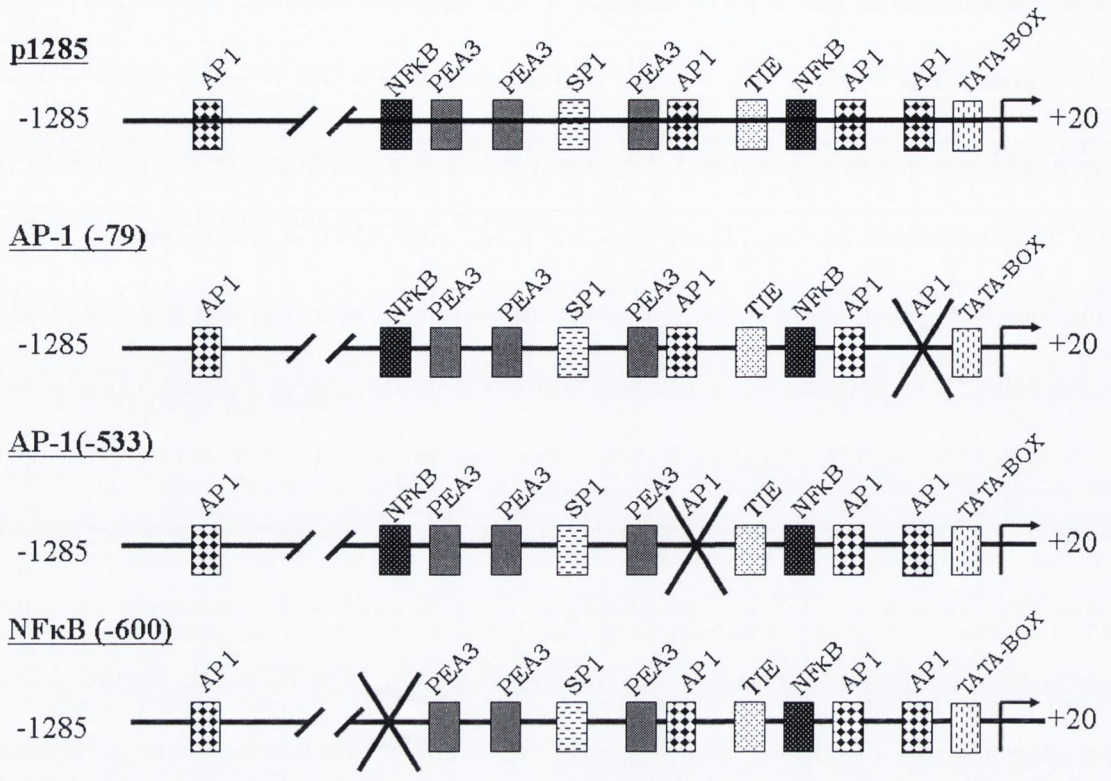


Figure 4.1 Schematic representation illustrating known transcription factor binding sites, and the location of the mutated AP-1 and NFκB binding sites on the p1285-luc MMP-9 promoter.

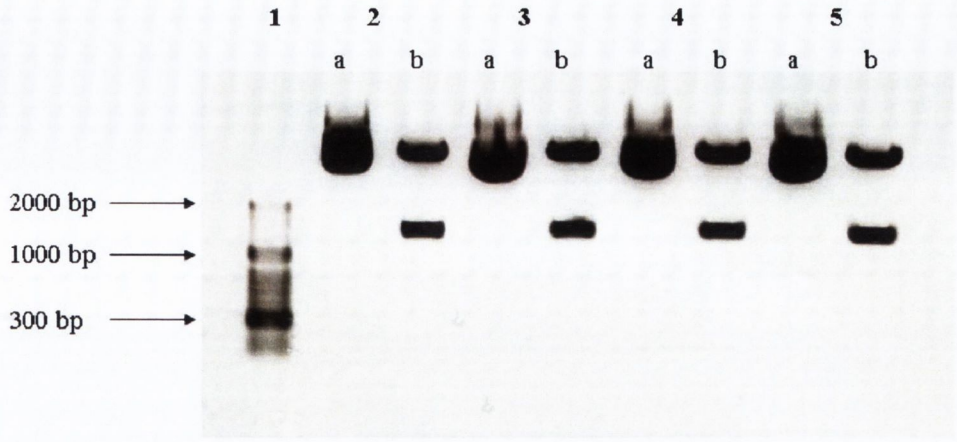


Figure 4.2 Characterisation of the pGL-3 Basic plasmids containing the mutated MMP-9 inserts by restriction enzyme digestion.

A representative mini gel (1% w/v agarose) showing the banding pattern of the p1285-luc (lane 2ab), p1285-luc AP-$1_{(-79)}$ (lane 3ab), p1285-luc AP-$1_{(-533)}$ (lane 4ab) and p1285-luc NFκ$B_{(-600)}$ construct (lane 5ab) along with a Hyperladder II DNA marker (Lane 1) following digestion with H*ind*III/*Xho*I (b). Undigested samples are represented in the lanes labelled (a). The blot is presented as a negative for clarity.

Table 4.1 A summary table showing sequence around the NFκB and AP-1 binding sites of the wild type and mutated MMP-9 promoters. Mutated bases are in bold and underlined.

	NFκB$_{(-600)}$	**AP-1$_{(-533)}$**	**AP-1$_{(-79)}$**
Wild type	5'-GTGGAATTCCCCAGCCTT-3'	5'-AGCTGAGTCAAAGAAGGC-3'	5'-CCCTGAGTCAGCACTTGC-3'
NFκB$_{(-600)}$ mutated	5'-GTGGAA**C**TC**A**CCAGCCTT-3'	As WT	As WT
AP-1$_{(-533)}$ mutated	As WT	5'-AGCTGAGT**TG**AAGAAGGC-3'	As WT
AP-1$_{(-79)}$ mutated	As WT	As WT	5'-CCCTGAGT**TG**GCACTTGC-3'

4.2.9 Western blot analysis

For the analysis of p38 MAPK and ERK1/2 MAPK phosphorylation, cells were seeded in 6-well plates ($3x10^5$ cells/well), and cultured in serum free DMEM for 5 hours prior to starting the experiment. For all other experiments, cells were seeded in 6-wellplates ($3x10^5$ cells/well) and medium was changed to phenol-red free DMEM containing 5% charcoal stripped foetal calf serum 18 hrs prior to the start of the experiment. Cells were treated with okadaic acid (40 nM), isoprenaline (1 μM), alone or in combination, along with the appropriate control (5% charcoal stripped foetal calf serum DMEM or DMEM) for 7.5 min, 30 min, 1 hr, 5 hrs or 24 hrs.

Western blot analysis was performed as described in section 3.2.10. In this study, anti-phospho-ERK1/2 MAPK (Thr^{202}/Tyr^{204}, 1:1000), anti-phospho-p38 MAPK (Thr^{180}/Tyr^{182}, 1:1000), anti-phospho-NFκB p65 (Ser^{536}, 1:1000), anti-IκBα (1:1000), and anti-β-actin HRP (1:7500) antibodies were used. Horseradish peroxidase (HRP) conjugated antibodies specific for swine anti-rabbit (1:1000) or horse anti-mouse (1:1000) IgG were employed as secondary antibodies.

4.2.10 Data and statistical analysis

Gelatinolytic activity, MMP-9 expression, cell viability, PP2A activity, and western blot data are normalised to their respective controls and either expressed as a percentage or a ratio as indicated. mRNA expression was analyzed according to Pfaffl[273] by determination of amplification efficiency for each primer set ($R^2 \geq 0.98$) as previously described (see section 3.2.7.2) and analysed in duplicate. MMP-9 reporter data are expressed as the ratio of firefly luciferase to *renilla* luciferase activity normalised to control (medium) and analysed in duplicate. Differences in the basal activity of the mutated p1285-luc promoter

constructs are expressed relative to the non-mutated p1285-luc construct. Data pertaining to the p1285-luc promoter assays were normalised to their respective control and expressed as a ratio to the p1285-luc construct. Data were analysed by one-way with *post hoc* analysis (Bonferroni, Dunnett's) as appropriate and expressed as mean ± S.E.M.. All experiments were repeated at least three independent times (n). A value of $P<0.05$ was taken to indicate statistical significance.

4.3 Results

4.3.1 Effects of okadaic acid on cell viability and MMP-9 activity

Okadaic acid (1-100 nM) did not alter cell viability in NIH3T3 fibroblasts at any concentration studied (OA 100 nM vs. control: 88.13±2.50 vs. 100±3.69%; Figure 4.3 A). Doxorubicin (2.5 μM) caused a ~50% reduction in cell viability compared to untreated cells (46.60±2.50 vs. 100±3.69%; $P<0.05$; Figure 4.3 A).

A representative *in vitro* zymogram (Figure 4.3 B) shows clear bands of gelatinolytic activity at approximately 62 kDa, 72 kDa and 105 kDa corresponding to MMP-2, proMMP-2 and proMMP-9 in all samples in NIH3T3 fibroblasts. No lytic activity corresponding to MMP-9 was detected. Okadaic acid caused a concentration dependent increase in proMMP-9 gelatinolytic activity in NIH3T3 fibroblasts (40 nM: OA vs. control: 1.38±0.03 vs. 1.0±0.07 AU; $P<0.05$; Figure 4.3 C). Similarly, in hepatic stellate cells okadaic acid increased MMP-9 activity at concentration above 10 nM compared to baseline (40 nM: OA vs. control: 2.83±0.40 vs. 1.0±0.16 AU; $P<0.05$; Figure 4.3 D). Furthermore, okadaic acid at the concentrations studied did not alter proMMP-2 or MMP-2 gelatinolytic activity in NIH3T3 fibroblasts and LX-2 cells.

4.3.2 Effect of isoprenaline on okadaic acid induced MMP-9 abundance

Okadaic acid increased (40 nM; $P<0.05$) proMMP-9 gelatinolytic activity by 40% in NIH3T3 cells compared to control. However, in combination with isoprenaline (10μM), the okadaic acid-mediated increase in proMMP-9 activity was not observed (OA vs. OA/ISO: 136.6±4.0 vs. 97.6±8.1%; $P<0.05$; Figure 4.4 A, B). As in the previous study, isoprenaline did not affect proMMP-9 activity.

To complement this, effects on total MMP-9 protein expression was assessed by Elisa in NIH3T3 fibroblasts. Okadaic acid (40 nM) increased MMP-9 protein from a control level of 4.72±0.50 ng/ml to 7.31±0.57 ng/ml ($P<0.05$; Figure 4.4 C). Again, in combination with isoprenaline this effect was abolished (OA vs. OA/ISO: 7.31±0.57 vs. 4.93±0.62 ng/ml; $P<0.05$; Figure 4.4 C), while isoprenaline alone did not alter MMP-9 protein expression. Furthermore, in human cardiac ventricular fibroblasts, okadaic acid increased MMP-9 mRNA expression by over 2 fold (OA vs. control: 3.4±0.56 vs. 1±0.0 AU; $P<0.05$; Figure 4.5). Similarly, in combination with isoprenaline this increase in MMP-9 mRNA expression was prevented (OA vs. OA/ISO: 3.4±0.56 vs. 1.11±0.45 AU; $P<0.05$; Figure 4.5). Isoprenaline had no effect on MMP-9 mRNA expression in HVCF (Figure 4.5).

4.3.3 The effect of β-arrestin 2 knockdown in NIH3T3 cells

Targeted knockdown of β-arrestin 2 by siRNA interference decreased β-arrestin expression by approximately 70% in NIH3T3 cells (Figure 4.6 A). Furthermore, siRNA treatment with NON-Target siRNA and β-arrestin 2 siRNA did not influence basal proMMP-9 activity (Figure 4.6 B). Okadaic acid (40 nM) increased proMMP-9 activity by 21±5% compared to control ($P<0.05$; Figure 4.6 B) following β-arrestin 2 knockdown. Interestingly, β-arrestin 2 knockdown prevented the inhibitory effect of isoprenaline (1 μM) on okadaic acid mediated proMMP-9 expression (OA vs. OA/ISO: 121.0±5.1 vs. 124.6±6.0%; Figure 4.6 C). Isoprenaline did not influence proMMP-9 activity in transfected cells.

4.3.4 Effect of okadaic acid and isoprenaline on PP2A activity

Okadaic acid (40 nM) caused a marked reduction in PP2A activity after 24 hrs in NIH3T3 cells (OA 40 nM vs. control: 26.8±3.36 vs. 100±1.42%; $P<0.05$; Figure 4.7 A).

Isoprenaline (1 μM) did not affect PP2A activity compared to untreated cells (isoprenaline vs. control: 97.6±4.44 vs. 100±1.42%; Figure 4.7 A), nor did it alter okadaic acid mediated inhibition of PP2A activity (OA vs. OA/ISO: 26.8±3.36 vs. 20.3±0.20%; Figure 4.7 A). However, isoprenaline transiently increased PP2A activity at 5 min (5 min vs. control: 152.9±11.01 vs. 100±3.00%; $P<0.05$; 4.7 B) and 15 min (15 min vs. control: 136.3±10.97 vs. 100±3.00%; $P<0.05$; 4.8 B). By 30 min, isoprenaline-induced PP2A activity had returned to baseline.

4.3.5 Effects of okadaic acid and isoprenaline on p38 and ERK1/2 MAPK signalling pathways

Prolonged exposure (24 hrs) to SB202190 (5 μM), a p38 MAPK pharmacological inhibitor, prevented okadaic acid induced MMP-9 expression (OA vs. OA/SB 202190: 43.31±6.51 vs. 14.77±3.68%; $P<0.05$; Figure 4.8 A). However, U0126 (5 μM), a MEK1/2 MAPK pharmacological inhibitor, did not block the effect of okadaic acid on total MMP-9 abundance (OA vs. OA/U0126: 35.80±6.34 vs. 36.45±8.50%; Figure 4.8 B). Of note, both SB202190 and U0126 decreased basal MMP-9 expression (U0126 vs. control: 37.10±11.18 vs. 0.00±7.44; SB 202190 vs. control: 71.13±8.93 vs. 0.00±6.43%; $P<0.05$; Figure 4.8 A, B).

Okadaic acid (40 nM) did not alter p38 MAPK phosphorylation after 7.5 min compared to control (OA vs. control; 1.01±0.06 vs. 1±0.12 AU; Figure 4.9 A). Although isoprenaline increased phospho-p38 MAPK expression, this was unaltered by okadaic acid in NIH3T3 fibroblasts (ISO vs. OA/ISO; 1.74±0.10 vs. 1.54±0.11 AU; Figure 4.9 A). Furthermore, at this time point, isoprenaline also caused a fold increase in phospho-ERK1/2 MAPK expression. This was not altered on addition of okadaic acid in NIH3T3 fibroblasts (Figure 4.9 A) and okadaic acid alone had no effect on phospho-ERK1/2 MAPK levels compared

to control (Figure 4.9 A). ERK1/2 phosphorylation was not studied at later time points (e.g. 24 hrs), as serum-free medium due to effects on cell viability. In HCVFs, isoprenaline and okadaic acid reduced ERK1/2 MAPK phosphorylation by ~80% and ~70% respectively after 30 min exposure ($P<0.05$; Figure 4.9 B). There was no further inhibition of ERK1/2 MAPK phosphorylation when cells were co-exposed to isoprenaline and okadaic acid (ISO vs. OA/ISO; 0.23±0.01 vs. 0.30±0.15 AU; Figure 4.9 B).

4.3.6 Assessment of the role of AP-1 and NFκB transcription factor binding sites on MMP-9 promoter activity

In NIH3T3 transfected cells, mutation of the proximal AP-1 binding site (-79 bp) attenuated basal promoter activity by 50% compared to the p1285-luc (wild type) MMP-9 promoter ($AP\text{-}1_{(-79)}$ vs. wild type: 49.3±3.7 vs. 100±6.0%; $P<0.05$; Figure 4.10 A). Mutation of the distal AP-1 binding site (-533 bp) did not influence basal wild type MMP-9 promoter activity ($AP\text{-}1_{(-533)}$ vs. wild type: 118.7±8.8 vs. 100±6.0%; Figure 4.10 A). Intriguingly, mutation of the NFκB p65 binding motif (-600 bp) augmented basal promoter activity by 30% compared to the wild type ($NF\kappa B_{(-600)}$ vs. wild type: 136.8±11.1 vs. 100±6.0%; $P<0.05$; Figure 4.10 A).

Okadaic acid (40 nM) increased wild type (p1285-luc) MMP-9 promoter activity by 60% compared to the untreated control (OA vs. control: 165.6±10.9 vs. 100±3.3%; $P<0.05$; Figure 4.10 B), whereas isoprenaline had no effect (ISO vs. control: 79.5±7.3 vs. 100±3.3%; Figure 4.10 B). When the $AP\text{-}1_{(-533)}$ and $AP\text{-}1_{(-79)}$ binding sites were mutated, okadaic acid-induced promoter activity was attenuated by ~50% when compared to the wild type MMP-9 promoter construct ($AP\text{-}1_{(-533)}$: 47.1±4.8 and $AP\text{-}1_{(-79)}$: 58.3±8.4 vs. control: 100±6.5%; $P<0.05$; Figure 4.10 C). Mutation of the $NF\kappa B_{(-600)}$ binding site did not

affect okadaic acid-mediated MMP-9 promoter activity ($NF\kappa B_{(-600)}$ vs. control: 83.5±6.5 vs. 100±6.5%; $P<0.05$; Figure 4.10 C).

In keeping with the zymography data, isoprenaline (1μM) did not alter p1286-luc AP-$1_{(-79)}$, p1285-luc AP-$1_{(-533)}$ or p1285-luc $NF\kappa B_{(-600)}$ promoter activity relative to the wild type MMP-9 promoter construct (AP-$1_{(-79)}$ vs. p1285-luc: 88.1±11.5 vs. 100±8.5 %; Figure 4.10 D). However, it prevented okadaic acid-mediated activation of the wild type MMP-9 promoter (OA vs. OA/ISO: 165.6±10.94 vs. 59.8±8.5%; $P<0.05$; Figure 4.10 B). Interestingly, in combination with okadaic acid, promoter activity of the $NF\kappa B_{(-600)}$ mutant construct increased relative to the wild type MMP-9 promoter construct (147.1±17.0 vs. 100±6.4 %; $P<0.05$; Figure 4.10 D). However, mutation of the AP-1 binding sites (-79 and -533 bp) did not affect wild type MMP-9 promoter activity following co-exposure to isoprenaline and okadaic acid (AP-$1_{(-533)}$: 91.1±11.4 and AP-$1_{(-79)}$: 99.9±13.3 vs. control: 100±6.4%; Figure 4.10 B).

4.3.7 Effects of okadaic acid and isoprenaline on NFκB and IκBα

To extend the data showing that NKκB is involved in modulating the effects of isoprenaline on okadaic acid-mediated MMP-9 promoter activity, the temporal effects on NFκB phosphorylation, IκBα degradation, and NFκB reporter activity were investigated. At the early time point of 7.5 min, isoprenaline (1 μM) caused a rapid decrease in phosphorylation of the NFκB p65 subunit (Ser^{536}) compared to control (0.50±0.04 vs. 1±0.13 AU; $P<0.05$, Figure 4.11 A). Surprisingly, this was not associated with a reciprocal increase in IκBα expression (Figure 4.11 A). Okadaic acid (40 nM) did not alter NFκB phosphorylation, or modify the effect of isoprenaline on NFκB when combined (Figure 4.11 A). Although it was not feasible to assess effects on NFκB promoter activity at 7.5 min, it was assessed at an intermediated time of 5 hrs. Okadaic acid, isoprenaline alone and in combination did not alter NFκB promoter activity at this time point (Figure 4.11 B).

However, TNFα (positive control, 100 ng/ml) caused a 4 fold increase in NFκB promoter activity (Figure 4.11 B).

When cells were exposed to okadaic acid (40 nM) for 24 hrs, phosphorylation of the p65 subunit of NFκB was increased by 1 fold (OA vs. control: 2.05±0.40 vs. 1±0.08 AU; $P<0.05$, Figure 4.12 A). Interestingly, this was not accompanied by a reciprocal change in IκBα expression (Figure 4.12 B). At this later time point, isoprenaline did not alter phospho-NFκB or IκBα expression compared to control. Furthermore, co-exposure to okadaic acid, isoprenaline did not alter the okadaic acid-induced increase in phospho-NFκB expression (OA/ISO vs. OA: 1.86±0.09 vs. 2.05±0.40 AU; Figure 4.12 A). Okadaic acid, isoprenaline alone and in combination did not alter NFκB promoter activity after 24 hrs (Figure 4.12 C). TNFα (positive control) increased NFκB promoter activity by approximately 30 fold (Figure 4.12 C). Incubation of NIH3T3 cells with a NFκB inhibitor (NFκB III Inhibitor; 1 μM) prior to stimulation with okadaic acid confirmed the lack of involvement of NFκB, as the NFκB inhibitor did not prevent okadaic acid induced MMP-9 expression (OA vs. OA/$NF\kappa B_{III}$: 40.08±7.93 vs. 34.13±5.87%; Figure 4.12 D). Okadaic acid increased MMP-9 expression by 40% compared to untreated cells (OA vs. control: 40.08±7.93 vs. 0.0±10.7%; $P<0.05$; Figure 4.12 D) at 24 hrs, while the NFκB inhibitor decreased basal expression of MMP-9 compared to untreated cells (NFκBIII vs. control: 38.41±9.65 vs. 0.00±10.73%; $P<0.05$; Figure 4.12 D).

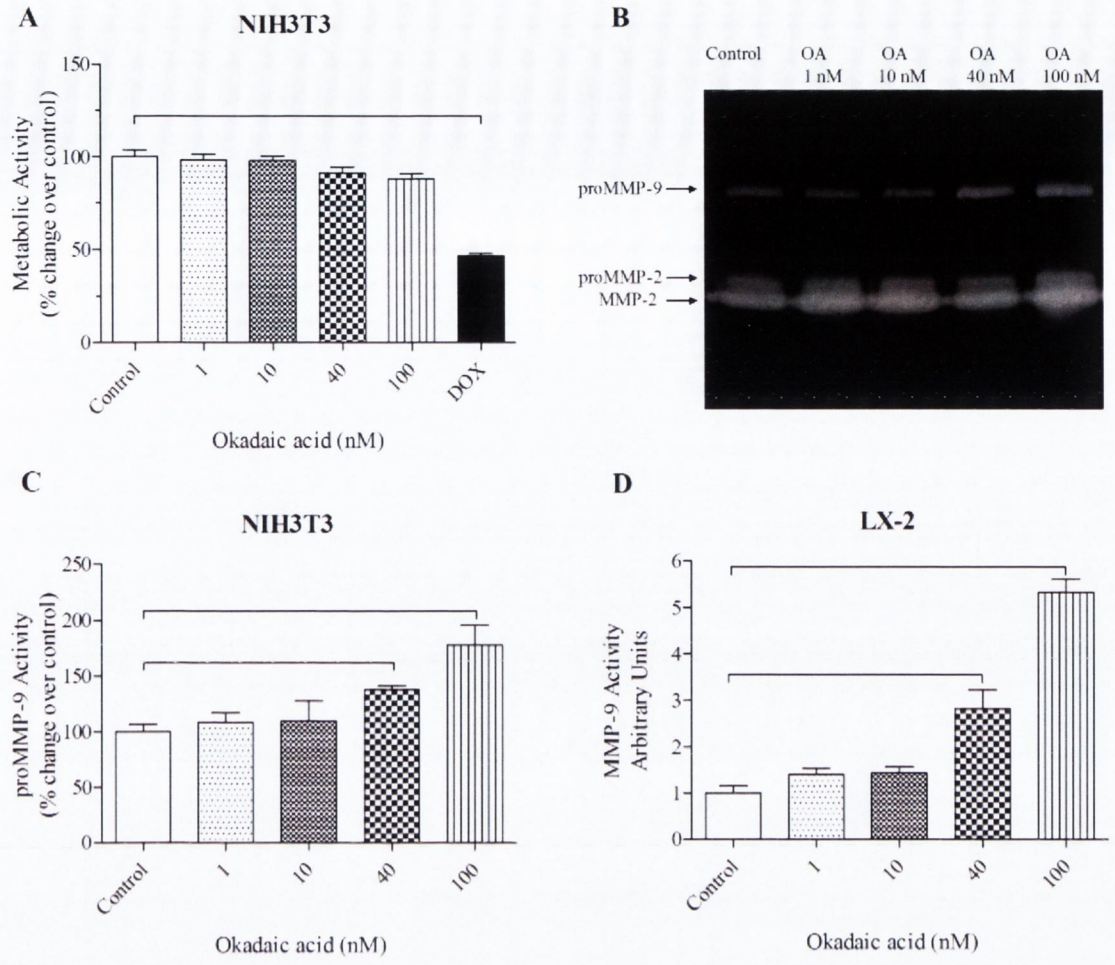


Figure 4.3 Effects of okadaic acid on cell viability and MMP-9 gelatinase activity in NIH3T3 fibroblasts and LX-2 cells.

(A) Cell viability was assessed in NIH3T3 cells following exposure to okadaic acid (1-100 nM), doxorubicin (DOX; 2.5 μM), or medium (control) for 24 hrs. (B) A representative zymogram showing the effects of OA (1-100nM) on gelatinolytic activity in NIH3T3 cells. (C) Concentration dependent effects of okadaic acid on proMMP-9 activity in conditioned medium from NIH3T3 cells. (D) Concentration dependent effects of okadaic acid on MMP-9 activity in conditioned medium from LX2 hepatic stellate cells. Data are expressed as fold increase of control (D; mean ± S.E.M.; n=4) or expressed as a percentage of untreated cells (A; C; mean ± S.E.M.; n=4). Data were analysed by one-way ANOVA with *post hoc* analysis (Dunnett's). Horizontal bars indicate a statistical significance of $P<0.05$.

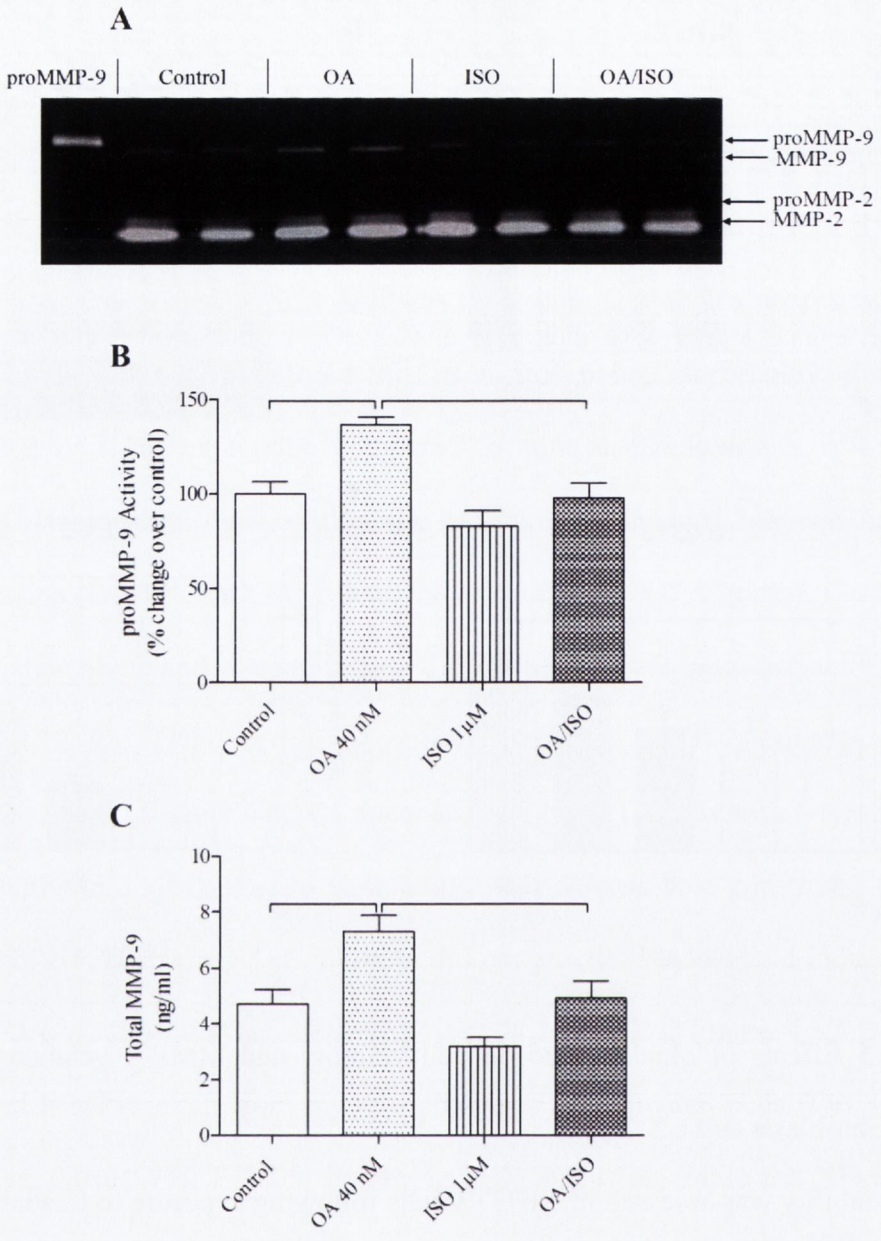


Figure 4.4 Effect of okadaic acid (OA; 40 nM) and isoprenaline (ISO; 1.0 μM), alone and in combination, on MMP-9 abundance in conditioned medium from NIH3T3 fibroblasts. (A) A representative zymogram, (B) MMP-9 activity and (C) total MMP-9 expression assessed by Elisa. Data are expressed as fold increase of control or in ng/ml (mean ± S.E.M.; n=4). Data were analysed by one-way ANOVA with *post hoc* analysis (Bonferroni). Horizontal bars indicate a statistical significance of $P<0.05$.

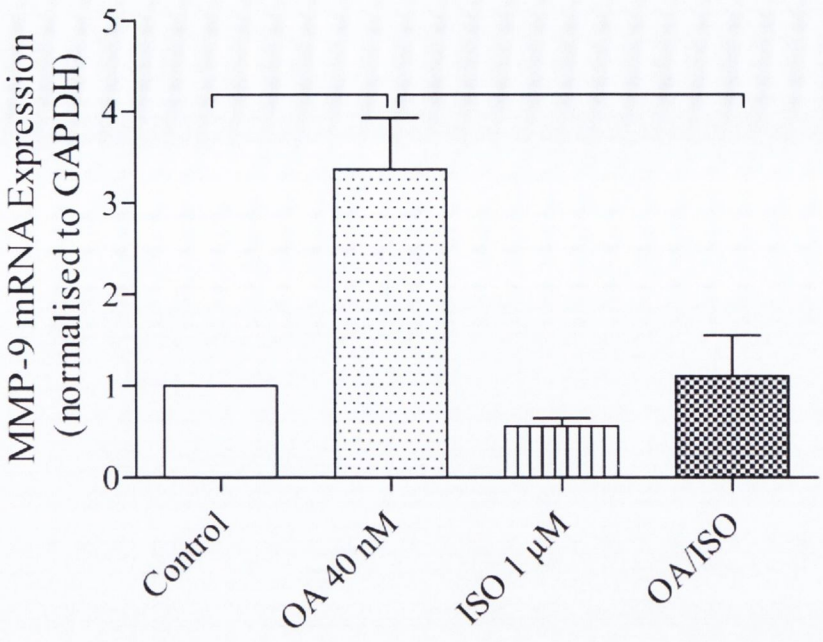


Figure 4.5 Effect of okadaic acid (OA; 40 nM) and isoprenaline (ISO; 1.0 μM), alone or in combination, on mRNA expression in HVCFs.

Relative mRNA expression was calculated according to the method of Pfaffl[273]. Data are expressed as fold increase of control (mean ± S.E.M.; n=4). Data were analysed by one-way ANOVA with *post hoc* analysis (Bonferroni). Horizontal bars indicate a statistical significance of $P<0.05$.

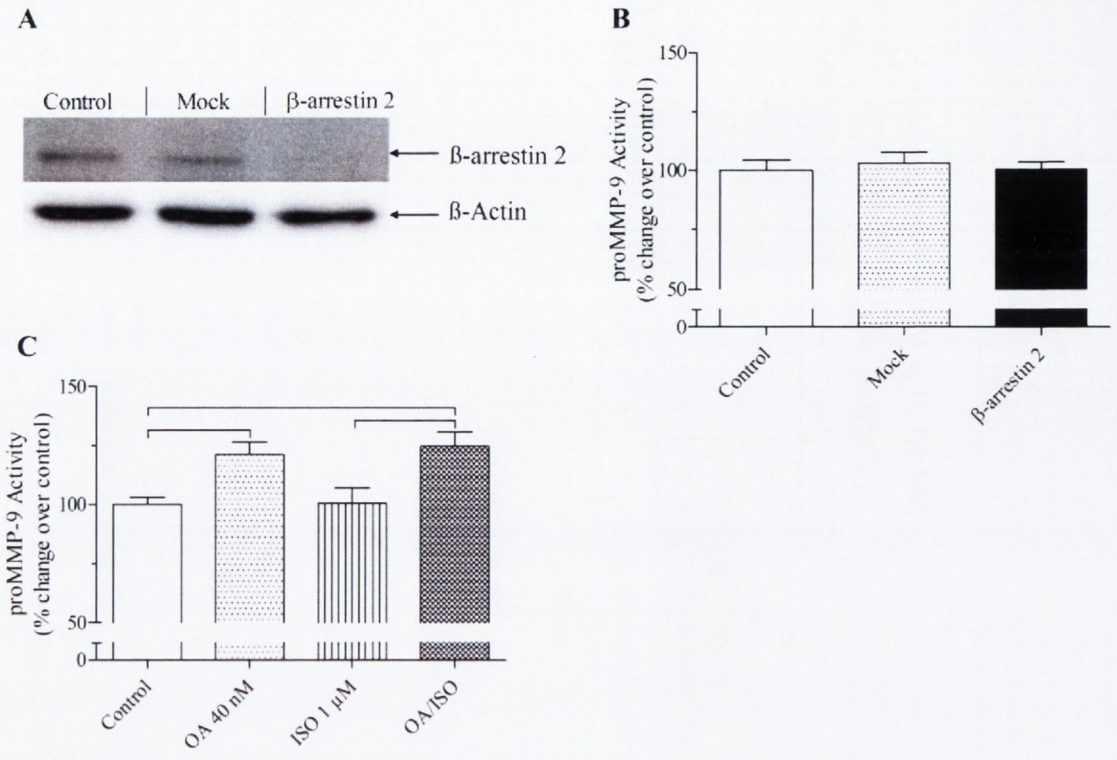


Figure 4.6 The effect of β-arrestin 2 knockdown on MMP-9 activity in NIH3T3 cells. Effects of transfection of NIH3T3 cells with β-arrestin 2 siRNA and NON-Target siRNA on: (A) β-arrestin 2 and β-actin (internal standard) expression in whole cell lysates, (B) basal proMMP-9 activity, and (C) proMMP-9 activity following exposure to okadaic acid (OA; 40 nM) and isoprenaline (ISO; 1 μM), alone and in combination, in β-arrestin 2 siRNA transfected cells. Data are expressed as a percentage of control (mean ± S.E.M.; n=6). Data were analysed by one-way ANOVA with *post hoc* analysis (Bonferroni and Dunnett's). Horizontal bars indicate a statistical significance of $P<0.05$.

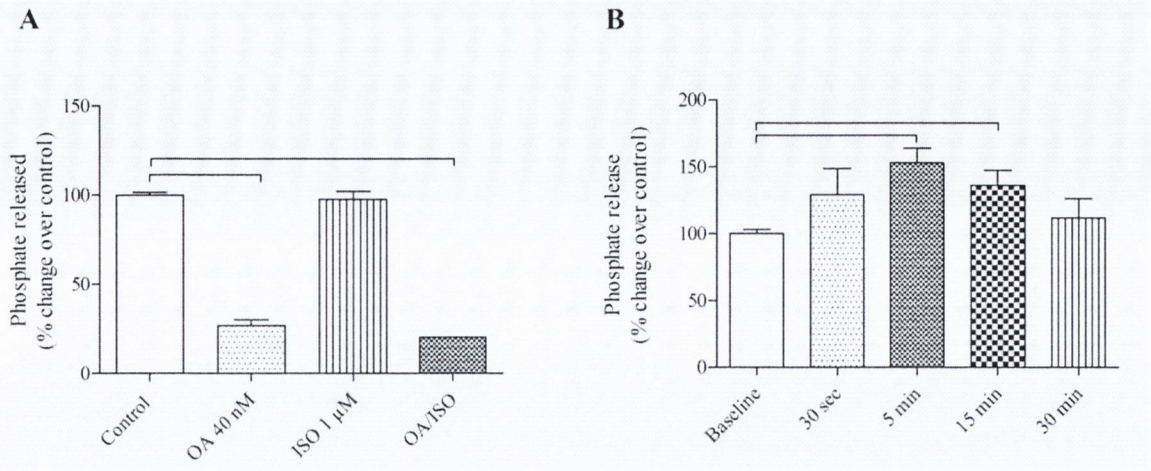


Figure 4.7 Effect of okadaic acid and isoprenaline on PP2A activity in NIH3T3 fibroblasts. (A) Cells were exposed to okadaic acid (OA; 40 nM), isoprenaline (ISO; 1.0 μM) alone and in combination or medium (control) for 24 hrs. (B) Short tern temporal effects of isoprenaline (1.0 μM) on PP2A activity in whole cell lysates. Data are expressed as a percentage of control (mean ± S.E.M.; n=3 (A); n=5 (B)). Data were analysed by one-way ANOVA with *post hoc* analysis (Bonferroni, Dunnett's). Horizontal bars indicate a statistical significance of $P<0.05$.

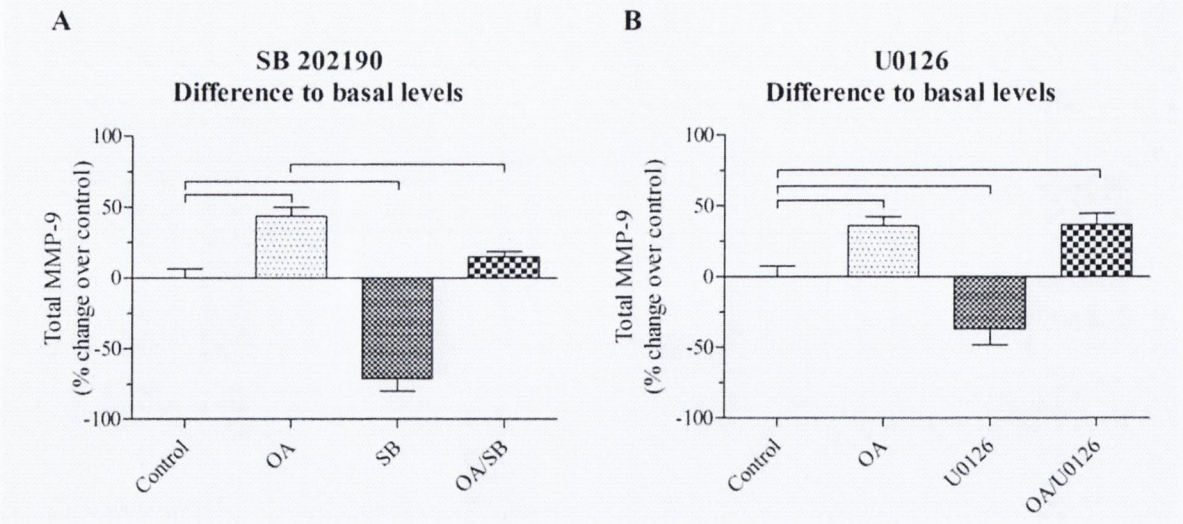


Figure 4.8 Effect of SB202190 and U0126 on okadaic acid induced MMP-9 expression. NIH3T3 cells were exposed to SB202190 (5 μM; p38 MAPK inhibitor; A), U0126 (5 μM; MEK 1/2 inhibitor; B) or medium (control) 1 hr prior to the addition of OA (40 nM) for 24 hrs. Data are expressed as percentage over control (mean ± S.E.M.; n=4). Data were analysed by one-way ANOVA with *post hoc* analysis (Bonferroni). Horizontal bars indicate a statistical significance of $P<0.05$.

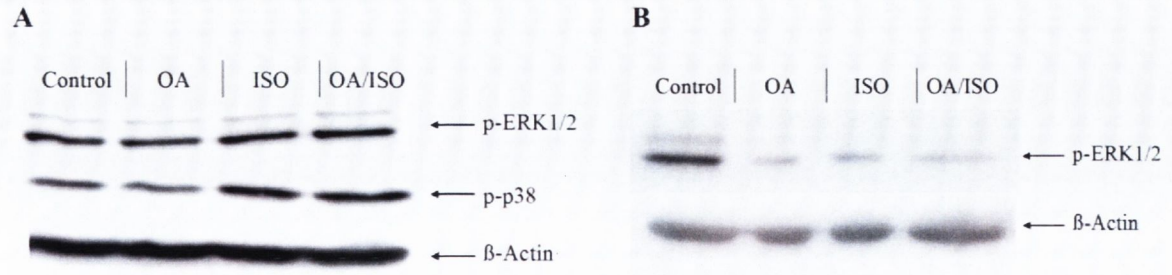


Figure 4.9 Effects of okadaic acid, isoprenaline alone and in combination on phospho-p38 and phospho-ERK1/2 levels in NIH3T3 and HCVF cells.

Effects of okadaic acid (OA, 40nM), isoprenaline (ISO, 1 μM) alone and in combination on phospho-p38 MAPK and phospho-ERK1/2 MAPK expression in NIH3T3 cells at 7.5 min, and (B) phospho-ERK1/2 expression in HCVF at 30 min in whole cell lysates. Cells exposed to medium were included as control. Expression of β-actin (internal standard) is presented in the lower blots in each image. The positions of phospho-ERK1/2 (Thr^{202}/Tyr^{204}) and p38-MAPK (Thr^{180}/Tyr^{182}) are indicated. Images are representative of three individual experiments.

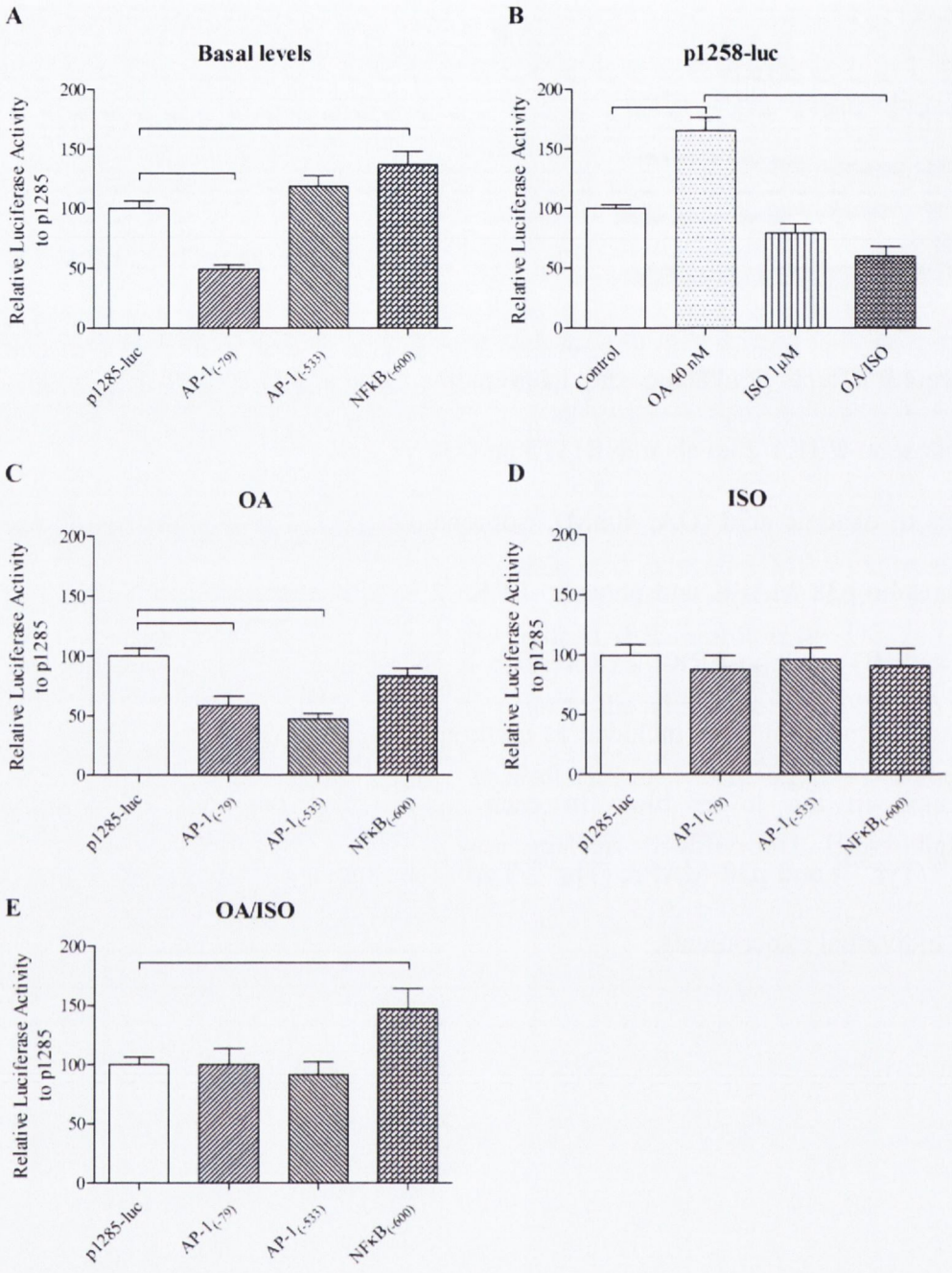


Figure 4.10 Effect of mutation of the AP-1 and NFκB transcription factor binding sites on MMP-9 promoter activity following exposure to okadaic acid and isoprenaline.

NIH3T3 fibroblasts were transfected with p1285-luc, p1285-luc AP-$1_{(-79)}$, p1285-luc AP-$1_{(-533)}$ and p1285-luc $NF\kappa B_{(-600)}$ promoter constructs and exposed to isoprenaline (ISO; 1.0 μM) alone and in combination with okadaic acid (OA; 40 nM). After 24 hrs, luciferase activity was determined in cell lysates. Promoter activity for each mutants was normalised to their individual control and expressed as a ratio to p1285-luc construct (mean ± S.E.M.; n=8). Data were analysed by one-way ANOVA with *post hoc* analysis (Bonferroni and Dunnett's). Horizontal bars indicate a statistical significance of $P<0.05$.

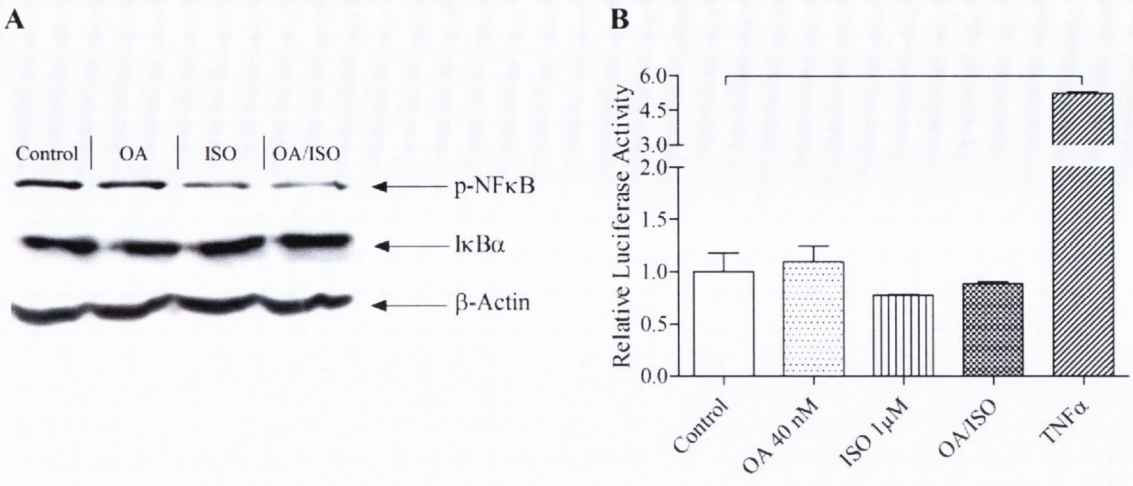


Figure 4.11 Early effects of okadaic acid and isoprenaline on NFκB and IκBα signalling. Effect of okadaic acid (OA; 40 nM) and isoprenaline (ISO; 1.0 μM) alone and in combination on: (A) phosphorylation of NFκB p65 (Ser^{536}) and IκBα expression after 7.5 min, and (B) NFκB promoter activity after 5 hrs. Expression of β-actin (internal standard) is presented in the lower blot in panel A. The positions of NFκB (Ser^{536}) and IκBα are indicated. Images are representative of four individual experiments. Luciferase activity was analysed in cell lysates. Data are expressed as fold increase over control (mean ± S.E.M.; n=3). Data were analysed by one-way ANOVA with *post hoc* analysis (Dunnett's). Horizontal bars indicate a statistical significance of $P<0.05$.

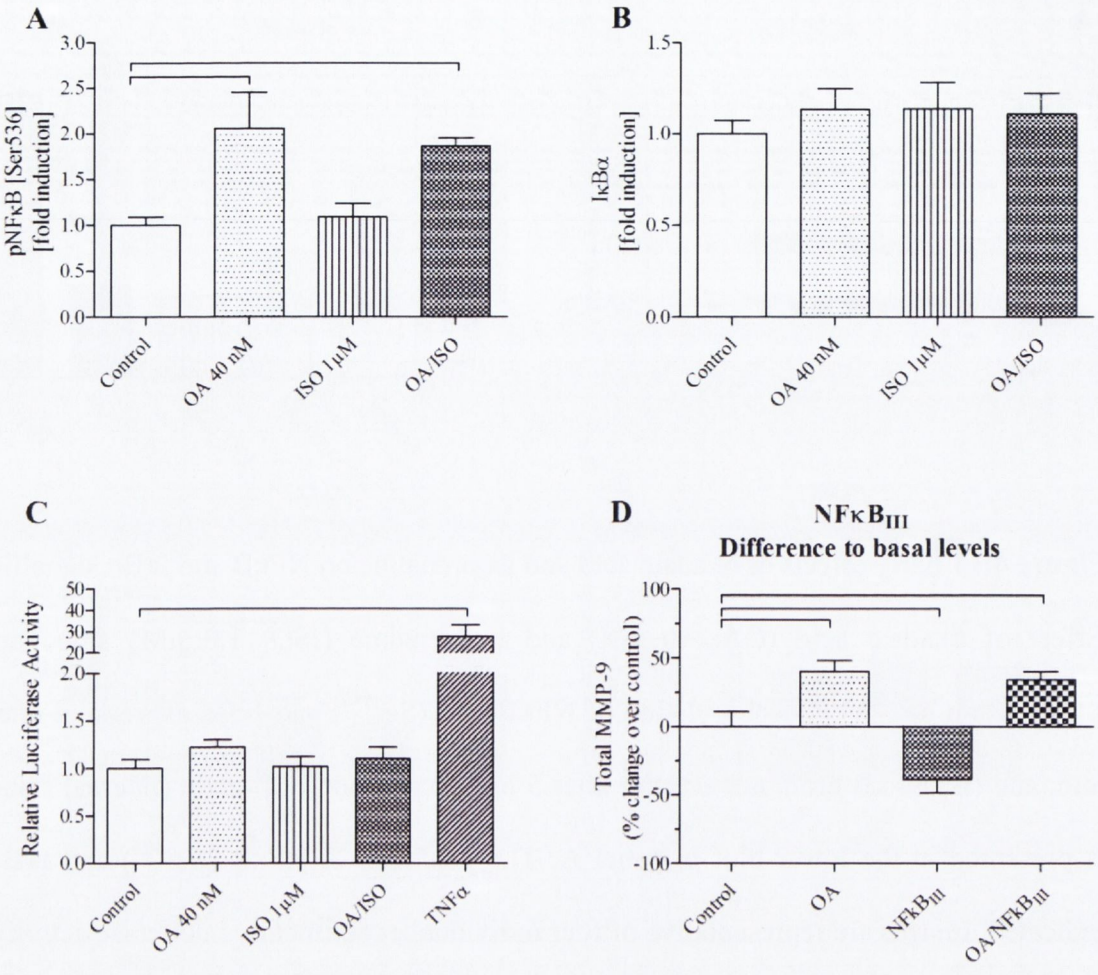


Figure 4.12 Late effects of okadaic acid and isoprenaline on NFκB and IκBα signalling. Effect of okadaic acid (OA; 40 nM) and isoprenaline (ISO; 1.0 μM) alone and in combination on: (A) phosphorylation of NFκB p65 (Ser^{536}), (B) IκBα expression, and (C) NFκB promoter activity after 24 hrs in NIH3T3 fibroblasts. D) Effects of pre-incubation with NFκB-Inhibitor III (1 μM) on MMP-9 expression for 24 hrs in NIH3T3 fibroblasts. MMP-9 abundance was analysed using Elisa and luciferase activity was measured in cell lysates. Data are expressed as fold increase over control or percentage change over control (mean ± S.E.M.; n=3). Data were analysed by one-way ANOVA with *post hoc* analysis (Bonferroni and Dunnett's). Horizontal bars indicate a statistical significance of $P<0.05$.

4.4 Discussion

The present study provides the first evidence that okadaic acid increases MMP-9 abundance in fibroblasts via activation of p38 MAPK, and requires functional AP-1 transcription factor binding sites on the promoter. Furthermore, it demonstrates that isoprenaline inhibits okadaic acid induced MMP-9 expression. This is mediated through β-arrestin 2 and an NFκB consensus motif on the promoter. However, it is not associated with transcriptional activation of NFκB or increased degradation of IκBα.

Okadaic acid is a non-phorbol ester like tumour promoter isolated from shellfish. In the current study, okadaic acid inhibited PP2A activity in keeping with its pharmacological properties[274, 275]. It also increased proMMP-9 gelatinase activity, MMP-9 expression, and MMP-9 promoter activity in NIH3T3 fibroblasts. While in hepatic stellate cells (LX-2) and human cardiac ventricular fibroblasts (HCVF) it increased MMP-9 activity and MMP-9 mRNA expression respectively. The effects on MMP-9 abundance are most likely ascribed to inhibition of PP2A activity, as okadaic acid inhibits PP2A with an IC_{50} of 1 nM in cell-free systems[274], and displays selective inhibition at concentrations below 1 μM in cell models[275]. Although it can also inhibit PP2B (calcineurin) and PP7, this is unlikely to have an influence in the present study as inhibition of PP2B is achieved at concentrations above 10 mM[276], and PP7 is insensitive to okadaic acid[277]. Nevertheless, effects on other protein phosphatase type 2A group members (PP4 and PP6) cannot be excluded.

How okadaic acid increases MMP-9 expression is not known. However, MAPK signalling is an important signalling cascade involved in the regulation of MMP-9 expression in endothelial cells[228], monocytes[266], and cardiac fibroblasts[83]. Therefore, we investigated the effects of okadaic acid on p38 and ERK1/2 MAPK signalling using a p38 MAPK inhibitor

(SB202190) and a MEK1/2 MAPK inhibitor. The latter inhibits MEK1/2 MAPK, which lies immediately up-stream of ERK1/2 MAPK. We found that SB202190 prevented okadaic acid-induced MMP-9 expression while U0126 had no effect in NIH3T3 cells, thus implicating involvement of p38 MAPK signalling. This was not accompanied by early changes (7.5 min) in p38 MAPK or ERK1/2 phosphorylation in NIH3T3 cells, although phospho-ERK1/2 MAPK expression was decreased in HCVF cells at 30 min. Nevertheless, this does not preclude okadaic acid from altering their phosphorylation at a later time point. Both inhibitors decreased basal expression of MMP-9 in NIH3T3 fibroblasts. This is not a universal finding as SB202190 increases MMP-9 activity and mRNA expression, while PD98059 (MEK1 inhibition) abolishes basal MMP-9 activity in monocytes[266]. Nonetheless, Westermarck *et al.*[271, 278] found that okadaic acid increases collagenase-1 (MMP-1) promoter activity in human fibrosarcoma (HT-1080) and NIH3T3 cells, which supports our data. Moreover, this was associated with a transient increase in ERK1/2, JNK/SAPK and p38 MAPK activation, peaking around 3-4 hrs post exposure. They also showed that PD98059 (MEK1 inhibitor) and SB203580 (p38 MAPK inhibitor) blocked okadaic acid induced MMP-1 mRNA expression. This is an interesting finding as MMP-1 and MMP-9 share commonality with regard to cis-acting elements in their promoter regions. This forms the basis of an alternative classification scheme. Under this alternative classification, MMP-1 and MMP-9, are group 1 members, and contain a TATA box and an activator protein-1 (AP-1) site in the proximal ~70 bp region of their promoters[126]. However, MMP-1 differs from MMP-9 in that it contains only NFκB-like elements in the promoter[279].

Intriguingly, isoprenaline prevented the effects of okadaic acid on MMP-9 mRNA expression in HCVF and MMP-9 abundance in NIH3T3 fibroblasts, while having no effect itself. Although, isoprenaline did not alter okadaic acid mediated inhibition of PP2A activity, it caused a transient increase in intracellular PP2A activity peaking at 5 minutes.

Others have also shown that β_1- and β_2-adrenoceptor stimulation is associated with a rapid increase PP2A activity in cardiac myocytes[206] and keratinocytes[207], but not in guinea pigs hearts[202]. Isoprenaline increased phospho-ERK1/2 MAPK and phospho-p38 MAPK expression was not altered in combination with okadaic acid in NIH3T3 fibroblasts. In keeping with this data, okadaic acid at comparable concentrations did not induce early phase p38 MAPK activation in mouse keratinocytes and T leukaemia cells[280, 281]. This would indicate that the effect of isoprenaline on okadaic acid mediated MMP-9 abundance is not simply a reversal of PP2A activity. However, Pullar *et al.* showed that okadaic acid reverses β_2-adrenoceptor mediated dephosphorylation of ERK1/2 MAPK in keratinocytes[207].

Following β-adrenoceptor activation, the receptor is phosphorylated and β-arrestins are recruited. The functional consequences of this are receptor desensitisation, uncoupling from their associated G-proteins and receptor internalisation. More recently, β-arrestins have emerged as scaffolding proteins, which can modify MAPK and other signalling pathways independent of G-protein involvement[50, 53]. Surprisingly, β-arrestin 2 knock down prevented the inhibitory effect of isoprenaline on okadaic acid-increased MMP-9 activity, while having no affect on okadaic acid augmented MMP-9 activity. The exact mechanism by which this occurs warrants further investigation. Although this effect has not been reported before, β-arrestin 2 can form a scaffolding complex with AKT/PP2A following dopaminergic stimulation, which prevents LiCl induced GSK-3β inactivation in mice brains[282, 283]. Interestingly, GSK-3β is a downstream target of p38 MAPK[284] and mediates MMP-9 expression in astrocytes[285].

MMP-9 contains multiple transcription factor binding sites including three AP-1 and one NFκB site. Using deletion mutants of the MMP9 promoter it was noted that both the

proximal AP-1 (-79 bp) and distal AP-1 (-533 bp) binding sites are required for full activation of the p1285-luc promoter by okadaic acid. However, the inhibitory effect of isoprenaline on okadaic acid induced MMP-9 promoter activity is mediated by a NFκB binding motif. This together with the data from the β-arrestin knock out experiments would indicate that isoprenaline inhibits the okadaic acid response through a pathway involving β-arrestin 2 and NFκB. In support of our data, Witherow *et al.* found that over-expression of β-arrestin 1 and β-arrestin 2 decreases NFκB promoter activity[286], and knockdown of β-arrestin 1 augments TNFα induced NFκB promoter activity. This would indicate that the NFκB binding site of the MMP-9 promoter might also have a negative regulatory role. This is supported by the observation that basal levels of MMP-9 promoter activity were increased when the NFκB site was mutated. In contrast, mutation of the AP-1 sites demonstrated that the proximal but not the distal AP-1 is required for basal activation of the MMP-9 promoter. Indeed, other studies show that the proximal AP-1 binding site is important in maintaining basal MMP-9 promoter activity[132, 145, 287]. However, the distal AP-1 (-533) is required for full promoter activity in Hela cells[145], as is the NFκB binding motif[132, 145, 287]. Nonetheless, okadaic acid induced MMP-9 promoter activation requires both AP-1 binding sites, but not the NFκB binding motif in NIH3T3 cells. These key findings along with the upstream signalling pathway in the NIH3T3 fibroblasts are presented as a schematic diagram in Figure 4.13.

Although the NFκB binding site in the MMP-9 promoter does not influence okadaic acid induced MMP-9 expression, other studies show that it can activate NFκB[288-291]. Therefore, we investigated this further by assessing the effects of okadaic acid and isoprenaline on NFκB phosphorylation and IκBα expression. Although okadaic acid increased phosphorylation of NFκB (Ser^{536}), IκBα degradation was unaffected. The former is most likely a direct consequence of PP2A inhibition, as the p65 unit of NFκB is de-

phosphorylated by PP2A *in vitro*[292]. This is at variance to work by Miskolci *et al.*, showing that okadaic acid mediated activation of NFκB is accompanied by a reciprocal degradation of IκBα in human neutrophils[290]. Nevertheless, we also show that okadaic acid did not alter NFκB reporter activity, while pharmacological inhibition of NFκB ($NF\kappa B_{III}$ Inhibitor) did not affect okadaic acid-mediated MMP-9 expression (Figure 4.13). These data in combination with data from the MMP-9 reporter assays strongly indicate that NFκB is not involved in regulation of MMP-9 by okadaic acid in NIH3T3 fibroblasts.

Although mutation of the NFκB binding motif in the p1285-luc construct prevented isoprenaline from inhibiting okadaic induced MMP-9 promoter activity, this was not accompanied by activation of NFκB promoter activity, IκBα expression, or alteration of okadaic acid induced NFκB phosphorylation. Indeed, isoprenaline caused a rapid decrease in NFκB (Ser^{536}) phosphorylation in NIH3T3 fibroblast, indicating an inhibition of the NFκB pathway. Nonetheless, this supports our suggestion that the NFκB binding motif in the MMP-9 promoter plays a negative regulatory role. Data pertaining to β-adrenoceptor or cAMP regulation of NFκB is confusing, as β-adrenoceptor stimulation activates NFκB in cardiomyocytes[253], while in monocytes β-adrenoceptor agonists exert anti-inflammatory properties by repression of the IκBα/NFκB signalling[257]. The latter is an interesting finding as okadaic acid per se did not activate NFκB in NIH3T3 fibroblasts. Nonetheless, Takemoto *et al.* found that chronic stimulation with isoprenaline enhances NFκB DNA binding activity in rats[255]. Therefore, it cannot be ruled out that isoprenaline may have altered NFκB DNA binding activity in the present study and hence regulate MMP-9 promoter in a non-classical manner.

In conclusion, it was found that okadaic acid increases MMP-9 activity via a p38 MAPK signalling cascade and requires both AP-1 binding sites. This effect was inhibited by β-

adrenoceptor stimulation, and mediated by β-arrestin 2 and the NFκB binding site on the MMP-9 promoter. The data extends our understanding of how MMP-9 expression is regulated, and has implications with regard to the pathophysiological progression of diseases with a neurohormonal component. Furthermore, it highlights a possible role of type 2A protein phosphatases in tissue remodelling, and by extension, the beneficial effects they may have in remodelling. Indeed, protein phosphatases may be a new therapeutic target worthy of future development.

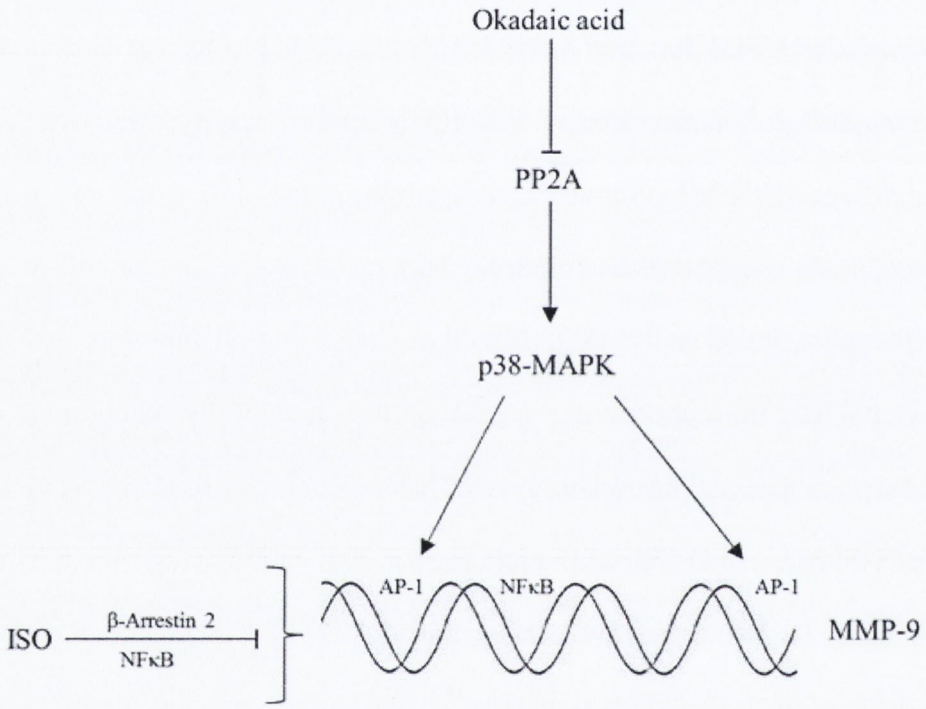


Figure 4.13 Schematic diagram presenting the key findings in NIH3T3 fibroblasts. Okadaic acid inhibited protein phosphatase 2 activity (PP2A) was unaltered by the addition of isoprenaline (ISO) after 24 hrs in NIH3T3 fibroblasts. Okadaic acid increased MMP-9 expression is mediated by p38-MAPK and involved both AP-1 binding site on the MMP-9 promoter. Okadaic acid increased MMP-9 abundance was inhibited by isoprenaline via β-arrestin 2 and the NFκB binding motif of the MMP-9 promoter.

Chapter 5.

Adrenoceptor antagonists differentially regulate TNFα-induced MMP-9 and TIMP-1 expression in NIH3T3 fibroblasts

5.1 Introduction

TNFα plays an important role in inflammation, and is implicated in the pathophysiology of several cardiovascular diseases[82, 293, 294]. Binding of TNFα to its receptors initiates signalling cascades culminating in activation of AP-1 and NFκB transcription factors. These in turn induce a multitude of genes, including many associated with tissue remodelling and fibrosis[125, 267, 295-298]. The latter is characterised by fibroblast proliferation, inflammation, and MMP/TIMP imbalance[90]. In particular, TNFα induces MMP-9 expression through activation of NFκB and subsequent binding to consensus sequence within the MMP-9 promoter. However, the MMP-9 promoter also contains several AP-1 binding sites, which allows regulation through transcription factors belonging to fos and jun families[127, 131, 134, 297].

MMP-9 expression is increased through activation of multiple signalling cascades including ERK1/2 MAPK, p38 MAPK, and SAPK. The cascade utilised, appears to be both cell type and stimulus dependent. For instance, TNFα induces MMP-9 through p38 MAPK and ERK1/2 MAPK in endothelial cells[228] and in skeletal cells[297], but via ERK1/2 MAPK in monocytes[266], and through ERK1/2 MAPK and JNK/SAPK in human trophoblastic cells[299]. IL-1β induces MMP-9 through a p38 MAPK pathway in cardiac fibroblasts[300]. To complicate things further, activation of an ERK1/2 signalling cascade by TNFα results in NFκB activation, while activation of the JNK/SAPK pathway is coupled to AP-1 activation in human trophoblastic cells[299], while in skeletal cells, TNFα activates both p38 MAPK and ERK1/2 MAPK[297].

Although TNFα is well known to increase MMP-9 expression, the data are less well defined with respect to its role in modulating TIMP-1, an endogenous inhibitor of MMP-9. TNFα increases TIMP-1 in human adult dermal fibroblasts[296] and in human retinal pigment

epithelial cells [301], but decreases TIMP-1 mRNA in human bronchial epithelial cells[302], and TIMP-1 expression in renal proximal tubular cells[303]. What's more, Ito *et al.* showed that low doses of TNFα increased TIMP-1, while high doses suppressed TIMP-1 production in human uterine cervical fibroblasts[304]. This is particularly interesting, as TNFα also inhibits and stimulates collagen production[298, 305]. Nevertheless, fibrosis is increased through the actions of extracellular matrix cells and cytokines that regulate collagen metabolism and up-regulate MMPs and TIMPs[179].

Several studies indicate that β-adrenoceptors are able to modulate TNFα abundance, although there is conflicting data. Chronic activation of β-adrenoceptors has been shown to increase TNFα levels in animal models and patients with heart failure[176, 254, 306]. However, Burger *et al.* demonstrate that adrenoceptor stimulation does not alter TNFα expression in cardiac fibroblasts[307], while others show that isoprenaline inhibits TNFα release[308, 309] or induce TNFα mRNA expression[310]. Furthermore, β-Adrenoceptor antagonists decrease serum levels of TNFα in patients with dilated cardiomyopathy[311]. How this occurs is not clear, but there is evidence that TNFα receptors crosstalk with GPCR receptors, as TNFα can enhance GPCR function by preventing agonist induced desensitation[312]. The TNFα receptor can also form a functional signalling complex with $G\alpha_{(q/11)}$/β-arrestin 1 in adipocytes[313]; β-arrestin is a key regulatory protein involved in GPCR signalling[45].

Based upon the above, β-adrenoceptor antagonists may modulate MMP-9 and TIMP-1 abundance in fibroblasts under pro-inflammatory conditions. However, this remains to be established. Therefore, the aims of the present study were to investigate in TNFα activated NIH3T3 fibroblasts: 1) the effects of adrenoceptor blockade on MMP-9 and TIMP-1 abundance, and 2) the involvement of NFκB, and 3) identify the cis-regulatory elements involved, using MMP-9 and TIMP-1 promoter constructs.

5.2 Methods

5.2.1 Cell culture

Mouse fibroblasts (NIH3T3; European Collection of Cell Cultures) were cultured as described previously (section 3.2.2). Cells were allowed to attach for 24 hrs, and medium was changed to phenol-red free DMEM containing 5% charcoal stripped foetal calf serum 18 hrs prior to the start of the experiment.

5.2.2 Drug treatment of NIH3T3 fibroblasts

All stock solutions were prepared in sterile water, except prazosin hydrochloride and (±)-carvedilol, which were dissolved in sterile DMSO (C_{final}= 0.4% and 0.2% v/v, respectively). All working solutions were prepared in medium. DMSO (0.4% v/v) was included in all experiments. Cells were treated with prazosin hydrochloride (PRAZ; 10 μM), (±)-carvedilol (CARV; 10 μM), (±)-propranolol hydrochloride (PROP; 10 μM), (±)-ICI 118,551 hydrochloride (ICI; 10 μM), (RS)-atenolol (ATENO; 10 μM), DMSO (DMSO; 0.4% v/v) or medium (control) for one hour, followed by incubation with 100 ng/ml mouse recombinant TNFα or medium for 24 hrs as indicated.

5.2.3 Gelatin-zymography

Cells were seeded in 24-wellplates ($4x10^4$ cells/well) and treated as above. After 24 hrs, the conditioned medium was collected and cell debris removed (5000 g, 5 min). In brief, equal volumes of conditioned medium were mixed with non-reducing Laemmli sample buffer and subjected to gelatin-zymography utilising 8% SDS-polyacrylamide gels containing 1 mg/ml gelatin. Gels were washed in Triton X-100 (2.5 % v/v) for 30 min and incubated for a further 18 hrs at 37°C in incubation buffer (section 3.2.6). Gelatinolytic

activity was assessed by staining of the gels with Coomassie Brilliant Blue R250, destaining and quantification using GeneGenius Gel documentation system (Syngene, Cambridge, UK).

5.2.4 Determination of MMP-9 and TIMP-1 protein expression

Cells were seeded in 24-wellplates ($4x10^4$ cells/well) and treated as described above. Conditioned medium was collected after 24 hrs, and cell debris removed (5000 g, 5 min). Samples were diluted by 1:8 or 1:20 in phenol-red free DMEM containing 5% charcoal stripped foetal calf serum prior to measurement of total MMP-9 and TIMP-1 abundance by ELISA (Total MMP-9, Quantikine ELISA Kit; mouse TIMP-1, DuoSet ELISA Kit; R&D Systems) according to manufactures protocol. The lower limit of detection for MMP-9 is 0.007 pg/ml. The intra-assay coefficients of variation and the inter-assay coefficients of variation for MMP-9 are 6.4% and 8.5%, respectively. Optical density was read at 450 nm with a reference wavelength of 540 nm. MMP-9 and TIMP-1 levels were determined by interpolation from their respective standard curves. Samples and standards were analysed in duplicate and expressed in ng/ml.

5.2.5 Transient transfection and Dual-Luciferase reporter assay

Transient transfection was performed as described in section 3.2.8. In brief, cells were transfected with 450 ng/well of the promoter constructs along with 1 ng pRL-CMV (internal standard) in Opti-Mem. The following constructs were used: NFκB, p1285-luc, p657-luc, p571-luc, p540-luc, p523-luc, p1285-luc $NF\kappa B_{(-600)}$, p1285-luc $AP\text{-}1_{(-533)}$, and p1285-luc $AP\text{-}1_{(-79)}$, $TIMP_{(-1718/+988)}$-luc and $TIMP_{(-738/+96)}$-luc. After exposure to the drugs (section 5.2.2), cells were harvested and lysates analysed for luciferase activity (Dual-Luciferase® Reporter Assay System, Promega). The TIMP-1 promoter constructs (pGL3-

basic backbone) were kindly provided by Professor Ian M. Clark, University of East Anglia, Norwich, UK. Details of the bases mutated in the NFκB, AP-$1_{(-533)}$ and AP-$1_{(-79)}$ deletion constructs are give in section 4.2.8.

5.2.6 Data and statistical analysis

proMMP-9 gelatinolytic activity is expressed as a percentage over TNFα. MMP-9 and TIMP-1 expression is expressed in ng/ml as a difference from control. Data from reporter assays are analysed in duplicate and expressed as the ratio of firefly luciferase to *renilla* luciferase activity normalised to control (medium). Data pertaining to the p1285-luc promoter assays were normalised to their individual control. Data were analysed by one-way ANOVA with *post hoc* analysis (Bonferroni or Dunnett's) as appropriate, and expressed as mean ± S.E.M.. All experiments were repeated at least three independent times (n). A value of $P<0.05$ was taken to indicate statistical significance.

5.3 Results

5.3.1 The effects of TNFα and adrenoceptor antagonists on MMP-9 activity and expression

A representative *in vitro* zymogram (Figure 5.1 A) shows clear bands of gelatinolytic activity at 62 kDa, 72 kDa, and 105 kDa corresponding to MMP-2, proMMP-2, and proMMP-9 in all samples. Lytic activity corresponding to MMP-9 (95 kDa) was detected, but was too low to quantify. None of the drugs altered either proMMP-2 or MMP-2 activity under basal or TNFα stimulated conditions. Propranolol, ICI 118,551, atenolol, carvedilol, prazosin, and DMSO did not alter proMMP-9 gelatinolytic activity in NIH3T3 cells under un-stimulated conditions. TNFα increased proMMP-9 activity by approximately 5 fold compared to control (TNFα vs. control: 100.0±3.97 vs. 21.1±2.97%; $P<0.05$; Figure 5.1 A, C). The response to TNFα was not altered in the presence of DMSO (TNFα/DMSO vs. TNFα: 89.1±7.11 vs. 1.00.0±3.98%; Figure 5.1 A, C). Prazosin and carvedilol inhibited TNFα mediated proMMP-9 activity by ~40% (TNFα/DMSO vs. TNFα/PRAZ: 89.1±7.11 vs. 54.6±5.32%) and ~50% (TNFα/DMSO vs. TNFα/CARV: 89.1±7.11 vs. 40.1±4.35%; $P<0.05$; Figure 5.1 A, C) respectively. Propranolol, atenolol and ICI 118,551 did not alter TNFα mediated proMMP9 activity (TNFα/ATENO vs. TNFα: 88.7±5.56 vs. 100.0±5.38%; Figure 5.1 B).

In keeping with the zymography data, carvedilol, prazosin, propranolol, ICI 118,551, atenolol and DMSO did not affect total MMP-9 protein expression in NIH3T3 cells (Figure 5.2 A and B). TNFα increased total MMP-9 expression by 4 fold in the conditioned medium of NIH3T3 fibroblasts (TNFα vs. control: 32.69±1.92 vs. 8.00±1.01 ng/ml; $P<0.05$; Figure 5.2 A). This response was not modified on co-exposure to DMSO (TNFα/DMSO vs. TNFα: 33.95±2.23 vs. 32.69±1.92 ng/ml; Figure 5.2 A). Prazosin and

carvedilol both attenuated TNFα mediated expression of MMP-9 expression by ~30% (TNFα/PRAZ and TNFα/CARV vs. TNFα/DMSO: 23.90±0.82 and 23.22±3.34 vs. 33.95±2.23 ng/ml; $P<0.05$; Figure 5.2 A). Propranolol, atenolol, and ICI 118,551 did not affect TNFα-induced MMP-9 expression (Figure 5.2 B).

5.3.2 Effect of 5'-end cis elements on TNFα modulated MMP-9 promoter activity

A schematic representation of cis-acting elements present in the 5'-end truncated MMP-9 promoter constructs is presented in figure 5.3, and following sequencing their presence was confirmed using AliBaba 2.1[272]. Under un-stimulated conditions, promoter activity was equivalent across the mutants, except for the p571-luc, which was decreased ($P<0.05$) compared to the p523-luc construct. TNFα increased p1285-luc promoter activity by 5 fold compared to the p523-luc reference construct (TNFα vs. control: 6.01±0.55 vs. 1±0.06; $P<0.05$; Figure 5.4). Upon removal of the distal AP-1 (-927 bp) binding site[134], TNFα increased p657-luc promoter activity by 1 fold compared to the reference construct (TNFα vs. control: 1.99±0.36 vs. 1±0.06; $P<0.05$; Figure 5.4). Truncation of the MMP-9 promoter region by a further 86 bp and 117 bp to generate the p571-luc and p540-luc constructs, completely removed the ability of TNFα to increase MMP-9 promoter activity (Figure 5.4).

5.3.3 Effects of TNFα and adrenoceptor antagonists on NFκB promoter activity

Carvedilol, prazosin and DMSO did not alter NFκB promoter activity in NIH3T3 cells under un-stimulated conditions. TNFα increased NFκB promoter activity by 30 fold in NIH3T3 fibroblasts (TNFα vs. control: 29.39±3.93 vs. 1±0.16; $P<0.05$; Figure 5.5 A), this was unaffected upon co-exposure with DMSO (TNFα/DMSO vs. TNFα: 26.61±3.76 vs. 29.39±3.93; Figure 5.5 A). The α_1-adrenoceptor antagonist prazosin, inhibited TNFα mediated NFκB promoter activity by 50% (TNFα/PRAZ vs. TNFα/DMSO: 14.02±2.22 vs. 26.61±3.76; $P<0.05$; Figure 5.5 A). Carvedilol also attenuated TNFα mediated NFκB promoter activity by 65% (TNFα/CARV vs. TNFα/DMSO: 9.37±1.24 vs. 26.61±3.76; $P<0.05$; Figure 5.5 A).

Propranolol, ICI 118,551 and atenolol, did not alter NFκB promoter activity in NIH3T3 cells under un-stimulated conditions. In NIH3T3 cells, propranolol decreased TNFα mediated NFκB promoter activity by 50% (TNFα/PROP vs. TNFα: 17.01±2.74 vs. 29.39±3.93; $P<0.05$; Figure 5.5 B). Atenolol caused a slight attenuation (25%) of TNFα mediated NFκB promoter activity, but this failed to reach statistical significance (TNFα/ATENO vs. TNFα: 22.32±3.38 vs. 29.39±3.93; Figure 5.5 B). ICI 118,551, a β_2-adrenoceptor antagonist, caused a robust decrease in TNFα mediated NFκB promoter activity by 50% (TNFα/ICI vs. TNFα: 15.20±1.76 vs. 29.39±3.93; $P<0.05$; Figure 5.5 B).

5.3.4 Effects of TNFα and adrenoceptor antagonism on MMP-9 promoter activity

Carvedilol (10 μM), prazosin (10 μM) and DMSO (0.4% v/v) did not alter MMP-9 promoter activity in NIH3T3 cells under un-stimulated conditions. TNFα increased p1285-luc promoter activity by 1 fold compared to control (TNFα vs. control: 2.33±0.13 vs. 1.00±0.11; $P<0.05$; Figure 5.6 A). This effect was unaltered by co-exposure to DMSO (TNFα/DMSO vs. TNFα: 2.29±0.16 vs. 2.33±0.13; $P<0.05$; Figure 5.6 A). Carvedilol and prazosin reduced TNFα mediated MMP-9 promoter activity by ~35% and ~30%, respectively (TNFα/PRAZ; TNFα/CARV vs. TNFα/DMSO: 1.59±0.17; 1.48±0.10 vs. 2.29±0.16, respectively; $P<0.05$; Figure 5.6 A). Propranolol (10 μM), ICI 118,551 (10 μM) and atenolol (10 μM) did not alter MMP-9 promoter activity under un-stimulated conditions. Furthermore, they did not alter TNFα mediated MMP-9 promoter activity (TNFα/ICI vs. TNFα: 2.06±0.14 vs. 2.33±0.12; Figure 5.6 B).

To delineate the relative importance of the NFκB and AP-1 cis-acting elements mediating these responses, cells were transfected with the wild type (p1285-luc) and MMP-9 reporter mutants (p1285-luc AP-$1_{(-79)}$, p1285-luc AP-$1_{(-533)}$, or p1285-luc NFκB$_{(-600)}$) of the p1285-luc. As in the earlier experiments, TNFα increased MMP-9 promoter activity in cells transfected with the wild type p1285-luc construct. In cells transfected with p1285-luc AP-$1_{(-79)}$ TNFα still caused a fold increase in promoter activity (TNFα/DMSO vs. control: 2.08±0.20 vs. 1.00±0.06; $P<0.05$; Figure 5.7 B). Interestingly, pre-incubation with prazosin did not alter TNFα mediated activity of this construct (TNFα/PRAZ vs. TNFα/DMSO: 2.02±0.20 vs. 2.08±0.20; Figure 5.7 B). Similarly, propranolol did not affect TNFα mediated p1285-luc AP-$1_{(-79)}$ promoter activity (TNFα/PROP vs. TNFα/DMSO: 1.89±0.08 vs. 2.08±0.20; Figure 5.7 B). However, these effects were different to that exerted by prazosin in cells transfected with the wild type p1285-luc construct (Figure 5.7 A).

Mutation of the distal AP-1 (-533) completely prevented TNFα mediated activation of the MMP-9 promoter compared to control (TNFα/DMSO vs. control: 1.04±0.16 vs. 1.00±0.03; Figure 5.7 C). This was not altered by pre-exposure to prazosin or propranolol (TNFα/PRAZ vs. TNFα/DMSO: 0.88±0.14 vs. 1.04±0.16; Figure 5.7 C).

Interestingly, when the NFκB binding site of MMP-9 promoter was mutated TNFα decreased promoter activity by 60% compared to un-stimulated control conditions (TNFα/DMSO vs. control: 0.39±0.03 vs. 1.00±0.08; $P<0.05$; Figure 5.7 D). This response was unaffected by prazosin and propranolol (TNFα/PRAZ; TNFα/PROP vs. TNFα/DMSO: 0.37±0.05; 0.44±0.03 vs. 0.39±0.03, respectively; Figure 5.7 D).

5.3.5 Effects of TNFα and adrenoceptor antagonists on TIMP-1 expression

Carvedilol (10 μM) decreased TIMP-1 expression in condition medium from unstimulated NIH3T3 cells (CARV vs. control: -5.33±1.54 vs. 0.0±1.08 ng/ml; $P<0.05$; Figure 5.8 A). ICI 118,551 also reduced basal TIMP-1 levels (ICI vs. control: -3.92±0.77 vs. 0.0±1.08 ng/ml; $P<0.05$; Figure 5.8 B), while prazosin, propranolol, atenolol and DMSO had no effect.

TNFα (100 ng/ml) increased TIMP-1 levels by ~10 ng/ml from a basal level of 30.53±1.08 ng/ml in conditioned medium of NIH3T3 cells ($P<0.05$; Figure 5.8 A). This effect was unaltered by co-exposure to DMSO (TNFα/DMSO vs. TNFα: 8.95±1.41 vs. 9.64±1.17 ng/ml; Figure 5.8 A). Although prazosin (10 μM) did not alter TNFα-mediated TIMP-1 expression, it was prevented by carvedilol (TNFα/CARV vs. TNFα/DMSO: -0.15±2.21 vs. 8.95±1.41 ng/ml; $P<0.05$; Figure 5.8 A). ICI 118,551 (β_2-adrenoceptor antagonist, 10 μM) also prevented TNFα-mediated expression of TIMP-1 (TNFα/ICI vs. TNFα: 2.89±0.88 vs. 9.64±1.17 ng/ml; $P<0.05$; Figure 5.8 B). Atenolol and propranolol did not modify TNFα

mediated TIMP-1 expression (TNFα/PROP vs. TNFα: 7.67±1.13 vs. 9.64±1.17 ng/ml; Figure 5.8 B).

5.3.6 Effects of TNFα and adrenoceptor antagonists on TIMP-1 promoter activity

A schematic representation of the transcription factor binding sites in the TIMP-$1_{(-1718/+988)}$-luc and TIMP-$1_{(-738/+96)}$-luc constructs is presented in Figure 5.9. Interestingly, TNFα reduced TIMP-$1_{(-1718/+988)}$-luc promoter activity by 50% compared to control (TNFα vs. control: 0.47±0.12 vs. 1.00±0.07; $P<0.05$; Figure 5.10 A, B). Likewise, carvedilol decreased basal TIMP-1 promoter activity (CARV vs. control: 0.42±0.04 vs. 1.00±0.07; $P<0.05$; Figure 5.10 A), while prazosin and DMSO had no effect. The β-adrenoceptor blockers propranolol, ICI 118,551, and atenolol did not alter basal TIMP-1 promoter activity (Figure 5.10 B).

TNFα also decreased TIMP-$1_{(-738/+96)}$-luc promoter activity compared to control in transfected NIH3T3 cells (TNFα vs. control: 0.42±0.09 vs. 1.00±0.11; $P<0.05$; Figure 5.10 C, D). Unlike in TIMP-$1_{(-1718/+998)}$-luc transfected cells, carvedilol did not alter basal TIMP-$1_{(-738/+96)}$-luc promoter activity (CARV vs. control: 0.80±0.21 vs. 1.00±0.11; Figure 5.10 C). Prazosin, propranolol, ICI 118,551, atenolol and DMSO did not alter basal TIMP-$1_{(-738/+96)}$-luc promoter activity (Figure 5.10 D).

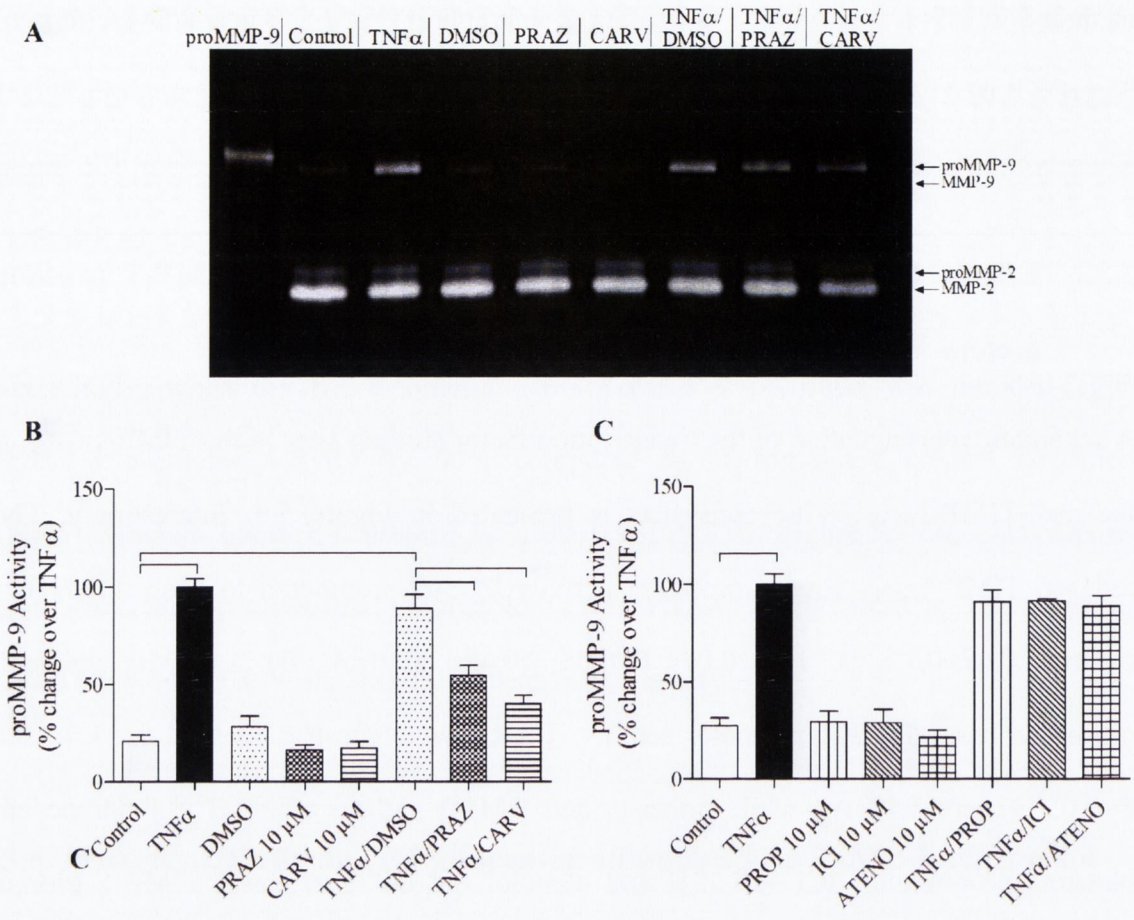


Figure 5.1 Effect of α_1- and β-adrenoceptor antagonists on basal or TNFα stimulated gelatinase activity in conditioned medium from NIH3T3 cells.

Cells were exposed to prazosin (PRAZ; 10 μM; A), carvedilol (CARV; 10 μM; A), propranolol (PROP; 10 μM; B), ICI 118,551 (ICI; 10 μM; B), atenolol (ATENO; 10 μM; B), DMSO (0.4% v/v; A) or medium (control) for 1 hr, prior to addition of TNFα (100 ng/ml) or medium as appropriate. Conditioned medium was collected after 24 hrs and gelatinase activity assessed. A representative zymogram (A), and summary data for α-adrenoceptor or mixed α/β-adrenoceptor antagonists (B) and β-adrenoceptor antagonists (C) are presented. Data are expressed as a percentage of TNFα treated cells (mean ± S.E.M.; n=9 (B); n=5 (C)). Data were analysed by one-way ANOVA with *post hoc* analysis (Bonferroni). Horizontal bars indicate a statistical significance of $P<0.05$.

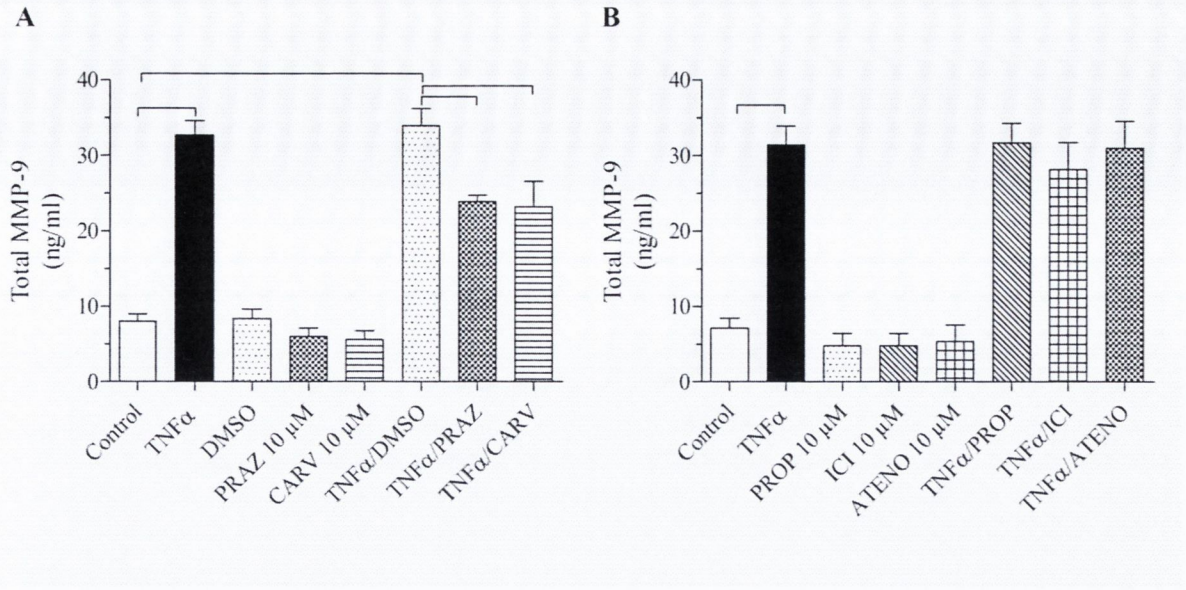


Figure 5.2 Effect of α_1- and β-adrenoceptor antagonists on basal or TNFα stimulated MMP-9 protein expression in conditioned medium from NIH3T3 cells.

Cells were exposed to prazosin (PRAZ; 10 μM; A), carvedilol (CARV; 10 μM; A), propranolol (PROP; 10 μM; B), ICI 118,551 (ICI; 10 μM; B), atenolol (ATENO; 10 μM; B), DMSO (0.4% v/v; A) or medium (control) for 1 hr, prior to addition of TNFα (100 ng/ml) or medium as appropriate. Conditioned medium was collected after 24 hrs and total MMP-9 protein expression determined by Elisa. Summary data for (A) α-adrenoceptor or mixed α/β-adrenoceptor antagonists and (B) β-adrenoceptor antagonists are presented. Data are expressed in ng/ml (mean ± S.E.M.; n=9 (A); n=6 (B)) and analysed by one-way ANOVA with *post hoc* analysis (Bonferroni). Horizontal bars indicate a statistical significance of $P<0.05$.

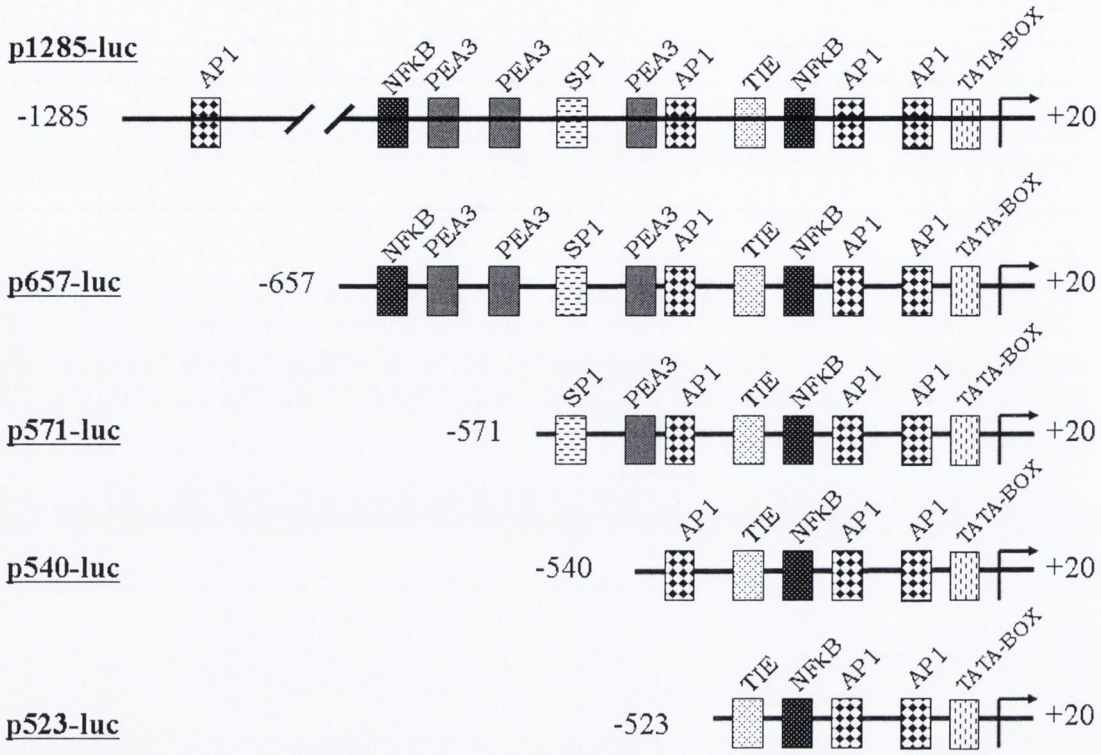


Figure 5.3 Schematic representation illustrating the position of the cis acting elements in the 5'-end deletion mutants of the MMP-9 promoter.

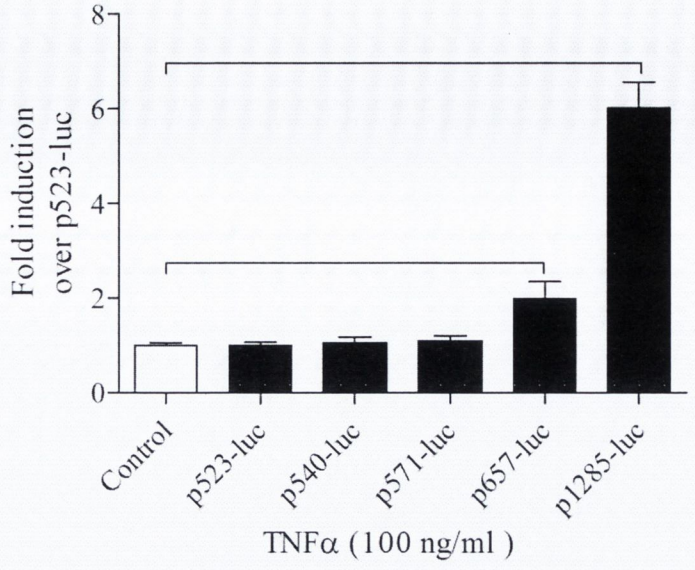


Figure 5.4 Effect of TNFα on promoter activity of the 5'-end deletion mutants of the MMP-9 promoter.

NIH3T3 cells transfected with p523-luc, p540-luc, p571-luc, p657-luc and p1285-luc promoter constructs were exposed to TNFα (100 ng/ml) or medium for 24 hrs, and luciferase activity was analysed in cell lysates. Data are expressed as fold increase over p523-luc (mean ± S.E.M.; n=7) and analysed by one-way ANOVA with *post hoc* analysis (Dunnett's). Horizontal bars indicate statistical a significance of $P<0.05$.

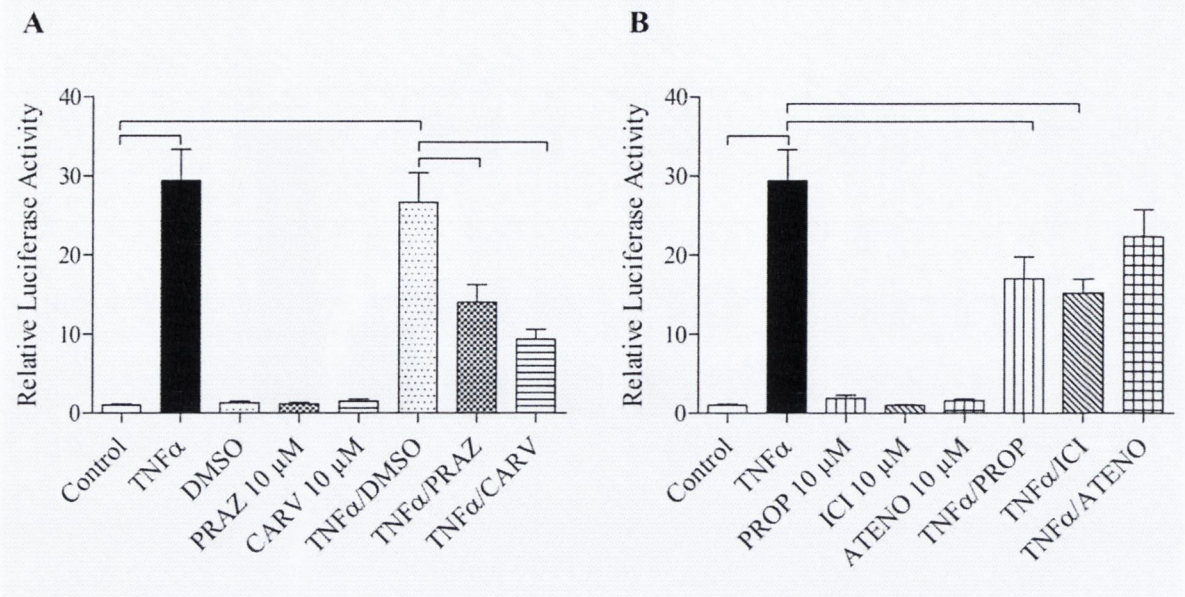


Figure 5.5 Effect of adrenoceptor antagonism on TNFα-induced NFκB promoter activity. NIH3T3 cells transfected with a NFκB promoter construct were pre-incubated prazosin (PRAZ; 10 μM; A), carvedilol (CARV; 10 μM; A), DMSO (0.4% v/v; A), propranolol (PROP; 10 μM; B), ICI 118,551 (ICI; 10 μM; B), atenolol (ATENO; 10 μM; B), or medium (control) for one hour. TNFα (100 ng/ml) or medium was then added and luciferase activity determined in cell lysates 24 hrs later. Data are expressed as fold increase (mean ± S.E.M.; n=5) relative to untreated cells transfected with pNFκB-luc. Data were analysed by one-way ANOVA with *post hoc* analysis (Bonferroni). Horizontal bars indicate a statistical significance of $P<0.05$.

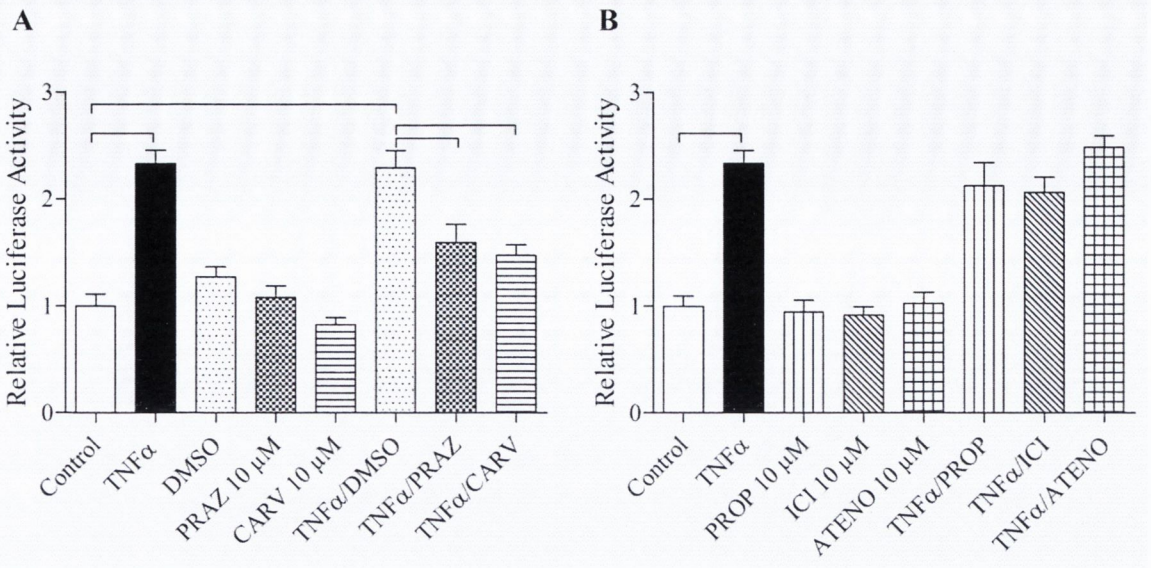


Figure 5.6 Effect of adrenoceptor antagonists on TNFα-mediated MMP-9 promoter activity in NIH3T3 cells transfected with p1285-luc.

Cells were pre-incubated with prazosin (PRAZ; 10 μM; A), carvedilol (CARV; 10 μM; A), DMSO (0.4% v/v, A); propranolol (PROP; 10 μM; B), ICI 118,551 (ICI; 10 μM; B), atenolol (ATENO; 10 μM; B) or medium (control) for 1 hr prior to addition of TNFα (100 ng/ml) or medium. After 24hrs, cells were lysed and luciferase activity assessed. Promoter activity was normalised to the control p1285-luc construct (mean ± S.E.M.; n=6). Data were analysed by one-way ANOVA with *post hoc* analysis (Bonferroni). Horizontal bars indicate a statistical significance of $P<0.05$.

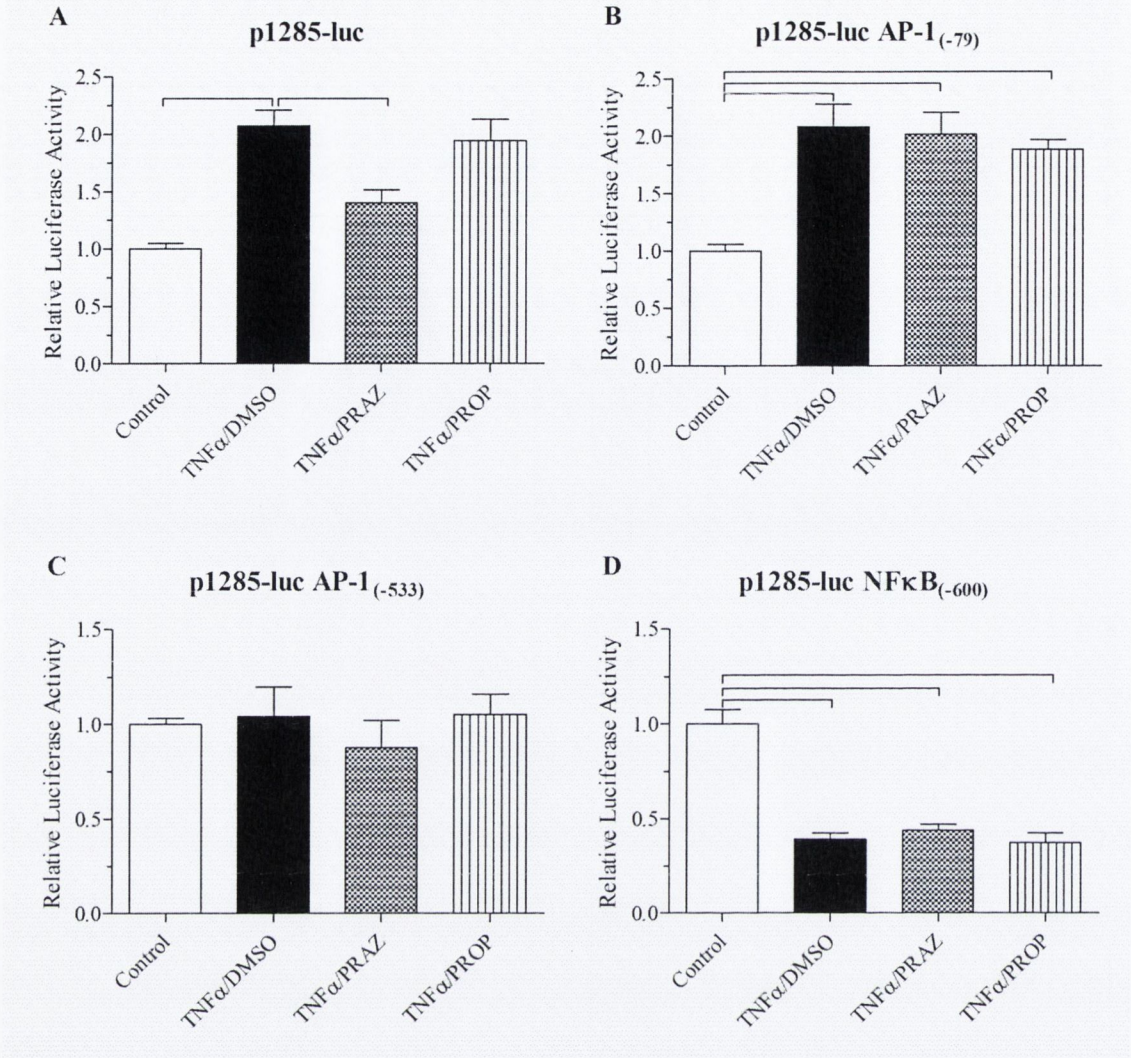


Figure 5.7 Effect of mutation of the AP-1 and NFκB transcription factor binding sites on TNFα-mediated MMP-9 promoter activity in NIH3T3 fibroblasts.

NIH3T3 cells were transfected with either (A) p1285-luc, (B) p1285-luc AP-$1_{(-79)}$. (C) p1285-luc AP-$1_{(-533)}$, or (B) p1285-luc $NF\kappa B_{(-600)}$. Cells were pre-incubated with prazosin (PRAZ; 10 μM; A), propranolol (PROP; 10 μM), DMSO (0.4% v/v), or medium (control) for 1 hr prior to the addition of TNFα (100 ng/ml) or medium. After 24 hrs, luciferase activity was determined in cell lysates. Promoter activity was normalised to control for the individual constructs, and expressed as mean ± S.E.M. (n=6). Data were analysed by one-way ANOVA with *post hoc* analysis (Bonferroni). Horizontal bars indicate a statistical significance of $P<0.05$.

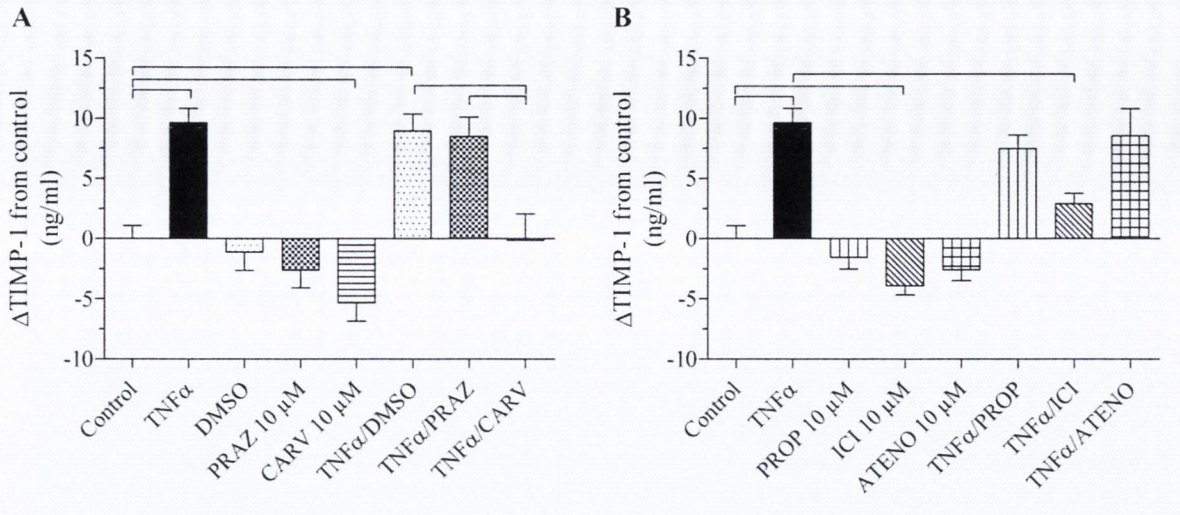


Figure 5.8 Effect of TNFα and adrenoceptor antagonists on TIMP-1 expression in NIH3T3 fibroblasts.

Cells were pre-incubated with prazosin (PRAZ; 10 μM; A), carvedilol (CARV; 10 μM; A), propranolol (PROP; 10 μM; B), ICI 118,551 (ICI; 10 μM; B), atenolol (ATENO; 10 μM; B), DMSO (0.4% v/v; A) or medium (control) one hr prior to addition of TNFα (100 ng/ml) or medium. TIMP-1 abundance was determined in conditioned medium by Elisa 24 hrs later. Data are expressed as a difference from control (ng/ml; mean ± S.E.M.; n=7 (A); n=4 (B)). Data were analysed by one-way ANOVA with *post hoc* analysis (Bonferroni). Horizontal bars indicate a statistical significance of $P<0.05$.

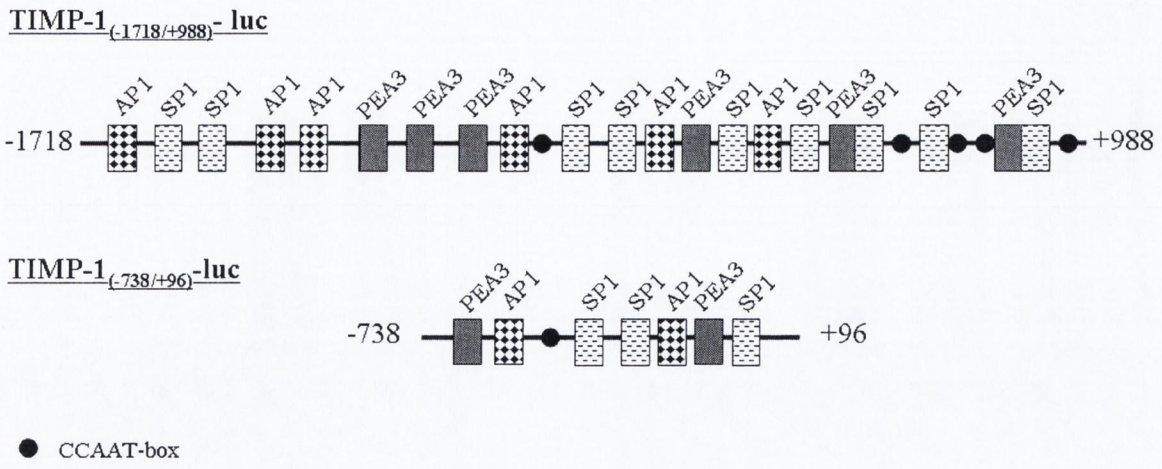


Figure 5.9 Schematic representation detailing the major transcription factors binding sites present in the TIMP-1 luciferase promoter constructs.

Modified from Clark *et al.*, 1993[314].

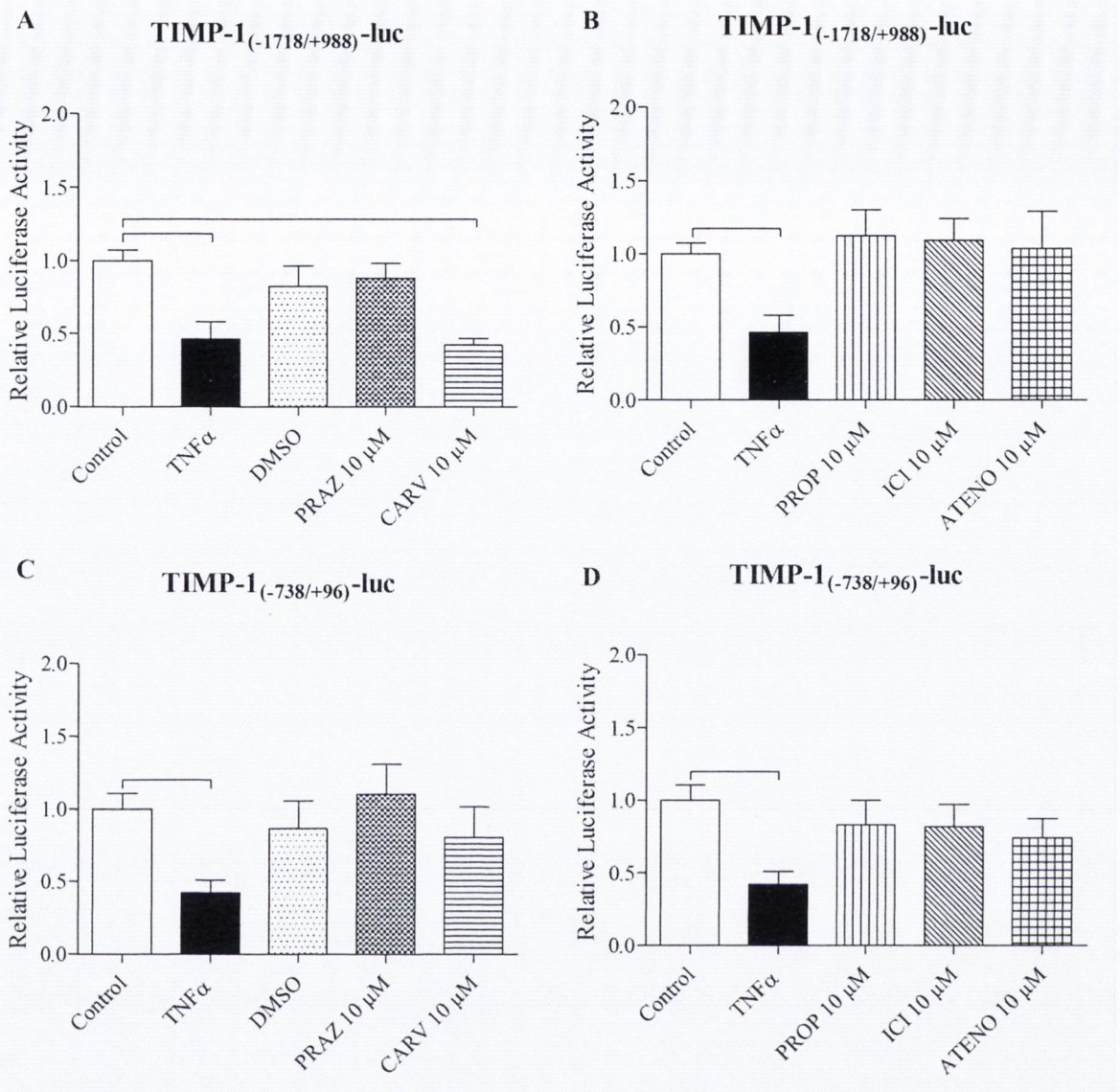


Figure 5.10 Effect of TNFα and adrenoceptor antagonism on TIMP-1 promoter activity. NIH3T3 cells were transfected with TIMP-$1_{(-1718/+988)}$-luc (full length; A, B) or TIMP-$1_{(-738/+96)}$-luc (truncated; C, D) promoter constructs. Cells were pre-exposed to prazosin (PRAZ; 10 μM; A, C), carvedilol (CARV; 10 μM; A, C), propranolol (PROP; 10 μM; B, D), ICI 118,551 (ICI; 10 μM; B, D), atenolol (ATENO; 10 μM; B, D), DMSO (0.4% v/v; A, C), medium (control) or TNFα (100 ng/ml). After 24 hrs, the cells were lysed and luciferase activity measured. Promoter activity was normalised to control for each construct. Data are expressed as mean ± S.E.M. (n=4 (A, B); n=3 (C, D)) and analysed by one-way ANOVA with *post hoc* analysis (Dunnett's). Horizontal bars indicate a statistical significance of $P<0.05$.

5.4 Discussion

The present study shows that TNFα increased MMP-9 abundance and promoter activity in NIH3T3 fibroblasts. The latter is mediated through the distal AP-1 (-533) and the NFκB (-600) binding motifs within the MMP-9 promoter. Although TNFα mediated NFκB promoter activity is prevented by α_1- and $\beta_{1/2}$-adrenoceptor blockade, these effects were not translated into changes in MMP-9 abundance. Only prazosin and carvedilol prevented TNFα induced MMP-9 expression. This effect was mediated by the proximal AP-1 (-79) binding site of the promoter. TNFα also increased TIMP-1 expression in NIH3T3 fibroblasts, an effect that was blocked by ICI 118,551 and carvedilol; ICI 118,551 and carvedilol also reduced basal expression of TIMP-1.

TNFα increased proMMP-9 activity, MMP-9 expression and MMP-9 promoter activity in NIH3T3 cells, which is in keeping with previous data from THP-1 monocytes, ECV304 cells and fibroblasts[228, 266, 267]. Propranolol, ICI 118,551, and atenolol did not alter MMP-9 abundance in NIH3T3 cells. Moreover, Propranolol, ICI 118,551 and atenolol did not prevent TNFα induced MMP-9 abundance in NIH3T3 cells. This is an interesting finding as noradrenaline induces MMP-9 secretion through $\beta_{1/2}$-adrenoceptors in tumour cell lines[315], while propranolol inhibits secretion of MMP-9 in brain microvascular endothelial cells following exposure to PMA[316]. However, in the present study prazosin and carvedilol prevented TNFα mediated induction of MMP-9 activity and expression in NIH3T3 cells. Similar findings have been reported for doxazosin (α_1-blocker) in THP-1 cells[317]. However, carvedilol attenuates TNFα induced MMP-9 activity in aortic smooth muscle cells independently of its α_1- or β-adrenoceptor antagonistic properties[172]. The latter study, differs from ours in that the cells were pre-treated with carvedilol (5 μM), propranolol (5-20 μM), or prazosin (5-20 μM) for 18 hrs prior to being exposed to TNFα for 24 hrs[172].

This together with cell type specific differences in adrenoceptor populations and signal transduction mechanisms may account for the discrepancies between studies.

Using 5'-end deletion mutants of the MMP-9 promoter (-1285/+20), it was established that the cis-acting elements upstream of -571 are required for TNFα to elicit a promoter response. The deleted region contains a recently described functional AP-1 binding site[134], along with a NFκB (-600) and two PEA3 binding sites. This is broadly in keeping with studies in HUVEC and ECV304 cells, although in these cell lines, TNFα increased MMP-9 promoter activity in the -571/+20 (HUVEC) and -540/+20 (ECV304) constructs[228]. As removal of the region from -657 bp to -571 bp, which contains a NFκB binding site, prevented the TNFα response we studied this further.

As widely reported[297, 318], TNFα also increased NFκB promoter activity by 30 fold in our cell line. Interestingly, prazosin, carvedilol, propranolol, and ICI 118,551, but not atenolol, inhibited this response. There is little data with which to compare this. However, Baouz *et al.*[318] found that salmeterol (β_2-adrenoceptor agonist) inhibits TNFα mediated translocation of NFκB to the nucleus in lung myofibroblasts. Furthermore, they showed that propranolol prevented the inhibitory effect. Propranolol itself had no effect on nuclear translocation of NFκB[318]. β-Adrenoceptor agonists such as isoprenaline, fenoterol, and albuterol also block LPS induced activation of NFκB in THP1-cells[257]. However, in human monocytes, carvedilol does not alter LPS induced NFκB activation[319].

Nonetheless, mutation of the NFκB binding site in the MMP-9 promoter construct confirmed the importance of the NFκB binding motif in mediating the inductive effect of TNFα on MMP-9 promoter activity in NIH3T3 cells. Interestingly, mutation of the NFκB binding site resulted in TNFα inhibiting MMP-9 promoter activity relative to control. The

requirement of the NFκB binding motif for TNFα mediated MMP-9 promoter activation is in keeping with previous reports utilizing a 670 bp-long MMP-9 promoter construct[287, 297]. However, these studies did not find TNFα to inhibit promoter activity in this truncated construct[287, 297]. Interestingly, PMA inhibits promoter activity of a genomic-integrated 2.2 kb MMP-9 promoter when the NFκB binding was mutated[320]. This may indicate that the region upstream of -670 bp on the MMP-9 promoter contains cis-acting elements which negatively regulate TNFα responses in cooperation with the NFκB binding site in NIH3T3 cells. Furthermore, we found that the distal AP-1 (-533) but not the proximal AP-1 (-79) binding site is necessary for TNFα induced MMP-9 activity in NIH3T3 fibroblasts. In contrast, previous reports indicate that the proximal AP-1 binding site is required for TNFα mediated activation of a 670 bp MMP-9 promoter construct in chondrocytes and skeletal muscle cells[287, 297]. Nonetheless, the proximal AP-1 binding site is required for basal MMP-9 promoter activity in NIH3T3 fibroblasts as previously shown (section 4.3.6), consistent with studies from other groups[132, 145, 287]. The regulatory function of the proximal AP-1 (-79) in regulating basal activity seems to be driven by the three different MAPK pathways (p38 MAPK, ERK1/2 MAPK and JNK/SAPK MAPK)[131]. As indicated earlier, TNFα differentially activates these three MAPK pathways depending on cell type. This might explain the observed discrepancies in the requirement of the proximal AP-1 binding site in response to TNFα.

The effects of the adrenoceptor antagonists on TNFα mediated p1285-luc promoter activity mirror those seen on MMP-9 abundance, as only prazosin and carvedilol inhibited TNFα-induced MMP-9 abundance. Following mutation of the NFκB (-600 bp), AP-1 (-533 bp) and AP-1 (-79 bp) motifs it was found that prazosin required a functional proximal AP-1 binding site (-79) in order to prevent TNFα mediated MMP-9 promoter activation in NIH3T3 fibroblast. This may explain the "disconnect" between the inhibitory effects of

propranolol and ICI 118,551 on TNFα induced NFκB promoter activity and the lack of effect on MMP-9 regulation. With regard to prazosin and carvedilol the effects are consistent with α_1-adreneoceptor antagonism of $G\alpha_{q/11}$ mediated signalling, as TNFα can mediate its actions through a $G\alpha_{q/11}$/β-arrestin 1 signalling complex in adipocytes[313].

As MMP activity is tightly regulated at multiple levels in including interaction with their tissue inhibitor, we also investigated the effects of TNFα and adrenoceptor antagonism on TIMP-1 expression. In keeping with previous reports studying human dermal fibroblasts[296] and retinal pigment epithelial cells[301], we found that TNFα increases TIMP-1 expression in NIH3T3 fibroblasts. However, others have demonstrated that TNFα decreases TIMP-1 expression in human bronchial epithelial cells[302], and renal proximal tubular cells[303]. Therefore, TNFα appears to regulate TIMP-1 expression in a cell type[296, 301-303] and a dose[304] dependent manner. Interestingly, TNFα inhibited TIMP-1 promoter activity in our study while increasing TIMP-1 expression. The reason for the disparity is unclear. Nevertheless, the decrease in promoter activity may simply indicate the start of a delayed down-regulation of TIMP-1 following prolonged exposure to TNFα, as protein expression was assessed at the same time point. Gardner *et al.* have shown that although interleukin-1β increases TIMP-1 protein expression after 24 hours, TIMP-1 promoter activity (-1718/+96) is unchanged in astrocytes[321]. They further showed that prolonged exposure to interleukin-1β decreases TIMP-1 expression and promoter activity. Alternatively, as the TIMP-1 promoter constructs used were limited to -1718 bp downstream and +988 bp upstream they may be missing more regulatory elements. TNFα can also modulate TIMP-1 expression by altering mRNA stability. In U937 cells, the early effect of PMA on TMP-1 expression is regulated through changes in mRNA stability, while delayed or later effects are associated with increased transcription[322].

Surprisingly, ICI 118,551 and carvedilol decreased basal TIMP-1 expression in NIH3T3 fibroblasts, while propranolol, atenolol, and prazosin had no effect. This is in keeping with previous studies which found β-adrenoceptor stimulation induces TIMP-1 expression in adipocytes[323] and ventricular myocytes[195]. However, ICI 118,551, prazosin, propranolol, and atenolol did not alter basal TIMP-$1_{(-1718/+988)}$-luc promoter activity, while carvedilol repressed basal TIMP-$1_{(-1718/+988)}$-luc promoter activity. Carvedilol-mediated inhibition of basal TIMP-1 promoter activity was abolished when the TIMP-$1_{(-738/+96)}$-luc promoter construct was used. These data would indicate that carvedilol directly modulates TIMP-1 expression in fibroblasts through an 1872 bp long region of the promoter, containing consensus sequences including four AP-1 binding sites, six Sp1 binding site and four PEA3 binding sites, while ICI 118,551 (β_2-adrenoceptor antagonist) may decrease TIMP-1 expression independent of transcriptional activation. However, it cannot be ruled out that ICI 118,551 may requires the full-length TIMP-1 promoter (3 kb)[314] to elicit its effect on TIMP-1 protein expression. Indeed, it may alter mRNA stability[322]. The effects of carvedilol and ICI 188,551 may also be independent of adrenoceptor blockade, as prazosin, propranolol, and atenolol did not alter TIMP-1 expression in the present study. For example, carvedilol also has antioxidant and anti-inflammatory effects independent of its adrenoceptor blocking properties. Furthermore, it has unique stimulatory effects on β-arrestin signalling independently from G-protein signalling[74].

In conclusion, the present study provides evidence that α_1- but not β-adrenoceptor antagonism attenuates TNFα stimulated MMP-9 abundance. This is mediated through the proximal AP-1 binding site on the MMP-9 promoter in NIH3T3 fibroblasts. Furthermore, ICI 118,551 and carvedilol reverse the effects of TNFα on TIMP-1 expression. Together these data provide evidence that α and β-adrenoceptor antagonists differentially regulate

MMP-9 and TIMP-1 expression in fibroblasts, which may account for their anti-remodelling effects in conditions with an inflammatory component.

Chapter 6.

Conclusions

6.1 Conclusions

The first study characterises adrenoceptor signalling pathways in NIH3T3 fibroblasts, and considers what effect these might have on MMP-9 abundance. Previous studies showed that β-adrenoceptor agonists increase MMP abundance *in vitro* and *in vivo*[174, 193, 195-198]. However, it remains to be established if fibroblasts respond in a similar manner. Therefore, we characterised key components of the adrenoceptor signalling pathways in murine embryonic (NIH3T3) and human cardiac ventricular fibroblasts (HCVF), and assessed if these are involved in MMP-9 regulation.

Isoprenaline increased cAMP, phospho-p38 MAPK and phospho-ERK1/2 MAPK levels, and induced nuclear translocation of phospho-CREB in NIH3T3 cells. In HCVFs, isoprenaline increased cAMP levels, but decreased phospho-ERK1/2 levels. The effects on cAMP were blocked by propranolol in both cell lines, while the decrease in phospho-ERK1/2 was prevented in HCVFs. Phenylephrine augmented phospho-p38 MAPK and phospho-ERK1/2 MAPK expression and caused nuclear translocation of phospho-CREB in NIH3T3 fibroblasts. In HCVFs, phenylephrine decreased phospho-ERK1/2 MAPK levels. These results demonstrate that α- and β-adrenoceptors are functionally active in NIH3T3 and HCVF cells. Interestingly, isoprenaline and phenylephrine did not activate NFκB in fibroblasts. In addition, α_1-and β-adrenoceptor activation did not alter MMP-9 abundance in fibroblasts. These findings indicate that although β-adrenoceptor signalling is functional in fibroblasts, they are unlikely to contribute to tissue remodelling by direct effects on MMP-9 abundance, or through transcriptional activation of genes containing a NFκB consensus motif.

Although isoprenaline and phenylephrine did not alter MMP-9 abundance in fibroblasts, it has been demonstrated that phosphoprotein phosphatases modulate β-adrenoceptor

signalling[202, 206, 212], and okadaic acid (phosphoprotein phosphatase inhibitor[274-277]) increases MMP-1 and stromelysin-1 mRNA expression[270, 271]. Therefore, we assessed if okadaic acid would alter MMP-9 expression and investigated the possibility that β-adrenoceptor agonists may modulate this effect.

Okadaic acid increased MMP-9 abundance and mRNA expression in fibroblasts and hepatic stellate cells, through activation of p38 MAPK. For this to occur there was an absolute dependence on the AP-1 consensus motifs at positions -79 bp and -533 bp on the MMP-9 promoter in NIH3T3 fibroblasts. Isoprenaline abolished the effect of okadaic acid on MMP-9 abundance and mRNA expression in NIH3T3 fibroblasts and HCVFs, respectively. This was found to involve β-arrestin 2 and the NFκB binding motif in the MMP-9 promoter, and is unlikely to be due to effects on PP2A activity as isoprenaline did not alter okadaic acid mediated PP2A inhibition. Since, okadaic acid did not alter the early effects of isoprenaline on ERK1/2 MAPK and p38 MAPK phosphorylation it would further support that the effects seen are not simply a reversal of PP2A activity. Despite okadaic acid increasing phospho-NFκB levels, there was not a reciprocal change in IκBα expression; this was not altered by isoprenaline. However, isoprenaline decreased phospho-NFκB expression, which would suggest that NFκB signalling is inhibited. The effects on NFκB and IκBα expression are in keeping with a lack of effect of isoprenaline and okadaic acid on NFκB promoter activity. In conclusion, the expression of MMP-9 in fibroblasts is mediated by type 2A protein phosphatases, and can be modulated by β-adrenoceptor activation through recruitment of β-arrestin 2. Although NFκB appears to be important, its involvement is not through a classical signalling pathway, and thus requires further investigation. These data shine a new light on the possible role of type 2A protein phosphatase in tissue remodelling and its regulation by β-adrenoceptors.

Interestingly, okadaic acid can mimic the effects of TNFα and IL-1 on protein phosphorylation and gene expression in human fibroblasts[324]. As TNFα is well documented to increase MMP-9 expression, we investigated if β-adrenoceptor antagonists modulate MMP-9 and TIMP-1 abundance in TNFα stimulated NIH3T3 fibroblasts.

Prazosin and carvedilol attenuated TNFα mediated MMP-9 expression and promoter activity in NIH3T3 cells. In contrast, selective β-adrenoceptor antagonists had no effect. Mutation of the NFκB and AP-1 binding sites and deletion mutants of the MMP-9 promoter confirmed the obligate role of the NFκB and distal AP-1 (-533) binding sites in TNFα mediated MMP-9 promoter activity. TNFα activation of the NFκB promoter was attenuated by α_1- and β-adrenoceptor antagonists. Mutational of the MMP-9 promoter revealed that prazosin requires a functional proximal AP-1 (-79) binding site to prevent TNFα mediated MMP-9 promoter activation. This may explain the discrepancy between the effects of β-adrenoceptor blockade on TNFα-mediated NFκB promoter activity and the obligatory requirement for the NFκB consensus motif in the MMP-9 promoter. In contrast, TNFα caused a marked increase in TIMP-1 abundance, which was abolished by ICI 118,551 and carvedilol, but not by atenolol, propranolol or prazosin. In the absence of TNFα, ICI 118,551 and carvedilol reduced TIMP-1 expression, but only carvedilol altered TIMP-1 promoter activity. This study shows that α_1 and β-adrenoceptors antagonists differentially regulate MMP-9 and TIMP-1 expression in fibroblasts.

This thesis is based on the hypothesis that adrenoceptor stimulation may modulate MMP-9 abundance in fibroblasts. This was founded upon several *in vitro* and *in vivo* studies[174, 193, 195-198], which indicated that β-adrenoceptor stimulation may increase MMP-9 abundance in fibroblasts. However, neither α_1-nor β-adrenoceptor stimulation increased MMP-9 abundance in murine embryonic and human cardiac ventricular fibroblasts, despite

functional adrenergic signalling mechanisms. However, β-adrenoceptor activation inhibited MMP-9 abundance following protein phosphatase inhibition, while α_1-but not β-adrenoceptor antagonism inhibited TNFα-increased MMP-9 abundance in fibroblasts. These imply a negative, rather than a positive regulatory function of the β-adrenoceptor signalling pathway in regards to MMP-9 abundance in fibroblasts. It appears that during chronic activation of β-adrenoceptors in man, other cells such as macrophages, smooth muscle cells are stimulated, which may secrete ECM proteins, growth factors or cytokines, which can activate fibroblasts. How does this theory agree with the observed inhibition by isoprenaline of MMP-9 expression during protein phosphatase inhibition? Based upon our data, the effects of β-adrenoceptor activation on MMP-9 production in fibroblasts might be a compensatory mechanism to prevent exacerbated secretion of MMP-9 by fibroblasts and slow pathological remodelling e.g. myocardial fibrosis in man. Our study also draws attention to the observation that adrenoceptor blockers with combined α_1-adrenoceptor and non-selective β-adrenoceptor antagonistic properties may maximize the beneficial anti-remodelling effect seen clinically. However, these results need to be confirmed in a tissue-like environment and/or in man, as our studies focussed on cell culture, in which the ECM itself and neighbouring cells are missing. This is important as collagens, growth factors and cytokines secreted and stored in the ECM are known activators of cells, including fibroblasts.

Together these studies expand our understanding of how adrenoceptors regulate MMP-9 and TIMP-1 expression in fibroblasts. It also highlights that adrenoceptor antagonists may alter tissue remodelling through modulation of MMP-9 in conditions with an inflammatory component. Finally, it indicates that phosphoprotein phosphatases regulate MMP-9 in fibroblasts.

Chapter 7.

Appendix

7.1 MMP-9 promoter insert sequences aligned to NCBI Accession NT_011362.10.

Table 7.1 Alignment of the MMP-9 promoter sequence from the p657-pGEM®-T Easy plasmid to that of NCBI Accession NT_011362.10.

Alignment was done using Basic Local Alignment Search Tool (BLAST). Differences in the $(CA)_n$-repeats of the microsatellite region are marked in red.

```
ref|NT_011362.10| Homo sapiens chromosome 20 genomic contig, GRCh37 reference primary
assembly
Length=31409461

 Features in this part of subject sequence:
   matrix metalloproteinase 9 preproprotein preproprotein

 Score = 1210 bits (655),  Expect = 0.0
 Identities = 675/683 (98%), Gaps = 8/683 (1%)
 Strand=Plus/Plus

Query  1         TACTGTCCCCTTTACTGCCCTGAAGATTCAGCCTGCGGAAGACAGGGGGTTGCCCCAGTG  60
                 ||||||||||||||||||||||||||||||||||||||||||||||||||||||||||||
Sbjct  14832976  TACTGTCCCCTTTACTGCCCTGAAGATTCAGCCTGCGGAAGACAGGGGGTTGCCCCAGTG  14833035

Query  61        GAATTCCCCAGCCTTGCCTAGCAGAGCCCATTCCTTCCGCCCCCAGATGAAGCAGGGAGA  120
                 ||||||||||||||||||||||||||||||||||||||||||||||||||||||||||||
Sbjct  14833036  GAATTCCCCAGCCTTGCCTAGCAGAGCCCATTCCTTCCGCCCCCAGATGAAGCAGGGAGA  14833095

Query  121       GGAAGCTGAGTCAAAGAAGGCTGTCAGGGAGGGAAAAAGAGGACAGAGCCTGGAGTGTGG  180
                 ||||||||||||||||||||||||||||||||||||||||||||||||||||||||||||
Sbjct  14833096  GGAAGCTGAGTCAAAGAAGGCTGTCAGGGAGGGAAAAAGAGGACAGAGCCTGGAGTGTGG  14833155

Query  181       GGAGGGGTTTGGGGAGGATATCTGACCTGGGAGGGGGTGTTGCAAAAGGCCAAGGATGGG  240
                 ||||||||||||||||||||||||||||||||||||||||||||||||||||||||||||
Sbjct  14833156  GGAGGGGTTTGGGGAGGATATCTGACCTGGGAGGGGGTGTTGCAAAAGGCCAAGGATGGG  14833215

Query  241       CCAGGGGGATCATTAGTTTCAGAAAGAAGTCTCAGGGAGTCTTCCATCACTTTCCCTTGG  300
                 ||||||||||||||||||||||||||||||||||||||||||||||||||||||||||||
Sbjct  14833216  CCAGGGGGATCATTAGTTTCAGAAAGAAGTCTCAGGGAGTCTTCCATCACTTTCCCTTGG  14833275

Query  301       CTGACCACTGGAGGCTTTCAGACCAAGGGATGGGGGATCCCTCCAGCTTCATCCCCCTCC  360
                 ||||||||||||||||||||||||||||||||||||||||||||||||||||||||||||
Sbjct  14833276  CTGACCACTGGAGGCTTTCAGACCAAGGGATGGGGGATCCCTCCAGCTTCATCCCCCTCC  14833335

Query  361       CTCCCTTTCATACAGTTCCCACAAGCTCTGCAGTTTGCAAAACCCTACCCCTCCCCTGAG  420
                 ||||||||||||||||||||||||||||||||||||||||||||||||||||||||||||
Sbjct  14833336  CTCCCTTTCATACAGTTCCCACAAGCTCTGCAGTTTGCAAAACCCTACCCCTCCCCTGAG  14833395

Query  421       GGCCTGCGGTTTCCTGCGGGTCTGGGGTCTTGCCTGACTTGGCAGTGGAGACTGCGGGCA  480
                 ||||||||||||||||||||||||||||||||||||||||||||||||||||||||||||
Sbjct  14833396  GGCCTGCGGTTTCCTGCGGGTCTGGGGTCTTGCCTGACTTGGCAGTGGAGACTGCGGGCA  14833455

Query  481       GTGGAGAGAGGAGGAGGTGGTGTAAGCCCTTTCTCATGCTGGTGCTGCCACACACACACA  540
                 ||||||||||||||||||||||||||||||||||||||||||||||||||||||||||||
Sbjct  14833456  GTGGAGAGAGGAGGAGGTGGTGTAAGCCCTTTCTCATGCTGGTGCTGCCACACACACACA  14833515

Query  541       CACACACACACACACACACACACACAC-C-C------TGACCCCTGAGTCAGCACTTGCC  592
                 |||||||||||||||||||||||||| | |      ||||||||||||||||||||||||
Sbjct  14833516  CACACACACACACACACACACACACACACACACACACCCTGACCCCTGAGTCAGCACTTGCC  14833575

Query  593       TGTCAAGGAGGGGTGGGGTCACAGGAGCGCCTCCTTAAAGCCCCCACAACAGCAGCTGCA  652
                 ||||||||||||||||||||||||||||||||||||||||||||||||||||||||||||
Sbjct  14833576  TGTCAAGGAGGGGTGGGGTCACAGGAGCGCCTCCTTAAAGCCCCCACAACAGCAGCTGCA  14833635

Query  653       GTCAGACACCTCTGCCCTCACCA  675
                 |||||||||||||||||||||||
Sbjct  14833636  GTCAGACACCTCTGCCCTCACCA  14833658
```

Table 7.2 Alignment of the MMP-9 promoter sequence from the p571-pGEM®-T Easy plasmid to that of NCBI Accession NT_011362.10.

Alignment was done using Basic Local Alignment Search Tool (BLAST). Differences in the $(CA)_n$-repeats of the microsatellite region are marked in red.

```
ref|NT_011362.10| Homo sapiens chromosome 20 genomic contig, GRCh37 reference primary
assembly
Length=31409461


 Features in this part of subject sequence:
   matrix metalloproteinase 9 preproprotein preproprotein

 Score = 1048 bits (567),  Expect = 0.0
 Identities = 587/595 (98%), Gaps = 8/595 (1%)
 Strand=Plus/Plus

Query  1         CATTCCTTCCGCCCCCAGATGAAGCAGGGAGAGGAAGCTGAGTCAAAGAAGGCTGTCAGG  60
                 ||||||||||||||||||||||||||||||||||||||||||||||||||||||||||||
Sbjct  14833064  CATTCCTTCCGCCCCCAGATGAAGCAGGGAGAGGAAGCTGAGTCAAAGAAGGCTGTCAGG  14833123

Query  61        GAGGGAAAAAGAGGACAGAGCCTGGAGTGTGGGGAGGGGTTTGGGGAGGATATCTGACCT  120
                 ||||||||||||||||||||||||||||||||||||||||||||||||||||||||||||
Sbjct  14833124  GAGGGAAAAAGAGGACAGAGCCTGGAGTGTGGGGAGGGGTTTGGGGAGGATATCTGACCT  14833183

Query  121       GGGAGGGGGTGTTGCAAAAGGCCAAGGATGGGCCAGGGGGATCATTAGTTTCAGAAAGAA  180
                 ||||||||||||||||||||||||||||||||||||||||||||||||||||||||||||
Sbjct  14833184  GGGAGGGGGTGTTGCAAAAGGCCAAGGATGGGCCAGGGGGATCATTAGTTTCAGAAAGAA  14833243

Query  181       GTCTCAGGGAGTCTTCCATCACTTTCCCTTGGCTGACCACTGGAGGCTTTCAGACCAAGG  240
                 ||||||||||||||||||||||||||||||||||||||||||||||||||||||||||||
Sbjct  14833244  GTCTCAGGGAGTCTTCCATCACTTTCCCTTGGCTGACCACTGGAGGCTTTCAGACCAAGG  14833303

Query  241       GATGGGGGATCCCTCCAGCTTCATCCCCCTCCCTCCCTTTCATACAGTTCCCACAAGCTC  300
                 ||||||||||||||||||||||||||||||||||||||||||||||||||||||||||||
Sbjct  14833304  GATGGGGGATCCCTCCAGCTTCATCCCCCTCCCTCCCTTTCATACAGTTCCCACAAGCTC  14833363

Query  301       TGCAGTTTGCAAAACCCTACCCCTCCCCTGAGGGCCTGCGGTTTCCTGCGGGTCTGGGGT  360
                 ||||||||||||||||||||||||||||||||||||||||||||||||||||||||||||
Sbjct  14833364  TGCAGTTTGCAAAACCCTACCCCTCCCCTGAGGGCCTGCGGTTTCCTGCGGGTCTGGGGT  14833423

Query  361       CTTGCCTGACTTGGCAGTGGAGACTGCGGGCAGTGGAGAGAGGAGGAGGTGGTGTAAGCC  420
                 ||||||||||||||||||||||||||||||||||||||||||||||||||||||||||||
Sbjct  14833424  CTTGCCTGACTTGGCAGTGGAGACTGCGGGCAGTGGAGAGAGGAGGAGGTGGTGTAAGCC  14833483

Query  421       CTTTCTCATGCTGGTGCTGCCACACACACACACACACACACACACACACACACACACAC-  479
                 ||||||||||||||||||||||||||||||||||||||||||||||||||||||||||| 
Sbjct  14833484  CTTTCTCATGCTGGTGCTGCCACACACACACACACACACACACACACACACACACACACA  14833543

Query  480       C-C------TGACCCCTGAGTCAGCACTTGCCTGTCAAGGAGGGGTGGGGTCACAGGAGC  532
                 | |      ||||||||||||||||||||||||||||||||||||||||||||||||||
Sbjct  14833544  CACACACCCTGACCCCTGAGTCAGCACTTGCCTGTCAAGGAGGGGTGGGGTCACAGGAGC  14833603

Query  533       GCCTCCTTAAAGCCCCCACAACAGCAGCTGCAGTCAGACACCTCTGCCCTCACCA  587
                 ||||||||||||||||||||||||||||||||||||||||||||||||||||||
Sbjct  14833604  GCCTCCTTAAAGCCCCCACAACAGCAGCTGCAGTCAGACACCTCTGCCCTCACCA  14833658

ref|NT_011362.10| Homo sapiens chromosome 20 genomic contig, GRCh37 reference primary
assembly
Length=31409461
```

Table 7.3 Alignment of the MMP-9 promoter sequence from the p540-pGEM®-T Easy plasmid to that of NCBI Accession NT_011362.10.

Alignment was done using Basic Local Alignment Search Tool (BLAST). Differences in the $(CA)_n$-repeats of the microsatellite region are marked in red.

```
Features in this part of subject sequence:
   matrix metalloproteinase 9 preproprotein preproprotein

 Score =  994 bits (538),  Expect = 0.0
 Identities = 558/566 (98%), Gaps = 8/566 (1%)
 Strand=Plus/Plus

Query  1         AGAGGAAGCTGAGTCAAAGAAGGCTGTCAGGGAGGGAAAAAGAGGACAGAGCCTGGAGTG  60
                 ||||||||||||||||||||||||||||||||||||||||||||||||||||||||||||
Sbjct  14833093  AGAGGAAGCTGAGTCAAAGAAGGCTGTCAGGGAGGGAAAAAGAGGACAGAGCCTGGAGTG  14833152

Query  61        TGGGGAGGGGTTTGGGGAGGATATCTGACCTGGGAGGGGGTGTTGCAAAAGGCCAAGGAT  120
                 ||||||||||||||||||||||||||||||||||||||||||||||||||||||||||||
Sbjct  14833153  TGGGGAGGGGTTTGGGGAGGATATCTGACCTGGGAGGGGGTGTTGCAAAAGGCCAAGGAT  14833212

Query  121       GGGCCAGGGGGATCATTAGTTTCAGAAAGAAGTCTCAGGGAGTCTTCCATCACTTTCCCT  180
                 ||||||||||||||||||||||||||||||||||||||||||||||||||||||||||||
Sbjct  14833213  GGGCCAGGGGGATCATTAGTTTCAGAAAGAAGTCTCAGGGAGTCTTCCATCACTTTCCCT  14833272

Query  181       TGGCTGACCACTGGAGGCTTTCAGACCAAGGGATGGGGGATCCCTCCAGCTTCATCCCCC  240
                 ||||||||||||||||||||||||||||||||||||||||||||||||||||||||||||
Sbjct  14833273  TGGCTGACCACTGGAGGCTTTCAGACCAAGGGATGGGGGATCCCTCCAGCTTCATCCCCC  14833332

Query  241       TCCCTCCCTTTCATACAGTTCCCACAAGCTCTGCAGTTTGCAAAACCCTACCCCTCCCCT  300
                 ||||||||||||||||||||||||||||||||||||||||||||||||||||||||||||
Sbjct  14833333  TCCCTCCCTTTCATACAGTTCCCACAAGCTCTGCAGTTTGCAAAACCCTACCCCTCCCCT  14833392

Query  301       GAGGGCCTGCGGTTTCCTGCGGGTCTGGGGTCTTGCCTGACTTGGCAGTGGAGACTGCGG  360
                 ||||||||||||||||||||||||||||||||||||||||||||||||||||||||||||
Sbjct  14833393  GAGGGCCTGCGGTTTCCTGCGGGTCTGGGGTCTTGCCTGACTTGGCAGTGGAGACTGCGG  14833452

Query  361       GCAGTGGAGAGAGGAGGAGGTGGTGTAAGCCCTTTCTCATGCTGGTGCTGCCACACACAC  420
                 ||||||||||||||||||||||||||||||||||||||||||||||||||||||||||||
Sbjct  14833453  GCAGTGGAGAGAGGAGGAGGTGGTGTAAGCCCTTTCTCATGCTGGTGCTGCCACACACAC  14833512

Query  421       ACACACACACACACACACACACACACAC-C-C------TGACCCCTGAGTCAGCACTT  472
                 |||||||||||||||||||||||||||| | |      ||||||||||||||||||||
Sbjct  14833513  ACACACACACACACACACACACACACACACACACACCCTGACCCCTGAGTCAGCACTT  14833572

Query  473       GCCTGTCAAGGAGGGGTGGGGTCACAGGAGCGCCTCCTTAAAGCCCCCACAACAGCAGCT  532
                 ||||||||||||||||||||||||||||||||||||||||||||||||||||||||||||
Sbjct  14833573  GCCTGTCAAGGAGGGGTGGGGTCACAGGAGCGCCTCCTTAAAGCCCCCACAACAGCAGCT  14833632

Query  533       GCAGTCAGACACCTCTGCCCTCACCA  558
                 |||||||||||||||||||||||||
Sbjct  14833633  GCAGTCAGACACCTCTGCCCTCACCA  14833658
```

Table 7.4 Alignment of the MMP-9 promoter sequence inserted into a p523-pGEM®-T Easy plasmid to that of NCBI Accession NT_011362.10.

Alignment was done using Basic Local Alignment Search Tool (BLAST). Differences in the $(CA)_n$-repeats of the microsatellite region are marked in red.

```
ref|NT_011362.10| Homo sapiens chromosome 20 genomic contig, GRCh37 reference primary
assembly
Length=31409461


 Features in this part of subject sequence:
   matrix metalloproteinase 9 preproprotein preproprotein

 Score =  963 bits (521),  Expect = 0.0
 Identities = 541/549 (98%), Gaps = 8/549 (1%)
 Strand=Plus/Plus

Query  1         AGAAGGCTGTCAGGGAGGGAAAAAGAGGACAGAGCCTGGAGTGTGGGGAGGGGTTTGGGG  60
                 ||||||||||||||||||||||||||||||||||||||||||||||||||||||||||||
Sbjct  14833110  AGAAGGCTGTCAGGGAGGGAAAAAGAGGACAGAGCCTGGAGTGTGGGGAGGGGTTTGGGG  14833169

Query  61        AGGATATCTGACCTGGGAGGGGGTGTTGCAAAAGGCCAAGGATGGGCCAGGGGGATCATT  120
                 ||||||||||||||||||||||||||||||||||||||||||||||||||||||||||||
Sbjct  14833170  AGGATATCTGACCTGGGAGGGGGTGTTGCAAAAGGCCAAGGATGGGCCAGGGGGATCATT  14833229

Query  121       AGTTTCAGAAAGAAGTCTCAGGGAGTCTTCCATCACTTTCCCTTGGCTGACCACTGGAGG  180
                 ||||||||||||||||||||||||||||||||||||||||||||||||||||||||||||
Sbjct  14833230  AGTTTCAGAAAGAAGTCTCAGGGAGTCTTCCATCACTTTCCCTTGGCTGACCACTGGAGG  14833289

Query  181       CTTTCAGACCAAGGGATGGGGGATCCCTCCAGCTTCATCCCCCTCCCTCCCTTTCATACA  240
                 ||||||||||||||||||||||||||||||||||||||||||||||||||||||||||||
Sbjct  14833290  CTTTCAGACCAAGGGATGGGGGATCCCTCCAGCTTCATCCCCCTCCCTCCCTTTCATACA  14833349

Query  241       GTTCCCACAAGCTCTGCAGTTTGCAAAACCCTACCCCTCCCCTGAGGGCCTGCGGTTTCC  300
                 ||||||||||||||||||||||||||||||||||||||||||||||||||||||||||||
Sbjct  14833350  GTTCCCACAAGCTCTGCAGTTTGCAAAACCCTACCCCTCCCCTGAGGGCCTGCGGTTTCC  14833409

Query  301       TGCGGGTCTGGGGTCTTGCCTGACTTGGCAGTGGAGACTGCGGGCAGTGGAGAGAGGAGG  360
                 ||||||||||||||||||||||||||||||||||||||||||||||||||||||||||||
Sbjct  14833410  TGCGGGTCTGGGGTCTTGCCTGACTTGGCAGTGGAGACTGCGGGCAGTGGAGAGAGGAGG  14833469

Query  361       AGGTGGTGTAAGCCCTTTCTCATGCTGGTGCTGCCACACACACACACACACACACACACA  420
                 ||||||||||||||||||||||||||||||||||||||||||||||||||||||||||||
Sbjct  14833470  AGGTGGTGTAAGCCCTTTCTCATGCTGGTGCTGCCACACACACACACACACACACACACA  14833529

Query  421       CACACACACACAC-C-C------TGACCCCTGAGTCAGCACTTGCCTGTCAAGGAGGGGT  472
                 |||||||||||| | |      ||||||||||||||||||||||||||||||||||||
Sbjct  14833530  CACACACACACACACACACACCCTGACCCCTGAGTCAGCACTTGCCTGTCAAGGAGGGGT  14833589

Query  473       GGGGTCACAGGAGCGCCTCCTTAAAGCCCCCACAACAGCAGCTGCAGTCAGACACCTCTG  532
                 ||||||||||||||||||||||||||||||||||||||||||||||||||||||||||||
Sbjct  14833590  GGGGTCACAGGAGCGCCTCCTTAAAGCCCCCACAACAGCAGCTGCAGTCAGACACCTCTG  14833649

Query  533       CCCTCACCA  541
                 |||||||||
Sbjct  14833650  CCCTCACCA  14833658
```

7.2 Predicted transcription factor binding site of the MMP-9 promoter mutants

Table 7.5 Predicted transcription factor binding sites of a p1285-luc sequence part (50 bp) containing the NFκB-binding site.

Transcription binding sites are predicted through AliBaba 2.1[272] and the NFκB consensus sequence is marked in green.

```
================================================================================
=========
seq(    0..   59)     gacaggggttgccccagtggaattccccagccttgcctagcagagccca
Segments:
4.1.1.0     18   28                        ====c-Rel==
9.9.590     19   28                         =NF-kappaB
9.9.594     19   28                         ====RelA==
2.3.1.0     23   33                             =====Sp1===
1.1.3.0     29   38                                  =C/EBPgam=

5 segments in this sequence identified as potential binding sites
```

Table 7.6 Predicted transcription factor binding sites of a p1285-luc sequence part (50 bp) containing the mutated NFκB-binding site.

Transcription binding sites are predicted through AliBaba 2.1[272] and the mutated NFκB consensus sequence is marked in green.

```
================================================================================
=========
seq(    0..   59)     gacaggggttgccccagtggaactcaccagccttgcctagcagagccca
Segments:
1.1.3.0     29   38                                  =C/EBPgam=

1 segments in this sequence identified as potential binding sites
```

Table 7.7 Predicted transcription factor binding sites of a p1285-luc sequence part (50 bp) containing the AP-$1_{(-533)}$ binding site.

Transcription binding sites are predicted through AliBaba 2.1[272] and the AP-1 consensus sequence is marked in green.

```
================================================================================
=========
seq(    0..   59)     agatgaagcagggagaggaagctgagtcaaagaaggctgtcagggaggga
Segments:
2.3.1.0     10   19              ====Sp1===
1.1.1.1     19   28                   ===c-Jun==
1.1.1.2     19   28                   ===Fra-1==
1.1.1.6     19   28                   ==CRE-BP1=
9.9.29      20   30                    ====AP-1===
1.1.1.5     22   31                      ====CPC1==
2.3.1.0     43   52
====Sp1===

7 segments in this sequence identified as potential binding sites
```

Table 7.8 Predicted transcription factor binding sites of a p1285-luc sequence part (50 bp) containing mutated AP-$1_{(-533)}$ binding site.

Transcription binding sites are predicted through AliBaba 2.1[272] and the mutated AP-1 consensus sequence is marked in green.

```
================================================================================
=========
seq(    0..   59)     agatgaagcagggagaggaagctgagttgaagaaggctgtcagggaggga
Segments:
2.3.1.0     10   19              ====Sp1===
2.3.1.0     43   52
====Sp1===

2 segments in this sequence identified as potential binding sites
```

Table 7.9 Predicted transcription factor binding sites of a p1285-luc sequence part (50 bp) containing the AP-$1_{(-79)}$ binding site.

Transcription binding sites are predicted through AliBaba 2.1[272] and the AP-1 consensus sequence is marked in green.

```
================================================================================
=========
seq(    0..   59)     cacacacacacacaccctgaccctgagtcagcacttgcctgtcaaggag
Segments:
2.3.2.3     5    14          =WT1 I -K=
4.6.1.0     5    14          ===Sox-2==
9.9.1840    5    14          ===WT1 I==
9.9.1841    5    14          ==WT1-del2
9.9.1842    5    14          =WT1 I-de=
2.1.1.4    12    21                =====ER===
2.1.2.3    14    23                  =REV-ErbA=
2.1.2.10   15    24                   ====COUP==
2.3.1.0    15    24                   ====Sp1===
9.9.45     16    25                    ===ARP-1==
2.1.2.2    17    26                     ==RXR-beta
1.1.1.1    21    30                         ===c-Jun==
1.1.1.2    21    30                         ===c-Fos==
9.9.29     21    33                         =====AP-1====
1.1.3.0    23    32                           =C/EBPalp=
9.9.32     23    32                           ====AP-1==
9.9.31     24    33                            ====AP-1==

17 segments in this sequence identified as potential binding sites
```

Table 7.10 Predicted transcription factor binding sites of a p1285-luc sequence part (50 bp) containing the mutated AP-$1_{(-79)}$ binding site.

Transcription binding sites are predicted through AliBaba 2.1[272] and the mutated AP-1 consensus sequence is marked in green.

```
================================================================================
=========
seq(    0..   59)     cacacacacacacaccctgacccctgagttggcacttgcctgtcaaggag
Segments:
2.3.2.3     5    14          =WT1 I -K=
4.6.1.0     5    14          ===Sox-2==
9.9.1840    5    14          ===WT1 I==
9.9.1841    5    14          ==WT1-del2
9.9.1842    5    14          =WT1 I-de=
2.1.1.4     12   21                =====ER===
2.1.2.3     14   23                  =REV-ErbA=
2.1.2.10    15   24                   ====COUP==
2.3.1.0     15   24                   ====Sp1===
9.9.45      16   25                    ===ARP-1==
2.1.2.2     17   26                     ==RXR-beta

11 segments in this sequence identified as potential binding sites
```

7.3 MMP-9 promoter mutant sequences aligned to wild type MMP-9 promoter construct

Table 7.11 Alignment of obtained sequence for p1285-luc $NF\kappa B_{(-600)}$ against p1285-luc using BLAST.

The NFκB binding site and the mutated NFκB binding site, containing the two base pairs targeted for mutation, are marked in green.

```
>lcl|9373
Length=1304

 Score = 2398 bits (1298),  Expect = 0.0
 Identities = 1302/1304 (99%), Gaps = 0/1304 (0%)
 Strand=Plus/Plus

Query 7   GGGAGGGAGGCTTGGCATAAGTGTGATAATTGGGGCTGGAGATTTGGCTGCATGGAGCAG  66
          ||||||||||||||||||||||||||||||||||||||||||||||||||||||||||||
Sbjct 1   GGGAGGGAGGCTTGGCATAAGTGTGATAATTGGGGCTGGAGATTTGGCTGCATGGAGCAG  60

Query 67  GGCTGGAGAACTGAAAGGGCTCCTATAGATTATTTTCCCCCATATCCTGCCCCAATTTGC  126
          ||||||||||||||||||||||||||||||||||||||||||||||||||||||||||||
Sbjct 61  GGCTGGAGAACTGAAAGGGCTCCTATAGATTATTTTCCCCCATATCCTGCCCCAATTTGC  120

Query 127 AGTTGAAGAATCCTAAGCTGACAAAGGGGAAGGCATTTACTCCAGGTTACACTGCAGCTT  186
          ||||||||||||||||||||||||||||||||||||||||||||||||||||||||||||
Sbjct 121 AGTTGAAGAATCCTAAGCTGACAAAGGGGAAGGCATTTACTCCAGGTTACACTGCAGCTT  180

Query 187 AGAGCCCAATAACCTGGTTTGGTGATTCCAAGTTAGAATCATGGTCTTTTGGCAGGGTCT  246
          ||||||||||||||||||||||||||||||||||||||||||||||||||||||||||||
Sbjct 181 AGAGCCCAATAACCTGGTTTGGTGATTCCAAGTTAGAATCATGGTCTTTTGGCAGGGTCT  240

Query 247 CGCTCTGTTGCCCAGGCTGGAGTGCAGTGACATAATCATGGCTCACTGTATCCTTGACCT  306
          ||||||||||||||||||||||||||||||||||||||||||||||||||||||||||||
Sbjct 241 CGCTCTGTTGCCCAGGCTGGAGTGCAGTGACATAATCATGGCTCACTGTATCCTTGACCT  300

Query 307 TCTTTCTGGGCTCAAGCAATCCTCCCACCTCGGCCTCCCAAAGTGCTAAGATTACAGGAA  366
          ||||||||||||||||||||||||||||||||||||||||||||||||||||||||||||
Sbjct 301 TCTTTCTGGGCTCAAGCAATCCTCCCACCTCGGCCTCCCAAAGTGCTAAGATTACAGGAA  360

Query 367 TGAGCCACCATACCTGGCCCTGAATCTTGGGTCTTGGCCTTAGTAATTAAAACCAATCAC  426
          ||||||||||||||||||||||||||||||||||||||||||||||||||||||||||||
Sbjct 361 TGAGCCACCATACCTGGCCCTGAATCTTGGGTCTTGGCCTTAGTAATTAAAACCAATCAC  420

Query 427 CACCATCCGTTGCGGACTTACAACCTACAGTGTTCTAAACATTTTATATGTTTGATCTCA  486
          ||||||||||||||||||||||||||||||||||||||||||||||||||||||||||||
Sbjct 421 CACCATCCGTTGCGGACTTACAACCTACAGTGTTCTAAACATTTTATATGTTTGATCTCA  480

Query 487 TTTAATCCTCACATCAATTTAGGGACAAAGAGccccccaccccccGttttttttttACA  546
          ||||||||||||||||||||||||||||||||||||||||||||||||||||||||||||
Sbjct 481 TTTAATCCTCACATCAATTTAGGGACAAAGAGCCCCCCACCCCCCGTTTTTTTTTTACA  540

Query 547 GCTGAGGAAACACTTCAAAGTGGTAAGACATTTGCCCGAGGTCCTGAAGGAAGAGAGTAA  606
          ||||||||||||||||||||||||||||||||||||||||||||||||||||||||||||
Sbjct 541 GCTGAGGAAACACTTCAAAGTGGTAAGACATTTGCCCGAGGTCCTGAAGGAAGAGAGTAA  600

Query 607 AGCCATGTCTGCTGTTTTCTAGAGGCTGCTACTGTCCCCTTTACTGCCCTGAAGATTCAG  666
          ||||||||||||||||||||||||||||||||||||||||||||||||||||||||||||
Sbjct 601 AGCCATGTCTGCTGTTTTCTAGAGGCTGCTACTGTCCCCTTTACTGCCCTGAAGATTCAG  660

Query 667 CCTGCGGAAGACAGGGGGTTGCCCCAGTGGAACTCACCAGCCTTGCCTAGCAGAGCCCAT  726
          ||||||||||||||||||||||||||||||||  ||||||||||||||||||||||||||
Sbjct 661 CCTGCGGAAGACAGGGGGTTGCCCCAGTGGAATTCCCCAGCCTTGCCTAGCAGAGCCCAT  720

Query 727 TCCTTCCGCCCCCAGATGAAGCAGGGAGAGGAAGCTGAGTCAAAGAAGGCTGTCAGGGAG  786
          ||||||||||||||||||||||||||||||||||||||||||||||||||||||||||||
Sbjct 721 TCCTTCCGCCCCCAGATGAAGCAGGGAGAGGAAGCTGAGTCAAAGAAGGCTGTCAGGGAG  780
```

```
Query 787 GGAAAAAGAGGACAGAGCCTGGAGTGTGGGGAGGGGTTTGGGGAGGATATCTGACCTGGG  846
          ||||||||||||||||||||||||||||||||||||||||||||||||||||||||||||
Sbjct 781 GGAAAAAGAGGACAGAGCCTGGAGTGTGGGGAGGGGTTTGGGGAGGATATCTGACCTGGG  840

Query 847 AGGGGGTGTTGCAAAAGGCCAAGGATGGGCCAGGGGGATCATTAGTTTCAGAAAGAAGTC  906
          ||||||||||||||||||||||||||||||||||||||||||||||||||||||||||||
Sbjct 841 AGGGGGTGTTGCAAAAGGCCAAGGATGGGCCAGGGGGATCATTAGTTTCAGAAAGAAGTC  900

Query 907 TCAGGGAGTCTTCCATCACTTTCCCTTGGCTGACCACTGGAGGCTTTCAGACCAAGGGAT  966
          ||||||||||||||||||||||||||||||||||||||||||||||||||||||||||||
Sbjct 901 TCAGGGAGTCTTCCATCACTTTCCCTTGGCTGACCACTGGAGGCTTTCAGACCAAGGGAT  960

Query 967 GGGGGATCCCTCCAGCTTCATCCCCCTCCCTCCCTTTCATACAGTTCCCACAAGCTCTGC  1026
          ||||||||||||||||||||||||||||||||||||||||||||||||||||||||||||
Sbjct 961 GGGGGATCCCTCCAGCTTCATCCCCCTCCCTCCCTTTCATACAGTTCCCACAAGCTCTGC  1020

Query 1027 AGTTTGCAAAACCCTACCCCTCCCCTGAGGGCCTGCGGTTTCCTGCGGGTCTGGGGTCTT  1086
           ||||||||||||||||||||||||||||||||||||||||||||||||||||||||||||
Sbjct 1021 AGTTTGCAAAACCCTACCCCTCCCCTGAGGGCCTGCGGTTTCCTGCGGGTCTGGGGTCTT  1080

Query 1087 GCCTGACTTGGCAGTGGAGACTGCGGGCAGTGGAGAGAGGAGGAGGTGGTGTAAGCCCTT  1146
           ||||||||||||||||||||||||||||||||||||||||||||||||||||||||||||
Sbjct 1081 GCCTGACTTGGCAGTGGAGACTGCGGGCAGTGGAGAGAGGAGGAGGTGGTGTAAGCCCTT  1140

Query 1147 TCTCATGCTGGTGCTGCcacacacacacacacacacacacacacacacacacacacacCCTG  1206
           ||||||||||||||||||||||||||||||||||||||||||||||||||||||||||||
Sbjct 1141 TCTCATGCTGGTGCTGCCACACACACACACACACACACACACACACACACACACACCCTG  1200

Query 1207 ACCCCTGAGTCAGCACTTGCCTGTCAAGGAGGGGTGGGGTCACAGGAGCGCCTCCTTAAA  1266
           ||||||||||||||||||||||||||||||||||||||||||||||||||||||||||||
Sbjct 1201 ACCCCTGAGTCAGCACTTGCCTGTCAAGGAGGGGTGGGGTCACAGGAGCGCCTCCTTAAA  1260

Query 1267 GCCCCCACAACAGCAGCTGCAGTCAGACACCTCTGCCCTCACCA  1310
           ||||||||||||||||||||||||||||||||||||||||||||
Sbjct 1261 GCCCCCACAACAGCAGCTGCAGTCAGACACCTCTGCCCTCACCA  1304
```

Table 7.12 Alignment of obtained sequence for p1285-luc AP-$1_{(-533)}$ against p1285-luc using BLAST.

The AP-$1_{(-533)}$ binding site and the mutated AP-$1_{(-533)}$ binding site, containing the two base pairs targeted for mutation, are marked in green.

```
>lcl|36865
Length=1304

 Score = 2398 bits (1298),  Expect = 0.0
 Identities = 1302/1304 (99%), Gaps = 0/1304 (0%)
 Strand=Plus/Plus

Query 29  GGGAGGGAGGCTTGGCATAAGTGTGATAATTGGGGCTGGAGATTTGGCTGCATGGAGCAG  88
          ||||||||||||||||||||||||||||||||||||||||||||||||||||||||||||
Sbjct 1   GGGAGGGAGGCTTGGCATAAGTGTGATAATTGGGGCTGGAGATTTGGCTGCATGGAGCAG  60

Query 89  GGCTGGAGAACTGAAAGGGCTCCTATAGATTATTTTCCCCCATATCCTGCCCCAATTTGC  148
          ||||||||||||||||||||||||||||||||||||||||||||||||||||||||||||
Sbjct 61  GGCTGGAGAACTGAAAGGGCTCCTATAGATTATTTTCCCCCATATCCTGCCCCAATTTGC  120

Query 149 AGTTGAAGAATCCTAAGCTGACAAAGGGGAAGGCATTTACTCCAGGTTACACTGCAGCTT  208
          ||||||||||||||||||||||||||||||||||||||||||||||||||||||||||||
Sbjct 121 AGTTGAAGAATCCTAAGCTGACAAAGGGGAAGGCATTTACTCCAGGTTACACTGCAGCTT  180

Query 209 AGAGCCCAATAACCTGGTTTGGTGATTCCAAGTTAGAATCATGGTCTTTTGGCAGGGTCT  268
          ||||||||||||||||||||||||||||||||||||||||||||||||||||||||||||
Sbjct 181 AGAGCCCAATAACCTGGTTTGGTGATTCCAAGTTAGAATCATGGTCTTTTGGCAGGGTCT  240

Query 269 CGCTCTGTTGCCCAGGCTGGAGTGCAGTGACATAATCATGGCTCACTGTATCCTTGACCT  328
          ||||||||||||||||||||||||||||||||||||||||||||||||||||||||||||
Sbjct 241 CGCTCTGTTGCCCAGGCTGGAGTGCAGTGACATAATCATGGCTCACTGTATCCTTGACCT  300

Query 329 TCTTTCTGGGCTCAAGCAATCCTCCCACCTCGGCCTCCCAAAGTGCTAAGATTACAGGAA  388
          ||||||||||||||||||||||||||||||||||||||||||||||||||||||||||||
Sbjct 301 TCTTTCTGGGCTCAAGCAATCCTCCCACCTCGGCCTCCCAAAGTGCTAAGATTACAGGAA  360

Query 389 TGAGCCACCATACCTGGCCCTGAATCTTGGGTCTTGGCCTTAGTAATTAAAACCAATCAC  448
          ||||||||||||||||||||||||||||||||||||||||||||||||||||||||||||
Sbjct 361 TGAGCCACCATACCTGGCCCTGAATCTTGGGTCTTGGCCTTAGTAATTAAAACCAATCAC  420

Query 449 CACCATCCGTTGCGGACTTACAACCTACAGTGTTCTAAACATTTTATATGTTTGATCTCA  508
          ||||||||||||||||||||||||||||||||||||||||||||||||||||||||||||
Sbjct 421 CACCATCCGTTGCGGACTTACAACCTACAGTGTTCTAAACATTTTATATGTTTGATCTCA  480

Query 509 TTTAATCCTCACATCAATTTAGGGACAAAGAGccccccaccccccGttttttttttACA  568
          ||||||||||||||||||||||||||||||||||||||||||||||||||||||||||||
Sbjct 481 TTTAATCCTCACATCAATTTAGGGACAAAGAGCCCCCCACCCCCCGTTTTTTTTTTACA  540

Query 569 GCTGAGGAAACACTTCAAAGTGGTAAGACATTTGCCCGAGGTCCTGAAGGAAGAGAGTAA  628
          ||||||||||||||||||||||||||||||||||||||||||||||||||||||||||||
Sbjct 541 GCTGAGGAAACACTTCAAAGTGGTAAGACATTTGCCCGAGGTCCTGAAGGAAGAGAGTAA  600

Query 629 AGCCATGTCTGCTGTTTTCTAGAGGCTGCTACTGTCCCCTTTACTGCCCTGAAGATTCAG  688
          ||||||||||||||||||||||||||||||||||||||||||||||||||||||||||||
Sbjct 601 AGCCATGTCTGCTGTTTTCTAGAGGCTGCTACTGTCCCCTTTACTGCCCTGAAGATTCAG  660

Query 689 CCTGCGGAAGACAGGGGGTTGCCCCAGTGGAATTCCCCAGCCTTGCCTAGCAGAGCCCAT  748
          ||||||||||||||||||||||||||||||||||||||||||||||||||||||||||||
Sbjct 661 CCTGCGGAAGACAGGGGGTTGCCCCAGTGGAATTCCCCAGCCTTGCCTAGCAGAGCCCAT  720

Query 749 TCCTTCCGCCCCCAGATGAAGCAGGGAGAGGAAGCTGAGTTCAAGAAGGCTGTCAGGGAG  808
          |||||||||||||||||||||||||||||||||||||||||||  ||||||||||||||||
Sbjct 721 TCCTTCCGCCCCCAGATGAAGCAGGGAGAGGAAGCTGAGTCAAAGAAGGCTGTCAGGGAG  780

Query 809 GGAAAAAGAGGACAGAGCCTGGAGTGTGGGGAGGGGTTTGGGGAGGATATCTGACCTGGG  868
          ||||||||||||||||||||||||||||||||||||||||||||||||||||||||||||
Sbjct 781 GGAAAAAGAGGACAGAGCCTGGAGTGTGGGGAGGGGTTTGGGGAGGATATCTGACCTGGG  840

Query 869 AGGGGGTGTTGCAAAAGGCCAAGGATGGGCCAGGGGGATCATTAGTTTCAGAAAGAAGTC  928
          ||||||||||||||||||||||||||||||||||||||||||||||||||||||||||||
Sbjct 841 AGGGGGTGTTGCAAAAGGCCAAGGATGGGCCAGGGGGATCATTAGTTTCAGAAAGAAGTC  900
```

```
Query 929 TCAGGGAGTCTTCCATCACTTTCCCTTGGCTGACCACTGGAGGCTTTCAGACCAAGGGAT  988
          ||||||||||||||||||||||||||||||||||||||||||||||||||||||||||||
Sbjct 901 TCAGGGAGTCTTCCATCACTTTCCCTTGGCTGACCACTGGAGGCTTTCAGACCAAGGGAT  960

Query 989 GGGGGATCCCTCCAGCTTCATCCCCCTCCCTCCCTTTCATACAGTTCCCACAAGCTCTGC  1048
          ||||||||||||||||||||||||||||||||||||||||||||||||||||||||||||
Sbjct 961 GGGGGATCCCTCCAGCTTCATCCCCCTCCCTCCCTTTCATACAGTTCCCACAAGCTCTGC  1020

Query 1049 AGTTTGCAAAACCCTACCCCTCCCCTGAGGGCCTGCGGTTTCCTGCGGGTCTGGGGTCTT  1108
           ||||||||||||||||||||||||||||||||||||||||||||||||||||||||||||
Sbjct 1021 AGTTTGCAAAACCCTACCCCTCCCCTGAGGGCCTGCGGTTTCCTGCGGGTCTGGGGTCTT  1080

Query 1109 GCCTGACTTGGCAGTGGAGACTGCGGGCAGTGGAGAGAGGAGGAGGTGGTGTAAGCCCTT  1168
           ||||||||||||||||||||||||||||||||||||||||||||||||||||||||||||
Sbjct 1081 GCCTGACTTGGCAGTGGAGACTGCGGGCAGTGGAGAGAGGAGGAGGTGGTGTAAGCCCTT  1140

Query 1169 TCTCATGCTGGTGCTGCcacacacacacacacacacacacacacacacacacacacacCCTG  1228
           ||||||||||||||||||||||||||||||||||||||||||||||||||||||||||||
Sbjct 1141 TCTCATGCTGGTGCTGCCACACACACACACACACACACACACACACACACACACACCCTG  1200

Query 1229 ACCCCTGAGTCAGCACTTGCCTGTCAAGGAGGGGTGGGGTCACAGGAGCGCCTCCTTAAA  1288
           ||||||||||||||||||||||||||||||||||||||||||||||||||||||||||||
Sbjct 1201 ACCCCTGAGTCAGCACTTGCCTGTCAAGGAGGGGTGGGGTCACAGGAGCGCCTCCTTAAA  1260

Query 1289 GCCCCCACAACAGCAGCTGCAGTCAGACACCTCTGCCCTCACCA  1332
             ||||||||||||||||||||||||||||||||||||||||||
Sbjct 1261 GCCCCCACAACAGCAGCTGCAGTCAGACACCTCTGCCCTCACCA  1304
```

Table 7.13 Alignment of obtained sequence for p1285-luc AP-$1_{(-79)}$ against p1285-luc using BLAST.

The AP-$1_{(-79)}$ binding site and the mutated AP-$1_{(-79)}$ binding site, containing the two base pairs targeted for mutation, are marked in green.

```
>lcl|22973
Length=1304

 Score = 2398 bits (1298),  Expect = 0.0
 Identities = 1302/1304 (99%), Gaps = 0/1304 (0%)
 Strand=Plus/Plus

Query 7   GGGAGGGAGGCTTGGCATAAGTGTGATAATTGGGGCTGGAGATTTGGCTGCATGGAGCAG  66
          ||||||||||||||||||||||||||||||||||||||||||||||||||||||||||||
Sbjct 1   GGGAGGGAGGCTTGGCATAAGTGTGATAATTGGGGCTGGAGATTTGGCTGCATGGAGCAG  60

Query 67  GGCTGGAGAACTGAAAGGGCTCCTATAGATTATTTTCCCCCATATCCTGCCCCAATTTGC  126
          ||||||||||||||||||||||||||||||||||||||||||||||||||||||||||||
Sbjct 61  GGCTGGAGAACTGAAAGGGCTCCTATAGATTATTTTCCCCCATATCCTGCCCCAATTTGC  120

Query 127 AGTTGAAGAATCCTAAGCTGACAAAGGGGAAGGCATTTACTCCAGGTTACACTGCAGCTT  186
          ||||||||||||||||||||||||||||||||||||||||||||||||||||||||||||
Sbjct 121 AGTTGAAGAATCCTAAGCTGACAAAGGGGAAGGCATTTACTCCAGGTTACACTGCAGCTT  180

Query 187 AGAGCCCAATAACCTGGTTTGGTGATTCCAAGTTAGAATCATGGTCTTTTGGCAGGGTCT  246
          ||||||||||||||||||||||||||||||||||||||||||||||||||||||||||||
Sbjct 181 AGAGCCCAATAACCTGGTTTGGTGATTCCAAGTTAGAATCATGGTCTTTTGGCAGGGTCT  240

Query 247 CGCTCTGTTGCCCAGGCTGGAGTGCAGTGACATAATCATGGCTCACTGTATCCTTGACCT  306
          ||||||||||||||||||||||||||||||||||||||||||||||||||||||||||||
Sbjct 241 CGCTCTGTTGCCCAGGCTGGAGTGCAGTGACATAATCATGGCTCACTGTATCCTTGACCT  300

Query 307 TCTTTCTGGGCTCAAGCAATCCTCCCACCTCGGCCTCCCAAAGTGCTAAGATTACAGGAA  366
          ||||||||||||||||||||||||||||||||||||||||||||||||||||||||||||
Sbjct 301 TCTTTCTGGGCTCAAGCAATCCTCCCACCTCGGCCTCCCAAAGTGCTAAGATTACAGGAA  360

Query 367 TGAGCCACCATACCTGGCCCTGAATCTTGGGTCTTGGCCTTAGTAATTAAAACCAATCAC  426
          ||||||||||||||||||||||||||||||||||||||||||||||||||||||||||||
Sbjct 361 TGAGCCACCATACCTGGCCCTGAATCTTGGGTCTTGGCCTTAGTAATTAAAACCAATCAC  420

Query 427 CACCATCCGTTGCGGACTTACAACCTACAGTGTTCTAAACATTTTATATGTTTGATCTCA  486
          ||||||||||||||||||||||||||||||||||||||||||||||||||||||||||||
Sbjct 421 CACCATCCGTTGCGGACTTACAACCTACAGTGTTCTAAACATTTTATATGTTTGATCTCA  480

Query 487 TTTAATCCTCACATCAATTTAGGGACAAAGAGccccccaccccccGttttttttttttACA  546
          ||||||||||||||||||||||||||||||||||||||||||||||||||||||||||||
Sbjct 481 TTTAATCCTCACATCAATTTAGGGACAAAGAGCCCCCCACCCCCCGTTTTTTTTTTTACA  540

Query 547 GCTGAGGAAACACTTCAAAGTGGTAAGACATTTGCCCGAGGTCCTGAAGGAAGAGAGTAA  606
          ||||||||||||||||||||||||||||||||||||||||||||||||||||||||||||
Sbjct 541 GCTGAGGAAACACTTCAAAGTGGTAAGACATTTGCCCGAGGTCCTGAAGGAAGAGAGTAA  600

Query 607 AGCCATGTCTGCTGTTTTCTAGAGGCTGCTACTGTCCCCTTTACTGCCCTGAAGATTCAG  666
          ||||||||||||||||||||||||||||||||||||||||||||||||||||||||||||
Sbjct 601 AGCCATGTCTGCTGTTTTCTAGAGGCTGCTACTGTCCCCTTTACTGCCCTGAAGATTCAG  660

Query 667 CCTGCGGAAGACAGGGGGTTGCCCCAGTGGAATTCCCCAGCCTTGCCTAGCAGAGCCCAT  726
          ||||||||||||||||||||||||||||||||||||||||||||||||||||||||||||
Sbjct 661 CCTGCGGAAGACAGGGGGTTGCCCCAGTGGAATTCCCCAGCCTTGCCTAGCAGAGCCCAT  720

Query 727 TCCTTCCGCCCCCAGATGAAGCAGGGAGAGGAAGCTGAGTCAAAGAAGGCTGTCAGGGAG  786
          ||||||||||||||||||||||||||||||||||||||||||||||||||||||||||||
Sbjct 721 TCCTTCCGCCCCCAGATGAAGCAGGGAGAGGAAGCTGAGTCAAAGAAGGCTGTCAGGGAG  780

Query 787 GGAAAAAGAGGACAGAGCCTGGAGTGTGGGGAGGGGTTTGGGGAGGATATCTGACCTGGG  846
          ||||||||||||||||||||||||||||||||||||||||||||||||||||||||||||
Sbjct 781 GGAAAAAGAGGACAGAGCCTGGAGTGTGGGGAGGGGTTTGGGGAGGATATCTGACCTGGG  840

Query 847 AGGGGGTGTTGCAAAAGGCCAAGGATGGGCCAGGGGGATCATTAGTTTCAGAAAGAAGTC  906
          ||||||||||||||||||||||||||||||||||||||||||||||||||||||||||||
Sbjct 841 AGGGGGTGTTGCAAAAGGCCAAGGATGGGCCAGGGGGATCATTAGTTTCAGAAAGAAGTC  900
```


Query 907 TCAGGGAGTCTTCCATCACTTTCCCTTGGCTGACCACTGGAGGCTTTCAGACCAAGGGAT 966
Sbjct 901 TCAGGGAGTCTTCCATCACTTTCCCTTGGCTGACCACTGGAGGCTTTCAGACCAAGGGAT 960
Query 967 GGGGGATCCCTCCAGCTTCATCCCCCTCCCTCCCTTTCATACAGTTCCCACAAGCTCTGC 1026
Sbjct 961 GGGGGATCCCTCCAGCTTCATCCCCCTCCCTCCCTTTCATACAGTTCCCACAAGCTCTGC 1020
Query 1027 AGTTTGCAAAACCCTACCCCTCCCCTGAGGGCCTGCGGTTTCCTGCGGGTCTGGGGTCTT 1086
Sbjct 1021 AGTTTGCAAAACCCTACCCCTCCCCTGAGGGCCTGCGGTTTCCTGCGGGTCTGGGGTCTT 1080
Query 1087 GCCTGACTTGGCAGTGGAGACTGCGGGCAGTGGAGAGAGGAGGAGGTGGTGTAAGCCCTT 1146
Sbjct 1081 GCCTGACTTGGCAGTGGAGACTGCGGGCAGTGGAGAGAGGAGGAGGTGGTGTAAGCCCTT 1140
Query 1147 TCTCATGCTGGTGCTGCcacacacacacacacacacacacacacacacacacacacCCTG 1206
Sbjct 1141 TCTCATGCTGGTGCTGCCACACACACACACACACACACACACACACACACACACCCTG 1200
Query 1207 ACCCCTGAGTTGGCACTTGCCTGTCAAGGAGGGGTGGGGTCACAGGAGCGCCTCCTTAAA 1266
Sbjct 1201 ACCCCTGAGTCAGCACTTGCCTGTCAAGGAGGGGTGGGGTCACAGGAGCGCCTCCTTAAA 1260
Query 1267 GCCCCCACAACAGCAGCTGCAGTCAGACACCTCTGCCCTCACCA 1310
Sbjct 1261 GCCCCCACAACAGCAGCTGCAGTCAGACACCTCTGCCCTCACCA 1304

Chapter 8.

Reference list

(1) Millar RP, Newton CL. The year in G protein-coupled receptor research. *Mol Endocrinol.* 2010;24:261-274.

(2) Fredriksson R, Lagerstrom MC, Lundin LG, Schioth HB. The G-protein-coupled receptors in the human genome form five main families. Phylogenetic analysis, paralogon groups, and fingerprints. *Mol Pharmacol.* 2003;63:1256-1272.

(3) Lefkowitz RJ. Historical review: a brief history and personal retrospective of seven-transmembrane receptors. *Trends Pharmacol Sci.* 2004;25:413-422.

(4) Walsh DA, Perkins JP, Krebs EG. An adenosine 3',5'-monophosphate-dependant protein kinase from rabbit skeletal muscle. *J Biol Chem.* 1968;243:3763-3765.

(5) Sutherland EW. On the biological role of cyclic AMP. *JAMA.* 1970;214:1281-1288.

(6) Bockaert J, Pin JP. Molecular tinkering of G protein-coupled receptors: an evolutionary success. *EMBO J.* 1999;18:1723-1729.

(7) Rivero-Muller A, Chou YY, Ji I, Lajic S, Hanyaloglu AC, Jonas K, Rahman N, Ji TH, Huhtaniemi I. Rescue of defective G protein-coupled receptor function in vivo by intermolecular cooperation. *Proc Natl Acad Sci U S A.* 2010;107:2319-2324.

(8) Lee C, Ji I, Ryu K, Song Y, Conn PM, Ji TH. Two defective heterozygous luteinizing hormone receptors can rescue hormone action. *J Biol Chem.* 2002;277:15795-15800.

(9) Downes GB, Gautam N. The G protein subunit gene families. *Genomics.* 1999;62:544-552.

(10) Oldham WM, Hamm HE. Heterotrimeric G protein activation by G-protein-coupled receptors. *Nat Rev Mol Cell Biol.* 2008;9:60-71.

(11) Karp G. *Cell and Molecular Biology: Concepts and Experiments.* 4th ed. Von Hoffmann Press: John Wiley & Sons; 2005.

(12) Luttrell LM, Lefkowitz RJ. The role of beta-arrestins in the termination and transduction of G-protein-coupled receptor signals. *J Cell Sci.* 2002;115:455-465.

(13) Ferguson SS. Evolving concepts in G protein-coupled receptor endocytosis: the role in receptor desensitization and signaling. *Pharmacol Rev.* 2001;53:1-24.

(14) AHLQUIST RP. A study of the adrenotropic receptors. *Am J Physiol.* 1948;153:586-600.

(15) Ruffolo RR, Jr. Relative agonist potency as a means of differentiating alpha-adrenoceptors and alpha-adrenergic mechanisms. *Clin Sci (Lond).* 1985;68 Suppl 10:9s-14s.

(16) Morrow AL, Creese I. Characterization of alpha 1-adrenergic receptor subtypes in rat brain: a reevaluation of [3H]WB4104 and [3H]prazosin binding. *Mol Pharmacol.* 1986;29:321-330.

(17) Graham RM, Perez DM, Hwa J, Piascik MT. alpha 1-adrenergic receptor subtypes. Molecular structure, function, and signaling. *Circ Res.* 1996;78:737-749.

(18) Civantos CB, Aleixandre de AA. Alpha-adrenoceptor subtypes. *Pharmacol Res.* 2001;44:195-208.

(19) Brodde OE. Beta-1 and beta-2 adrenoceptor polymorphisms: functional importance, impact on cardiovascular diseases and drug responses. *Pharmacol Ther.* 2008;117:1-29.

(20) Reiter MJ. Cardiovascular drug class specificity: beta-blockers. *Prog Cardiovasc Dis.* 2004;47:11-33.

(21) Brodde OE, Michel MC. Adrenergic and muscarinic receptors in the human heart. *Pharmacol Rev.* 1999;51:651-690.

(22) Insel PA. Seminars in medicine of the Beth Israel Hospital, Boston. Adrenergic receptors--evolving concepts and clinical implications. *N Engl J Med.* 1996;334:580-585.

(23) Warne T, Serrano-Vega MJ, Baker JG, Moukhametzianov R, Edwards PC, Henderson R, Leslie AG, Tate CG, Schertler GF. Structure of a beta1-adrenergic G-protein-coupled receptor. *Nature.* 2008;454:486-491.

(24) Rosenbaum DM, Rasmussen SG, Kobilka BK. The structure and function of G-protein-coupled receptors. *Nature.* 2009;459:356-363.

(25) Rasmussen SG, Choi HJ, Rosenbaum DM, Kobilka TS, Thian FS, Edwards PC, Burghammer M, Ratnala VR, Sanishvili R, Fischetti RF, Schertler GF, Weis WI, Kobilka BK. Crystal structure of the human beta2 adrenergic G-protein-coupled receptor. *Nature.* 2007;450:383-387.

(26) McCarron JG, Olson ML, Rainbow RD, MacMillan D, Chalmers S. Ins(1,4,5)P3 receptor regulation during 'quantal' Ca2+ release in smooth muscle. *Trends Pharmacol Sci.* 2007;28:271-279.

(27) Bell RM, Burns DJ. Lipid activation of protein kinase C. *J Biol Chem.* 1991;266:4661-4664.

(28) Perez DM, DeYoung MB, Graham RM. Coupling of expressed alpha 1B- and alpha 1D-adrenergic receptor to multiple signaling pathways is both G protein and cell type specific. *Mol Pharmacol.* 1993;44:784-795.

(29) Gallego M, Setien R, Puebla L, Boyano-Adanez MC, Arilla E, Casis O. alpha1-Adrenoceptors stimulate a Galphas protein and reduce the transient outward K+ current via a cAMP/PKA-mediated pathway in the rat heart. *Am J Physiol Cell Physiol.* 2005;288:C577-C585.

(30) Docherty JR. Subtypes of functional alpha1-adrenoceptor. *Cell Mol Life Sci.* 2010;67:405-417.

(31) Docherty JR. Subtypes of functional alpha1- and alpha2-adrenoceptors. *Eur J Pharmacol.* 1998;361:1-15.

(32) Michelotti GA, Price DT, Schwinn DA. Alpha 1-adrenergic receptor regulation: basic science and clinical implications. *Pharmacol Ther.* 2000;88:281-309.

(33) Weiss H, Friedrich F, Paulmichl M, Woll E, Lang F. Effect of BHT 920 on calcium-activated K+ channels in renal epithelioid MDCK cells. *Biochim Biophys Acta.* 1991;1069:165-170.

(34) MacNulty EE, McClue SJ, Carr IC, Jess T, Wakelam MJ, Milligan G. Alpha 2-C10 adrenergic receptors expressed in rat 1 fibroblasts can regulate both adenylylcyclase and phospholipase D-mediated hydrolysis of phosphatidylcholine by interacting with pertussis toxin-sensitive guanine nucleotide-binding proteins. *J Biol Chem.* 1992;267:2149-2156.

(35) Michel MC, Brass LF, Williams A, Bokoch GM, LaMorte VJ, Motulsky HJ. Alpha 2-adrenergic receptor stimulation mobilizes intracellular Ca2+ in human erythroleukemia cells. *J Biol Chem.* 1989;264:4986-4991.

(36) Della Rocca GJ, van BT, Daaka Y, Luttrell DK, Luttrell LM, Lefkowitz RJ. Ras-dependent mitogen-activated protein kinase activation by G protein-coupled receptors. Convergence of Gi- and Gq-mediated pathways on calcium/calmodulin, Pyk2, and Src kinase. *J Biol Chem.* 1997;272:19125-19132.

(37) Karkoulias G, Mastrogianni O, Lymperopoulos A, Paris H, Flordellis C. alpha(2)-Adrenergic receptors activate MAPK and Akt through a pathway involving arachidonic acid metabolism by cytochrome P450-dependent epoxygenase, matrix metalloproteinase activation and subtype-specific transactivation of EGFR. *Cell Signal.* 2006;18:729-739.

(38) Cussac D, Schaak S, Denis C, Paris H. alpha 2B-adrenergic receptor activates MAPK via a pathway involving arachidonic acid metabolism, matrix metalloproteinases, and epidermal growth factor receptor transactivation. *J Biol Chem.* 2002;277:19882-19888.

(39) Xiao RP, Zhu W, Zheng M, Cao C, Zhang Y, Lakatta EG, Han Q. Subtype-specific alpha1- and beta-adrenoceptor signaling in the heart. *Trends Pharmacol Sci.* 2006;27:330-337.

(40) Gao T, Yatani A, Dell'Acqua ML, Sako H, Green SA, Dascal N, Scott JD, Hosey MM. cAMP-dependent regulation of cardiac L-type Ca2+ channels requires membrane targeting of PKA and phosphorylation of channel subunits. *Neuron.* 1997;19:185-196.

(41) El-Armouche A, Eschenhagen T. Beta-adrenergic stimulation and myocardial function in the failing heart. *Heart Fail Rev.* 2009;14:225-241.

(42) Xiao RP, Ji X, Lakatta EG. Functional coupling of the beta 2-adrenoceptor to a pertussis toxin-sensitive G protein in cardiac myocytes. *Mol Pharmacol.* 1995;47:322-329.

(43) Daaka Y, Luttrell LM, Lefkowitz RJ. Switching of the coupling of the beta2-adrenergic receptor to different G proteins by protein kinase A. *Nature.* 1997;390:88-91.

(44) Zamah AM, Delahunty M, Luttrell LM, Lefkowitz RJ. Protein kinase A-mediated phosphorylation of the beta 2-adrenergic receptor regulates its coupling to Gs and Gi. Demonstration in a reconstituted system. *J Biol Chem.* 2002;277:31249-31256.

(45) DeWire SM, Ahn S, Lefkowitz RJ, Shenoy SK. Beta-arrestins and cell signaling. *Annu Rev Physiol.* 2007;69:483-510.

(46) Lohse MJ, Klenk C. Blocking them all: beta-arrestins inhibit cellular signaling. *Mol Cell.* 2008;31:619-621.

(47) Baillie GS, Sood A, McPhee I, Gall I, Perry SJ, Lefkowitz RJ, Houslay MD. beta-Arrestin-mediated PDE4 cAMP phosphodiesterase recruitment regulates beta-adrenoceptor switching from Gs to Gi. *Proc Natl Acad Sci U S A.* 2003;100:940-945.

(48) Kendall RT, Luttrell LM. Diversity in arrestin function. *Cell Mol Life Sci.* 2009;66:2953-2973.

(49) Shenoy SK, Barak LS, Xiao K, Ahn S, Berthouze M, Shukla AK, Luttrell LM, Lefkowitz RJ. Ubiquitination of beta-arrestin links seven-transmembrane receptor endocytosis and ERK activation. *J Biol Chem.* 2007;282:29549-29562.

(50) Kobayashi H, Narita Y, Nishida M, Kurose H. Beta-arrestin2 enhances beta2-adrenergic receptor-mediated nuclear translocation of ERK. *Cell Signal.* 2005;17:1248-1253.

(51) DeFea KA, Vaughn ZD, O'Bryan EM, Nishijima D, Dery O, Bunnett NW. The proliferative and antiapoptotic effects of substance P are facilitated by formation of a beta -arrestin-dependent scaffolding complex. *Proc Natl Acad Sci U S A.* 2000;97:11086-11091.

(52) Defea K. Beta-arrestins and heterotrimeric G-proteins: collaborators and competitors in signal transduction. *Br J Pharmacol.* 2008;153 Suppl 1:S298-S309.

(53) Shenoy SK, Drake MT, Nelson CD, Houtz DA, Xiao K, Madabushi S, Reiter E, Premont RT, Lichtarge O, Lefkowitz RJ. beta-arrestin-dependent, G protein-independent ERK1/2 activation by the beta2 adrenergic receptor. *J Biol Chem.* 2006;281:1261-1273.

(54) Williamson AP, Seifen E, Lindemann JP, Kennedy RH. Alpha 1a-adrenergic receptor mediated positive chronotropic effect in right atria isolated from rats. *Can J Physiol Pharmacol.* 1994;72:1574-1579.

(55) Tanoue A, Koshimizu TA, Shibata K, Nasa Y, Takeo S, Tsujimoto G. Insights into alpha1 adrenoceptor function in health and disease from transgenic animal studies. *Trends Endocrinol Metab.* 2003;14:107-113.

(56) Gilsbach R, Schneider J, Lother A, Schickinger S, Leemhuis J, Hein L. Sympathetic alpha(2)-adrenoceptors prevent cardiac hypertrophy and fibrosis in mice at baseline but not after chronic pressure overload. *Cardiovasc Res.* 2010;86:432-442.

(57) Ma D, Rajakumaraswamy N, Maze M. alpha2-Adrenoceptor agonists: shedding light on neuroprotection? *Br Med Bull.* 2004;71:77-92.

(58) Hoeks J, van Baak MA, Hesselink MK, Hul GB, Vidal H, Saris WH, Schrauwen P. Effect of beta1- and beta2-adrenergic stimulation on energy expenditure, substrate oxidation, and UCP3 expression in humans. *Am J Physiol Endocrinol Metab.* 2003;285:E775-E782.

(59) Levine MA, Leenen FH. Role of beta 1-receptors and vagal tone in cardiac inotropic and chronotropic responses to a beta 2-agonist in humans. *Circulation.* 1989;79:107-115.

(60) McConville P, Spencer RG, Lakatta EG. Temporal dynamics of inotropic, chronotropic, and metabolic responses during beta1- and beta2-AR stimulation in the isolated, perfused rat heart. *Am J Physiol Endocrinol Metab.* 2005;289:E412-E418.

(61) Philipp M, Hein L. Adrenergic receptor knockout mice: distinct functions of 9 receptor subtypes. *Pharmacol Ther.* 2004;101:65-74.

(62) Hahn HS, Marreez Y, Odley A, Sterbling A, Yussman MG, Hilty KC, Bodi I, Liggett SB, Schwartz A, Dorn GW. Protein kinase Calpha negatively regulates systolic and diastolic function in pathological hypertrophy. *Circ Res.* 2003;93:1111-1119.

(63) Akhter SA, Luttrell LM, Rockman HA, Iaccarino G, Lefkowitz RJ, Koch WJ. Targeting the receptor-Gq interface to inhibit in vivo pressure overload myocardial hypertrophy. *Science.* 1998;280:574-577.

(64) Wettschureck N, Rutten H, Zywietz A, Gehring D, Wilkie TM, Chen J, Chien KR, Offermanns S. Absence of pressure overload induced myocardial hypertrophy after conditional inactivation of Galphaq/Galpha11 in cardiomyocytes. *Nat Med.* 2001;7:1236-1240.

(65) Bristow MR, Ginsburg R, Umans V, Fowler M, Minobe W, Rasmussen R, Zera P, Menlove R, Shah P, Jamieson S, . Beta 1- and beta 2-adrenergic-receptor subpopulations in nonfailing and failing human ventricular myocardium: coupling of both receptor subtypes to muscle contraction and selective beta 1-receptor down-regulation in heart failure. *Circ Res.* 1986;59:297-309.

(66) Bristow MR, Ginsburg R, Minobe W, Cubicciotti RS, Sageman WS, Lurie K, Billingham ME, Harrison DC, Stinson EB. Decreased catecholamine sensitivity and beta-adrenergic-receptor density in failing human hearts. *N Engl J Med.* 1982;307:205-211.

(67) Wang GY, Yeh CC, Jensen BC, Mann MJ, Simpson PC, Baker AJ. Heart failure switches the RV alpha1-adrenergic inotropic response from negative to positive. *Am J Physiol Heart Circ Physiol.* 2010;298:H913-H920.

(68) Brodde OE, Bruck H, Leineweber K, Seyfarth T. Presence, distribution and physiological function of adrenergic and muscarinic receptor subtypes in the human heart. *Basic Res Cardiol.* 2001;96:528-538.

(69) Baker JG, Hall IP, Hill SJ. Agonist and inverse agonist actions of beta-blockers at the human beta 2-adrenoceptor provide evidence for agonist-directed signaling. *Mol Pharmacol.* 2003;64:1357-1369.

(70) Marano G, Palazzesi S, Fadda A, Vergari A, Ferrari AU. Attenuation of aortic banding-induced cardiac hypertrophy by propranolol is independent of beta-adrenoceptor blockade. *J Hypertens.* 2002;20:763-769.

(71) Bristow MR, Feldman AM, Adams KF, Jr., Goldstein S. Selective versus nonselective beta-blockade for heart failure therapy: are there lessons to be learned from the COMET trial? *J Card Fail.* 2003;9:444-453.

(72) Poole-Wilson PA, Swedberg K, Cleland JG, Di LA, Hanrath P, Komajda M, Lubsen J, Lutiger B, Metra M, Remme WJ, Torp-Pedersen C, Scherhag A, Skene A. Comparison of carvedilol and metoprolol on clinical outcomes in patients with chronic heart failure in the Carvedilol Or Metoprolol European Trial (COMET): randomised controlled trial. *Lancet.* 2003;362:7-13.

(73) Packer M, Coats AJ, Fowler MB, Katus HA, Krum H, Mohacsi P, Rouleau JL, Tendera M, Castaigne A, Roecker EB, Schultz MK, DeMets DL. Effect of carvedilol on survival in severe chronic heart failure. *N Engl J Med.* 2001;344:1651-1658.

(74) Wisler JW, DeWire SM, Whalen EJ, Violin JD, Drake MT, Ahn S, Shenoy SK, Lefkowitz RJ. A unique mechanism of beta-blocker action: carvedilol stimulates beta-arrestin signaling. *Proc Natl Acad Sci U S A.* 2007;104:16657-16662.

(75) Metra M, Cas LD, Di LA, Poole-Wilson P. Beta-blockers in heart failure: are pharmacological differences clinically important? *Heart Fail Rev.* 2004;9:123-130.

(76) Waagstein F, Caidahl K, Wallentin I, Bergh CH, Hjalmarson A. Long-term beta-blockade in dilated cardiomyopathy. Effects of short- and long-term metoprolol treatment followed by withdrawal and readministration of metoprolol. *Circulation.* 1989;80:551-563.

(77) Sigmund M, Jakob H, Becker H, Hanrath P, Schumacher C, Eschenhagen T, Schmitz W, Scholz H, Steinfath M. Effects of metoprolol on myocardial beta-adrenoceptors and Gi alpha-proteins in patients with congestive heart failure. *Eur J Clin Pharmacol.* 1996;51:127-132.

(78) Hall JA, Kaumann AJ, Brown MJ. Selective beta 1-adrenoceptor blockade enhances positive inotropic responses to endogenous catecholamines mediated through beta 2-adrenoceptors in human atrial myocardium. *Circ Res.* 1990;66:1610-1623.

(79) Yoshikawa T, Port JD, Asano K, Chidiak P, Bouvier M, Dutcher D, Roden RL, Minobe W, Tremmel KD, Bristow MR. Cardiac adrenergic receptor effects of carvedilol. *Eur Heart J.* 1996;17 Suppl B:8-16.

(80) Gheorghiade M, Colucci WS, Swedberg K. Beta-blockers in chronic heart failure. *Circulation.* 2003;107:1570-1575.

(81) Sorrell JM, Caplan AI. Fibroblasts-a diverse population at the center of it all. *Int Rev Cell Mol Biol.* 2009;276:161-214.

(82) Porter KE, Turner NA. Cardiac fibroblasts: at the heart of myocardial remodeling. *Pharmacol Ther.* 2009;123:255-278.

(83) Brown RD, Jones GM, Laird RE, Hudson P, Long CS. Cytokines regulate matrix metalloproteinases and migration in cardiac fibroblasts. *Biochem Biophys Res Commun.* 2007;362:200-205.

(84) Porter KE, Turner NA, O'Regan DJ, Ball SG. Tumor necrosis factor alpha induces human atrial myofibroblast proliferation, invasion and MMP-9 secretion: inhibition by simvastatin. *Cardiovasc Res.* 2004;64:507-515.

(85) Cleutjens JP, Verluyten MJ, Smiths JF, Daemen MJ. Collagen remodeling after myocardial infarction in the rat heart. *Am J Pathol.* 1995;147:325-338.

(86) Sun Y, Zhang JQ, Zhang J, Lamparter S. Cardiac remodeling by fibrous tissue after infarction in rats. *J Lab Clin Med.* 2000;135:316-323.

(87) Cleutjens JP, Kandala JC, Guarda E, Guntaka RV, Weber KT. Regulation of collagen degradation in the rat myocardium after infarction. *J Mol Cell Cardiol.* 1995;27:1281-1292.

(88) Virag JI, Murry CE. Myofibroblast and endothelial cell proliferation during murine myocardial infarct repair. *Am J Pathol.* 2003;163:2433-2440.

(89) Kondalenko VF, Babaev VR, Rukosuev VS. [Myofibroblasts in a myocardial infarct zone]. *Biull Eksp Biol Med.* 1981;92:740-743.

(90) Kisseleva T, Brenner DA. Mechanisms of fibrogenesis. *Exp Biol Med (Maywood).* 2008;233:109-122.

(91) Willems IE, Havenith MG, De Mey JG, Daemen MJ. The alpha-smooth muscle actin-positive cells in healing human myocardial scars. *Am J Pathol.* 1994;145:868-875.

(92) Leicht M, Greipel N, Zimmer H. Comitogenic effect of catecholamines on rat cardiac fibroblasts in culture. *Cardiovasc Res.* 2000;48:274-284.

(93) Kadler KE, Baldock C, Bella J, Boot-Handford RP. Collagens at a glance. *J Cell Sci.* 2007;120:1955-1958.

(94) Koch M, Laub F, Zhou P, Hahn RA, Tanaka S, Burgeson RE, Gerecke DR, Ramirez F, Gordon MK. Collagen XXIV, a vertebrate fibrillar collagen with structural features of invertebrate collagens: selective expression in developing cornea and bone. *J Biol Chem.* 2003;278:43236-43244.

(95) Boot-Handford RP, Tuckwell DS, Plumb DA, Rock CF, Poulsom R. A novel and highly conserved collagen (pro(alpha)1(XXVII)) with a unique expression pattern and unusual molecular characteristics establishes a new clade within the vertebrate fibrillar collagen family. *J Biol Chem.* 2003;278:31067-31077.

(96) Hulmes DJ, Miller A. Quasi-hexagonal molecular packing in collagen fibrils. *Nature*. 1979;282:878-880.

(97) Gelse K, Poschl E, Aigner T. Collagens--structure, function, and biosynthesis. *Adv Drug Deliv Rev*. 2003;55:1531-1546.

(98) Niyibizi C, Eyre DR. Bone type V collagen: chain composition and location of a trypsin cleavage site. *Connect Tissue Res*. 1989;20:247-250.

(99) Fleischmajer R, MacDonald ED, Perlish JS, Burgeson RE, Fisher LW. Dermal collagen fibrils are hybrids of type I and type III collagen molecules. *J Struct Biol*. 1990;105:162-169.

(100) Myllyharju J, Kivirikko KI. Collagens and collagen-related diseases. *Ann Med*. 2001;33:7-21.

(101) Hudson BG, Reeders ST, Tryggvason K. Type IV collagen: structure, gene organization, and role in human diseases. Molecular basis of Goodpasture and Alport syndromes and diffuse leiomyomatosis. *J Biol Chem*. 1993;268:26033-26036.

(102) von der MH, Aumailley M, Wick G, Fleischmajer R, Timpl R. Immunochemistry, genuine size and tissue localization of collagen VI. *Eur J Biochem*. 1984;142:493-502.

(103) Keene DR, Engvall E, Glanville RW. Ultrastructure of type VI collagen in human skin and cartilage suggests an anchoring function for this filamentous network. *J Cell Biol*. 1988;107:1995-2006.

(104) Bonaldo P, Braghetta P, Zanetti M, Piccolo S, Volpin D, Bressan GM. Collagen VI deficiency induces early onset myopathy in the mouse: an animal model for Bethlem myopathy. *Hum Mol Genet*. 1998;7:2135-2140.

(105) Werb Z. ECM and cell surface proteolysis: regulating cellular ecology. *Cell*. 1997;91:439-442.

(106) Iozzo RV. Matrix proteoglycans: from molecular design to cellular function. *Annu Rev Biochem*. 1998;67:609-652.

(107) Bode W, Grams F, Reinemer P, Gomis-Ruth FX, Baumann U, McKay DB, Stocker W. The metzincin-superfamily of zinc-peptidases. *Adv Exp Med Biol*. 1996;389:1-11.

(108) Sternlicht MD, Werb Z. How matrix metalloproteinases regulate cell behavior. *Annu Rev Cell Dev Biol*. 2001;17:463-516.

(109) Brauer PR. MMPs--role in cardiovascular development and disease. *Front Biosci*. 2006;11:447-478.

(110) Bode W, Fernandez-Catalan C, Tschesche H, Grams F, Nagase H, Maskos K. Structural properties of matrix metalloproteinases. *Cell Mol Life Sci*. 1999;55:639-652.

(111) Overall CM. Molecular determinants of metalloproteinase substrate specificity: matrix metalloproteinase substrate binding domains, modules, and exosites. *Mol Biotechnol.* 2002;22:51-86.

(112) Ra HJ, Parks WC. Control of matrix metalloproteinase catalytic activity. *Matrix Biol.* 2007;26:587-596.

(113) Stocker W, Grams F, Baumann U, Reinemer P, Gomis-Ruth FX, McKay DB, Bode W. The metzincins--topological and sequential relations between the astacins, adamalysins, serralysins, and matrixins (collagenases) define a superfamily of zinc-peptidases. *Protein Sci.* 1995;4:823-840.

(114) Butler GS, Tam EM, Overall CM. The canonical methionine 392 of matrix metalloproteinase 2 (gelatinase A) is not required for catalytic efficiency or structural integrity: probing the role of the methionine-turn in the metzincin metalloprotease superfamily. *J Biol Chem.* 2004;279:15615-15620.

(115) Hege T, Baumann U. The conserved methionine residue of the metzincins: a site-directed mutagenesis study. *J Mol Biol.* 2001;314:181-186.

(116) Rowsell S, Hawtin P, Minshull CA, Jepson H, Brockbank SM, Barratt DG, Slater AM, McPheat WL, Waterson D, Henney AM, Pauptit RA. Crystal structure of human MMP9 in complex with a reverse hydroxamate inhibitor. *J Mol Biol.* 2002;319:173-181.

(117) Visse R, Nagase H. Matrix metalloproteinases and tissue inhibitors of metalloproteinases: structure, function, and biochemistry. *Circ Res.* 2003;92:827-839.

(118) Allan JA, Docherty AJ, Barker PJ, Huskisson NS, Reynolds JJ, Murphy G. Binding of gelatinases A and B to type-I collagen and other matrix components. *Biochem J.* 1995;309 (Pt 1):299-306.

(119) Steffensen B, Wallon UM, Overall CM. Extracellular matrix binding properties of recombinant fibronectin type II-like modules of human 72-kDa gelatinase/type IV collagenase. High affinity binding to native type I collagen but not native type IV collagen. *J Biol Chem.* 1995;270:11555-11566.

(120) Pourmotabbed T. Relation between substrate specificity and domain structure of 92-kDa type IV collagenase. *Ann N Y Acad Sci.* 1994;732:372-374.

(121) Page-McCaw A, Ewald AJ, Werb Z. Matrix metalloproteinases and the regulation of tissue remodelling. *Nat Rev Mol Cell Biol.* 2007;8:221-233.

(122) Elkins PA, Ho YS, Smith WW, Janson CA, D'Alessio KJ, McQueney MS, Cummings MD, Romanic AM. Structure of the C-terminally truncated human ProMMP9, a gelatin-binding matrix metalloproteinase. *Acta Crystallogr D Biol Crystallogr.* 2002;58:1182-1192.

(123) **The PyMOL Molecular Graphics System** [computer program]. **DeLano Scientific**; 2002.

(124) Vincenti MP, Brinckerhoff CE. Signal transduction and cell-type specific regulation of matrix metalloproteinase gene expression: can MMPs be good for you? *J Cell Physiol.* 2007;213:355-364.

(125) Mackay AR, Ballin M, Pelina MD, Farina AR, Nason AM, Hartzler JL, Thorgeirsson UP. Effect of phorbol ester and cytokines on matrix metalloproteinase and tissue inhibitor of metalloproteinase expression in tumor and normal cell lines. *Invasion Metastasis.* 1992;12:168-184.

(126) Yan C, Boyd DD. Regulation of matrix metalloproteinase gene expression. *J Cell Physiol.* 2007;211:19-26.

(127) Bond M, Fabunmi RP, Baker AH, Newby AC. Synergistic upregulation of metalloproteinase-9 by growth factors and inflammatory cytokines: an absolute requirement for transcription factor NF-kappa B. *FEBS Lett.* 1998;435:29-34.

(128) Jin YJ, Park I, Hong IK, Byun HJ, Choi J, Kim YM, Lee H. Fibronectin and vitronectin induce AP-1-mediated matrix metalloproteinase-9 expression through integrin alpha(5)beta(1)/alpha(v)beta(3)-dependent Akt, ERK and JNK signaling pathways in human umbilical vein endothelial cells. *Cell Signal.* 2010.

(129) Yan C, Wang H, Toh Y, Boyd DD. Repression of 92-kDa type IV collagenase expression by MTA1 is mediated through direct interactions with the promoter via a mechanism, which is both dependent on and independent of histone deacetylation. *J Biol Chem.* 2003;278:2309-2316.

(130) Sopata I, Dancewicz AM. Presence of a gelatin-specific proteinase and its latent form in human leucocytes. *Biochim Biophys Acta.* 1974;370:510-523.

(131) Van den Steen PE, Dubois B, Nelissen I, Rudd PM, Dwek RA, Opdenakker G. Biochemistry and molecular biology of gelatinase B or matrix metalloproteinase-9 (MMP-9). *Crit Rev Biochem Mol Biol.* 2002;37:375-536.

(132) Sato H, Kita M, Seiki M. v-Src activates the expression of 92-kDa type IV collagenase gene through the AP-1 site and the GT box homologous to retinoblastoma control elements. A mechanism regulating gene expression independent of that by inflammatory cytokines. *J Biol Chem.* 1993;268:23460-23468.

(133) Sato H, Seiki M. Regulatory mechanism of 92 kDa type IV collagenase gene expression which is associated with invasiveness of tumor cells. *Oncogene.* 1993;8:395-405.

(134) Song Y, Qian L, Song S, Chen L, Zhang Y, Yuan G, Zhang H, Xia Q, Hu M, Yu M, Shi M, Jiang Z, Guo N. Fra-1 and Stat3 synergistically regulate activation of human MMP-9 gene. *Mol Immunol.* 2008;45:137-143.

(135) Han YP, Tuan TL, Hughes M, Wu H, Garner WL. Transforming growth factor-beta - and tumor necrosis factor-alpha -mediated induction and proteolytic activation of MMP-9 in human skin. *J Biol Chem.* 2001;276:22341-22350.

(136) Huhtala P, Tuuttila A, Chow LT, Lohi J, Keski-Oja J, Tryggvason K. Complete structure of the human gene for 92-kDa type IV collagenase. Divergent regulation

of expression for the 92- and 72-kilodalton enzyme genes in HT-1080 cells. *J Biol Chem.* 1991;266:16485-16490.

(137) Ogawa K, Chen F, Kuang C, Chen Y. Suppression of matrix metalloproteinase-9 transcription by transforming growth factor-beta is mediated by a nuclear factor-kappaB site. *Biochem J.* 2004;381:413-422.

(138) Demacq C, Vasconcellos VB, Marcaccini AM, Gerlach RF, Silva WA, Jr., Tanus-Santos JE. Functional polymorphisms in the promoter of the matrix metalloproteinase-9 (MMP-9) gene are not linked with significant plasma MMP-9 variations in healthy subjects. *Clin Chem Lab Med.* 2008;46:57-63.

(139) Fiotti N, Altamura N, Fisicaro M, Carraro N, Uxa L, Grassi G, Torelli L, Gobbato R, Guarnieri G, Baxter BT, Giansante C. MMP-9 microsatellite polymorphism and susceptibility to carotid arteries atherosclerosis. *Arterioscler Thromb Vasc Biol.* 2006;26:1330-1336.

(140) Fiotti N, Zivadinov R, Altamura N, Nasuelli D, Bratina A, Tommasi MA, Bosco A, Locatelli L, Grop A, Cazzato G, Guarnieri G, Giansante C, Zorzon M. MMP-9 microsatellite polymorphism and multiple sclerosis. *J Neuroimmunol.* 2004;152:147-153.

(141) Huang TS, Lee CC, Chang AC, Lin S, Chao CC, Jou YS, Chu YW, Wu CW, Whang-Peng J. Shortening of microsatellite deoxy(CA) repeats involved in GL331-induced down-regulation of matrix metalloproteinase-9 gene expression. *Biochem Biophys Res Commun.* 2003;300:901-907.

(142) Zhao X, Benveniste EN. Transcriptional activation of human matrix metalloproteinase-9 gene expression by multiple co-activators. *J Mol Biol.* 2008;383:945-956.

(143) Munaut C, Salonurmi T, Kontusaari S, Reponen P, Morita T, Foidart JM, Tryggvason K. Murine matrix metalloproteinase 9 gene. 5'-upstream region contains cis-acting elements for expression in osteoclasts and migrating keratinocytes in transgenic mice. *J Biol Chem.* 1999;274:5588-5596.

(144) Chicoine E, Esteve PO, Robledo O, Van TC, Potworowski EF, St-Pierre Y. Evidence for the role of promoter methylation in the regulation of MMP-9 gene expression. *Biochem Biophys Res Commun.* 2002;297:765-772.

(145) Ma Z, Shah RC, Chang MJ, Benveniste EN. Coordination of cell signaling, chromatin remodeling, histone modifications, and regulator recruitment in human matrix metalloproteinase 9 gene transcription. *Mol Cell Biol.* 2004;24:5496-5509.

(146) Pei D, Weiss SJ. Furin-dependent intracellular activation of the human stromelysin-3 zymogen. *Nature.* 1995;375:244-247.

(147) Wang Z, Juttermann R, Soloway PD. TIMP-2 is required for efficient activation of proMMP-2 in vivo. *J Biol Chem.* 2000;275:26411-26415.

(148) Hahn-Dantona E, Ramos-DeSimone N, Sipley J, Nagase H, French DL, Quigley JP. Activation of proMMP-9 by a plasmin/MMP-3 cascade in a tumor cell model. Regulation by tissue inhibitors of metalloproteinases. *Ann N Y Acad Sci.* 1999;878:372-387.

(149) Ramos-DeSimone N, Hahn-Dantona E, Sipley J, Nagase H, French DL, Quigley JP. Activation of matrix metalloproteinase-9 (MMP-9) via a converging plasmin/stromelysin-1 cascade enhances tumor cell invasion. *J Biol Chem.* 1999;274:13066-13076.

(150) Fang KC, Wolters PJ, Steinhoff M, Bidgol A, Blount JL, Caughey GH. Mast cell expression of gelatinases A and B is regulated by kit ligand and TGF-beta. *J Immunol.* 1999;162:5528-5535.

(151) Tchougounova E, Lundequist A, Fajardo I, Winberg JO, Abrink M, Pejler G. A key role for mast cell chymase in the activation of pro-matrix metalloprotease-9 and pro-matrix metalloprotease-2. *J Biol Chem.* 2005;280:9291-9296.

(152) Gu Z, Kaul M, Yan B, Kridel SJ, Cui J, Strongin A, Smith JW, Liddington RC, Lipton SA. S-nitrosylation of matrix metalloproteinases: signaling pathway to neuronal cell death. *Science.* 2002;297:1186-1190.

(153) Nagase H, Itoh Y, Binner S. Interaction of alpha 2-macroglobulin with matrix metalloproteinases and its use for identification of their active forms. *Ann N Y Acad Sci.* 1994;732:294-302.

(154) Van den Steen PE, Van A, I, Hvidberg V, Piccard H, Fiten P, Jacobsen C, Moestrup SK, Fry S, Royle L, Wormald MR, Wallis R, Rudd PM, Dwek RA, Opdenakker G. The hemopexin and O-glycosylated domains tune gelatinase B/MMP-9 bioavailability via inhibition and binding to cargo receptors. *J Biol Chem.* 2006;281:18626-18637.

(155) Lambert E, Bridoux L, Devy J, Dasse E, Sowa ML, Duca L, Hornebeck W, Martiny L, Petitfrere-Charpentier E. TIMP-1 binding to proMMP-9/CD44 complex localized at the cell surface promotes erythroid cell survival. *Int J Biochem Cell Biol.* 2009;41:1102-1115.

(156) Yu Q, Stamenkovic I. Cell surface-localized matrix metalloproteinase-9 proteolytically activates TGF-beta and promotes tumor invasion and angiogenesis. *Genes Dev.* 2000;14:163-176.

(157) Brew K, Nagase H. The tissue inhibitors of metalloproteinases (TIMPs): an ancient family with structural and functional diversity. *Biochim Biophys Acta.* 2010;1803:55-71.

(158) O'Connell JP, Willenbrock F, Docherty AJ, Eaton D, Murphy G. Analysis of the role of the COOH-terminal domain in the activation, proteolytic activity, and tissue inhibitor of metalloproteinase interactions of gelatinase B. *J Biol Chem.* 1994;269:14967-14973.

(159) Nguyen Q, Willenbrock F, Cockett MI, O'Shea M, Docherty AJ, Murphy G. Different domain interactions are involved in the binding of tissue inhibitors of metalloproteinases to stromelysin-1 and gelatinase A. *Biochemistry.* 1994;33:2089-2095.

(160) Baragi VM, Fliszar CJ, Conroy MC, Ye QZ, Shipley JM, Welgus HG. Contribution of the C-terminal domain of metalloproteinases to binding by tissue inhibitor of metalloproteinases. C-terminal truncated stromelysin and matrilysin

exhibit equally compromised binding affinities as compared to full-length stromelysin. *J Biol Chem.* 1994;269:12692-12697.

(161) Howard EW, Bullen EC, Banda MJ. Preferential inhibition of 72- and 92-kDa gelatinases by tissue inhibitor of metalloproteinases-2. *J Biol Chem.* 1991;266:13070-13075.

(162) Hamze AB, Wei S, Bahudhanapati H, Kota S, Acharya KR, Brew K. Constraining specificity in the N-domain of tissue inhibitor of metalloproteinases-1; gelatinase-selective inhibitors. *Protein Sci.* 2007;16:1905-1913.

(163) Marom B, Rahat MA, Lahat N, Weiss-Cerem L, Kinarty A, Bitterman H. Native and fragmented fibronectin oppositely modulate monocyte secretion of MMP-9. *J Leukoc Biol.* 2007;81:1466-1476.

(164) Awasthi N, Wang-Su ST, Wagner BJ. Downregulation of MMP-2 and -9 by proteasome inhibition: a possible mechanism to decrease LEC migration and prevent posterior capsular opacification. *Invest Ophthalmol Vis Sci.* 2008;49:1998-2003.

(165) Catalgol B, Ziaja I, Breusing N, Jung T, Hohn A, Alpertunga B, Schroeder P, Chondrogianni N, Gonos ES, Petropoulos I, Friguet B, Klotz LO, Krutmann J, Grune T. The proteasome is an integral part of solar ultraviolet a radiation-induced gene expression. *J Biol Chem.* 2009;284:30076-30086.

(166) Hedhli N, Lizano P, Hong C, Fritzky LF, Dhar SK, Liu H, Tian Y, Gao S, Madura K, Vatner SF, Depre C. Proteasome inhibition decreases cardiac remodeling after initiation of pressure overload. *Am J Physiol Heart Circ Physiol.* 2008;295:H1385-H1393.

(167) Spiers JP, Kelso EJ, Siah WF, Edge G, Song G, McDermott BJ, Hennessy M. Alterations in vascular matrix metalloproteinase due to ageing and chronic hypertension: effects of endothelin receptor blockade. *J Hypertens.* 2005;23:1717-1724.

(168) Wang M, Takagi G, Asai K, Resuello RG, Natividad FF, Vatner DE, Vatner SF, Lakatta EG. Aging increases aortic MMP-2 activity and angiotensin II in nonhuman primates. *Hypertension.* 2003;41:1308-13016.

(169) McNulty M, Spiers P, McGovern E, Feely J. Aging is associated with increased matrix metalloproteinase-2 activity in the human aorta. *Am J Hypertens.* 2005;18:504-509.

(170) Bonnema DD, Webb CS, Pennington WR, Stroud RE, Leonardi AE, Clark LL, McClure CD, Finklea L, Spinale FG, Zile MR. Effects of age on plasma matrix metalloproteinases (MMPs) and tissue inhibitor of metalloproteinases (TIMPs). *J Card Fail.* 2007;13:530-540.

(171) Messerli FH. TIMPs, MMPs and cardiovascular disease. *Eur Heart J.* 2004;25:1475-1476.

(172) Wu TC, Chen YH, Leu HB, Chen YL, Lin FY, Lin SJ, Chen JW. Carvedilol, a pharmacological antioxidant, inhibits neointimal matrix metalloproteinase-2 and -9 in experimental atherosclerosis. *Free Radic Biol Med.* 2007;43:1508-1522.

(173) Peterson JT, Li H, Dillon L, Bryant JW. Evolution of matrix metalloprotease and tissue inhibitor expression during heart failure progression in the infarcted rat. *Cardiovasc Res*. 2000;46:307-315.

(174) Spinale FG, Coker ML, Thomas CV, Walker JD, Mukherjee R, Hebbar L. Time-dependent changes in matrix metalloproteinase activity and expression during the progression of congestive heart failure: relation to ventricular and myocyte function. *Circ Res*. 1998;82:482-495.

(175) Miura S, Ohno I, Suzuki J, Suzuki K, Okada S, Okuyama A, Nawata J, Ikeda J, Shirato K. Inhibition of matrix metalloproteinases prevents cardiac hypertrophy induced by beta-adrenergic stimulation in rats. *J Cardiovasc Pharmacol*. 2003;42:174-181.

(176) Wilson EM, Gunasinghe HR, Coker ML, Sprunger P, Lee-Jackson D, Bozkurt B, Deswal A, Mann DL, Spinale FG. Plasma matrix metalloproteinase and inhibitor profiles in patients with heart failure. *J Card Fail*. 2002;8:390-398.

(177) Li YY, McTiernan CF, Feldman AM. Interplay of matrix metalloproteinases, tissue inhibitors of metalloproteinases and their regulators in cardiac matrix remodeling. *Cardiovasc Res*. 2000;46:214-224.

(178) Coker ML, Thomas CV, Clair MJ, Hendrick JW, Krombach RS, Galis ZS, Spinale FG. Myocardial matrix metalloproteinase activity and abundance with congestive heart failure. *Am J Physiol*. 1998;274:H1516-H1523.

(179) Polyakova V, Loeffler I, Hein S, Miyagawa S, Piotrowska I, Dammer S, Risteli J, Schaper J, Kostin S. Fibrosis in endstage human heart failure: Severe changes in collagen metabolism and MMP/TIMP profiles. *Int J Cardiol*. 2010.

(180) Reinhardt D, Sigusch HH, Hensse J, Tyagi SC, Korfer R, Figulla HR. Cardiac remodelling in end stage heart failure: upregulation of matrix metalloproteinase (MMP) irrespective of the underlying disease, and evidence for a direct inhibitory effect of ACE inhibitors on MMP. *Heart*. 2002;88:525-530.

(181) Agewall S. Matrix metalloproteinases and cardiovascular disease. *Eur Heart J*. 2006;27:121-122.

(182) Galis ZS, Khatri JJ. Matrix metalloproteinases in vascular remodeling and atherogenesis: the good, the bad, and the ugly. *Circ Res*. 2002;90:251-262.

(183) Brown DL, Hibbs MS, Kearney M, Loushin C, Isner JM. Identification of 92-kD gelatinase in human coronary atherosclerotic lesions. Association of active enzyme synthesis with unstable angina. *Circulation*. 1995;91:2125-2131.

(184) Kim HE, Dalal SS, Young E, Legato MJ, Weisfeldt ML, D'Armiento J. Disruption of the myocardial extracellular matrix leads to cardiac dysfunction. *J Clin Invest*. 2000;106:857-866.

(185) Ducharme A, Frantz S, Aikawa M, Rabkin E, Lindsey M, Rohde LE, Schoen FJ, Kelly RA, Werb Z, Libby P, Lee RT. Targeted deletion of matrix metalloproteinase-9 attenuates left ventricular enlargement and collagen accumulation after experimental myocardial infarction. *J Clin Invest*. 2000;106:55-62.

(186) Hemmann S, Graf J, Roderfeld M, Roeb E. Expression of MMPs and TIMPs in liver fibrosis - a systematic review with special emphasis on anti-fibrotic strategies. *J Hepatol.* 2007;46:955-975.

(187) Schonbeck U, Mach F, Libby P. Generation of biologically active IL-1 beta by matrix metalloproteinases: a novel caspase-1-independent pathway of IL-1 beta processing. *J Immunol.* 1998;161:3340-3346.

(188) Gearing AJ, Beckett P, Christodoulou M, Churchill M, Clements J, Davidson AH, Drummond AH, Galloway WA, Gilbert R, Gordon JL, . Processing of tumour necrosis factor-alpha precursor by metalloproteinases. *Nature.* 1994;370:555-557.

(189) Briest W, Holzl A, Rassler B, Deten A, Leicht M, Baba HA, Zimmer HG. Cardiac remodeling after long term norepinephrine treatment in rats. *Cardiovasc Res.* 2001;52:265-273.

(190) Cimmino G, Ibanez B, Giannarelli C, Prat-Gonzalez S, Hutter R, Garcia M, Sanz J, Fuster V, Badimon JJ. Carvedilol administration in acute myocardial infarction results in stronger inhibition of early markers of left ventricular remodeling than metoprolol. *Int J Cardiol.* 2010.

(191) Bernstein M., Tyagi S.C. beta-Blocker Improves Cardiac Function by Reducing Oxidative Stress and Metalloproteinase Activity After Myocardial Infarction. *The Journal of Applied Research.* 2001;1.

(192) Senzaki H, Paolocci N, Gluzband YA, Lindsey ML, Janicki JS, Crow MT, Kass DA. beta-blockade prevents sustained metalloproteinase activation and diastolic stiffening induced by angiotensin II combined with evolving cardiac dysfunction. *Circ Res.* 2000;86:807-815.

(193) Coker ML, Jolly JR, Joffs C, Etoh T, Holder JR, Bond BR, Spinale FG. Matrix metalloproteinase expression and activity in isolated myocytes after neurohormonal stimulation. *Am J Physiol Heart Circ Physiol.* 2001;281:H543-H551.

(194) Banfi C, Cavalca V, Veglia F, Brioschi M, Barcella S, Mussoni L, Boccotti L, Tremoli E, Biglioli P, Agostoni P. Neurohormonal activation is associated with increased levels of plasma matrix metalloproteinase-2 in human heart failure. *Eur Heart J.* 2005;26:481-488.

(195) Menon B, Singh M, Singh K. Matrix metalloproteinases mediate beta-adrenergic receptor-stimulated apoptosis in adult rat ventricular myocytes. *Am J Physiol Cell Physiol.* 2005;289:C168-C176.

(196) Speidl WS, Toller WG, Kaun C, Weiss TW, Pfaffenberger S, Kastl SP, Furnkranz A, Maurer G, Huber K, Metzler H, Wojta J. Catecholamines potentiate LPS-induced expression of MMP-1 and MMP-9 in human monocytes and in the human monocytic cell line U937: possible implications for peri-operative plaque instability. *FASEB J.* 2004;18:603-605.

(197) Song G, Hennessy M, Zhao YL, Li Q, Han WD, Qi Y, Zhao WN, Silke B, Barry M, Doyle R, Spiers JP. Adrenoceptor blockade alters plasma gelatinase activity in patients with heart failure and MMP-9 promoter activity in a human cell line (ECV304). *Pharmacol Res.* 2006;54:57-64.

(198) Pavlovic S, Du B, Sakamoto K, Khan KM, Natarajan C, Breyer RM, Dannenberg AJ, Falcone DJ. Targeting prostaglandin E2 receptors as an alternative strategy to block cyclooxygenase-2-dependent extracellular matrix-induced matrix metalloproteinase-9 expression by macrophages. *J Biol Chem.* 2006;281:3321-3328.

(199) Staun-Ram E, Goldman S, Gabarin D, Shalev E. Expression and importance of matrix metalloproteinase 2 and 9 (MMP-2 and -9) in human trophoblast invasion. *Reprod Biol Endocrinol.* 2004;2:59.

(200) Shi Y. Serine/threonine phosphatases: mechanism through structure. *Cell.* 2009;139:468-484.

(201) Gallego M, Virshup DM. Protein serine/threonine phosphatases: life, death, and sleeping. *Curr Opin Cell Biol.* 2005;17:197-202.

(202) Gupta RC, Neumann J, Watanabe AM, Sabbah HN. Inhibition of type 1 protein phosphatase activity by activation of beta-adrenoceptors in ventricular myocardium. *Biochem Pharmacol.* 2002;63:1069-1076.

(203) Carr AN, Schmidt AG, Suzuki Y, del MF, Sato Y, Lanner C, Breeden K, Jing SL, Allen PB, Greengard P, Yatani A, Hoit BD, Grupp IL, Hajjar RJ, DePaoli-Roach AA, Kranias EG. Type 1 phosphatase, a negative regulator of cardiac function. *Mol Cell Biol.* 2002;22:4124-4135.

(204) Neumann J, Gupta RC, Schmitz W, Scholz H, Nairn AC, Watanabe AM. Evidence for isoproterenol-induced phosphorylation of phosphatase inhibitor-1 in the intact heart. *Circ Res.* 1991;69:1450-1457.

(205) El-Armouche A, Rau T, Zolk O, Ditz D, Pamminger T, Zimmermann WH, Jackel E, Harding SE, Boknik P, Neumann J, Eschenhagen T. Evidence for protein phosphatase inhibitor-1 playing an amplifier role in beta-adrenergic signaling in cardiac myocytes. *FASEB J.* 2003;17:437-439.

(206) De A, V, Soto D, Xiang Y. Phosphodiesterase 4 and phosphatase 2A differentially regulate cAMP/protein kinase a signaling for cardiac myocyte contraction under stimulation of beta1 adrenergic receptor. *Mol Pharmacol.* 2008;74:1453-1462.

(207) Pullar CE, Chen J, Isseroff RR. PP2A activation by beta2-adrenergic receptor agonists: novel regulatory mechanism of keratinocyte migration. *J Biol Chem.* 2003;278:22555-22562.

(208) El-Armouche A, Bednorz A, Pamminger T, Ditz D, Didie M, Dobrev D, Eschenhagen T. Role of calcineurin and protein phosphatase-2A in the regulation of phosphatase inhibitor-1 in cardiac myocytes. *Biochem Biophys Res Commun.* 2006;346:700-706.

(209) Neumann J, Eschenhagen T, Jones LR, Linck B, Schmitz W, Scholz H, Zimmermann N. Increased expression of cardiac phosphatases in patients with end-stage heart failure. *J Mol Cell Cardiol.* 1997;29:265-272.

(210) Gergs U, Boknik P, Buchwalow I, Fabritz L, Matus M, Justus I, Hanske G, Schmitz W, Neumann J. Overexpression of the catalytic subunit of protein phosphatase 2A impairs cardiac function. *J Biol Chem.* 2004;279:40827-40834.

(211) Weinbrenner C, Baines CP, Liu GS, Armstrong SC, Ganote CE, Walsh AH, Honkanen RE, Cohen MV, Downey JM. Fostriecin, an inhibitor of protein phosphatase 2A, limits myocardial infarct size even when administered after onset of ischemia. *Circulation.* 1998;98:899-905.

(212) Boknik P, Fockenbrock M, Herzig S, Knapp J, Linck B, Luss H, Muller FU, Muller T, Schmitz W, Schroder F, Neumann J. Protein phosphatase activity is increased in a rat model of long-term beta-adrenergic stimulation. *Naunyn Schmiedebergs Arch Pharmacol.* 2000;362:222-231.

(213) El-Armouche A, Gocht F, Jaeckel E, Wittkopper K, Peeck M, Eschenhagen T. Long-term beta-adrenergic stimulation leads to downregulation of protein phosphatase inhibitor-1 in the heart. *Eur J Heart Fail.* 2007;9:1077-1080.

(214) El-Armouche A, Wittkopper K, Degenhardt F, Weinberger F, Didie M, Melnychenko I, Grimm M, Peeck M, Zimmermann WH, Unsold B, Hasenfuss G, Dobrev D, Eschenhagen T. Phosphatase inhibitor-1-deficient mice are protected from catecholamine-induced arrhythmias and myocardial hypertrophy. *Cardiovasc Res.* 2008;80:396-406.

(215) Davies SP, Reddy H, Caivano M, Cohen P. Specificity and mechanism of action of some commonly used protein kinase inhibitors. *Biochem J.* 2000;351:95-105.

(216) TODARO GJ, GREEN H. Quantitative studies of the growth of mouse embryo cells in culture and their development into established lines. *J Cell Biol.* 1963;17:299-313.

(217) Xu L, Hui AY, Albanis E, Arthur MJ, O'Byrne SM, Blaner WS, Mukherjee P, Friedman SL, Eng FJ. Human hepatic stellate cell lines, LX-1 and LX-2: new tools for analysis of hepatic fibrosis. *Gut.* 2005;54:142-151.

(218) Baudino TA, Carver W, Giles W, Borg TK. Cardiac fibroblasts: friend or foe? *Am J Physiol Heart Circ Physiol.* 2006;291:H1015-H1026.

(219) Weber KT, Brilla CG. Pathological hypertrophy and cardiac interstitium. Fibrosis and renin-angiotensin-aldosterone system. *Circulation.* 1991;83:1849-1865.

(220) Akers WS, Cross A, Speth R, Dwoskin LP, Cassis LA. Renin-angiotensin system and sympathetic nervous system in cardiac pressure-overload hypertrophy. *Am J Physiol Heart Circ Physiol.* 2000;279:H2797-H2806.

(221) Kiriazis H, Wang K, Xu Q, Gao XM, Ming Z, Su Y, Moore XL, Lambert G, Gibbs ME, Dart AM, Du XJ. Knockout of beta(1)- and beta(2)-adrenoceptors attenuates pressure overload-induced cardiac hypertrophy and fibrosis. *Br J Pharmacol.* 2008;153:684-692.

(222) HORI Y, KUNIHIRO S, Sato S, Yoshioka K, Hara Y, KANAI K, HOSHI F, ITOH N, HIGUCHI S. Doxycycline attenuates isoproterenol-induced myocardial fibrosis and matrix metalloproteinase activity in rats. *Biol Pharm Bull.* 2009;32:1678-1682.

(223) Kuwahara F, Kai H, Tokuda K, Takeya M, Takeshita A, Egashira K, Imaizumi T. Hypertensive myocardial fibrosis and diastolic dysfunction: another model of inflammation? *Hypertension*. 2004;43:739-745.

(224) Spinale FG, Coker ML, Bond BR, Zellner JL. Myocardial matrix degradation and metalloproteinase activation in the failing heart: a potential therapeutic target. *Cardiovasc Res*. 2000;46:225-238.

(225) Gutkind JS. Regulation of mitogen-activated protein kinase signaling networks by G protein-coupled receptors. *Sci STKE*. 2000;2000:RE1.

(226) McCoy CE, Campbell DG, Deak M, Bloomberg GB, Arthur JS. MSK1 activity is controlled by multiple phosphorylation sites. *Biochem J*. 2005;387:507-517.

(227) Arthur JS. MSK activation and physiological roles. *Front Biosci*. 2008;13:5866-5879.

(228) Genersch E, Hayess K, Neuenfeld Y, Haller H. Sustained ERK phosphorylation is necessary but not sufficient for MMP-9 regulation in endothelial cells: involvement of Ras-dependent and -independent pathways. *J Cell Sci*. 2000;113 Pt 23:4319-4330.

(229) Doyle K, Miles J. Ligation of plasmid vector and insert DNA. *Promega protocols and applications guide*. 1996;45.

(230) Pfaffl MW. A new mathematical model for relative quantification in real-time RT-PCR. *Nucleic Acids Res*. 2001;29:e45.

(231) Haan C, Behrmann I. A cost effective non-commercial ECL-solution for Western blot detections yielding strong signals and low background. *J Immunol Methods*. 2007;318:11-19.

(232) Garcia-Cazarin ML, Smith JL, Clair DK, Piascik MT. The alpha1D-adrenergic receptor induces vascular smooth muscle apoptosis via a p53-dependent mechanism. *Mol Pharmacol*. 2008;74:1000-1007.

(233) Seaman CW, Toseland CD, Maile PA, Francis I, White DJ. Study of the cardiotoxic potential of pharmaceutical compounds in chick myocardial myocyte reaggregate cultures. *Toxicol In Vitro*. 1994;8:543-544.

(234) Purcell NH, Tang G, Yu C, Mercurio F, DiDonato JA, Lin A. Activation of NF-kappa B is required for hypertrophic growth of primary rat neonatal ventricular cardiomyocytes. *Proc Natl Acad Sci U S A*. 2001;98:6668-6673.

(235) Chandrasekar B, Marelli-Berg FM, Tone M, Bysani S, Prabhu SD, Murray DR. Beta-adrenergic stimulation induces interleukin-18 expression via beta2-AR, PI3K, Akt, IKK, and NF-kappaB. *Biochem Biophys Res Commun*. 2004;319:304-311.

(236) Masure S, Paemen L, Van A, I, Fiten P, Proost P, Billiau A, Van DJ, Opdenakker G. Production and characterization of recombinant active mouse gelatinase B from eukaryotic cells and in vivo effects after intravenous administration. *Eur J Biochem*. 1997;244:21-30.

(237) Fry SA, Van den Steen PE, Royle L, Wormald MR, Leathem AJ, Opdenakker G, McDonnell JM, Dwek RA, Rudd PM. Cancer-associated glycoforms of gelatinase B exhibit a decreased level of binding to galectin-3. *Biochemistry.* 2006;45:15249-15258.

(238) Fry SA, Van den Steen PE, Royle L, Wormald MR, Leathem AJ, Opdenakker G, Rudd PM, Dwek RA. Differential glycosylation of gelatinase B from neutrophils and breast cancer cells. *Adv Exp Med Biol.* 2005;564:103-112.

(239) Song G, Hennessy M, Zhao YL, Li Q, Han WD, Qi Y, Zhao WN, Silke B, Barry M, Doyle R, Spiers JP. Adrenoceptor blockade alters plasma gelatinase activity in patients with heart failure and MMP-9 promoter activity in a human cell line (ECV304). *Pharmacol Res.* 2006;54:57-64.

(240) Boutillier AL, Barthel F, Roberts JL, Loeffler JP. Beta-adrenergic stimulation of cFOS via protein kinase A is mediated by cAMP regulatory element binding protein (CREB)-dependent and tissue-specific CREB-independent mechanisms in corticotrope cells. *J Biol Chem.* 1992;267:23520-23526.

(241) Delghandi MP, Johannessen M, Moens U. The cAMP signalling pathway activates CREB through PKA, p38 and MSK1 in NIH 3T3 cells. *Cell Signal.* 2005;17:1343-1351.

(242) Markou T, Hadzopoulou-Cladaras M, Lazou A. Phenylephrine induces activation of CREB in adult rat cardiac myocytes through MSK1 and PKA signaling pathways. *J Mol Cell Cardiol.* 2004;37:1001-1011.

(243) Ozgen N, Obreztchikova M, Guo J, Elouardighi H, Dorn GW, Wilson BA, Steinberg SF. Protein kinase D links Gq-coupled receptors to cAMP response element-binding protein (CREB)-Ser133 phosphorylation in the heart. *J Biol Chem.* 2008;283:17009-17019.

(244) Arthur JS, Cohen P. MSK1 is required for CREB phosphorylation in response to mitogens in mouse embryonic stem cells. *FEBS Lett.* 2000;482:44-48.

(245) Sun P, Enslen H, Myung PS, Maurer RA. Differential activation of CREB by Ca2+/calmodulin-dependent protein kinases type II and type IV involves phosphorylation of a site that negatively regulates activity. *Genes Dev.* 1994;8:2527-2539.

(246) Zhang GX, Kimura S, Nishiyama A, Shokoji T, Rahman M, Yao L, Nagai Y, Fujisawa Y, Miyatake A, Abe Y. Cardiac oxidative stress in acute and chronic isoproterenol-infused rats. *Cardiovasc Res.* 2005;65:230-238.

(247) Lazou A, Sugden PH, Clerk A. Activation of mitogen-activated protein kinases (p38-MAPKs, SAPKs/JNKs and ERKs) by the G-protein-coupled receptor agonist phenylephrine in the perfused rat heart. *Biochem J.* 1998;332 (Pt 2):459-465.

(248) Alexandrov A, Keffel S, Goepel M, Michel MC. Stimulation of alpha1A-adrenoceptors in Rat-1 cells inhibits extracellular signal-regulated kinase by activating p38 mitogen-activated protein kinase. *Mol Pharmacol.* 1998;54:755-760.

(249) Barron AJ, Finn SG, Fuller SJ. Chronic activation of extracellular-signal-regulated protein kinases by phenylephrine is required to elicit a hypertrophic response in cardiac myocytes. *Biochem J.* 2003;371:71-79.

(250) Ford AP, Daniels DV, Chang DJ, Gever JR, Jasper JR, Lesnick JD, Clarke DE. Pharmacological pleiotropism of the human recombinant alpha1A-adrenoceptor: implications for alpha1-adrenoceptor classification. *Br J Pharmacol.* 1997;121:1127-1135.

(251) Argyle SA, McGrath JC. An alpha(1A)/alpha(1L)-adrenoceptor mediates contraction of canine subcutaneous resistance arteries. *J Pharmacol Exp Ther.* 2000;295:627-633.

(252) Freund C, Schmidt-Ullrich R, Baurand A, Dunger S, Schneider W, Loser P, El-Jamali A, Dietz R, Scheidereit C, Bergmann MW. Requirement of nuclear factor-kappaB in angiotensin II- and isoproterenol-induced cardiac hypertrophy in vivo. *Circulation.* 2005;111:2319-2325.

(253) Chandrasekar B, Marelli-Berg FM, Tone M, Bysani S, Prabhu SD, Murray DR. Beta-adrenergic stimulation induces interleukin-18 expression via beta2-AR, PI3K, Akt, IKK, and NF-kappaB. *Biochem Biophys Res Commun.* 2004;319:304-311.

(254) Davel AP, Fukuda LE, De Sa LL, Munhoz CD, Scavone C, Sanz-Rosa D, Cachofeiro V, Lahera V, Rossoni LV. Effects of isoproterenol treatment for 7 days on inflammatory mediators in the rat aorta. *Am J Physiol Heart Circ Physiol.* 2008;295:H211-H219.

(255) Takemoto Y, Yoshiyama M, Takeuchi K, Omura T, Komatsu R, Izumi Y, Kim S, Yoshikawa J. Increased JNK, AP-1 and NF-kappa B DNA binding activities in isoproterenol-induced cardiac remodeling. *J Mol Cell Cardiol.* 1999;31:2017-2030.

(256) Poppers DM, Schwenger P, Vilcek J. Persistent tumor necrosis factor signaling in normal human fibroblasts prevents the complete resynthesis of I kappa B-alpha. *J Biol Chem.* 2000;275:29587-29593.

(257) Farmer P, Pugin J. beta-adrenergic agonists exert their "anti-inflammatory" effects in monocytic cells through the IkappaB/NF-kappaB pathway. *Am J Physiol Lung Cell Mol Physiol.* 2000;279:L675-L682.

(258) Gao H, Sun Y, Wu Y, Luan B, Wang Y, Qu B, Pei G. Identification of β-arrestin2 as a G protein-coupled receptor-stimulated regulator of NF-kappaB pathways. *Mol Cell.* 2004;14:303-317.

(259) Witherow DS, Garrison TR, Miller WE, Lefkowitz RJ. β-Arrestin inhibits NF-κB activity by means of its interaction with the NF-κB inhibitor IκBα. *Proc Natl Acad Sci U S A.* 2004;101:8603-8607.

(260) Ieda M, Tsuchihashi T, Ivey KN, Ross RS, Hong TT, Shaw RM, Srivastava D. Cardiac fibroblasts regulate myocardial proliferation through beta1 integrin signaling. *Dev Cell.* 2009;16:233-244.

(261) Coker ML, Doscher MA, Thomas CV, Galis ZS, Spinale FG. Matrix metalloproteinase synthesis and expression in isolated LV myocyte preparations. *Am J Physiol.* 1999;277:H777-H787.

(262) Speidl WS, Toller WG, Kaun C, Weiss TW, Pfaffenberger S, Kastl SP, Furnkranz A, Maurer G, Huber K, Metzler H, Wojta J. Catecholamines potentiate LPS-induced expression of MMP-1 and MMP-9 in human monocytes and in the human monocytic cell line U937: possible implications for peri-operative plaque instability. *FASEB J.* 2004;18:603-605.

(263) Chen LF, Greene WC. Shaping the nuclear action of NF-kappaB. *Nat Rev Mol Cell Biol.* 2004;5:392-401.

(264) Parry GC, Mackman N. Role of cyclic AMP response element-binding protein in cyclic AMP inhibition of NF-kappaB-mediated transcription. *J Immunol.* 1997;159:5450-5456.

(265) Sheppard KA, Rose DW, Haque ZK, Kurokawa R, McInerney E, Westin S, Thanos D, Rosenfeld MG, Glass CK, Collins T. Transcriptional activation by NF-kappaB requires multiple coactivators. *Mol Cell Biol.* 1999;19:6367-6378.

(266) Heidinger M, Kolb H, Krell HW, Jochum M, Ries C. Modulation of autocrine TNF-alpha-stimulated matrix metalloproteinase 9 (MMP-9) expression by mitogen-activated protein kinases in THP-1 monocytic cells. *Biol Chem.* 2006;387:69-78.

(267) Bond M, Fabunmi RP, Baker AH, Newby AC. Synergistic upregulation of metalloproteinase-9 by growth factors and inflammatory cytokines: an absolute requirement for transcription factor NF-kappa B. *FEBS Lett.* 1998;435:29-34.

(268) Brewis N, Ohst K, Fields K, Rapacciuolo A, Chou D, Bloor C, Dillmann W, Rockman H, Walter G. Dilated cardiomyopathy in transgenic mice expressing a mutant A subunit of protein phosphatase 2A. *Am J Physiol Heart Circ Physiol.* 2000;279:H1307-H1318.

(269) Larsen KO, Lygren B, Sjaastad I, Krobert KA, Arnkvaern K, Florholmen G, Larsen AK, Levy FO, Tasken K, Skjonsberg OH, Christensen G. Diastolic dysfunction in alveolar hypoxia: a role for interleukin-18-mediated increase in protein phosphatase 2A. *Cardiovasc Res.* 2008;80:47-54.

(270) Grumbles RM, Shao L, Jeffrey JJ, Howell DS. Regulation of rat interstitial collagenase gene expression in growth cartilage and chondrocytes by vitamin D3, interleukin-1 beta, and okadaic acid. *J Cell Biochem.* 1996;63:395-409.

(271) Westermarck J, Lohi J, Keski-Oja J, Kahari VM. Okadaic acid-elicited transcriptional activation of collagenase gene expression in HT-1080 fibrosarcoma cells is mediated by JunB. *Cell Growth Differ.* 1994;5:1205-1213.

(272) **Alibaba 2.1** [computer program]. 2000.

(273) Pfaffl MW. A new mathematical model for relative quantification in real-time RT-PCR. *Nucleic Acids Res.* 2001;29:e45.

(274) Cohen P, Klumpp S, Schelling DL. An improved procedure for identifying and quantitating protein phosphatases in mammalian tissues. *FEBS Lett.* 1989;250:596-600.

(275) Millward TA, Zolnierowicz S, Hemmings BA. Regulation of protein kinase cascades by protein phosphatase 2A. *Trends Biochem Sci.* 1999;24:186-191.

(276) Fernandez JJ, Candenas ML, Souto ML, Trujillo MM, Norte M. Okadaic acid, useful tool for studying cellular processes. *Curr Med Chem.* 2002;9:229-262.

(277) Huang X, Honkanen RE. Molecular cloning, expression, and characterization of a novel human serine/threonine protein phosphatase, PP7, that is homologous to Drosophila retinal degeneration C gene product (rdgC). *J Biol Chem.* 1998;273:1462-1468.

(278) Westermarck J, Holmstrom T, Ahonen M, Eriksson JE, Kahari VM. Enhancement of fibroblast collagenase-1 (MMP-1) gene expression by tumor promoter okadaic acid is mediated by stress-activated protein kinases Jun N-terminal kinase and p38. *Matrix Biol.* 1998;17:547-557.

(279) Borghaei H, Borghaei RC, Ni X, Pease E, Thornton R, Mochan E. Evidence that suppression of IL-1 induced collagenase mRNA expression by dihomo-gamma-linolenic acid (DGLA) involves inhibition of NF kappa B binding. *Inflamm Res.* 1997;46 Suppl 2:S177-S178.

(280) Boudreau RT, Conrad DM, Hoskin DW. Apoptosis induced by protein phosphatase 2A (PP2A) inhibition in T leukemia cells is negatively regulated by PP2A-associated p38 mitogen-activated protein kinase. *Cell Signal.* 2007;19:139-151.

(281) Rosenberger SF, Gupta A, Bowden GT. Inhibition of p38 MAP kinase increases okadaic acid mediated AP-1 expression and DNA binding but has no effect on TRE dependent transcription. *Oncogene.* 1999;18:3626-3632.

(282) Beaulieu JM, Sotnikova TD, Marion S, Lefkowitz RJ, Gainetdinov RR, Caron MG. An Akt/beta-arrestin 2/PP2A signaling complex mediates dopaminergic neurotransmission and behavior. *Cell.* 2005;122:261-273.

(283) Beaulieu JM, Marion S, Rodriguiz RM, Medvedev IO, Sotnikova TD, Ghisi V, Wetsel WC, Lefkowitz RJ, Gainetdinov RR, Caron MG. A beta-arrestin 2 signaling complex mediates lithium action on behavior. *Cell.* 2008;132:125-136.

(284) Thornton TM, Pedraza-Alva G, Deng B, Wood CD, Aronshtam A, Clements JL, Sabio G, Davis RJ, Matthews DE, Doble B, Rincon M. Phosphorylation by p38 MAPK as an alternative pathway for GSK3beta inactivation. *Science.* 2008;320:667-670.

(285) Kim SD, Yang SI, Kim HC, Shin CY, Ko KH. Inhibition of GSK-3beta mediates expression of MMP-9 through ERK1/2 activation and translocation of NF-kappaB in rat primary astrocyte. *Brain Res.* 2007;1186:12-20.

(286) Witherow DS, Garrison TR, Miller WE, Lefkowitz RJ. beta-Arrestin inhibits NF-kappaB activity by means of its interaction with the NF-kappaB inhibitor IkappaBalpha. *Proc Natl Acad Sci U S A.* 2004;101:8603-8607.

(287) Ray A, Bal BS, Ray BK. Transcriptional induction of matrix metalloproteinase-9 in the chondrocyte and synoviocyte cells is regulated via a novel mechanism: evidence for functional cooperation between serum amyloid A-activating factor-1 and AP-1. *J Immunol.* 2005;175:4039-4048.

(288) Traenckner EB, Pahl HL, Henkel T, Schmidt KN, Wilk S, Baeuerle PA. Phosphorylation of human I kappa B-alpha on serines 32 and 36 controls I kappa B-alpha proteolysis and NF-kappa B activation in response to diverse stimuli. *EMBO J.* 1995;14:2876-2883.

(289) Sun SC, Maggirwar SB, Harhaj E. Activation of NF-kappa B by phosphatase inhibitors involves the phosphorylation of I kappa B alpha at phosphatase 2A-sensitive sites. *J Biol Chem.* 1995;270:18347-18351.

(290) Miskolci V, Castro-Alcaraz S, Nguyen P, Vancura A, Davidson D, Vancurova I. Okadaic acid induces sustained activation of NFkappaB and degradation of the nuclear IkappaBalpha in human neutrophils. *Arch Biochem Biophys.* 2003;417:44-52.

(291) Rieckmann P, Thevenin C, Kehrl JH. Okadaic acid is a potent inducer of AP-1, NF-kappa B, and tumor necrosis factor-alpha in human B lymphocytes. *Biochem Biophys Res Commun.* 1992;187:51-57.

(292) Yang J, Fan GH, Wadzinski BE, Sakurai H, Richmond A. Protein phosphatase 2A interacts with and directly dephosphorylates RelA. *J Biol Chem.* 2001;276:47828-47833.

(293) Dutka DP, Elborn JS, Delamere F, Shale DJ, Morris GK. Tumour necrosis factor alpha in severe congestive cardiac failure. *Br Heart J.* 1993;70:141-143.

(294) Ono K, Matsumori A, Shioi T, Furukawa Y, Sasayama S. Cytokine gene expression after myocardial infarction in rat hearts: possible implication in left ventricular remodeling. *Circulation.* 1998;98:149-156.

(295) Baud V, Karin M. Signal transduction by tumor necrosis factor and its relatives. *Trends Cell Biol.* 2001;11:372-377.

(296) Dasu MR, Barrow RE, Spies M, Herndon DN. Matrix metalloproteinase expression in cytokine stimulated human dermal fibroblasts. *Burns.* 2003;29:527-531.

(297) Srivastava AK, Qin X, Wedhas N, Arnush M, Linkhart TA, Chadwick RB, Kumar A. Tumor necrosis factor-alpha augments matrix metalloproteinase-9 production in skeletal muscle cells through the activation of transforming growth factor-beta-activated kinase 1 (TAK1)-dependent signaling pathway. *J Biol Chem.* 2007;282:35113-35124.

(298) Theiss AL, Simmons JG, Jobin C, Lund PK. Tumor necrosis factor (TNF) alpha increases collagen accumulation and proliferation in intestinal myofibroblasts via TNF receptor 2. *J Biol Chem.* 2005;280:36099-36109.

(299) Cohen M, Meisser A, Haenggeli L, Bischof P. Involvement of MAPK pathway in TNF-alpha-induced MMP-9 expression in human trophoblastic cells. *Mol Hum Reprod.* 2006;12:225-232.

(300) Brown RD, Jones GM, Laird RE, Hudson P, Long CS. Cytokines regulate matrix metalloproteinases and migration in cardiac fibroblasts. *Biochem Biophys Res Commun*. 2007;362:200-205.

(301) Eichler W, Friedrichs U, Thies A, Tratz C, Wiedemann P. Modulation of matrix metalloproteinase and TIMP-1 expression by cytokines in human RPE cells. *Invest Ophthalmol Vis Sci*. 2002;43:2767-2773.

(302) Yao PM, Maitre B, Delacourt C, Buhler JM, Harf A, Lafuma C. Divergent regulation of 92-kDa gelatinase and TIMP-1 by HBECs in response to IL-1beta and TNF-alpha. *Am J Physiol*. 1997;273:L866-L874.

(303) Nee LE, McMorrow T, Campbell E, Slattery C, Ryan MP. TNF-alpha and IL-1beta-mediated regulation of MMP-9 and TIMP-1 in renal proximal tubular cells. *Kidney Int*. 2004;66:1376-1386.

(304) Ito A, Sato T, Iga T, Mori Y. Tumor necrosis factor bifunctionally regulates matrix metalloproteinases and tissue inhibitor of metalloproteinases (TIMP) production by human fibroblasts. *FEBS Lett*. 1990;269:93-95.

(305) Mauviel A, Daireaux M, Redini F, Galera P, Loyau G, Pujol JP. Tumor necrosis factor inhibits collagen and fibronectin synthesis in human dermal fibroblasts. *FEBS Lett*. 1988;236:47-52.

(306) Jaffre F, Callebert J, Sarre A, Etienne N, Nebigil CG, Launay JM, Maroteaux L, Monassier L. Involvement of the serotonin 5-HT2B receptor in cardiac hypertrophy linked to sympathetic stimulation: control of interleukin-6, interleukin-1beta, and tumor necrosis factor-alpha cytokine production by ventricular fibroblasts. *Circulation*. 2004;110:969-974.

(307) Burger A, Benicke M, Deten A, Zimmer HG. Catecholamines stimulate interleukin-6 synthesis in rat cardiac fibroblasts. *Am J Physiol Heart Circ Physiol*. 2001;281:H14-H21.

(308) Yokoyama T, Sekiguchi K, Tanaka T, Tomaru K, Arai M, Suzuki T, Nagai R. Angiotensin II and mechanical stretch induce production of tumor necrosis factor in cardiac fibroblasts. *Am J Physiol*. 1999;276:H1968-H1976.

(309) Newman WH, Castresana MR, Webb JG, Wang Z, Warejcka DJ. Stimulation of beta-adrenergic receptors inhibits the release of tumor necrosis factor-alpha from the isolated rat heart. *Crit Care Med*. 2000;28:3593-3598.

(310) Liu B, Li W, Li Y, Wang Z, Li H, Liu P, Fu J. Protective effects of N-acetylcysteine in isoproterenol-induced myocardium injury in rats. *Mol Biol Rep*. 2009;36:761-765.

(311) Ohtsuka T, Hamada M, Saeki H, Ogimoto A, Hara Y, Shigematsu Y, Higaki J. Serum levels of matrix metalloproteinases and tumor necrosis factor-alpha in patients with idiopathic dilated cardiomyopathy and effect of carvedilol on these levels. *Am J Cardiol*. 2003;91:1024-7, A8.

(312) Khoa ND, Postow M, Danielsson J, Cronstein BN. Tumor necrosis factor-alpha prevents desensitization of Galphas-coupled receptors by regulating GRK2 association with the plasma membrane. *Mol Pharmacol*. 2006;69:1311-1319.

(313) Kawamata Y, Imamura T, Babendure JL, Lu JC, Yoshizaki T, Olefsky JM. Tumor necrosis factor receptor-1 can function through a G alpha q/11-beta-arrestin-1 signaling complex. *J Biol Chem.* 2007;282:28549-28556.

(314) Clark IM, Rowan AD, Edwards DR, Bech-Hansen T, Mann DA, Bahr MJ, Cawston TE. Transcriptional activity of the human tissue inhibitor of metalloproteinases 1 (TIMP-1) gene in fibroblasts involves elements in the promoter, exon 1 and intron 1. *Biochem J.* 1997;324 (Pt 2):611-617.

(315) Yang EV, Sood AK, Chen M, Li Y, Eubank TD, Marsh CB, Jewell S, Flavahan NA, Morrison C, Yeh PE, Lemeshow S, Glaser R. Norepinephrine up-regulates the expression of vascular endothelial growth factor, matrix metalloproteinase (MMP)-2, and MMP-9 in nasopharyngeal carcinoma tumor cells. *Cancer Res.* 2006;66:10357-10364.

(316) Annabi B, Lachambre MP, Plouffe K, Moumdjian R, Beliveau R. Propranolol adrenergic blockade inhibits human brain endothelial cells tubulogenesis and matrix metalloproteinase-9 secretion. *Pharmacol Res.* 2009;60:438-445.

(317) Kintscher U, Wakino S, Kim S, Jackson SM, Fleck E, Hsueh WA, Law RE. Doxazosin inhibits retinoblastoma protein phosphorylation and G(1)-->S transition in human coronary smooth muscle cells. *Arterioscler Thromb Vasc Biol.* 2000;20:1216-1224.

(318) Baouz S, Giron-Michel J, Azzarone B, Giuliani M, Cagnoni F, Olsson S, Testi R, Gabbiani G, Canonica GW. Lung myofibroblasts as targets of salmeterol and fluticasone propionate: inhibition of alpha-SMA and NF-kappaB. *Int Immunol.* 2005;17:1473-1481.

(319) Mizuochi Y, Okajima K, Harada N, Molor-Erdene P, Uchiba M, Komura H, Tsuda T, Katsuya H. Carvedilol, a nonselective beta-blocker, suppresses the production of tumor necrosis factor and tissue factor by inhibiting early growth response factor-1 expression in human monocytes in vitro. *Transl Res.* 2007;149:223-230.

(320) Yan C, Wang H, Aggarwal B, Boyd DD. A novel homologous recombination system to study 92 kDa type IV collagenase transcription demonstrates that the NF-kappaB motif drives the transition from a repressed to an activated state of gene expression. *FASEB J.* 2004;18:540-541.

(321) Gardner J, Borgmann K, Deshpande MS, Dhar A, Wu L, Persidsky R, Ghorpade A. Potential mechanisms for astrocyte-TIMP-1 downregulation in chronic inflammatory diseases. *J Neurosci Res.* 2006;83:1281-1292.

(322) Doyle GA, Saarialho-Kere UK, Parks WC. Distinct mechanisms regulate TIMP-1 expression at different stages of phorbol ester-mediated differentiation of U937 cells. *Biochemistry.* 1997;36:2492-2500.

(323) Kralisch S, Lossner U, Bluher M, Paschke R, Stumvoll M, Fasshauer M. Tissue inhibitor of metalloproteinase 1 expression and secretion are induced by beta-adrenergic stimulation in 3T3-L1 adipocytes. *J Endocrinol.* 2006;189:665-670.

(324) Guy GR, Cao X, Chua SP, Tan YH. Okadaic acid mimics multiple changes in early protein phosphorylation and gene expression induced by tumor necrosis factor or interleukin-1. *J Biol Chem*. 1992;267:1846-1852.